İSTANBUL TECHNICAL UNIVERSITY ★ INSTITUTE OF SCIENCE AND TECHNOLOGY

WATER QUALITY MODELING OF KÖYCEĞİZ – DALYAN LAGOON

Ph.D. Thesis by

Alpaslan EKDAL, M.Sc.

Department : Environmental Engineering

Programme : Environmental Engineering

JANUARY 2008

İSTANBUL TECHNICAL UNIVERSITY ★ INSTITUTE OF SCIENCE AND TECHNOLOGY

WATER QUALITY MODELING OF KÖYCEĞİZ – DALYAN LAGOON

Ph.D. Thesis by

Alpaslan EKDAL, M.Sc.

(501002352)

Date of submission: 31 July 2007

Date of defence examination: 30 January 2008

Supervisor (Chairman): Prof. Dr. Ayşegül TANIK

Members of the Examining Committee Prof.Dr. İ. Ethem GÖNENÇ (Retired)

Prof.Dr. Günay KOCASOY (BÜ)

Prof.Dr. Bilsen BELER BAYKAL (İTÜ)

Prof.Dr. Mehmet KARPUZCU (GYTE)

JANUARY 2008

İSTANBUL TEKNİK ÜNİVERSİTESİ ★ FEN BİLİMLERİ ENSTİTÜSÜ

KÖYCEĞİZ – DALYAN LAGÜNÜ'NÜN SU KALİTESİ MODELLEMESİ

DOKTORA TEZİ

Y. Müh. Alpaslan EKDAL
(501002352)

Tezin Enstitüye Verildiği Tarih: 31 Temmuz 2007

Tezin Savunulduğu Tarih: 30 Ocak 2008

Tez Danışmanı: Prof. Dr. Ayşegül TANIK

Diğer Jüri Üyeleri Prof.Dr. İ. Ethem GÖNENÇ (Emekli)

Prof.Dr. Günay KOCASOY (BÜ)

Prof.Dr. Bilsen BELER BAYKAL (İTÜ)

Prof.Dr. Mehmet KARPUZCU (GYTE)

OCAK 2008

FOREWORD

Without a doubt, this study is a product of the influence of many special people. It never would have been completed without their support and belief in me.

I appreciate my supervisor, Prof. Dr. Ayşegül TANIK, not only for her invaluable guidance for conducting this Ph D study, but also for her support and encouragement during the desperate moments of my life. I am grateful to Prof. Dr. İ. Ethem GÖNENÇ, for sharing his advices and visions for the study, and for his encouragement to think in a broader manner in our studies. I would like to thank to Prof. Dr. Günay KOCASOY, for her valuable contributions to the study, as the thesis progress monitoring committee member. Special thanks go to Prof. Dursun Z. ŞEKER for his valuable contribution throughout the work and help in generating GIS figures. I would like to thank to the staff of Istanbul University Institute of Marine Sciences and Management for their contribution in the field studies in memory of Prof. Dr. Erdoğan OKUŞ.

I express my deepest thanks to Dr. Rosemarie C. RUSSO, for providing me the opportunity to work as a visiting scientist at the USEPA NERL ERD, and for encouraging me to attend Tai Chi practices. I owe much to Mr. Robert B. AMBROSE, Jr., for his supervision in applying WASP, and for his support in my daily life in Athens, GA. I would like to thank to all people at ERD for their lovely friendship in the name of him.

I would like to express my warm thanks to Melike GÜREL and Ali ERTÜRK for their endless help and contribution throughout the study, and for their friendship. I am also grateful to Elif PEHLİVANOĞLU MANTAŞ and Egemen AYDIN, for listening me long hours with great patience during my hard times. My special thanks go to my dear friends Serdar DOĞRUEL and Gülsüm Emel ZENGİN, for their invaluable friendship since the undergraduate days at the Yıldız Technical University. I hope we will always walk together in this way.

I would like to thank all my friends at İTÜ Environmental Engineering Department for their encouragement.

Last but not the least; I would like to express my warm thanks to my beloved family, for their support and belief in me in every moment of my life. I dedicate this dissertation to my dad; I know that he is following me somewhere up in the sky.

January 2008 **Alpaslan EKDAL**

TABLE OF CONTENTS

ABBREVIATIONS

WASP : Water Quality Analysis Simulation Program
USEPA : United States Environmental Protection Agency
TMDL : Total Maximum Daily Loads
PEM : Potomac Eutrophication Model
SOD : Sediment Oxygen Demand
DRP : Dissolved Reactive Phosphorus
TSS : Total Suspended Solids
TRP : Total Reactive Phosphorus
TDP : Total Dissolved Phosphorus
PP : Particulate Phosphorus
PIP : Particulate Inorganic Phosphorus
POP : Particulate Organic Phosphorus
TP : Total Phosphorus
TN : Total Nitrogen
DON : Dissolved Organic Nitrogen
DIN : Dissolved Inorganic Nitrogen
PON : Particulate Organic Nitrogen
POC : Particulate Organic Carbon
DO : Dissolved Oxygen
BOD_5 : 5 days Biochemical Oxygen Demand
CBOD : Carbonaceous Biochemical Oxygen Demand
Chl-a : Chlorophyll-a

LIST OF TABLES

LIST OF FIGURES

Page No

KÖYCEĞİZ – DALYAN LAGÜNÜ'NÜN SU KALİTESİ MODELLEMESİ

ÖZET

Kıyı ekosistemlerinde gerçekleştirilen insan faaliyetleri son yıllarda önemli çevre sorunlarının ortaya çıkmasına neden olmuştur. Dolayısıyla, oldukça yüksek ekonomik değere sahip, bu hassas su kaynaklarında meydana gelen bozulmalar en önemli çevresel sorunlar arasında yerini almıştır.

Bilgisayar teknolojisinde meydana gelen hızlı gelişmeler sayesinde, matematik modellerin kirlenme sorunlarının iyileştirilmesi ve çevrenin bir birim olarak nasıl çalıştığının anlaşılması amacıyla kullanılması, büyük önem kazanmıştır. Matematik modeller, sadece zaman ve ekonomik tasarruflar sağladığı için değil, aynı zamanda ekolojik sorunların daha kolay çözülmesine olanak sağladıkları ve sürdürülebilir yönetim için uygun yönetim seçeneklerinin seçilmesine yardımcı oldukları için oldukça yararlı araçlardır.

Kıyı lagünleri kara ve deniz ekosistemleri arasında bir ara yüz gibi davrandıklarından, hem karadan hem de denizden gelen etkilerin altında kalırlar. Fosfor ve azot yüklerinin bu hassas su ortamlarının üzerinde oldukça önemli etkileri mevcuttur. Dolayısıyla, bu gibi ekosistemlerin sürdürülebilir gelişimi ve yönetiminden sorumlu kişilerin karşılarına çıkan en önemli sorunlardan biri olarak ötrofikasyon görülmektedir. Bu hassas su ortamlarının ve doğal kaynakların sürdürülebilir gelişimi ve yönetimi için, modeller kullanılarak gelecekteki durumlarının bugünden öngörülmesi gerekmektedir.

Bu çalışmada, seçilen bir pilot bölgeye bir su kalitesi modeli uygulanmış ve bu hassas ekosistemin sürdürülebilir yönetimi için karar vericilere sistemin su kalitesi durumu hakkında bilgi üretilmiştir.

Türkiye'nin en önemli ve hassas ekosistemlerinden olan Köyceğiz – Dalyan Lagünü, pilot bölge olarak seçilmiştir. Yapılan literatür taramasının ardından, Amerika Birleşik Devletleri Çevre Koruma Teşkilatı tarafından geliştirilen Water Quality Analysis Simulation Program (WASP), en uygun model olarak seçilmiştir.

Uygun modelin seçiminin ardından su kalitesi modelleme çalışmalarına başlanmıştır. Su kalitesi modelleme çalışmaları sırasında, sistemdeki süreçlerin ve mekanizmaların daha iyi anlaşılabilmesi amacıyla simülasyonlar basitten başlayıp, karmaşığa doğru gerçekleştirilmiştir. Bu amaçla, simülasyonlar 5 adımda yapılarak, her adımda bir veya birkaç durum değişkeni ilave edilmiştir.

Birinci simülasyon adımında, modele tanıtılan akımların analiz edilebilmesi ve kontrolü için tuzluluk simülasyonları gerçekleştirilmiştir. Tuzluluk sonuçlarına göre, öngörülen konsantrasyonların çoğu izleme çalışmalarında ölçülen değerlerle uyum göstermektedir. Simülasyon sonuçları; modele tanıtılan akımların, akım yollarının ve

difüzyon katsayılarının su kalitesi simülasyonlarının gerçekleştirilebilmesi için yeterli doğrulukta olduğunu göstermektedir.

İkinci simülasyon adımında, WASP modelinde yer alan bütün azot türleri (NH_3 – N, NO_3^- – N, organik azot ve detrital azot) ve fitoplankton simüle edilmiştir.

Üçüncü simülasyon adımında, fosfor türleri simülasyonlara ilave edilmiştir. Böylece, WASP modelinde yer alan bütün azot türleri (NH_3 – N, NO_3^- – N, organik azot ve detrital azot), fosfor türleri (PO_4^{3-} – P, organik fosfor ve detrital fosfor) ve fitoplankton, birlikte simüle edilmiştir.

Dördüncü simülasyon adımında, üçüncü adımda yer alan durum değişkenlerine çözünmüş oksijen, $KBOİ_1$, detrital karbon ve tuzluluk parametreleri ilave edilmiş ve toplamda 12 durum değişkeni simüle edilmiştir.

Beşinci simülasyon adımında, noktasal ve yayılı yüklerin sistem üzerindeki etkilerinin analiz edilebilmesi için, yük senaryoları geliştirilmiştir. Birinci yük senaryosunda; bütün amonyak azotu, nitrat azotu, organik azot, ortofosfat fosforu, organik fosfor, $KBOİ_1$, detrital azot ve detrital fosfor yükleri %50 arttırılmıştır. İkinci senaryoda ise, aynı durum değişkenlerine ait yükler %100 oranında arttırılarak iki katına çıkarılmıştır. Üçüncü senaryoda, bu kez sözü edilen yükler %50 oranında azaltılmıştır.

Simülasyon sonuçlarına göre, fosfor sistemdeki kısıtlayıcı element olarak gözükmektedir. Fosfor türleri simülasyonlara eklendiklerinde toplam klorofil-a konsantrasyonlarında önemli değişiklikler meydana gelmiş, bu da azot türlerinde konsantrasyon değişimlerine neden olmuştur.

WATER QUALITY MODELING OF KÖYCEĞİZ – DALYAN LAGOON

SUMMARY

The human activities on coastal ecosystems started to cause severe environmental problems in the last few decades. Therefore, deterioration of these sensitive water resources, which have high economic importance, has become a major environmental concern.

The fast and recent advances in computer technology provided mathematical models to be utilized in the remediation of pollution problems and in understanding how the environment works as a unit. Mathematical models are useful tools, not only for saving time and money, but also for solving ecological problems easier and for helping to choose an appropriate management alternative for sustainable management.

Coastal lagoons act as an interface between the terrestrial and marine environments, therefore, they are affected both by continental and marine influences. Phosphorous and nitrogen loadings have a major impact on the water quality of such sensitive and vulnerable water bodies; thus, control of eutrophication is one of the major problems faced by those responsible of the sustainable development and management of these ecosystems. Sustainable development and management requires the use of such models to foresee the future status of such natural resources and sensitive water bodies.

In this study, a water quality model was applied to a selected pilot area, for generating information to the decision-makers about the water quality status of this sensitive ecosystem for its sustainable management.

Köyceğiz – Dalyan Lagoon, was selected as the pilot area, which is one of the most important and sensitive ecosystems in Turkey. Water Quality Analysis Simulation Program (WASP), developed by the United States Environmental Protection Agency (USEPA), was selected as the appropriate model.

After the selection of the appropriate model, water quality modeling studies were conducted. During the modeling studies, the simulations were run from the simplest complexity level to higher complexity levels in order to better understand the processes and mechanisms that occur in the system. Therefore, the simulations were carried out in 5 steps. One or more state variables were added in each simulation step.

In Simulation Step 1, salinity simulations were conducted for analyzing the flows and exchanges defined to the model. According to the salinity simulation results, most of them are in high compliance with monitoring data. The simulation results

indicate that the flow rates, pathways, exchanges and exchange coefficients, are estimated satisfactorily to run water quality simulations.

In Simulation Step 2, all the nitrogen state variables (NH_3 – N, NO_3^- – N, organic nitrogen and detrital nitrogen) available in WASP and phytoplankton were simulated.

In Simulation Step 3, phosphorus species were added to the simulations. All the available state variables of WASP regarding nitrogen (NH_3 – N, NO_3^- – N, organic nitrogen and detrital nitrogen), phosphorus (PO_4^{3-} – P, organic phosphorus and detrital phosphorus) and phytoplankton are simulated together.

In Simulation Step 4, dissolved oxygen, $CBOD_1$, detrital carbon and salinity parameters were added to Simulation Step 3. Thus, a total number of 12 state variables were simulated.

In order to analyze the effects of point and diffuse pollutant loads on the system, load scenarios were developed. In the first load scenario, all the ammonia nitrogen, nitrate nitrogen, organic nitrogen, orthophosphate phosphorus, organic phosphorus, $CBOD_1$, detrital nitrogen and detrital phosphorus loads are increased by 50%. In the second scenario, the loads of the same state variables were increased by 100%, and in the last scenario these loads were decreased by 50%.

According to the simulation results, phosphorus seems to be the limiting nutrient in the system. When phosphorus species were included into the simulations significant changes were observed in total chlorophyll- a concentrations, which also affected the concentrations of nitrogen species.

1. INTRODUCTION

1.1 Aim and Scope

The human activities on coastal ecosystems started to cause severe environmental problems in the last few decades. Therefore, deterioration of these sensitive water resources, which have high economic importance, has become a major environmental concern.

The fast and recent advances in computer technology provided mathematical models to be utilized in the remediation of pollution problems and in understanding how the environment works as a unit. Mathematical models are useful tools, not only for saving time and money, but also for solving ecological problems easier and for helping to choose an appropriate management alternative for sustainable management. Therefore, using models has a broader function and they help the users to visualize the problems in detail.

Coastal lagoons act as an interface between the terrestrial and marine environments, therefore, they are affected both by continental and marine influences. Phosphorous and nitrogen loading have a major impact on the water quality of such sensitive and vulnerable water bodies; thus, control of eutrophication is one of the major problems faced by those responsible for the sustainable development and management of these ecosystems. Sustainable development and management requires the use of such models to foresee the future status of such natural resources and sensitive water bodies.

In the study, the main objective is application and adaptation of a complex water quality model to a complex lagoon system. The second objective is to prepare a guideline for the future water quality modeling studies in such complex systems by emphasizing on the difficulties faced in developing countries such as Turkey.

Köyceğiz – Dalyan Lagoon, selected as the area of interest, is one of the most sensitive ecosystems in Turkey. The lagoon is located in the southwest of Turkey within the boundaries of Muğla Province along the Mediterranean Sea coast. Two drainage systems comprise the lagoon system. The first drainage system consists of the Köyceğiz Lake, whereas the second one consists of Dalyan Channel Network, Alagöl Lake, Sülüngür Lake and İztuzu Lake. The Köyceğiz Lake is connected to the Mediterranean Sea via the lagoon and its branches.

Water Quality Analysis Simulation Program (WASP), which is developed by the United States Environmental Protection Agency (USEPA), was selected as the appropriate model to be implemented to Köyceğiz – Dalyan Lagoon for the study. WASP helps users to interpret and predict water quality responses to natural phenomena and man-made pollution for various pollution management decisions. The model has been especially applied to many water bodies in USA. It is also aimed to give the guidelines of using the model and evaluating the findings.

The following chapters are included within the context of the dissertation.

The second chapter includes the literature survey on surface water quality modeling. Firstly, the effects of eutrophication on aquatic ecosystems are put forth. Then, the concepts and historical development of surface water quality modeling is stated.

Information about the Köyceğiz – Dalyan Lagoon is referred in Chapter 3. Some information is given about the coastal lagoons. It is then that the location and the characteristics of Köyceğiz – Dalyan Lagoon is described. The characteristics of the lagoon include; meteorology, hydrodynamic and hydrogeological conditions, socio-demographical structure and population, land use and soil characteristics, and the pollutant sources.

In Chapter 4 the modeling process applied for Köyceğiz – Dalyan Lagoon is described. Initially the objective is defined and then model selection stage is explained. The subsequent stages of modeling process such as preliminary application, calibration, verification and sensitivity analysis are also mentioned in this chapter.

Chapter 5 is devoted to WASP program. The overview of WASP model and the modeling system is given at the beginning of this chapter. Then, the mass balance equation used in the model is presented. After that, information on the model network, the model transport scheme and the application of the model is mentioned. The overview of the eutrophication module, the state variables simulated, and the kinetics and nutrient cycles used in the model are also presented in Chapter 5.

The data analyses and water quality modeling studies with WASP are given in Chapter 6. Initially, the collection of monitoring data is presented in this chapter. Then, generation of input data is provided that includes the subsections of; initial concentrations, and the boundary conditions (pollutant loads, water temperature function, air temperature, daily solar radiation, wind speed, flows and exchanges). The water quality modeling studies conducted with WASP are presented at the end of this chapter.

Chapter 7 includes the results and the discussion of the water quality modeling studies conducted with WASP.

Conclusions and recommendations of this study are presented in Chapter 8.

1.2 Significance of the Study

Models and simulations allow the rapid evaluation of pollution in terms of cause and effect relationships. Models are required for forecasting the effects of eutrophication on aquatic ecosystems. The main advantage is that they enable analyses of different future scenarios. The models are also useful since they allow making more objective and reliable assessments and predictions. Water quality models, which predict nutrient levels within a water body using catchment variables, are especially developed for predicting nutrient levels in the water body. Surface water quality models are used both in research as well as in designing and assessing the water quality management measures. Water quality models attempt to describe the major spatial and temporal changes of constituents of concern.

Developing countries around the world are beginning to recognize that environmental protection must be coupled with socioeconomic development. For

these countries, cost-effective, model-based control strategies could provide a means to control pollution and sustain a high quality of life while maintaining economic growth.

This study is a leading one in the world, where WASP is applied to a lagoon system. Köyceğiz – Dalyan Lagoon is a highly complex system regarding its geomorphology, hydrodynamics and hydrology. WASP has so far been applied especially in developed countries, where modelers may obtain systematic and continuous data for long periods of time that enables to apply the model quite easily, compared to similar conditions in developing countries. In developing countries like Turkey, one of the major constraints in running models is the lack of sufficient input data that represent the conditions of the water systems under investigation. Besides, continuous data availability, systematic database is also necessary for fulfilling the minimum data requirement of models. Under such conditions, WASP has been attempted to be applied in a complex lagoon system in Turkey where data constraints evolved certain difficulties during various stages of the modeling study. Therefore, it can be stated that, besides applying the model to a water system in Turkey, the main idea behind the target of the study is to put forth the difficulties faced in applying the model and the assumptions made to overcome these difficulties that any of the developing countries may face in modeling efforts. The significance of the work conducted is therefore based on the fact that it will in the future act as a guideline for other developing countries that aim to apply water quality modeling studies.

2. SURFACE WATER QUALITY MODELING

Clean water is an important resource for different beneficial uses such as drinking, irrigation, industry, transportation, recreation, fishing, hunting, and aesthetic enjoyment (Carpenter et al., 1998). Pollutant inputs have increased in the last few decades and have deteriorated water quality of many rivers, lakes, and coastal waters. Deterioration of these important water resources can be considered as loss of natural systems, their component species, and the amenities that they provide (EPA, 1996; Postel and Carpenter, 1997). Eutrophication and oxygen depletion are among the common principal problems addressed in surface water quality studies. Depletion of dissolved oxygen and acceleration of undesired aquatic growth due to nutrients cause severe surface water quality problems (Erturk et al., 2004). Eutrophication of most waters is dependent on supplies of nitrogen and phosphorus (Vollenweider, 1968). There are coastal areas that suffer from eutrophication due to increased mineralization of organic matter and decreased oxygen concentrations based on their local natural characteristics like the geomorphology of the systems, shape of the tidal curve, mean depth of the entire system, its channels and tidal flats (de Jonge et al., 2002). Apart from natural eutrophication, human- induced eutrophication occurs due to nutrient loadings from point and diffuse inputs. Nutrients arise especially from the application of commercial fertilizers and animal manure on agricultural land, forest run-offs, wastewater effluent, atmospheric deposition, and urban surface run-off (Carpenter et al., 1998; de Jonge et al., 2002; Erturk et al., 2004; Nijboer and Verdonschot, 2004). As point sources are under control in many cases, the contribution of nutrients from diffuse (non-point) sources is becoming more important (Carpenter et al., 1998; de Jonge et al., 2002; Mainstone and Parr, 2002).

Eutrophication is also widespread and rapidly expanding in estuaries and coastal seas of the world (NRC, 1993; Nixon 1995). For most temperate estuaries and coastal ecosystems, nitrogen is the most limiting element of primary production and highly responsible for eutrophication (Howarth, 1988; NRC, 1993; Howarth et al., 1996;

Nixon et al., 1996). Although nitrogen is the major factor of eutrophication in most of the estuaries and coastal seas, phosphorus is also determined to be an essential element that contributes to coastal eutrophication. It is, in fact, the dominant control of primary production in some coastal ecosystems (Carpenter et al., 1998).

Mathematical modeling, which forms an integral part of the decision-making process for water resources management, has been in use since the late 1960s as a tool in environmental sciences. Models and simulations allow the rapid evaluation of pollution in terms of cause and effect relationships. Models are required for forecasting the effects of eutrophication on aquatic ecosystems (Nijboer and Verdonschot, 2004). The main advantage is that they enable analyses of different future scenarios (Erturk et al., 2004). The models are also useful since they allow making more objective and reliable assessments and predictions (Gertsev and Gertseva, 2004).

Water quality models, which predict nutrient levels within a water body using catchment variables, are especially developed for predicting nutrient levels in the water body. Surface water quality models are used both in research as well as in designing and assessing the water quality management measures. Water quality models attempt to describe the major spatial and temporal changes of constituents of concern. Many of these models couple catchment's hydrology and water quality in the water body (there is a large overlap with hydrological models), including variables such as catchment area, soil type, land use, nutrient input, and/or runoffs (Nijboer and Verdonschot, 2004).

2.1 Effects of Eutrophication on the Aquatic Ecosystems

Eutrophication has many negative effects on aquatic ecosystems. The increased growth of algae and aquatic weeds that interfere with the use of water for fisheries, recreation, industry, agriculture and drinking is the well known indicator among the others. Oxygen shortages caused by the decomposition of nuisance plants lead to fish kills. Eutrophication causes the loss of habitats, including aquatic plant beds in fresh and marine waters and coral reefs of tropical coasts (NRC, 1993; Jeppesen et al.,

1998). Eutrophication is accepted as an important factor in the loss of aquatic biodiversity (Seehausen et al., 1997).

2.1.1 Toxicity

Toxicity is one of the aspects of eutrophication that has a direct effect on the functioning of organisms in the ecosystem. Ammonia, nitrite and sulphide are the toxic substances that develop due to eutrophication processes (Sladecek, 1973). These toxicants can be lethal to species at high concentrations. These direct effects are very clear, but they only occur under extreme conditions of high concentrations together with oxygen depletion. More importantly, there are also less visible and indirect effects of eutrophication (Nijboer and Verdonschot, 2004).

Explosive growths of nuisance algae are among the most destructive effects of eutrophication (Anderson and Garrison, 1997). These algae are harmful to livestock, humans, and other organisms. In marine ecosystems, algal blooms (red or brown tides) cause widespread problems by releasing toxins and by causing anoxia when oxygen is consumed as dead algae decompose (Carpenter et al., 1998). Harmful algal blooms seem to be more common today than it was in the past. They can have severe effects in fish kills and neuro-toxin production (PSP, DSP, and ASP) affecting animals with complex nervous systems (de Jonge et al., 2002). The blooms also have severe negative impacts on aquaculture and shellfisheries (Shumway, 1990). They cause shellfish poisoning in humans and significant mortality in marine mammals (Anderson, 1994).

2.1.2 Primary Production Rate

Emergent plants, aquatic bryophytes, epiphytic green and blue-green algae and phytoplankton are the organism groups that contribute to the primary production. The benthic and epiphytic algae contribute largely to primary production in rapidly flowing waters. These algae attach themselves to the substrate as long as the current is not too strong (Nijboer and Verdonschot, 2004).

A high algal biomass results in ecological and management problems in fast as well as slowly flowing parts of streams and rivers. Attention should be focused on the

periphyton, the dominant community in running waters, as referred by Wetzel and Ward (1992).

An increase in nutrient ratios may cause a change in the algal species composition based on the differences in affinity of algae to nutrients (de Jonge et al., 2002).

The algal growth can be limited by the depletion of nitrogen or phosphorus (Winterbourn, 1990). The uptake of dissolved nutrients from the water layer is high in a river that is dominated by phytoplankton. Phytoplankton is capable of reducing the amount of phosphorus originating from a sewer discharge to a limiting level (Decamps et al., 1984). Many researchers have investigated whether phosphorus or nitrogen limits the algal growth. If the nutrient concentration is high, light or temperature can also be the limiting factor. Limitation by light especially occurs in forested and turbid streams. When the layer of algae or macrophytes is getting too dense to permit light penetration through the water column, limitation by self-shading occurs. Low turbidity systems may change from macrophyte-dominated into a phytoplankton-dominated system even with micro algal blooms affecting the integrity of the system (de Jonge et al., 2002). If a stream is shaded, primary production will not incline by addition of nutrients.

Eutrophication resulting in enlarged production is also dependent on the light availability. In highly turbid systems where primary production is light limited the situation usually differs from low turbid systems, because benthic communities are usually poor in vascular plants like eelgrass and large brown algae (de Jonge et al., 2002).

Hydrological variables can also play a role on primary production. The photosynthesis, the respiration and the nutrient uptake can be stimulated by a high current velocity (Stevenson, 1984). This is explained by the higher diffusion rate of nutrients by high current velocities with continuous nutrient fluxes. On the other hand, current can have a negative effect by flushing away loosely attached algae and reducing the algal biomass (Biggs, 1996).

Water transport processes dictate that the effects of nutrient enrichment occur either in the lower reaches of the estuary or in the coastal area itself (de Jonge et al., 2002).

To sum up, primary production increases after nutrient addition as long as the added nutrient is limiting. Other factors, such as light, current velocity, spates, and temperature play a major role as well. In modeling, all those factors and processes should be taken into account.

2.1.3 Oxygen Depletion

Eutrophication with inorganic nutrients can result in oxygen depletion. In running waters, it causes an increase in production rate. Since primary producers play an important role in the oxygen balance of the water, this has an impact on the water quality. Primary production is a strong link between nutrient fluxes and deterioration of water quality (Novotny and Zheng, 1988). Oxygen consuming processes occur during day and night, while oxygen producing processes only take place during daylight. Therefore, oxygen content can fluctuate strongly over the day as mentioned by Thomann and Mueller (1987). An increase in production causes an enhanced oxygen use, especially during the night. A higher decomposition rate can cause oxygen depletion as well, because organisms which breakdown the organic matter consume oxygen. Increase in the decomposition of organic matter may lead to hypoxia and even anoxia, although these effects are strongly dependent on the turbulence of the system (de Jonge et al., 2002).

A combined effect of both increased production and decomposition rates results in extremely low oxygen contents, because during the night time no oxygen is produced and both groups, autotrophic and heterotrophic organisms will grow and consume oxygen (Nijboer and Verdonschot, 2004).

Oxygen decline can be a result of oxygen-consuming processes, bacterial carbon oxidation and nitrification but also a result of a decrease in algal biomass (Nijboer and Verdonschot, 2004).

2.2 Concepts of Surface Water Quality Modeling

Surface water quality models can be categorized in different ways, out of which one is regarding their formulation. The models may be classified as follows on that basis:

- *Physical versus mathematical/numerical*: Physical models are difficult and expensive to construct and the repetition of the results are not so satisfactory, whereas they provide good solutions for the simulation of cases where systems cannot be constructed with the virtual media. In some cases, they do not require field measurements. It is hard to consider living components in a physical model. Physical models occupy space when they are constructed, therefore, the model must be destroyed after a while. Besides, mathematical models are cheaper in terms of model construction; but they require field measurements to provide some external conditions for running the model. These field measurements sometimes need high budgets. If the user is familiar with the mathematical model, it is much easier to run the model and to make a change. For most of the cases, the results are repeatable and it is possible to use a model with a different scenario after a long time.

- *Mechanistic versus empirical*: Empirically – based models are capable of analyzing data rather than depending on theoretical principles, whereas mechanistic models are based more on theoretical principles than on fitting data sets. A mechanistic model will employ equations developed from theories such as the laws of thermodynamics to predict a certain parameter (Reckhow and Chapra, 1983). Empirical models are sometimes referred as black – box models because output from these models only reflect the effect of changes in input data, but the model does not represent the causes of these effects (Beck, 1983; Jørgensen, 1988).

- *Deterministic versus stochastic models*: Stochastic models use probability density functions for certain parameters and variables, and the model predictions are therefore also act as probability density functions (Reckhow and Chapra, 1983). If it is assumed that the variability and random error of the input data and parameters are zero, then the model is considered as deterministic, and its predicted values do not allow quantification of variability or random error (Beck, 1983; Jørgensen, 1988).

- *Steady versus unsteady*: Unsteady models describe systems that vary with time, while steady state models describe behavior that is assumed constant over time (Beck, 1983; Jørgensen, 1988; Reckhow and Chapra, 1983).

2.3 Historical Development of Surface Water Quality Models

This section is compiled from the book "Surface Water Quality Modeling" written by Chapra (1997).

Surface water quality modeling has developed significantly since the early years of the twentieth century. Four main stages can be included in this development. Public concerns and the computational capabilities that were available during each of the periods determined these stages.

The early modeling work mostly focused on the urban waste load allocation problem. The model developed by Streeter and Phelps (1925) on the Ohio River was the determining work in the field. The following studies provided the evaluation of dissolved oxygen levels in streams and estuaries (Velz, 1938; Velz, 1947; O'Connor, 1960; O'Connor, 1967). Bacteria models were also developed (O'Connor, 1962).

Since the computers were not available, model solutions were realized in closed form, which meant that applications were usually limited to linear kinetics, simple geometries, and steady-state receiving waters. Thus, the availability of computational tools limited the scope of the problems that could be addressed.

In the 1960s, digital computers became widely available, which led to major advances in both the models and the ways they could be applied. Numerical expressions of the analytical frameworks were the subject of the first modeling studies. The computer allowed analysts to address more complicated system geometries, kinetics, and time variable simulations; however, oxygen was still the main focus. In particular, the models were extended to two-dimensional systems such as wide estuaries and bays.

The ways in which the models were applied also changed in 1960s. The computer allowed a more comprehensive approach to water quality problems. The drainage basin could be analyzed as an entire system, rather than focusing on local effects of single point sources. As tools developed originally in the field of operations, research were coupled with the models to generate cost effective treatment alternatives (Thomann and Sobel, 1964; Deininger, 1965; Ravelle et al., 1967). Although point

sources were still the focus, the computer allowed a more holistic perspective to be adopted.

In the 1970s public awareness moved beyond dissolved oxygen and urban point sources to a more general concern for the environment. An ecological movement was born and, in some quarters, environmental remediation became an end in itself.

Eutrophication was the principal water quality problem addressed during this period. Consequently, more mechanistic representations of biological processes were included by the modelers. As more oceanographic researches were conducted, detailed nutrient/food-chain models were developed (Chen, 1970; Chen and Orlob, 1975; Di Toro et al., 1971; Canale et al., 1974; Canale et al., 1976). Because of the existing computational capabilities, feedback and nonlinear kinetics could be employed in these frameworks.

During this period, major work proceeded in taking the urban point-source problem under control. In fact, most municipalities in the United States installed secondary treatment of their effluents. Besides improving the dissolved oxygen problem in many local areas, for areas where point-source control was insufficient, this had the additional effect of diverting attention towards diffuse sources of especially oxygen-demanding wastes. The emphasis on eutrophication dominated over diffuse inputs; as such sources are also prime contributors of nutrients.

The environmental awareness in the early 1970s should have led to an increased dependence on the systems approach to water quality management, which was not the case for three reasons. Firstly, eutrophication is a more dynamic problem than urban point-source control, since it deals with seasonal growth. Although systems analysis methods could be developed to optimize such dynamic problems, they are much more complicated and computationally intensive than for the linear, steady-state, point-source problem. Secondly, the environmental movement encouraged an atmosphere of urgency regarding cleanup. A mentality of remediation “at any cost” led to concepts such as “zero discharge” being expressed as a national goal. Finally, the economy was successful during this period. Therefore, the economic feasibility of such a strategy was not seriously questioned. Although progress was made during this period, the unrealistic goals have never been achieved.

The most recent stage of model development evolved during the energy crisis of the mid-seventies. The pollution control effort was brought back to economic reality with the energy crisis. Attention turned to problems such as toxic substances (and to lesser extent acid rain) that, although they certainly represented a major threat to human and ecosystem health, could also be marketed effectively in the political arena.

The re-organization of the important role of solid matter in the transport and fate of toxicants was the major modeling advance in this period (Thomann and Di Toro; 1983; Chapra and Reckhow; 1983; O'Connor, 1988). In particular, the association of toxicants with settling and re-suspending particles represents a major mechanism controlling their transport and fate in natural waters. Further, small organic particles, such as phytoplankton and detritus, can be ingested and passed along to higher organisms (Thomann, 1981). Such food-chain interactions have led the modelers to view nature's organic carbon cycle as more than an end itself. Rather, the food chain is viewed as a conveyor and concentrator of contaminants.

Today, another stage is occurring in the development and application of surface water quality modeling. There is a strong recognition that environmental protection is so critical for the maintenance of a high quality of life, as was the case in the late 1960s and early 1970s. However, besides this awareness, the following four factors should make the coming decade different from the past.

1. Economic pressures are more severe than during the late 1970s. Thus, incentives for cost effective solutions are stronger than ever. Treatment currently deals with the steepest part of the cost curve for point sources. Further, reductions of diffuse sources are typically more expensive than point-source controls. Today, better models are needed to avoid the severe economic penalties associated with wrong decisions.

2. Developing countries around the world are beginning to recognize that environmental protection must be coupled with economic development. For these countries, cost-effective, model-based control strategies could provide a means to control pollution and sustain a high quality of life while maintaining economic growth.

3. Computer hardware and software have undergone a revolution over the past decade that rivals the initial advances made during the 1960s. In particular, graphical user interfaces and decision-support systems are being developed that facilitate the generation and visualization of model output. Further, hardware advances are removing computational constraints that limited the scope of earlier models. Today, two and three dimensional models with highly mechanistic kinetics can be simulated at a reasonable cost.

4. Finally, significant research advances have occurred in the recent past. In particular, mechanistic characterizations of sediment-water interactions and hydrodynamics have advanced to the point that they can effectively be integrated into surface water quality modeling frameworks. Apart from the scientific advances involved in developing these mechanisms, their subsequent integration into usable frameworks is being made possible by the advances in computer technology.

Although infrequently used, there are a number of systems analysis techniques that could be linked with the simulation models to provide cost-effective engineering solutions. Together with strong public concern for the environment, these factors have provided a trend for a new management-oriented, computer-aided phase in surface water quality modeling. There is a possible down side to this new phase of surface water quality modeling; that is, widespread and easy use of models could lead to their being applied without insight as “black boxes”. Models must be applied with insight and with regard to their underlying assumptions (Chapra, 1997).

2.4 Models Addressing Organic Wastes and Nutrients

Depletion of dissolved oxygen and stimulation of undesired aquatic growth due to organic waste and nutrients causes water quality problems. Also, high levels of nitrate and ammonia can be harmful to aquatic life. Nutrients, such as nitrogen and phosphorous applied to agricultural fields as fertilizer, can reach surface waters by runoff and leaching. Nitrogen is soluble and is easily mobilized by runoff or leaching. Phosphorous is strongly bound to soil, but may be carried by erosion. The organic matter and nutrients contained in agricultural runoff can play an important role in the trophic state and water quality of receiving waters. Dissolved oxygen

(DO) and biochemical oxygen demand (BOD) can be used as a general measure of the system for the models focusing on conventional pollutants, or when major concern is eutrophication, it can be primary productivity. Temperature, major nutrients, other chemical characteristics, detritus, bacteria, and primary producers are usually included in these models. Water quality models for surface waters may include higher trophic levels (i.e. zooplankton and fish) because of their effect on other more important variables, such as phytoplankton, BOD and DO. Zooplankton and fish also provide a means of controlling lower trophic levels, which can effect nutrients and DO (biomanipulation). Because the source of agricultural organic waste and nutrients is driven by the hydrologic cycle, the most appropriate modeling approaches are dynamic. However, for leaching or irrigation situations steady-state or quasi-dynamic models may be adequate (Stefan et al., 1990).

3. THE STUDY AREA

The studies conducted in Köyceğiz – Dalyan Lagoon were realized with couple of projects supported by various institutions and many master theses carried out at the Istanbul Technical University. The main projects which constitute the major part of these studies are as follows:

- Ecosystem Modeling of Coastal Lagoons for Sustainable Management supported by NATO – CCMS.
- Modeling and Land Use Planning of Köyceğiz – Dalyan Lagoon and its Watershed supported by the Istanbul Technical University Research Fund, Project No: 937
- Ecosystem Modeling for the Sustainable Management of the Lagoons supported by The Scientific and Technological Research Council of Turkey (TÜBİTAK), Project No: YDABCAG 100Y047.

The studies were initiated with the NATO – CCMS project in 1995. The main purpose of all these projects conducted since 1995 are gathering data and information to realize the modeling studies which are utilized as tools to provide necessary information to the decision makers for the sustainable management of the study area.

These studies require cooperation with experts from other disciplines and high budgets. Therefore, the water quality monitoring studies were carried out in parallel with the field surveys. The data gathered with these projects, which provides the required data for running the water quality modeling studies, have been completed a few years ago. The watershed loading modeling studies are still ongoing and this dissertation gives the results of water quality modeling studies.

3.1 Coastal Lagoons

Lagoons are the most valuable components of coastal areas in terms of both the ecosystem and natural capital (Gönenç and Wolflin, 2005). They are inland water bodies, usually oriented parallel to the coast, either separated from the sea by a barrier, or connected to the sea by one or more restricted inlets which remain open at least intermittently and have water depths rarely exceeding a few meters (Kjerfve, 1994).

Coastal lagoon ecosystems are dynamic and open systems, dominated and subsidized by physical energies, and characterized by particular features (such as shallowness, presence of physical and ecological boundaries, and isolation) that distinguish them from other marine ecosystems (UNESCO, 1981). Shallowness usually provides a lighted bottom, and the wind affects the entire water column, promoting re-suspension of materials, nutrients, and small organisms from the sediment to the surface layer. The various boundaries (between water and sediment, pelagic and benthic communities, and among lagoon, marine, freshwater, and terrestrial systems, and with the atmosphere) involve intense gradients and, consequently, a high potential to do work (UNESCO, 1981). Because of that, coastal lagoons are usually among the marine habitats with the highest biological productivity (Alongi, 1998). Nutrient input from various sources like surface runoff, irrigated land waters, and from the currents through tidal channels contribute to increasing the primary productivity affecting the structure of the communities (Gamito et al., 2005).

Although lagoons have complex connections to surrounding environments, they develop mechanisms for structural and functional regulation, which result in specific biological productivity and carrying capacities. As a consequence of high levels of biological productivity, lagoons play an important ecological role among the coastal ecosystems, providing a collection of habitat types for many species and maintaining high levels of biological diversity (Clark, 1998). Today, many lagoons are deteriorating because of over-use of their natural capital. Most lagoons are subjected to human activities like fishing, aquaculture, tourism, and urban, industrial and agricultural developments, inducing changes that affect their ecology. The environmental deterioration can be characterized by dissolved oxygen deficits, aquatic toxicity, variation in organism structure, disappearance of benthic animals,

turbidity and odors, fish mortality, sedimentation, and clogging of channels. These problems hinder the future use of lagoons and surrounding environments, and lead to loss of agriculture, fisheries, and aquatic production and also retard the tourism activities.

A high diversity of environments can be found in lagoons. Size can vary from a few hundred square meters to extensive areas of shallow coastal sea. The salinity range can vary from nearly fresh to hyperhaline waters, with concentrations of salt reaching three times the salinity of the adjacent sea (Sanders, 1968). Salt balance relies on several factors such as the exchange of water with the open sea, the inputs of continental waters from rivers, watercourses and groundwater, and on the precipitation-evaporation balance. The variability of salinity can also be observed inside the lagoon both spatially and temporally. From a hydrographical point of view, most of this variability between lagoons can be summarized by a set of quantitative parameters or indexes that describe the lagoon orientation and structure, as well as spatial variability and the potential sea influence.

In biological terms, heterogeneity can be applied to both the structure (species composition and abundance) and functioning (productivity, trophic webs, and fluxes) of the lagoon ecosystem at a wide range of spatial and temporal scales, from biogeographic (thousands of kilometers) to regional (hundred to thousands of kilometers, including distinct lagoons in the same area) and local (the inside of the lagoon).

Coastal lagoons experience river input, wind stress, tides, precipitation-evaporation balance, surface heat balance, and respond differently to these forcing functions. Water and salt balances, lagoon water quality and eutrophication depend critically on lagoon circulation, salt and material dispersion, water exchange through the canal(s), and turnover, residence or flushing times. The understanding of physical, chemical, geological and ecological dynamics of lagoons is important for planning and implementation of coastal management strategies in coastal lagoons (Kjerfve, 1994).

3.1.1 Köyceğiz – Dalyan Lagoon – The Pilot Area

Köyceğiz–Dalyan Lagoon is selected as the pilot area for the implementation of the water quality model. Köyceğiz – Dalyan Lagoon and its watershed is located at the southwest of Turkey within the boundaries of Muğla Province along the Mediterranean Sea Coast. Two drainage systems comprise the lagoon system. The first drainage system consists of the Köyceğiz Lake, whereas the second one consists of Dalyan Channel Network, Alagöl Lake, Sülüngür Lake and İztuzu Lake. The Köyceğiz Lake is connected to the Mediterranean Sea via the lagoon and its branches. The location of Köyceğiz – Dalyan Lagoon and its sub-watersheds are given in Figure 3.1. The boundary of the watershed is given in Figure 3.2. Part of the area is an officially declared Special Protection Area, as it is a unique and important ecosystem with high diversity of species. It hosts one of the rare breeding and nesting sites for endangered sea turtles, *Caretta Caretta*. The watershed is divided into 24 sub-watersheds covering a total area of approximately 1,200 km^2. When the Köyceğiz Lake Watershed is excluded, Lagoon drainage area equals to approximately 130 km^2.

3.2 Characteristics of Köyceğiz – Dalyan Lagoon

3.2.1 Meteorological Conditions

The area is under the influence of Mediterranean climate characteristics, with a hot, dry summer season and a warm, rainy winter season. Although the region is controlled by the terrestrial, marine or semi-marine, and semi-terrestrial low-and high-pressure systems, the high-pressure system is more effective. Precipitation usually occurs during the cold winter period and drought occurs during the hot summer period.

Five meteorology stations are located within and the vicinity of the watershed. The coordinates and the elevations of these meteorology stations are given in Table 3.1. Among these stations Köyceğiz Meteorology Station was found to be the representative station for modeling studies.

Table 3.1: Location and Elevation of Meteorology Stations

Meteorology Station	Latitude	Longitude	Elevation, m
Muğla	37°13′	28°22′	+646
Marmaris	36°51′	28°16′	+19
Fethiye	36°37′	29°07′	+3
Dalaman	36°45′	28°47′	+13
Köyceğiz	36°58′	28°41′	+24

3.2.1.1 Precipitation

Annual total precipitation data obtained from Köyceğiz Meteorology station and the resulting trend line of the precipitation analysis for the years 1985–2000 is given in Figure 3.3. According to Figure 3.3, the minimum annual precipitation occurred in 1990 with 685 mm and the maximum occurred in 1998 with 1535 mm. Although a decreasing trend is observed between years 1989 and 1993, the overall trend covering years between 1985 and 2000 is increasing.

3.2.1.2 Evaporation

Determining the losses through evaporation is as important as precipitation for calculating the water budget of a watershed. Evaporation is the major sink of the hydrological system in a watershed.

Annual total evaporation data obtained from Köyceğiz Meteorology Station and the resulting trend line of the evaporation analysis for the years 1983–2000 is given in Figure 3.4. The evaporation analysis was conducted for the months between April and October since this period has the most reliable data for evaporation. According to Figure 3.4 the minimum annual evaporation occurred in 2000 with 1042 mm and the maximum occurred in 1985 with 1459 mm. The peak values on the trend line are observed in 1985, 1990 and 1996. A decreasing trend for evaporation between 1983 and 2000 is also observed.

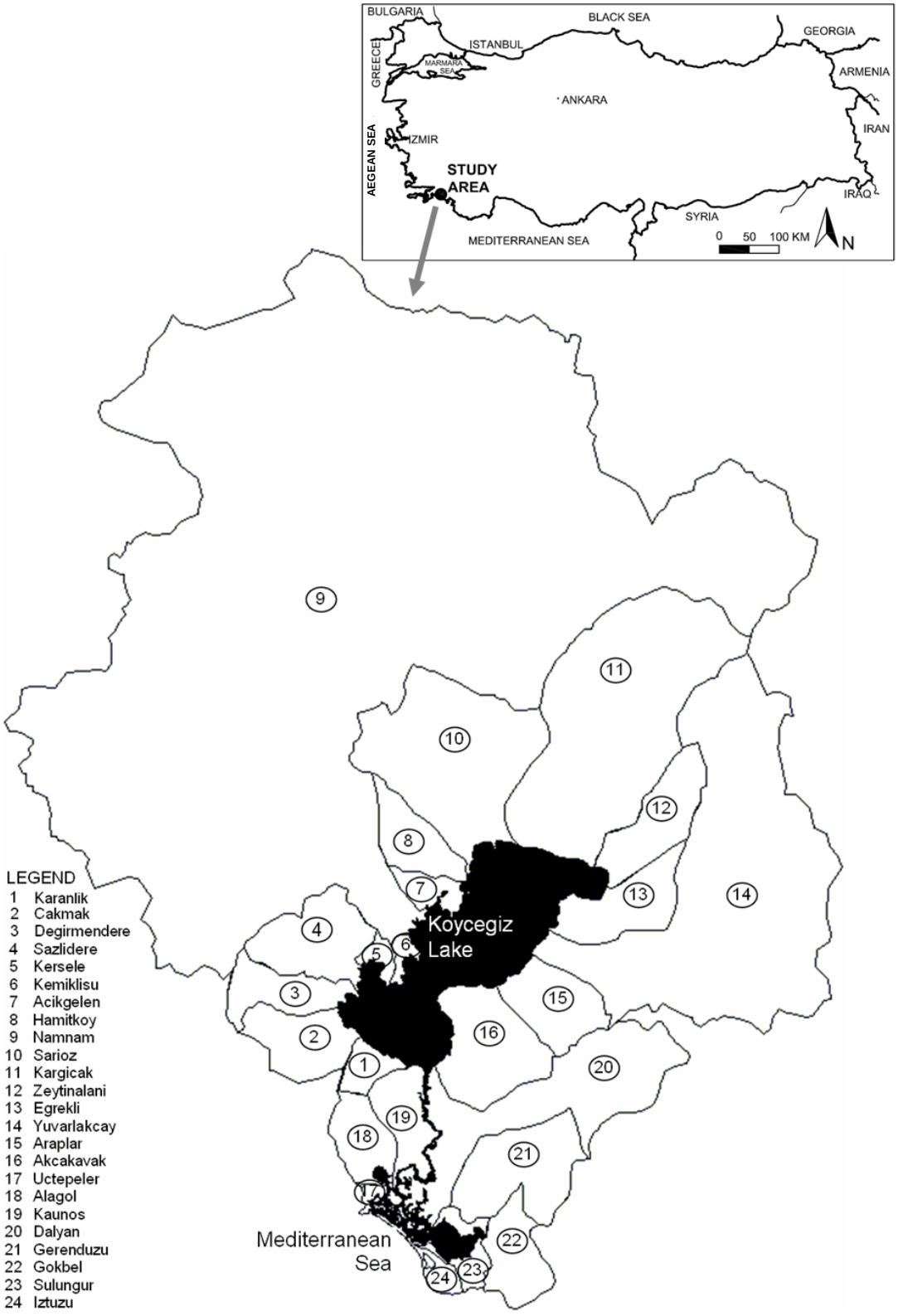

Figure 3.1: Location of Köycegiz - Dalyan Lagoon and its Sub-watersheds (Yuceil et al., 2007)

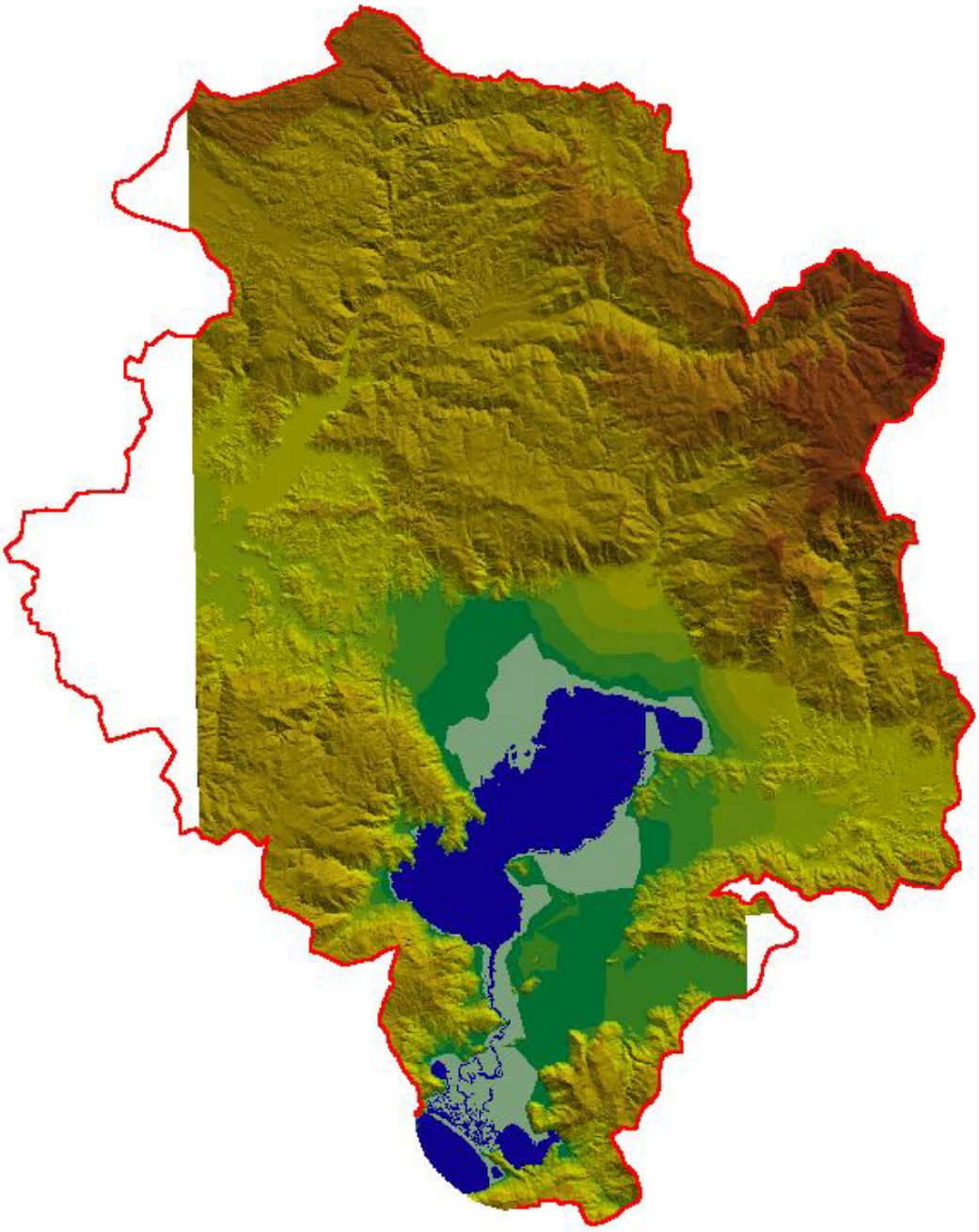

Figure 3.2: The Boundary of Köyceğiz – Dalyan Lagoon Watershed

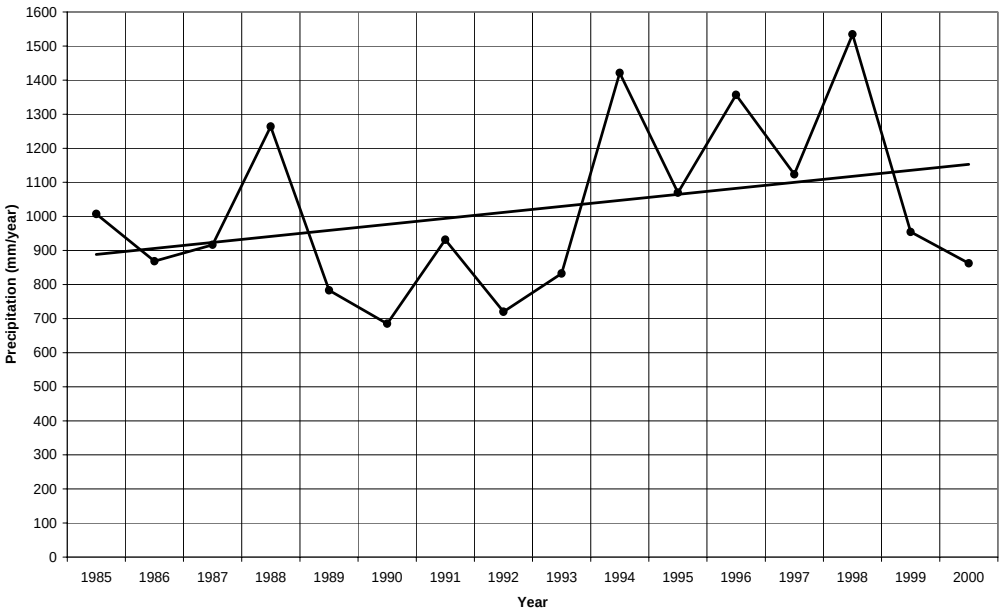

Figure 3.3: Annual Total Precipitation between 1985 and 2000 (Gönenç et al., 2004)

Figure 3.4: Annual Total Evaporation between 1983 and 2000 (Gönenç et al., 2004)

3.2.1.3 Temperature

Temperature is a major parameter which affects various reactions in terrestrial and aquatic ecosystems. On the other hand, it governs the movement of water with either precipitation or evaporation in the hydrological cycle.

Temperature is measured three times a day at 7:00, 14:00 and 21:00 hours by the General Directorate of State Meteorology Services. The temperature data obtained from the Köyceğiz Meteorology Station belongs to the years between 1976 and 2000. The monthly distribution of average temperature for 7:00, 14:00 and 21:00 hours between 1976 and 2000 is given in Figure 3.5. According to Figure 3.5 the maximum temperature values are measured in July and August at 14:00 with 35°C and the minimum values are measured in January and February at 7:00 with 6°C.

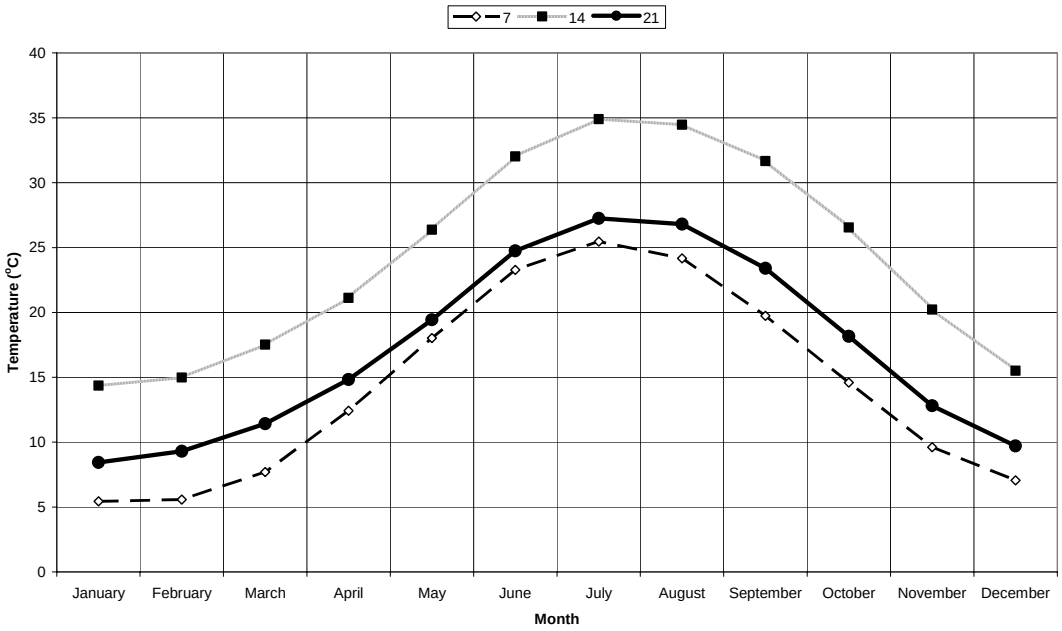

Figure 3.5: The Monthly Distribution of Average Temperature for 7:00, 14:00 and 21:00 Hours between 1976 and 2000 (Gönenç et al., 2004)

3.2.1.4 Wind

Wind velocity and direction cause mixing especially at the surface of shallow water bodies, which affects the formation of stratification due to temperature and/or salinity. Temperature and density changes affect the hydraulics of the system and water quality regarding the biochemical and physical conditions.

Wind data obtained from Köyceğiz Meteorology Station covers the period starting from 1969 to 1990. The average values illustrated in Figure 3.6 show that the prevailing wind directions are west northwest (WNW) and southeast (SE). The fastest wind speeds occur in north northwest (NNW) and north northeast (NNE)

directions with velocities of 2.2 m/s and 2.3 m/s, respectively. The fastest wind speed in the prevailing directions has an average value of 2 m/s.

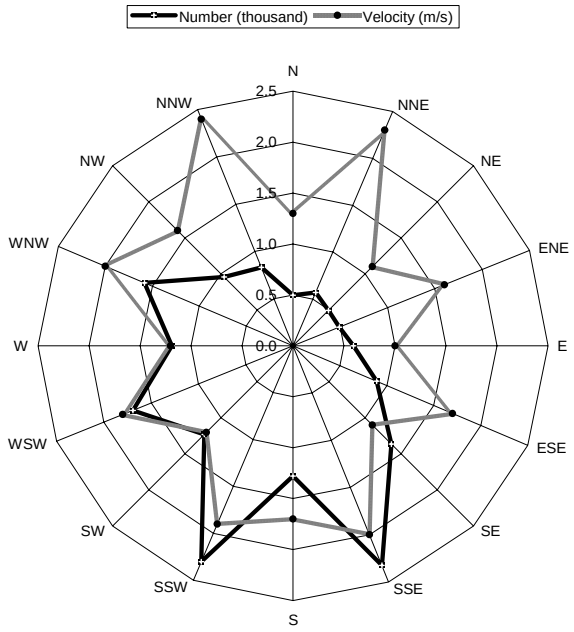

Figure 3.6: Wind Velocity and Frequency Distribution for the period 1969–1990 (Gönenç et al., 2004)

3.2.1.5 Solar Radiation

Solar radiation is measured in terms of dispersed heat energy. It defines the potential light energy which can be utilized by photosynthetic living organisms thus; it is particularly of great importance for water quality. Duration is as important as intensity, since it determines the total energy amount utilized.

The data obtained from Köyceğiz Meteorology Station covers the period 1985–1990 for duration and 1987–1990 for intensity. The relation between duration and intensity is given Figure 3.7.

Solar radiation parameter has the highest intensity value in June with 564 cal/cm^2/min, and the highest duration in July with 11:15 hours. The lowest values are measured in December with 175 cal/cm^2/min, and 4:25 hours for intensity and duration, respectively.

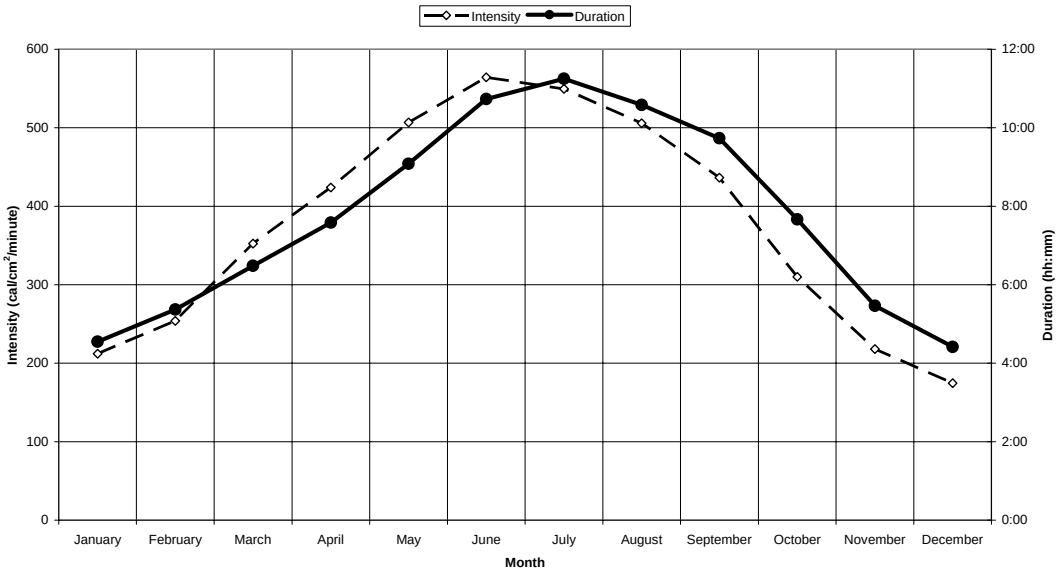

Figure 3.7: Average Monthly Distribution of Daily Average Solar Radiation Duration and Intensity for the Period 1985 – 1990 (Gönenç et al., 2004)

3.2.2 Hydrodynamic and Hydrogeological Conditions

The major streams flowing into Köyceğiz Lake and Dalyan Channel, which are the two most important main components of Köyceğiz–Dalyan Lagoon are; Yuvarlak Stream, Kargıcak and Yangı Creeks, Kocagöz Stream, Hamitköy Collection Channel, Namnam Stream, Çamlıdüzü Creek, Değirmendere Creek, and Çakmak Creek. Namnam and Yuvarlak are the biggest streams among them.

The conclusions of the hydrodynamic data evaluation derived, and the water movement analysis studied by Gönenç et al., (2004) in the system are summarized below.

Köyceğiz – Dalyan Lagoon system has a dynamic character and the processes that take place in the system indicate high uncertainty. When the overall system is considered, there exist two boundary conditions. The upper boundary condition is the Köyceğiz Lake watershed, which is highly affected by Namnam and Yuvarlakçay Streams. The lower boundary condition is the Mediterranean Sea, which has a high stability and low uncertainty compared to the upper boundary condition.

Namnam Stream has the highest effect on the system since it carries the highest amount of fresh water from its large watershed. The flow rate of Namnam fluctuates

significantly. The uncertainty of the flow rate affects the water level of Köyceğiz Lake and increases the uncertainty of this parameter.

During winter months, components of Dalyan Lagoon (Alagöl, Sülüngür Lake, Dalyan Channel, Dalyan Channel Network and İztuzu Region) are under the effect of Köyceğiz Lake. The effect decreases as it comes closer to the lower boundary condition, but it specifies the temperature and salinity of the system.

The salinity of Dalyan Channel varies spatially and temporally, with depth and distance from Köyceğiz Lake. It is concluded that there exist salinity stratification in the Lagoon. The upper layer flows from Köyceğiz Lake to Mediterranean Sea, and the bottom layer flows from the Mediterranean Sea to the Köyceğiz Lake.

The stratification of Alagöl and Sülüngür Lake is more stable than Dalyan Channel. As the stratification depth remains constant, the salinity of the upper layer vary seasonally and the salinity of bottom layer remains constant.

There are two major fault lines in the region. One lies to the south of Köyceğiz Lake in the S-SW direction. Sultaniye Hot Spring, with a high level of radioactivity, is located on it. Velibey, Rıza Çavuş, and Kokargirme Springs and hot springs are located on another fault line and are separated from the major line. A second major fault line penetrates through Köyceğiz Lake and lies in the NW–SE direction. At the north of the watershed, there is a fault line in the NW–SE direction (Gurel et al., 2005a).

The coastal geological structure of the system allows seawater flow into the Köyceğiz–Dalyan Lagoon. Seasonal groundwater level varies between 0.05 m and 6.55 m during May and November. Because of the carstic rock structure of the area, groundwater resources mainly feed this lake (Gurel et al., 2005a).

3.2.3 Socio-demographical Structure and Population

The total population of the Köyceğiz–Dalyan Lagoon watershed is 45890 according to the 2000 census. Köyceğiz is the largest residential area with 7523 inhabitants in the lake drainage area. Dalyan is the largest town in the Dalyan Channel Network

area with a population of 4848. There are also a number of small communities bounded to Ortaca and Ula (SIS, 2000).

As there are no significant industrial activities in this area the population increase in the lagoon area does not reflect a rapid increase. Agriculture, tourism, fishery, and forestry are the main sectors driving the economy in the watershed (Gurel et al., 2005a).

Agricultural activities are the major sources of income in the watershed. The area of land used for agriculture in Köyceğiz is 7111 ha. Cotton, citrus fruits, wheat, corn, peas, and horticulture are the main cultivated crops, and citrus fruits have the highest percentage among them. Potato, melon, onion, and garlic are the other crops grown in the area. About 3259 ha of land is used for agriculture in Dalyan, and product distribution is the same with Köyceğiz (Gurel et al., 2005a).

Tourism is a major industry in Köyceğiz and Dalyan. The ruins of the ancient city of Caunos are located in this area and the 4th century B.C. Lycian rock tombs are near the seaside. İztuzu Beach on the Mediterranean coast is one of the most beautiful beaches in Turkey and the nesting and breeding ground of *Caretta caretta* sea turtles, which have played a significant role in the increase of tourism. The other important tourist attractions are mud baths and hot springs.

Fishing activities in the region is conducted by Dalyan Fisheries Cooperative (DALKO) and are carried out in Köycegiz, Alagöl, Sülüklügöl, and Sülüngür Lakes, and along the İztuzu coast. Fishing in the Lagoon is made by printer and trammel nets in addition to weirs. Mullet species are of primary importance. Apart from the mullets, the other dominant species are sea bass, eel and crap (Bilecik et al., 1994).

Surrounding hills and mountains are covered with scrubs and pine forests. Sığla forests, which are peculiar to Southwest Anatolia, are present in the region. The oil extracted from these trees is used in pharmaceutical and cosmetic industries.

3.2.4 Land Use and Soil Characteristics

Since towns and small communities of the lagoon drainage area are scattered in agricultural lands, thus they cannot be shown separately. Forests and agricultural

land cover approximately 85% of the watershed. Figure 3.8 represents the land use of the study area, and Table 3.2 gives the related areal and percent distribution.

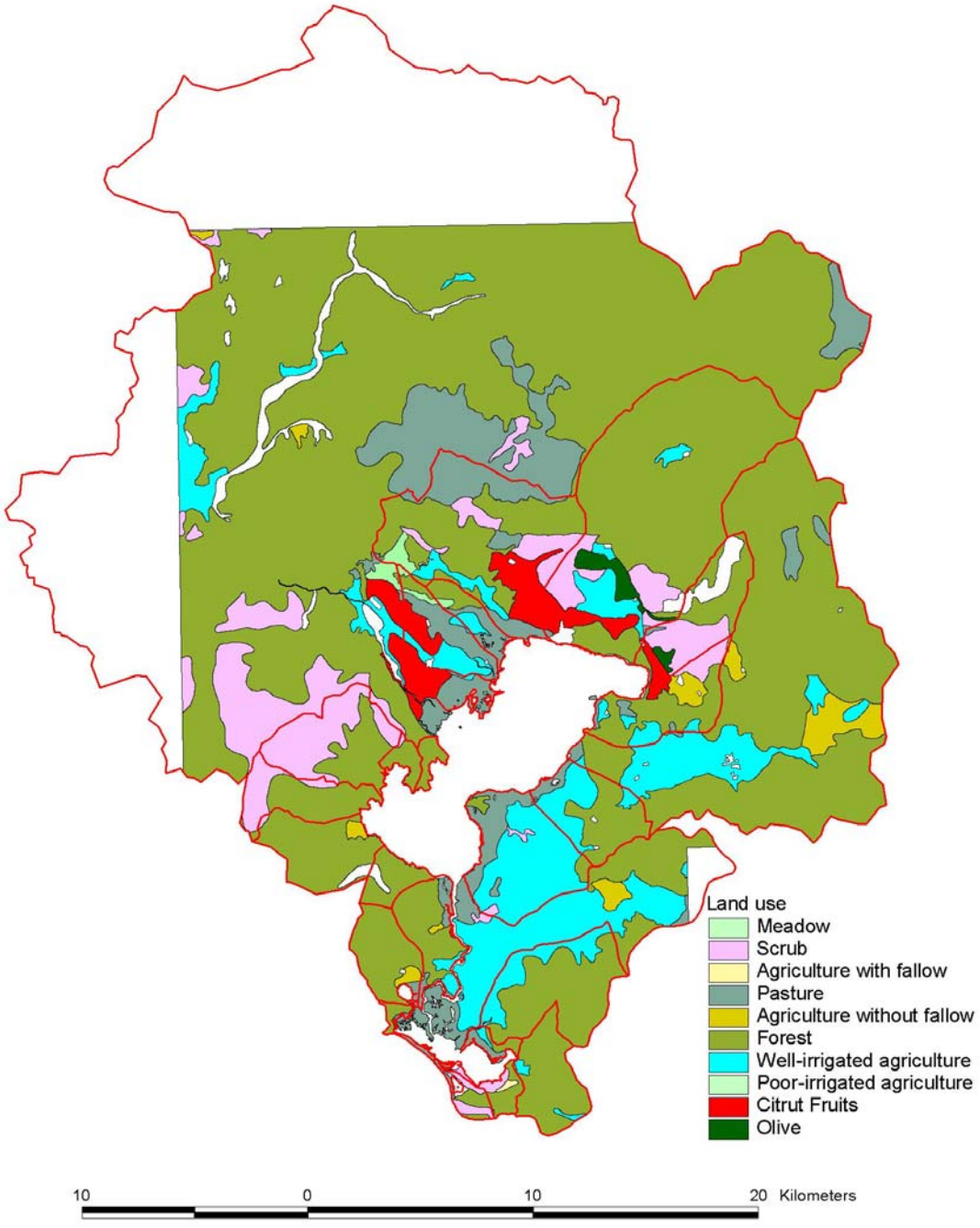

Figure 3.8: Land Use of the Study Area

Table 3.2: Current Land Use of the Köyceğiz – Dalyan Lagoon Watershed (Gurel et al., 2005a)

Land Use	Area (km^2)	% Distribution
Forests	80.93	62.55
Agriculture	29.70	22.95
Wetlands	6.56	5.07
Sülüngür Lake	3.01	2.33
Alagöl Lake	0.55	0.43
İztuzu Lake	0.19	0.15
Lagoon	2.50	1.93
Others (historical sites and springs)	5.94	4.59
Total	129.38	100

Land capability classification, soil types, soil subgroups, land use, and other soil characteristics of the area are studied and presented using different thematic maps obtained from the National Information Centre (NIC) of the General Directorate of Rural Affairs of Turkish Republic (TRGDRA). Concurrent with these studies, field soil surveys are carried out to investigate soil fertility, drainage and erosion conditions, and irrigation and fertilization requirements. The aim of such a comprehensive study was to investigate an alternative approach for sustainable land-use planning. The location of the soil sampling stations is plotted in Figure 3.9, which also summarizes the overlaid thematic maps. Detailed information on the soil characteristics derived from the soil analyses is given in Yuceil et al. (2007).

3.2.5 Pollutant Sources

Since there is no major industrial activity in the area, domestic wastewater is accepted as the only point source. The infrastructure of towns and small communities has been constructed and the centralized wastewater treatment plant for the area is under operation since mid 2002. The infrastructure and wastewater treatment project is designed in two stages. The first stage is planned until 2010 and the second stage is planned until 2020. According to this planning, some of the settlements will be connected to the treatment plant during the second stage. Sewer systems of both regions are realized within the development and construction area of the Köyceğiz and Dalyan Municipalities. First stage is planned for the centre of Köyceğiz, Dalyan and the foreseen areas where the population density would increase. The rest of non-dense settlements will continue to use their individual septic tanks. Toparlar, located in the northwest of Köyceğiz will connect to the wastewater treatment plant at the second stage.

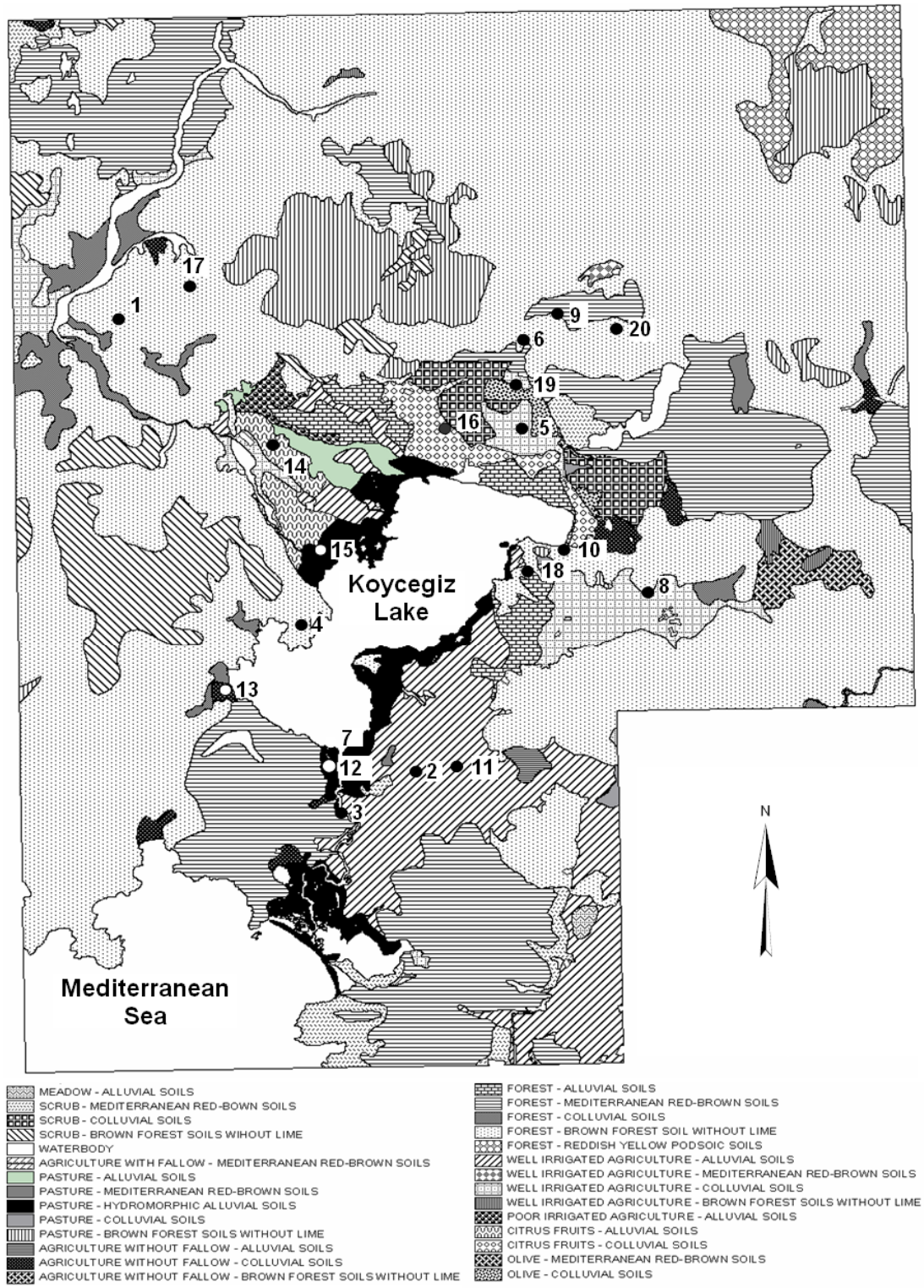

Figure 3.9: Overlaid Thematic Soil Maps (Yuceil et al., 2007)

However, the monitoring studies were conducted prior to the construction of the sewage system and the operation of the treatment plant. The wastewater from domestic uses was collected in septic tanks. Thus, domestic wastewater loads were

estimated by using unit load coefficients for nitrogen, phosphorus, biochemical oxygen demand and suspended solids. The unit loads were selected as 10 g N/capita.day, 3 g P/capita.day, 50 g BOD/capita.day and 60 g SS /capita.day. It is assumed that nitrogen and phosphorus are removed by 25%, BOD by 50%, and suspended solids by 70% in the septic tank. Nutrient, BOD and suspended solids load estimations originating from domestic wastewater in Dalyan Lagoon sub-watershed are given in Table 3.3 and Table 3.4.

Agricultural area and forest land are of great importance in terms of diffuse pollution generation since these areas are the major components of land-use. Nutrient loads (N and P) originating from forests are calculated by utilizing the unit load values from literature by taking into account the regional climatic characteristics and forest types. Fertilizer use is the major source of nutrient loads from agriculture. The type, amount and frequency of application of fertilizer in agriculture are investigated in detail according to the crop types for Dalyan Channel network sub-watershed (Karak, 2000). The surplus fertilizer remaining after crop uptake and the processes that take place in the soil, and its fate until it reaches the receiving water are listed by Karak (2000). The main nitrogen reactions were assumed to be denitrification, ammonia volatilization, surface run-off, and leaching, and were defined as certain percentages of the amounts remaining after crop uptake. The loads remaining after the reactions are calculated on monthly basis. Monthly load distributions are calculated for with irrigation and without irrigation applications separately, since there is intense irrigation requirement for some crop types during the summer months. The annual total load does not change in these calculations. The surplus nitrogen and phosphorus loads from fertilizer use in Dalyan and Köyceğiz Subwatersheds are given in Table 3.5 and Table 3.6, respectively (Tanik et al., 2002). Citrus fruit, cotton, corn and common vetch are the major crops. Citrus fruit and cotton require high irrigation during summer months. Olive groves are located at higher elevations. The number of greenhouses is increasing in the region. N and P loads originate from fertilizer use in Köyceğiz sub watershed is calculated by selecting unit loads. The cultivated area in this sub-watershed is devoted approximately 60% for field crops, 22% for citrus fruit and 13% for olive (Gönenç et al., 2004).

Table 3.3: Domestic Wastewater Nutrient Loads from Dalyan Lagoon Subwatersheds

Subwatershed	Village	Population	N- Influent Load (kg/year)	N-Removal Efficiency	N- Effluent Load (kg/year)	P- Influent Load (kg/year)	P-Removal Efficiency	P- Effluent Load (kg/year)
Alagöl Havzası	Çandır	437	1594	0.25	1195	478	0.25	359
Dalyan Riverbasin	Dalyan	6302	23004	0.25	17253	6901	0.25	5176
	Kemaliye	1071	3910	0.25	2933	1173	0.25	880
	Ekşiliyurt	2214	8083	0.25	6062	2425	0.25	1819
	Gölbaşı	610	2228	0.25	1671	668	0.25	501
	Karadonlar	261	952	0.25	714	286	0.25	214
	Tepearası	445	1625	0.25	1219	488	0.25	366
Gökbel Riverbasin	Gökbel	422	1542	0.25	1156	463	0.25	347
	Mergenli	626	2287	0.25	1715	686	0.25	514
	Eskiköy	1279	4668	0.25	3501	1400	0.25	1050
Permanent		13669	49892		37419	14968		11226
Temporary (Tourism)		18000	33120	0.25	24840	9936	0.25	7452
Total		31669	83012		62259	24904		18678

Table 3.4: Domestic Wastewater BOD and SS Loads from Dalyan Lagoon Subwatersheds

Subwatershed	Village	Population	BOD Influent Load (kg/year)	BOD-Removal Efficiency	BOD-Effluent Load (kg/year)	SS-Influent Load (kg/year)	SS-Removal Efficiency	SS- Effluent Load (kg/year)
Alagöl	Çandır	437	7968	0.50	3984	9561	0.70	2868
Dalyan	Dalyan	6302	115019	0.50	57509	138023	0.70	41407
	Kemaliye	1071	19550	0.50	9775	23460	0.70	7038
	Ekşiliyurt	2214	40414	0.50	20207	48496	0.70	14549
	Gölbaşı	610	11138	0.50	5569	13366	0.70	4010
	Karadonlar	261	4762	0.50	2381	5715	0.70	1714
	Tepearası	445	8125	0.50	4063	9751	0.70	2925
Gökbel	Gökbel	422	7710	0.50	3855	9252	0.70	2775
	Mergenli	626	11433	0.50	5716	13719	0.70	4116
	Eskiköy	1279	23340	0.50	11670	28008	0.70	8402
Permanent		13669	249459		124729	299350		89805
Temporary (Tourism)		18000	165600	0.50	82800	198720	0.70	59616
Total		31669	415059		207529	498070		149421

Table 3.5: Surplus Nitrogen and Phosphorus Loads from Fertilizer Use in Dalyan Channel Network Sub-watershed (with irrigation) (Tanik et al., 2002; Gönenç et al., 2004)

Month	N Load (kg/month)	P Load (kg/month)
January	2157	196
February	5825	505
March	2697	242
April	12081	1087
May	11326	1019
June	17151	1544
July	16396	1476
August	17043	1534
September	10894	981
October	-	-
November	4746	427
December	7766	699
Toplam (kg/year)	108082	9710

Table 3.6: Surplus Nitrogen and Phosphorus Loads from Fertilizer Use in Köyceğiz Sub-watershed (with irrigation) (Tanik et al., 2002; Gönenç et al., 2004)

Month	N Load (kg/month)	P Load (kg/month)
January	7128	648
February	19246	1669
March	8910	802
April	39918	3594
May	37423	3370
June	56669	5103
July	54174	4878
August	56312	5070
September	35997	3241
October	-	-
November	15682	1412
December	25661	2311
Total (kg/year)	357120	32098

Pesticide use for agriculture in Dalyan Channel Network Sub-watershed is investigated by Güvensoy (2000) through the same methodology used for fertilizers. The impact of 41 pesticides on the soil system based on the main mechanisms like persistence and mobility are investigated, and findings are then used to determine the changes in pesticide amount being lost via run-off or by leaching with the aim of detecting their probable existence in the lagoon environment. Pesticide use in the area is approximately 12 kg-L/ha, which is quite high compared to overall annual consumption value for all of Turkey (1.25 kg-L/ha).

Urban runoff originating from the residential areas in Köyceğiz Sub-watershed is calculated by utilizing values from the cited literature. However, urban runoff loads for residential areas of Dalyan Channel Network suwatershed cannot be calculated since the residential areas are scattered between the agricultural land, which does not allow the evaluation of this area for land use (Gönenç et al., 2004).

N and P loads originated from atmospheric deposition contribute especially to agricultural areas. Unit loads widely used in the literature for atmospheric deposition are selected for both sub watersheds (Gönenç et al., 2004).

A detailed forest survey has not yet been carried out. Because the mechanisms are too complex in these systems, unit polluting loads were selected from the literature, representing and reflecting similar climatic conditions and forestry, as 2 kg/ha/year for nitrogen and 0.2 kg/ha/year for phosphorus (Gurel et al., 2005a).

Total pollutant loads from point (domestic) and diffuse (agriculture and forestry) sources and their distribution are given in Table 3.7 for the entire watershed.

Table 3.7: Total Pollutant Loads and Their Distribution in the Watershed (Gönenç et al., 2004)

Source	TN (kg/year)	TP (kg/year)	TN Distribution (%)	TP Distribution (%)
Domestic	21629	3261	3	7
Agricultural	464107	41805	74	86
Forest	143326	3583	23	7

4. MODELING PROCESS APPLIED FOR KÖYCEĞİZ – DALYAN LAGOON

The water quality model, results from a multi-step model development and application process. This multi-step process is given in Figure 4.1. The modeling process applied for Köyceğiz – Dalyan Lagoon is given in this chapter by the following steps shown in Figure 4.1.

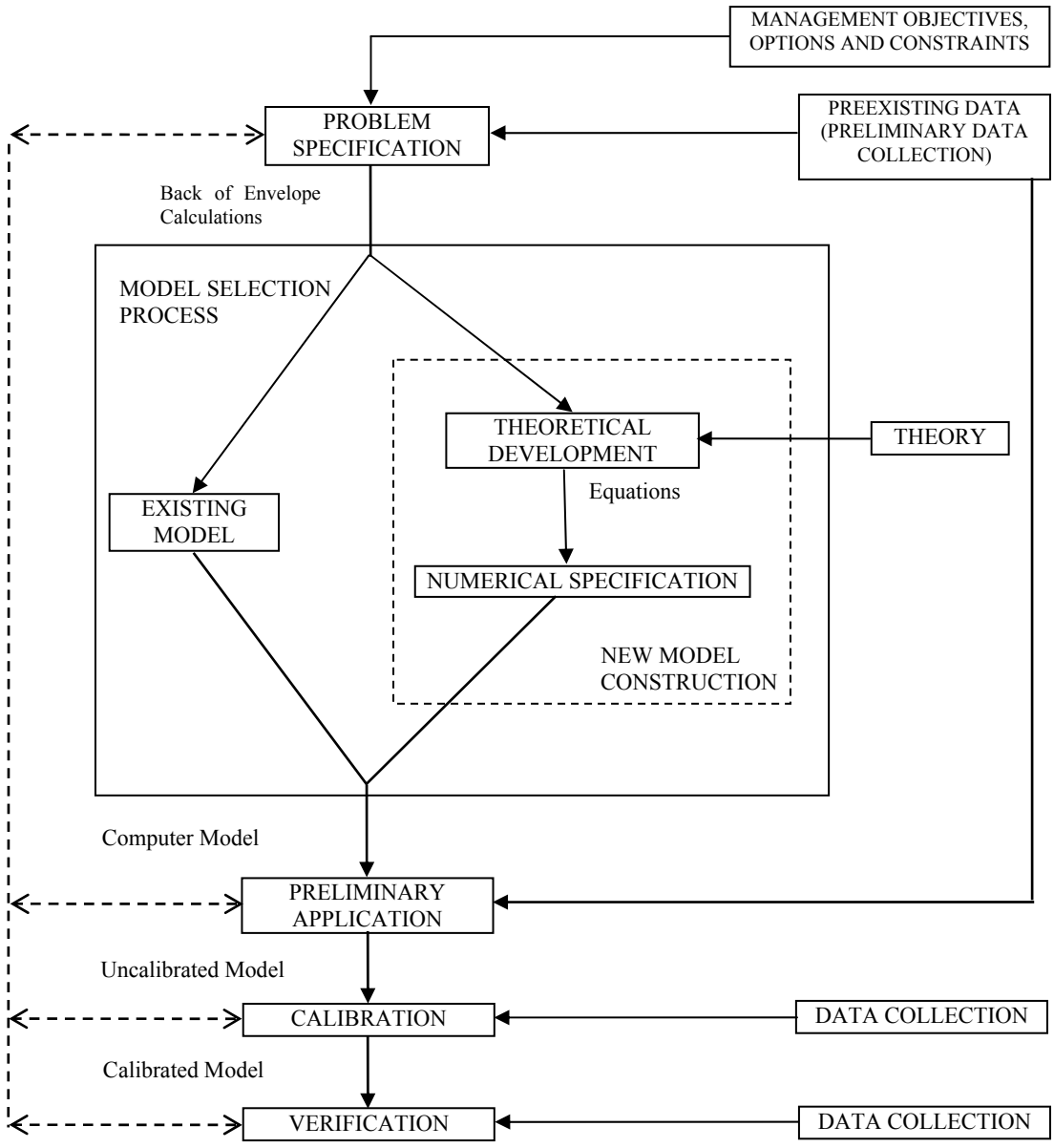

Figure 4.1: The Modeling Process (adapted from Chapra, 1997)

4.1 Problem Specification

The first step of a modeling process is the problem specification phase. The modeler must be provided with a clear definition of the objectives and the context of the study.

Two primary sources provide information for this step. Management objectives, options and constraints are the first one, which might include physical constraints, legal, regulatory and economic information.

Data related to the physics, chemistry and biology of the water body and its watershed is the second source, providing information for problem specification. Usually this kind of information is scarce or does not exist. Therefore, some preliminary premodeling data could be in order.

The objectives of this study, which is also given in Chapter 1.1, are the application and adaptation of a complex water quality model to a complex lagoon system, and to prepare a guideline for the future water quality modeling studies in such complex systems by emphasizing on the difficulties faced in developing countries such as Turkey. This study is a leading one, which applies a water quality model to a lagoon having a high level of ecosystem complexity. Köyceğiz – Dalyan Lagoon has a complex structure in terms of its geomorphology, hydraulics and hydrology.

4.2 Model Selection

The second step of modeling process is obtaining a model. Sometimes an existing software package can be selected to achieve this goal. The first advantage of using an existing model is, the work has already done. The second one is several models are widely used; therefore, they have a certain reputability in legal and regulatory contexts, which provides them credibility among judges and decision-makers.

However, many water quality problems can not be solved by existing software packages, since the models are not adequate or available. These reflect both kinetics and the time – space scale considerations. Therefore, a new model must be developed

to solve the problem. Model development comprised of two phases, theoretical development, and numerical specification and validation.

4.2.1 Implementation of Model Selection Process for Köyceğiz – Dalyan Lagoon

Water quality modeling studies conducted on coastal lagoons are much more complicated and challenging than the other water bodies. As mentioned in Chapter 3 Köyceğiz – Dalyan Lagoon, selected as the study area, is a complex and dynamic system. Hydrodynamic and ecological parameters vary spatially and temporally. When all these information are considered, an ideal ecosystem model for Köyceğiz – Dalyan Lagoon should be able to involve the following:

- Physical processes such as circulation, mixing and thermal stratification, and physical parameters such as solar radiation, water/air temperature, pressure and density.
- Chemical processes such as oxidation/reduction, gas solution and precipitation/dissolution, and water quality parameters such as dissolved oxygen, dissolved organic and inorganic substances.
- Nutrient dynamics.
- Biological processes such as primary production, photosynthesis, respiration, mortality, competition, grazing and predation, and biological parameters such as phytoplankton, zooplankton, benthic organisms, macrophytes and fish.

The model also should involve the interrelations between these processes and components.

Design and application of such a comprehensive model is challenging and complicated. Moreover, calibration and verification of this model does not seem possible with the available data. According to the literature survey conducted the possible models which might be applied to Köyceğiz – Dalyan Lagoon were determined and compared. After the model comparison, WASP/EUTRO was found to be the most appropriate model for the lagoon system (Gönenç et al., 2004). The details of the model selection step are given in the following sections.

4.2.2 Classification of Surface Water Quality Models

Various classifications are available for surface water quality models. The models applied to coastal areas are classified in 4 levels by EPA (2001). According to this classification, it is possible to calculate the seasonal and yearly variations of the parameters with Level – I models by taking into consideration the steady-state conditions. Level – II models are either steady-state or quasi-dynamic models averaged over tidal cycle. These models can be used for predictions with a time resolution of 2 weeks or a month, in cases where parameters change slower than seasonal variations. Level – III models are one dimensional (longitudinal) dynamic model. If the models boxes are located into a special geometry, two dimensional (longitudinal and lateral) model networks could be generated. These models are used for modeling shallow lagoons by assuming complete mixing in the vertical direction, with a time resolution considering the variations during each tidal event. Level – IV models are multidimensional dynamic models. These models simulate the processes in the mixing zones and sea boundaries, and are more realistic than Level – III models. Other classifications are also available for surface water quality models. For example, it is possible to make classification according to the grids used for model computational network discretization or the numerical solution method used (finite difference, finite elements, etc.) by the model.

4.2.3 Criteria Used for Surface Water Quality Model Selection

The criteria used for selecting the appropriate model for the study area are as follows:

- Model should involve the components to characterize the boundary conditions. 5 different boundary conditions can be defined for lagoons including atmosphere, benthos, and interaction with the sea, coastal line and stream. The effects from the system boundaries might have steady-state or dynamic characteristics. Internal dynamics of the system may be affected considerably with the energy or load flux originating from system boundaries.

- Model computational network should represent the lagoon geometry. Defining the model dimensions is of utmost importance and affects the model selection directly.

- Model should characterize the transport mechanism in the lagoon. Transport mechanisms (advection and dispersion) are affected directly by the lagoon geometry and boundary conditions. Some surface water quality models are able to read the hydrodynamic model outputs to get advection parameters such as flow rate and velocity, whereas some models involve the hydrodynamic codes in their own codes.

- Model should involve the reaction kinetics to simulate the chemical and biochemical processes in the lagoon and the related water quality/ecosystem components.

4.2.4 Selection of the Appropriate Surface Water Quality Model

A literature survey was conducted utilizing the data analysis carried out on Köyceğiz – Dalyan Lagoon together with considering the criteria given in Chapter 4.2.3. The following models were designated as candidates to be the appropriate model for the surface water quality modeling of Köyceğiz – Dalyan Lagoon:

- Water Quality for River and Reservoir Systems - WQRRS (HEC, 1978): The model was developed by the U.S. Army Corps of Engineers (USACE), Hydraulic Engineering Center (HEC). It is a one dimensional (vertical direction) dynamic water quality model. The model was developed to analyze the effects of dam operation conditions on the water quality of stream/reservoir systems. However, the process kinetics and the water quality variables included, select the model as a candidate for modeling the lagoon systems. The model simulates a number of water quality variables together with phytoplankton, zooplankton, fish and benthic organisms.

- EGÖLEM: The model is a recompiled version of the reservoir module of WQRRS model to make it compatible with IBM – PC by Gönenç et al., (1990). No changes were applied to the process kinetics and other model properties.

- CE-QUAL-R1 (Environmental Laboratory, 1995): The model was developed by the U.S. Army Corps of Engineers (USACE), Waterways Experiment Station (WES) instead of the reservoir module of WQRSS. It is a one dimensional (vertical direction) dynamic water quality model. Most of its properties are similar to WQRSS, whereas Fe and Mg are included to the parameters to be modeled. Model simulates the anaerobic processes as well.

- CE-QUAL-W2 (Cole and Wells, 2002): The model was developed by U.S. Army Corps of Engineers (USACE). It is a two dimensional model (x, z) and consists of directly coupled hydrodynamic and water quality transport models. The model simulates salinity, temperature, dissolved oxygen, carbonaceous biochemical oxygen demand, carbon, nitrogen and phosphorus containing organic matter (dissolved readily degradable, dissolved refractory degradable, particulate readily degradable, particulate refractory degradable), ammonium, nitrate, phosphate, dissolved and particulate silica and chlorophyll-a. Sediment processes are not widely considered.

- CE-QUAL-ICM (Cerco and Cole, 1994; Cerco and Cole, 1995): The model is also known as the Chesapeake Bay Model (USA – West Coast), however, it includes only the water quality code. It is developed by the US Army Corps of Engineers. The output files of CH3D hydrodynamic model, which is developed by the same institution, are required to run the model. It is possible to conduct three dimensional water quality simulations with CH3D/CE-QUAL-ICM. The model can be obtained from the developers. The model simulates the sediment comprehensively; however, it is not user friendly model since basic FORTRAN knowledge is required to run the model.

- Hydrological Simulation Program-FORTRAN (HSPF) (Johanson et al., 1984; Donigian et al., 1984): HSPF is a comprehensive package for simulation of watershed hydrology and water quality for both conventional and toxic organic pollutants. HSPF incorporates the watershed scale ARM (Agricultural Runoff Model) and NPS (Non-Point Source) models into a basin-scale analysis framework that includes pollutant transport and transformation in stream channels. The model uses information such as the time history of rainfall, temperature, and solar radiation; land surface

characteristics such as land-use patterns and soil properties; and land management practices to simulate the processes that occur in a watershed. The result of this simulation is a time history of the quantity and quality of runoff from an urban or agricultural watershed. Flow rate, sediment load, and nutrient and pesticide concentrations are predicted. The program takes these results along with the information about the stream network and point-source discharges, and simulates in-stream processes to produce a time history of water quantity and quality at any point in a watershed. HSPF includes an internal data base management system to process the large amounts of simulation input and output.

- WASP (Ambrose et al., 1993a; Wool et al., 2001): The transport structure of Water Quality Analysis Simulation Program (WASP) includes advection – dispersion and sediment movements. The model provides the user a couple of sub-models to be used for various water quality simulations. EUTRO module is used for the simulation of eutrophication and includes principal water quality state variables and nutrient cycles. TOXI module is used for simulating the fate of toxic organic matter. Mercury module is a special version of TOXI module which is developed for this element. Six transport fields are defined in the model including water column, pore water, 3 different settling/re-suspension sediment group and transport with precipitation/evaporation. Three options are available for the calculation of transport with advection in the water column. These options are net flows, gross flows and linkage to a hydrodynamic model to get depth, velocity and flow rate data. Couple of hydrodynamic models generate output files which can be linked to WASP, such as DYNHYD5 (Ambrose et al., 1993b), RIVMOD (Hosseinipour and Martin 1990), SED3D (Sheng et al., 1991) and EFDC (Hamrick, 1992; Hamrick, 1996; Tetratech, 2002). Since WASP is a box model, it allows generating 0, 1, 2 and 3 dimensional model networks with the number of segments and their locations. A three dimensional water quality model could be developed by using EFDC – WASP models.

- COHERENS (Luyten et al., 1999): It is a three dimensional hydrodynamic – ecological model developed for the North Sea by the Management Unit of the

Mathematical Models of the North Sea (MUMM). The model is provided with its source code for scientific purposes. The model simulates only the nitrogen cycle as the nutrient.

- ERSEM (Pätsch, 2001): European Regional Seas Ecosystem Model (ERSEM) is developed for the North Sea by the European Union. The model can be downloaded from the internet free of charge with its source code. Phytoplankton is considered by the model.

- MIKE3: The model is developed by the Danish Hydraulic Institute (DHI). It is a robust three dimensional model with a modular structure. The model includes hydrodynamic, advection, dispersion, water quality, eutrophication, and toxic organic and heavy metal modules. ECOLAB is a component of the model which allows conducting ecosystem simulations with the specific parameters defined by the user. Since the price of the model is very high and the comprehensive and expensive education required for the user makes this model to be used widely, especially for the projects with a high budget.

4.2.5 Selection of the Appropriate Surface Water Quality Model for the Köyceğiz – Dalyan Lagoon

Köyceğiz – Dalyan Lagoon consists of many channels and most of them have stratification due to density gradient. Sülüngür Lake and Alagöl, which are designated as separate zones in the lagoon, are relatively small lakes and they are not considerably affected by the Coriolis forces. The widths of the other channels are very narrow. Therefore, variations in lateral (y) direction are not of great importance in the lagoon. A two dimensional model network, which makes calculations in longitudinal (x) and vertical (z) directions, is adequate for most of the modeling purposes.

COHERENS and ERSEM are not appropriate for Köyceğiz – Dalyan Lagoon because of their water quality sub-models. In the COHERENS model, nitrogen is the limiting parameter for primary production and phosphorus cycle is not included. ERSEM model is used just for the North Sea. According to the literature survey no information exists regarding the application of the model to the temperate lagoons.

WQRRS/EGÖLEM and CE–QUAL–R1 are not appropriate for the lagoon since they are capable of making simulations only in vertical direction. These models can be applied to Sülüngür Lake instead of the whole system.

MIKE3 is not appropriate because of its high cost.

CE–QUAL–W2 is appropriate for most of the system; however, the model seems to be inadequate for modeling the sediment processes in the lagoon. On the other hand, hydrodynamic modules of the model are capable of characterizing adequately most of the lagoon.

CE–QUAL–ICM is not a user-friendly model and requires programming knowledge. It is not considered as appropriate due to the difficulties in applying the model.

HSPF has a water quality module (RCHRES) which has the capability of modeling the streams longitudinally (x direction) and the lakes and reservoirs vertically in one dimension. However, due to the complex structure of transport mechanisms in Köyceğiz – Dalyan Lagoon RCHRES cannot represent the system good enough for modeling. Therefore, HSPF was not found to be appropriate for the water quality modeling study.

WASP does not have any of the disadvantages, which the above mentioned models have. It is possible to define two types of sediment segment and the model allows generating an appropriate model network for Köyceğiz – Dalyan Lagoon. The model is developed to be run under Windows operating system and includes a graphical user interface for generating input files and visualizing the output files for the evaluation of simulation results easily. The outputs of WASP can be transferred to programs used for Geographical Information System (GIS) and water quality statistics. WASP has an interface to read the results generated by Hydrological Simulation Program – FORTRAN (HSPF). When all these capabilities are considered, WASP was found to be the most appropriate model for Köyceğiz – Dalyan Lagoon. It can also be downloaded from the internet free of charge.

More detailed information about WASP7, which is the most recent version of the WASP series, is given in Chapter 5.

4.3 Preliminary Application

Preliminary application is useful for identifying data deficiencies and theoretical gaps. Particularly it can provide an important context for designing the field and laboratory studies to fill the gaps.

This step is also useful in identifying the important model parameters. The other way to identify the important model parameters is conducting a model sensitivity analysis. Sensitivity analysis is conducted by varying each of the parameters by a set percent and observing how the predictions vary.

Salinity simulations, which were conducted for analyzing the flows and exchanges defined to the model, also provided information for preliminary application purposes of the modeling study. The simulation results were compared with the salinity data collected during the field studies. Figure 4.2 is given as an example to show the results of salinity simulations, and the salinity profile obtained along the main channel is for November 1999 cruise is provided in Figure 4.3. More results from salinity simulations are given and discussed in Chapter 7.2.

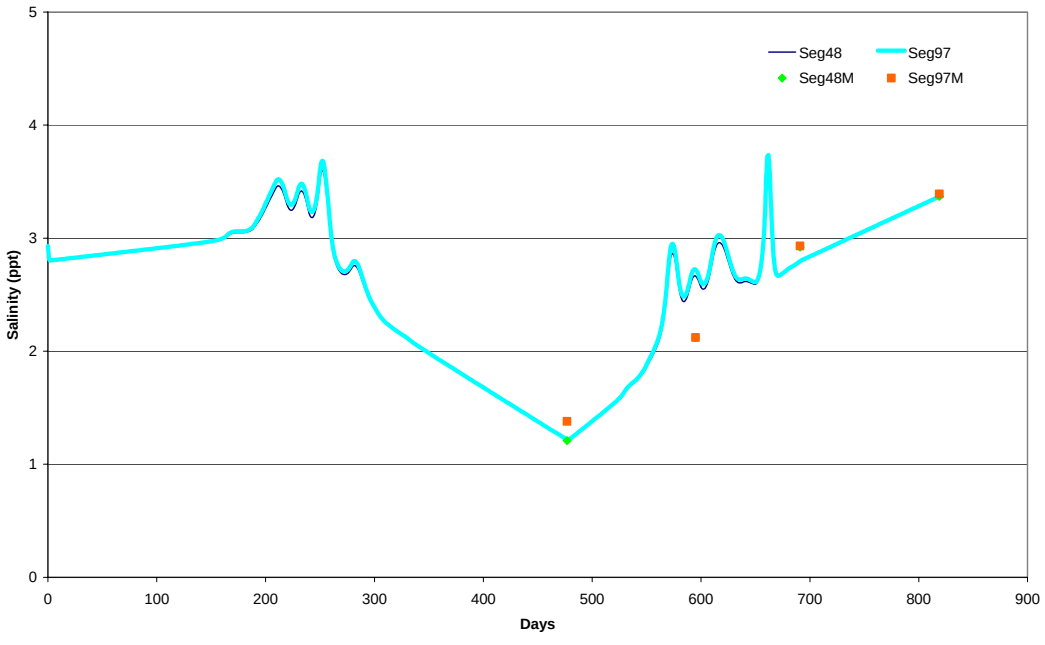

Figure 4.2: Salinity Simulation Result for the Köyceğiz Lake Boundary Condition

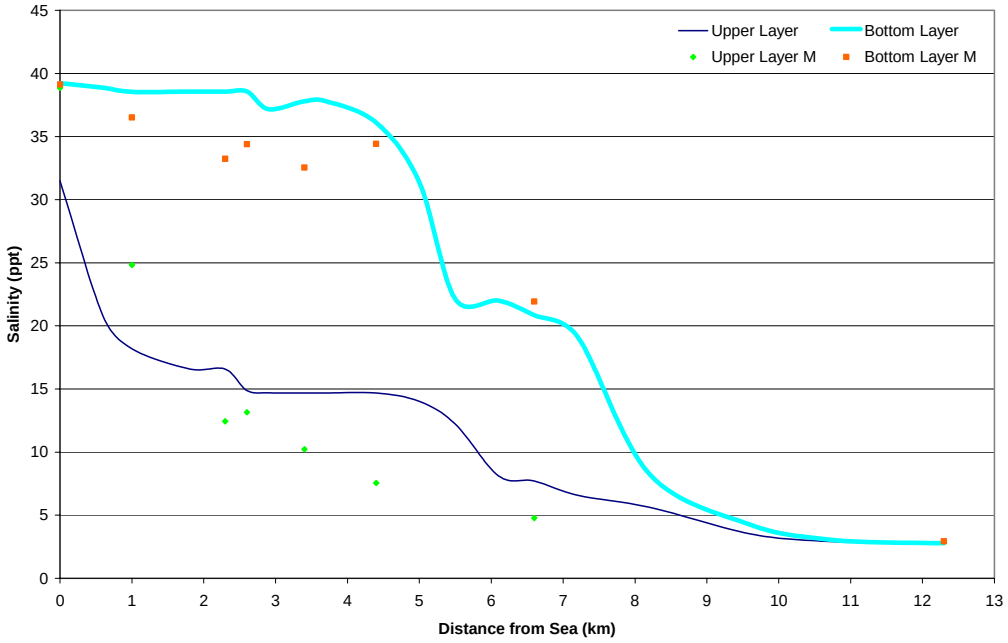

Figure 4.3: Salinity Simulation Results and the Measured Values along the Main Channel for November 1999 Cruise

4.4 Calibration

Model calibration involves a comparison between simulation results and field measurements. Model calibration consists of changing values of model input parameters in an attempt to match field conditions within some acceptable criteria. This requires that field conditions at a site be properly characterized.

Prior to the beginning of calibration process the system's loads, boundary conditions, and initial conditions must be measured with adequate precision that they are considered not as a significant source of uncertainty. The system's geometry and hydraulics characteristics must be developed accurately. As this is completed the physical parameters should not be varied.

After this, adjustment of the kinetic parameters is the focus of the calibration process. Adjustments are made until the simulation matches the data in some optimal sense.

The model was calibrated through changing the parameters and coefficients affecting the phytoplankton kinetics such as; maximum growth rate, death rate constant (non-

zooplankton), phytoplankton settling, detrital settling, endogenous respiration rate and phytoplankton half-saturation constant for nitrogen uptake and phosphorus uptake in the study. The other calibration components are related to nitrogen conversion reactions included in the nitrogen cycle, which are nitrification and detritus dissolution rate constants. Vertical eddy dispersion coefficients of some segments were also changed for calibration.

4.5 Verification

The model must be verified before it is used with confidence for making management predictions. The calibrated model should be run for a new data set, with the physical parameters and the forcing functions changed to reflect the new conditions. On the other hand the kinetic coefficients must be kept fixed at the values derived during calibration. It is subsequent testing of a calibrated model to additional field data preferably under different external conditions to further examine model validity.

In this study, model verification was conducted as a parallel process to model calibration. The data obtained Cruise 4 was selected as the verification set, since it is the only winter cruise conducted during the water quality modeling monitoring studies. After the model was calibrated, it was run again to check its compatibility with the verification data set. When the model results did not fit well enough with the verification data set, the model was recalibrated. A plot obtained during the verification step is given in Figure 4.4, which indicates high compatibility with the water quality monitoring studies.

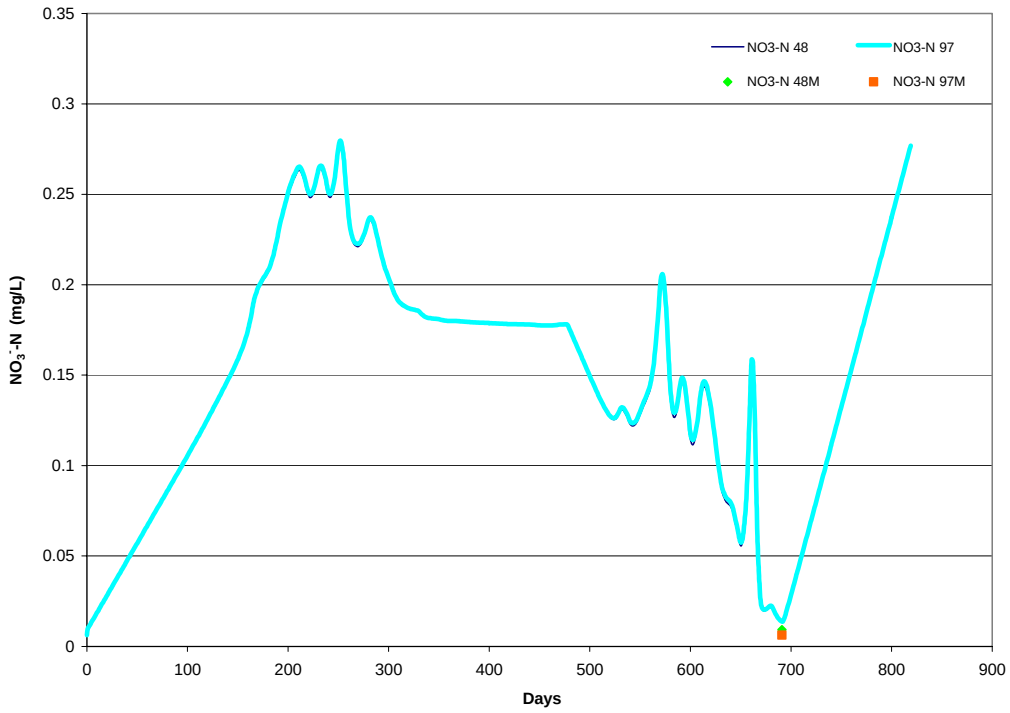

Figure 4.4: The Comparison of Simulation Results and Measured Concentrations of Nitrate Nitrogen at the Köyceğiz Lake Boundary Condition for the Verification Step

4.6 Sensitivity Analysis

Sensitivity analysis is the determination of the effect of a small change in model parameters on the results either by numerical simulation or mathematical techniques. Sensitivity analysis was conducted by numerical simulation in this study.

The parameters and their values used in the sensitivity analysis are given in Table 4.1. The ranges of the selected parameters vary according to the geomorphology, hydrologic and hydrodynamic characteristics of the water body; therefore, the values used in the modeling studies vary within a wide range. The literature values given in Table 4.1 are abstracted from different sources by Gurel et al. (2005).

Table 4.1: Parameters and the Values Used for the Sensitivity Analysis

Parameters	Literature Values (Gurel et al., 2005)	Values Used in This Study
Phytoplankton Max Growth Rate Constant at 20°C, day^{-1}	0.2 – 3.9	0.8, 1, 1.25, 1.5, 2
Phytoplankton Endogenous Respiration Rate Constant at 20°C, day^{-1}	0.004 – 0.2	0.03, 0.05, 0.07
Phytoplankton Half Saturation Constant for Nitrogen Uptake, mg N/L	0.001 – 0.4	0.005, 0.05, 0.2
Phytoplankton Half Saturation Constant for Phosphorus Uptake, mg P/L	0.0005 – 0.05	0.005, 0.03, 0.05

According to the sensitivity analysis total chlorophyll-a was found to be the most sensitive parameter. This parameter indicated response in each change applied to the parameters given in Table 4.1. However, dissolved oxygen and CBOD parameters did not response to any of the changes made during the sensitivity analysis.

5. WATER QUALITY ANALYSIS SIMULATION PROGRAM (WASP)

Water Quality Analysis Simulation Program (WASP) version 7, developed by the United States Environmental Protection Agency (USEPA) is described in this Chapter. This model will be applied to the pilot area within the framework of the study as mentioned in Chapter 2.

5.1 Overview of WASP

WASP7 is an enhancement of the original WASP (Di Toro et al., 1983; Connolly and Winfield, 1984; Ambrose et al., 1988). The model is used for interpreting and predicting water quality responses to natural events and anthropogenic pollution for different pollution management scenarios and decisions. WASP7 is a dynamic compartment – modeling program for aquatic systems, including the water column and the underlying benthos. Advection, dispersion, point and diffuse pollution loading processes, which vary with time and boundary exchange are represented in the basic program.

Water quality processes are represented in special kinetic subroutines that are either selected from the library existing in WASP or written by the user. WASP is structured to allow easy substitution of kinetic subroutines into the overall package to form problem-specific models. Technical assistance is provided by the developers to the users of the model in case of any problem regarding to the implementation and application of the model through EPA's Watershed and Water Quality Modeling Technical Support Center. However, the main mission of the Center is to provide assistance to EPA Regions, State and Local Governments, and their contractors in the implementation of the Clean Water Act. The Center which is part of EPA's Office of Research and Development (ORD) is committed to providing access to technically defensible tools and approaches that can be used in the development of Total Maximum Daily Loads (TMDL), waste load allocations, and watershed

protection plans. The Center will reach out to experts throughout EPA and States to bring technical expertise to the Center. The users can reach to the center via the web address **http://www.epa.gov/athens/wwqtsc/index.html**. Technical assistance is limited to supply of help any kind of change in the source code is under the responsibility of the user.

WASP7 consists of two models – TOXI for toxicants and EUTRO for conventional water quality. In addition to the general toxicant module, WASP7 offers a specific mercury module. Basic WASP7 structure and kinetics is provided in Figure 5.1. It has a unique flexibility. The model can be structured as one, two, and three dimensional. Time – variable exchange coefficients, advective flows, waste loads and water quality boundary conditions can be specified to the model.

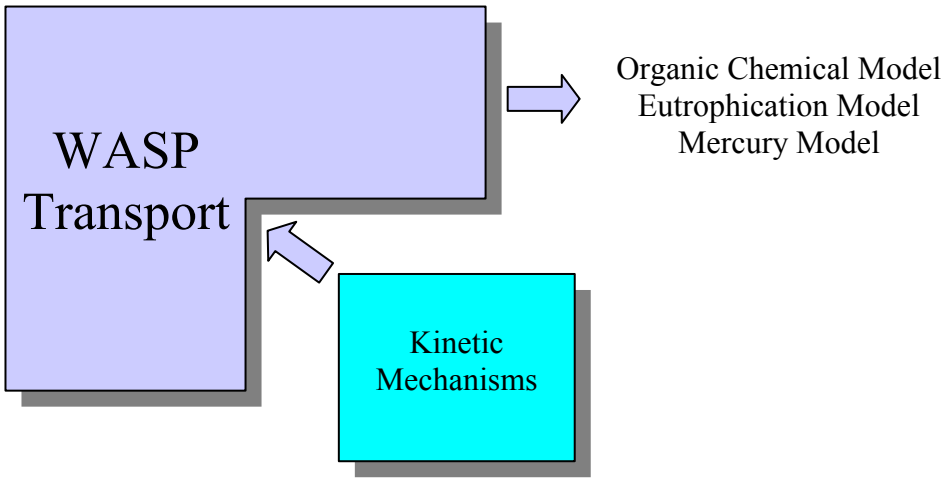

Figure 5.1: Basic WASP Structure and Kinetic Systems

5.2 Overview of the WASP Modeling System

The more detailed information on the kinetics, processes and equations included in WASP model and how the model is used, is available in the "WASP User's Manual" (Wool et al., 2001). The user's manual and other course material about WASP can be downloaded from http://www.epa.gov/athens/wwqtsc/html/wasp.html.

WASP7 simulates the movement and interaction of pollutants within the water. The key principle of '*the conservation of mass*' forms the basis of the equations solved by WASP7. The mass of each water quality constituent must be taken into consideration

in some way to fulfill this principle. WASP7 traces each water quality constituent from the point of spatial and temporal input to its final point, conserving mass in space and time. The input data, which defines the seven important categories, must be provided to WASP7 to compute the mass balance. These categories stated in the manual are as follows;

- Simulation and output control,
- Model segmentation,
- Advective and dispersive transport,
- Boundary concentrations,
- Point and diffuse pollutant loads,
- Kinetic parameters, constants, and time functions,
- Initial concentrations.

The general WASP7 mass balance equations, the specific chemical kinetics equations and the input data, uniquely define a special set of water quality equations. WASP7 integrates these numerically as the simulation proceeds in time. WASP7 saves the values of all display variables for subsequent retrieval by the post – processor program, at user – specified print intervals. These programs allow the user to interactively produce graphs and tables of all display variables.

5.2.1 General Mass Balance Equation

A mass balance equation for dissolved constituents in a water body must take into consideration all the materials entering and leaving through point and/or diffuse loading; advective and dispersive transport; and physical, chemical and biological transformation. If one considers the coordinate system shown in Figure 5.2, where the x- and y-coordinates are in the horizontal plane and the z-coordinate is in the vertical plane. The mass balance equation around an infinitesimally small fluid volume can be written accordingly as given in Equation (5.1).

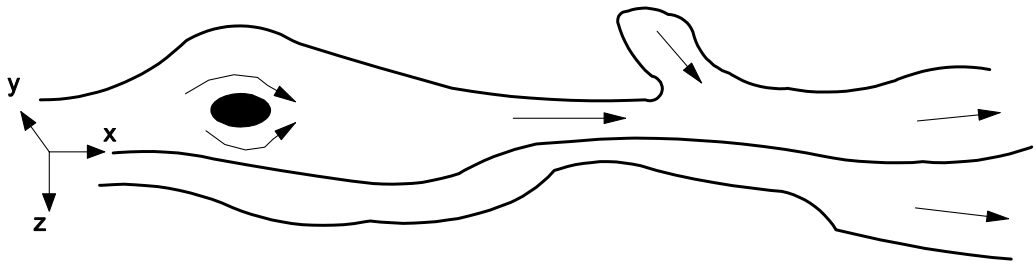

Figure 5.2: Coordinate System for Mass Balance Equation

$$\frac{\partial C}{\partial t} = -\frac{\partial}{\partial x}(U_x C) - \frac{\partial}{\partial y}(U_y C) - \frac{\partial}{\partial z}(U_z C) + \frac{\partial}{\partial x}(E_x \frac{\partial C}{\partial x}) + \frac{\partial}{\partial y}(E_y \frac{\partial C}{\partial y}) + \frac{\partial}{\partial z}(E_z \frac{\partial C}{\partial z}) + S_L + S_B + S_K \quad \textbf{(5.1)}$$

where,

C : concentration of the water quality constituent, mg/L or g/m^3

t : time, days

U_x, U_y, U_z : longitudinal, lateral, and vertical advective velocities, m/day

E_x, E_y, E_z : longitudinal, lateral, and vertical diffusion coefficients, m^2/day

S_L : point and diffuse loading rate, g/m^3-day

S_B : boundary loading rate (including upstream, downstream, benthic, and atmospheric), g/m^3-day

S_K : total kinetic transformation rate; (+) is source, (–) is sink, g/m^3-day

By expanding the infinitesimally small control volumes into larger adjoining "segments", and by specifying proper transport, loading, and transformation parameters, WASP implements a finite difference form of equation (5.1). For conciseness and simplicity, however, the derivation of the finite difference form of the mass balance equation will be for a one dimensional reach. Assuming vertical and lateral homogeneity, equation (5.1) can be integrated over y- and z- axis to obtain equation (5.2).

$$\frac{\partial}{\partial t}(AC) = \underbrace{\frac{\partial}{\partial x}\left(-U_x AC + E_x A\frac{\partial C}{\partial x}\right)}_{\text{Transport}} + \underbrace{A(S_L + S_B)}_{\text{Loading}} + \underbrace{A S_K}_{\text{Transformation}} \qquad \textbf{(5.2)}$$

where,

A: cross-sectional area, m^2

The three major classes of water quality processes transport, loading, and transformation are represented in this equation.

5.2.2 The Model Network

The physical configuration of the water body is represented by the model network, which is a group of expanded control volumes, or "segments". As illustrated in Figure 5.3, the network may subdivide the water body laterally, vertically and longitudinally. Benthic segments can be included along with water column segments. Water column segments must correspond to the hydrodynamic junctions if the water quality model is being linked to the hydrodynamic model. Concentrations of water quality constituents are calculated within each segment. The transport rates of water quality constituents are calculated across the interface of adjoining segments.

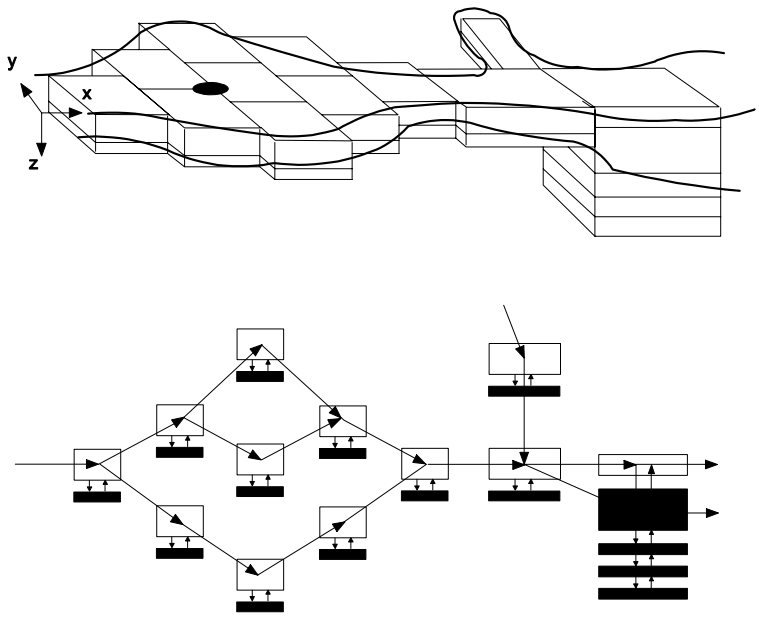

Figure 5.3: Model Segmentation

Segments in WASP may be one of the four types: epilimnion (surface water), hypolimnion layers (subsurface), upper sediment layer, and lower sediment layers. The segment type plays an important role in bed sedimentation and in certain transformation processes. Specifying vertical segment alignment is important when light has to pass from one segment to the next in the water column, or when material is buried or eroded in the bed.

Segment volumes and the simulation time step are directly related. As one increases or decreases, the other must do the same to ensure stability and accuracy. Segment size can vary significantly, governed by the spatial and temporal scale of the problem being analyzed rather than by the characteristics of the water body or the pollutant by itself.

As part of the problem definition, the user must determine how much of the water quality frequency distribution must be predicted. Predicting average values is easier than predicting extreme concentration values. Reducing the model time step (and consequently, the segment size) allows better simulation of the frequency distribution. However, this increase in predictive ability also entails an increase in the resolution of the input data.

The temporal variability of the water body and input loadings must be taken into consideration after the characteristics of the problem has been determined. Generally, the model time step must be slightly less than the period of variation of the important driving variables. In some cases, this restriction can be relaxed by averaging the input over its period of variation.

The spatial variability of the water body must be taken into consideration after the temporal variability has been determined. Generally, the important spatial characteristics must be homogeneous within a segment. In some cases, this restriction can be relaxed by well- judged averaging over width, depth, and/or length. Depending upon the problem being analyzed temperature, light penetration, velocity, pH, benthic characteristics or fluxes, and sediment concentrations are other important spatial characteristics to be considered.

The segment sizes are also affected by the expected spatial variability of the water quality concentrations. The user must determine how much averaging of the concentration gradients is acceptable.

Water column volumes should be roughly the same for obtaining accurate simulations. If flows vary significantly downstream, then segment volumes should increase proportionally. The user should first choose the proper segment volume and time step in the critical reaches of the water body (V_c, Δt_c), and then scale upstream and downstream segments accordingly;

$$V_i = V_c \, Q_i / Q_c \qquad \textbf{(5.3)}$$

Actual volumes specified must be adjusted to best represent the actual spatial variability. This guideline will allow larger time steps and result in greater numerical accuracy over the entire model network.

5.2.3 The Model Transport Scheme

Transport includes advection and dispersion of water quality constituents. Advection and dispersion in WASP are each divided into six distinct types, or “fields”. The first transport field involves advective flow and dispersive mixing in the water column. Advective flow carries water quality constituents "downstream" with the water and takes into consideration the instream dilution. Dispersion causes further mixing and dilution between regions of high concentrations and regions of low concentrations.

The movement of water in the sediment bed is specified in the second transport field. Dissolved water quality constituents are carried through the bed by water flow and are exchanged between the bed and the water column by diffusion.

The transport of particulate pollutants is specified in the third, fourth, and fifth transport fields by the settling, resuspension, and sedimentation of solids. Water quality constituents sorbed onto solid particles are transported between the water column and the sediment bed. The three solids fields are defined as size fractions, such as sand, silt, and clay, or as inorganic, phytoplankton, and organic solids.

Evaporation or precipitation from or to surface water segments are represented in the sixth transport field.

Most transport data, such as flows or settling velocities, must be specified by the user in a WASP input dataset. However, WASP may be "linked" with a hydrodynamic model for water column flow. If this option is specified, WASP will read the contents of a hydrodynamic file for unsteady flows, volumes, depths, and velocities during the simulation.

5.3 Application of the Model

Defining the problem to be solved is the first step of applying the model. A water quality model can do three basic tasks; to describe existing water quality conditions, and to provide generic, and site-specific predictions. The first is a descriptive task to extend in some way a limited site-specific database. As monitoring is expensive, data seldom give the spatial and temporal resolution needed to fully characterize a water body. A simulation model can be used to interpolate between observed data, such a model can be used to guide future monitoring efforts. The important processes that control existing water quality could be determined by using descriptive models. Second type of modeling task is providing generic predictions. Generic predictions may adequately deal with the management problem to be solved, or they may be a preliminary step in detailed site-specific analyses.

The most stringent modeling task is to provide site-specific predictions. Calibration to a good set of monitoring data is definitely required to provide reliable predictions. However, the model must also have sufficient process integrity, since predictions often try to extrapolate outside the existing database.

The spatial and temporal scales for the modeling analysis should be stated by the analysis of the problem. The network must be extended upstream and downstream beyond the influence of the waste loads being studied. If this is not possible, the user should extend the network far enough so that errors in specifying future boundary concentrations do not propagate into the studied reaches.

Aligning the network should be taken into account so that the sampling stations and significant points (such as water withdrawals) fall near the center of a segment. Point pollutant loads in streams and rivers with unidirectional flow should be located near the upper end of a segment. In estuaries and other water bodies with fluctuating flow, polluting loads are best centered within segments.

When the network set up is completed, the model study will go through hydrodynamics, mass transport, water quality transformations, and environmental toxicology steps. Hydrodynamics identifies where the water goes. This study can be done by a combination of gauging, special studies, and hydrodynamic modeling. Flow data can be interpolated or extrapolated using the principle of continuity. Very simple flow routing models can be used. Besides, very complicated multi-dimensional hydrodynamic models can also be used with proper averaging over time and space.

Mass transport identifies where the material in the water is transported. This study can be done by a combination of tracer studies and model calibration. Dye and salinity are often used as tracers.

Water quality transformations answer how the material in the water and sediment is transformed and what the fate of the material is, constitutes the main focus of many studies. Answers depend on a combination of laboratory studies, field monitoring, parameter estimation, calibration, and testing. The net result is called model validation and/or verification.

Environmental toxicology identifies how the material is likely to affect anything of interest, such as people, fish, or the ecological balance. Often, predicted concentrations are simply compared with water quality criteria adopted to protect the general aquatic environment. Care must be given to make sure that the temporal and spatial scales assumed in developing the criteria are compatible with those predicted by the model.

5.4 Various Application Examples of WASP

WASP has a long history of application to a variety of water bodies for a variety of water quality problems. Earlier versions of WASP were used to examine eutrophication and PCB pollution of the Great Lakes (Thomann, 1975; Thomann et al., 1976; Thomann et al., 1979; Di Toro and Connolly, 1980), eutrophication of the Potomac Estuary (Thomann and Fitzpatrick, 1982), kepone pollution of the James River Estuary (O'Connor et al., 1983), heavy metal pollution of the Deep River, North Carolina (JRB, 1984), and volatile organic pollution of the Delaware River Estuary (Ambrose, 1987). In addition to these, numerous applications are listed in Di Toro et al., (1983).

Published applications of more recent versions of WASP include eutrophication and mixing in Prince William Sound embayments (Lung et al., 1993), eutrophication in the inner shelf of the Gulf of Mexico (Bierman et al., 1994), eutrophication in the Mississippi River and Lake Pepin (Lung and Larson, 1995), water quality of the Speed River (Gualtieri and Rotono, 1996a, b), pollutant loading for the Black and Chehalis Rivers in Washington (Pickett, 1997), hydrodynamics and water quality in a large South Carolina reservoir (Tufford and McKellar, 1999; Tufford et al., 1999), and eutrophication in the Neuse River Estuary (Wool et al., 2003).

5.5 Applicability of the Model for Lagoons

The success of applying a model in a specific watershed area depends mainly on clearly defining the pilot watershed area and on supplying the required input data, as much as possible. The determination of the model area is of utmost importance as well as investigating the existing land-use distribution. Land-use distribution and detailed field surveys on land give the scientists a rough idea on the types and amount of land based sources of pollutants that might lead to the water body either through surface runoff or leaching depending on the geological structure of the soil media. Such transportation basically incorporates with the meteorological data and climatic conditions of the watershed. The model should reflect the yearly seasonal variations.

Although some estimates can be made from chemical properties and environmental characteristics, site-specific calibration is to be preferred. This is especially true in the case of coastal lagoons since the effect of intermittent salinity in the water body needs to be investigated. Such an impact may have both temporal and spatial dimensions.

5.6 Eutrophication

Nutrient enrichment and eutrophication are ongoing concerns in many water bodies. High concentrations of nitrogen and phosphorus can cause periodic phytoplankton blooms and change the natural trophic balance. Dissolved oxygen levels can fluctuate widely, and low DO concentrations can be measured in bottom waters.

Eutrophication has been modeled for approximately 30 years. The equations implemented in WASP were derived from the Potomac Eutrophication Model (PEM) developed by Thomann and Fitzpatrick (1982), and are fairly standard.

5.6.1 Overview of WASP7 Eutrophication

The EUTRO program simulates the nutrient enrichment, eutrophication, and dissolved oxygen depletion processes. Several physical-chemical processes can affect the transport and interaction among the nutrients, phytoplankton, carbonaceous material, and dissolved oxygen in the aquatic environment. The principal kinetic interactions for the nutrient cycles and dissolved oxygen are provided in Figure 5.4.

The transport and transformation reactions of up to sixteen state variables are simulated by EUTRO as illustrated in Figure 5.4 and given in Table 5.1. Phytoplankton kinetics, periphyton kinetics, phosphorus cycling, nitrogen cycling, dissolved oxygen balance and sediment diagenesis are the processes, which are considered to be the interacting systems. The general WASP7 mass balance equation is solved for each state variable. To this general equation, the EUTRO subroutines add specific transformation processes to modify the general mass balance for the sixteen state variables in the water column and benthos.

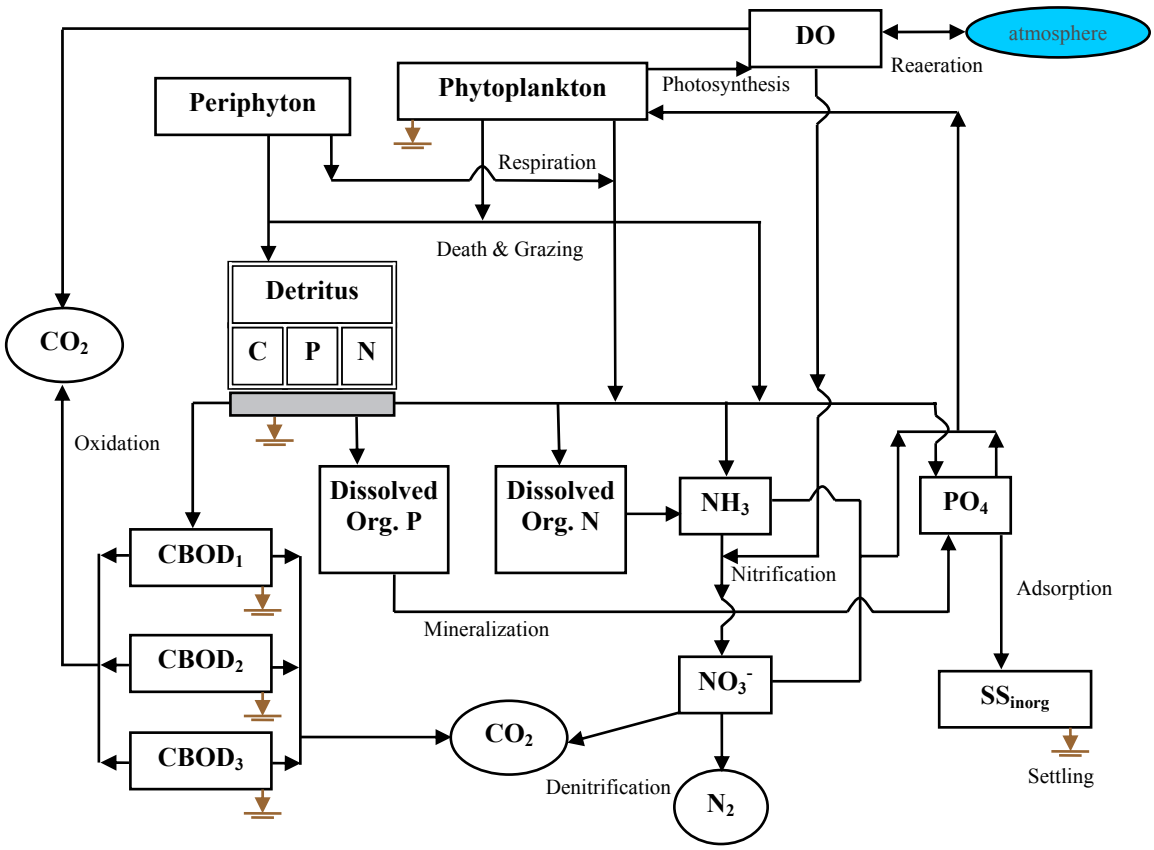

Figure 5.4: WASP 7 Eutrophication Kinetics Diagram

Table 5.1: WASP7 State Variables

Ammonia	Detrital Carbon (Particulate)
Nitrate	Detrital Nitrogen (Particulate)
Orthophosphate	Detrital Phosphorus (Particulate)
Dissolved Oxygen	CBOD (1) (Dissolved Organic Matter)
Salinity	CBOD (2) (Dissolved Organic Matter)
Phytoplankton	CBOD (3) (Dissolved Organic Matter)
Periphyton	DON (Dissolved Organic Nitrogen)
Solids	DOP (Dissolved Organic Phosphorus)

WASP7 eutrophication model can be implemented at different levels of complexity as given in Table 5.2. Some or all of these variables and interactions can be used according to the selected level of complexity.

Table 5.2: Levels of Complexity in Implementing WASP7 Eutrophication Model

Name	Level of Complexity					
	1	2	3	4	5	6
Ammonia		*	*	*	*	*
Nitrate			*	*	*	*
Inorganic Phosphorus				*	*	*
Phytoplankton Carbon				*	*	*
Periphyton Carbon						*
Carbonaceous BOD	*	*	*	*	*	*
Dissolved Oxygen	*	*	*	*	*	*
Organic Nitrogen			*	*	*	*
Organic Phosphorus				*	*	*
Sediment Diagenesis					*	*

The description of each complexity level is given in Table 5.3.

Table 5.3: Description of Complexity Levels

Level	Description
1	Streeter – Phelps DO / BOD and Descriptive Sediment Oxygen Demand
2	Modified Streeter – Phelps with Nitrogenous BOD
3	Linear DO Balance with Nitrification
4	Simple Eutrophication with Descriptive Sediment Oxygen Demand
5	Intermediate Eutrophication with Sediment Diagenesis
6	Advanced Eutrophication with Sediment Diagenesis and Periphyton

5.6.1.1 Phytoplankton Kinetics

Phytoplankton kinetics assumes a central role in eutrophication, affecting all other systems, as given in Figure 5.5.

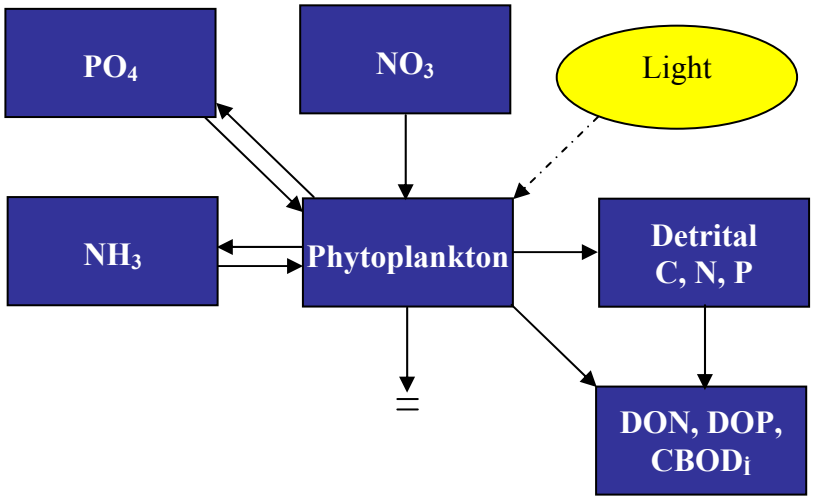

Figure 5.5: Phytoplankton Kinetics

The phytoplankton kinetics in WASP7 is represented by equation (5.4).

$$\frac{\partial C_p}{\partial t} = (R_G - R_D - R_S)C_P \qquad \textbf{(5.4)}$$

where,

C_p : phytoplankton carbon concentration, mg C/L

R_G : growth rate constant, day^{-1}

R_D : death rate constant, day^{-1}

R_S : settling rate constant, day^{-1}

Phytoplankton Growth

Phytoplankton growth kinetics is given in Figure 5.6 and in equation (5.5).

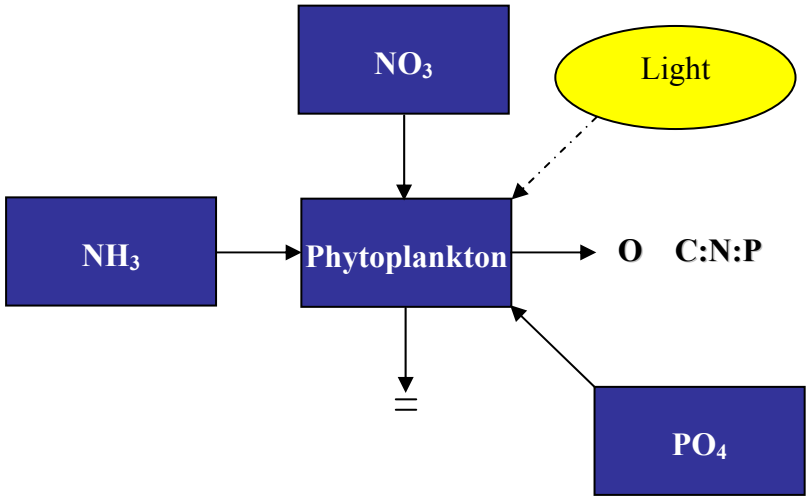

Figure 5.6: Phytoplankton Growth Kinetics

$$R_G = G_{max} X_T X_L X_N \qquad \textbf{(5.5)}$$

R_G : growth rate constant, day^{-1}

G_{max} : maximum specific growth rate constant at 20°C, 0.5 – 4.0, day^{-1}

X_T : temperature growth multiplier, dimensionless

X_L : light growth multiplier, dimensionless

X_N : nutrient growth multiplier, dimensionless

In a natural environment, the growth rate of a phytoplankton population is a complex function of the existing species of phytoplankton and their distinctive reactions to solar radiation, temperature, and the balance between nutrient availability and phytoplankton requirements. It is not possible to specify the growth kinetics for individual algal species in a natural environment since the available information is limited. EUTRO characterizes the population as a whole by the total biomass of the phytoplankton present instead of considering the problem of different species and their associated environmental and nutrient requirements.

Chlorophyll *a*, is used as the collective variable, which is a simple measure of total biomass that is characteristic of all phytoplankton. The main advantages are that the measurement is direct, it integrates cell types and ages, and it takes into consideration the cell viability. The principal disadvantage is that it is a community measurement with no differentiation of functional groups (e.g., diatoms, blue-greens); also, it is not necessarily a good measurement of standing crop in dry weight or carbon units because the chlorophyll-to-dry-weight and carbon ratios are variable and non-active chlorophyll (phaeopigments) must be measured to determine viable chlorophyll concentrations.

No simple collective measurement is entirely satisfactory. Since extensive chlorophyll data is available, its use as a collective measure of the phytoplankton population or biomass for calibration and verification purposes is essentially dictated from a practical point of view. However, EUTRO uses phytoplankton carbon as a measure of algal biomass for internal computational purposes. Phytoplankton chlorophyll *a* may be computed and used as the calibration and verification variable to be compared against observed chlorophyll *a* field data by using either a fixed or variable carbon to chlorophyll mechanism.

Temperature Effects on Phytoplankton

Phytoplankton growth rate is directly affected by the water temperature. The selected maximum growth rate is temperature-corrected using temporally- and spatially-

variable water column temperatures as reported in many field studies. The temperature multiplier is calculated as follows:

$$X_T = \theta_G^{T-20} \quad \textbf{(5.6)}$$

where

θ_G : temperature correction factor for growth (1.0 – 1.1)

T : water temperature, °C

Light Effects on Phytoplankton

In the natural environment, the light intensity to which the phytoplankton is exposed is not uniformly distributed at the optimum value. At the surface and near-surface of the air-water interface, photo-inhibition can occur at high light intensities, whereas at depths below the euphotic zone, light is not available for photosynthesis because of turbidity arising from natural and algal sources.

Modeling frameworks developed by Di Toro et al. (1971), and by Smith (1980), extending upon a light curve analysis formulated by Steele (1962), take into consideration both the effects of supersaturated light intensities and light attenuation through the water column. The instantaneous depth – averaged growth rate reduction developed by Di Toro is given in equation (5.7), which is obtained by integrating the specific growth rate over depth.

$$X_L(t) = \frac{e}{K_e H}\left[\exp\left\{-\frac{I_0}{I_s}\exp(-K_e H)\right\} - \exp\left\{-\frac{I_0}{I_s}\right\}\right] \quad \textbf{(5.7)}$$

H : average depth of segment, m

K_e : total light extinction coefficient, m^{-1}

I_0 : time variable incident light intensity just below the surface, langleys/day (assumes 10% reflectance)

I_s : saturating light intensity of phytoplankton, langleys/day

where,

$$I_0(t) = \left(\frac{\pi}{2}\frac{I}{f}\right) SIN\left(\frac{\pi t}{f}\right), \; t = 0 - f \qquad \textbf{(5.8)}$$

$$= 0, \qquad t = f - 1$$

and

$$I_S = \frac{G_{\max} X_T \theta_C e}{\Phi_{\max} K_c f_u} \qquad \textbf{(5.9)}$$

I_0 : the time variable incident light intensity just below the surface, assumed to follow a half sine function over daylight hours, langleys/day

Φ_{max} : the quantum yield, mg carbon fixed per mole of light quanta absorbed

K_c : the extinction coefficient per unit of chlorophyll, m^2/mg chlorophyll *a*

f_u : units conversion factor (0.083, assuming 43% incident light is visible and 1 mole photons is equivalent to 52,000 cal), mole photons/m^2-langleys

Θ_c : the ratio of carbon to chlorophyll in the phytoplankton, mg carbon/mg chlorophyll *a*

e : the base of natural logarithms (2.71828), dimensionless

Total light extinction is calculated as follows:

$$K_e = K_{eback} + K_{eshd} + K_{esolid} + K_{eDOC} \qquad \textbf{(5.10)}$$

where,

K_{eback} : background light extinction due to ligands, color, etc.

K_{eshd} : algal self shading

K_{esolid} : solids light extinction

K_{eDOC} : DOC light extinction

Light extinction components are calculated as follows:

$$K_{e\,back} = K_{eB\,const} \cdot K_{eB\,parameter} \cdot K_{eB\,time\,function} \quad \textbf{(5.11)}$$

$$K_{e\,solids} = K_{eS\,const} \cdot \left[C_{Detritus} \cdot ADC + C_{Solids}\right] \quad \textbf{(5.12)}$$

$$K_{e\,DOC} = K_{eDOC\,const} \cdot DOC;\ DOC = \frac{12}{32} \cdot \sum_i CBOD_i \cdot frac_{diss\,i} \quad \textbf{(5.13)}$$

$$K_{e\,shd} = K_{eshd\,mult} \cdot Chl_a^{Ke\,shd\,\exp} \quad \textbf{(5.14)}$$

When equation (5.7) is integrated over time, it becomes

$$X_L = \frac{e}{K_e H} f\left[\exp\left\{-\frac{I_{AV}}{I_S}\exp\left(-K_e H\right)\right\} - \exp\left\{-\frac{I_{AV}}{I_S}\right\}\right] \quad \textbf{(5.15)}$$

f : fraction of day, that is daylight

I_{TOT} : total daily light intensity, langleys/day

I_{AV} : average light intensity during daylight, langleys/day

$= I_{TOT} / f$

Nutrient Effects on Phytoplankton

Investigations on the effects of various nutrient concentrations on the growth of phytoplankton have quite complex results. The first approach to the effect of nutrient concentration on the growth rate, assumes that the concerned phytoplankton population follows Monod growth kinetics with respect to the significant nutrients as shown in Figure 5.7. This is interpreted as, at an adequate level of substrate concentration, the growth rate proceeds at the saturated rate for the existing ambient temperature and light conditions. However, the growth rate becomes linearly

proportional to substrate concentration at low substrate concentration. The constant, K_m (Michaelis or half-saturation constant), is the nutrient concentration at which the growth rate is half of the maximum growth rate.

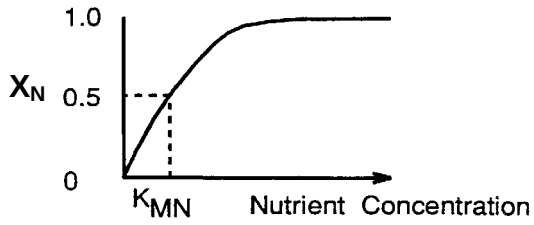

Figure 5.7: Effect of Nutrient Concentration on Growth Rate

$$X_N = \frac{N}{K_{MN} + N} \tag{5.16}$$

where,

X_N : nutrient limitation factor, dimensionless

N : nutrient concentration, mg/L

K_{MN} : half-saturation concentration, mg/L

Since the two nutrients, nitrogen and phosphorus, are taken into consideration in this study, the Michaelis-Menten expression is evaluated for the dissolved inorganic forms of both nutrients and the minimum value is chosen to reduce the maximum growth rate, as given by equation (5.17).

$$X_N = \min\left(\frac{DIN}{K_{mN} + DIN}, \frac{DIP}{K_{mP} + DIP}\right) \tag{5.17}$$

where,

$DIN = \left[NH_4 + NO_3\right]_{dissolved}$, mg/L

$DIP = \left[PO_4\right]_{dissolved}$, mg/L

K_{MN} : half–saturation constant for N, mg/L

K_{MP} : half–saturation constant for P, mg/L

Phytoplankton Death

Endogenous respiration, grazing by herbivorous zooplankton, and parasitization are the mechanisms that contribute to the biomass reduction rate of phytoplankton. Endogenous respiration and grazing by herbivorous zooplankton have shown to be of general importance, which have been included in the previous models for phytoplankton dynamics.

The endogenous respiration rate of phytoplankton is the rate at which the phytoplankton oxidizes their organic carbon to carbondioxide per unit weight of phytoplankton organic carbon. Respiration is the reverse of the photosynthesis process and therefore, contributes to the reduction in the biomass of the phytoplankton population. There is a net loss of phytoplankton carbon or biomass, when the respiration rate of the phytoplankton as a whole is greater than the growth rate.

$$R_D = k_{1R}\,\theta_{1R}^{T-20} + k_{1D} + k_{1G}\,Z(t) \qquad \textbf{(5.18)}$$

R_D : death rate constant, day^{-1}

k_{1R} : endogenous respiration rate constant, day^{-1}

θ_{1R} : temperature correction factor, dimensionless

k_{1D} : mortality rate constant, day^{-1}

k_{1G} : grazing rate constant, day^{-1} or $m^3/gZ\text{-day}$ if Z (t) specified

Z (t) : zooplankton biomass time function, gZ/m^3 (defaults to 1.0)

The zooplankton population dynamics are not simulated; they are described by the user. Simulating zooplankton and their grazing may be considered if population fluctuations are important in controlling phytoplankton levels in a particular body of water. On the other hand, many studies need only a constant first order-grazing rate

constant, where grazing rates are assumed proportional to phytoplankton levels. In that case, k_{1G} can be set to the first order constant with Z (t) omitted.

Phytoplankton Settling

An important contribution to the overall mortality of the phytoplankton population is the settling of phytoplankton, particularly in lakes and coastal oceanic waters. Actual settling in natural waters is a complex phenomenon, affected by vertical turbulence, density gradients, and the physiological state of the different phytoplankton species. Although the effective settling rate of phytoplankton is greatly reduced in a relatively shallow, well-mixed river or estuary due to vertical turbulence, it still can contribute to the overall mortality of the algal population. The settling phytoplankton can be a significant source of nutrients to the sediments and can play an important role in the sediment oxygen demand.

$$R_S = v_S A_S / V \quad \textbf{(5.19)}$$

R_S : settling rate constant, day^{-1}

v_S : settling velocity, m/day

A_S : surface area, m^2

V : segment volume, m^3

5.6.1.2 Nitrogen Cycle

NH_3, NO_3^-, organic nitrogen and detrital nitrogen state variables are modeled within EUTRO. The nitrogen cycle state variables and processes taken into consideration by EUTRO are given in Figure 5.8.

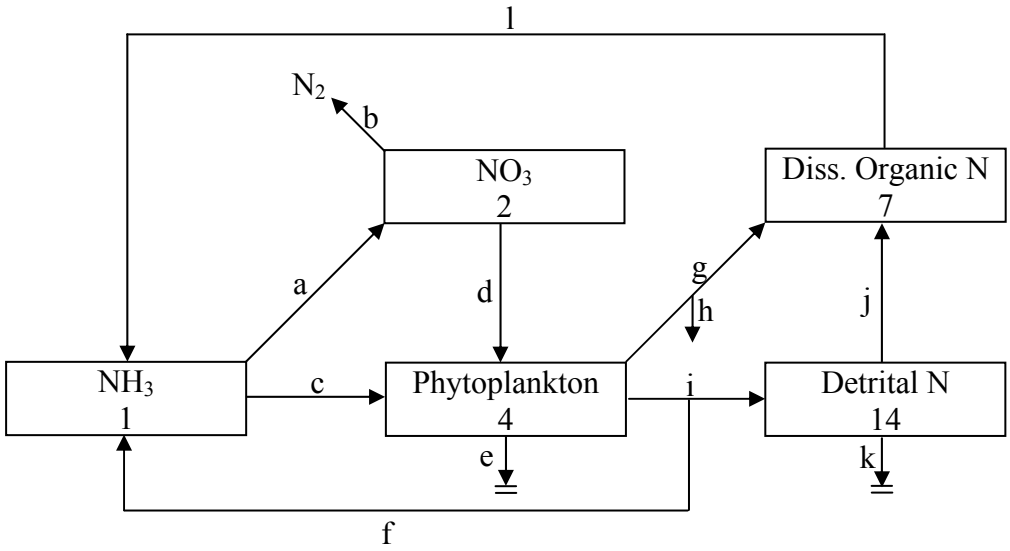

Figure 5.8: Nitrogen Cycle of EUTRO

The processes represented by letters in Figure 5.8 are described as follows:

(a): Nitrification, $k_{12}\theta_{12}^{T-20}\left(\frac{C_6}{K_{nit}+C_6}\right)C_1$ **(5.20)**

(b): Denitrification, $k_{2D}\theta_{2D}^{T-20}\left(\frac{k_{NO_3}}{k_{NO_3}+C_6}\right)C_2$ **(5.21)**

(c): Growth (Uptake), $G_p\, a_{nc}\, P_{NH3}\, C_4$ **(5.22)**

(d): Growth (Uptake), $G_p a_{nc}\left(1-P_{NH_3}\right)C_4$ **(5.23)**

(e): Settling, $\frac{v_{s4}}{H}C_4 a_{nc}$ **(5.24)**

(f): Respiration, $R_p C_4 a_{nc}(1-f_{ON})$ + Death, $D_p C_4 a_{nc}(1-f_{ON})$ **(5.25)**

(g): Respiration, $R_p C_4 f_{ON} a_{nc}$ **(5.26)**

(h): Respiration, $R_p C_4 (1-f_{ON}) a_{nc}$ **(5.27)**

(i): Death, $D_p\ C_4 f_{ON}\ a_{nc}$ **(5.28)**

(j): Dissolution, $k_{diss}\ \theta_{diss}^{T-20}\ C_{14}$ **(5.29)**

(k): Settling, $\frac{v_{s14}}{H}$ **(5.30)**

(l): Mineralization, $k_{\min}\ \theta_{\min}^{T-20}\left(\frac{C_4}{K_{mpc}+C_4}\right)C_7$ **(5.31)**

where,

C_4 : phytoplankton carbon concentration, mg C/L

k_{12} : nitrification rate at 20°C, day^{-1}

θ_{12} : temperature coefficient, dimensionless

K_{nit} : half saturation constant for oxygen limitation of nitrification, mg O_2/L

K_{2D} : denitrification rate at 20°C, day^{-1}

Θ_{2D} : temperature coefficient, dimensionless

k_{NO3} : Michaelis constant for denitrification, mg O_2/L

a_{nc} : nitrogen to carbon ratio, mg N/mg C

P_{NH3} : preference for ammonia uptake term, dimensionless

v_{S4} : phytoplankton settling velocity, m/day

H : depth, m

f_{ON} : fraction of dead and respired phytoplankton recycled to the organic nitrogen pool, dimensionless

1 - f_{ON} : fraction of dead and respired phytoplankton recycled to the ammonia nitrogen pool, dimensionless

k_{diss} : dissolution rate at 20°C, day^{-1}

Θ_{diss} : temperature coefficient, dimensionless

v_{S14} : detritus settling velocity, m/day

k_{min} : mineralization rate at 20°C, day^{-1}

Θ_{min} : temperature coefficient, dimensionless

K_{mpc} : half-saturation constant for phytoplankton recycled to the nitrogen pool, mg C/L

G_p : phytoplankton growth rate, day^{-1}

D_p : phytoplankton death rate, day^{-1}

R_p : phytoplankton respiration rate, day^{-1}

The nitrogen cycle equations used by EUTRO are;

Phytoplankton Nitrogen

$$\frac{\partial C_4 a_{nc}}{\partial t} = \left(G_p - R_p - D_p - \frac{v_{s4}}{H} \right) C_4 a_{nc} \qquad \textbf{(5.32)}$$

Detrital Nitrogen

$$\frac{\partial C_{14}}{\partial t} = D_p C_4 f_{ON} a_{nc} - k_{diss} \theta_{diss}^{T-20} C_{14} - \frac{v_{s14}}{H} \qquad \textbf{(5.33)}$$

Dissolved Organic Nitrogen

$$\frac{\partial C_7}{\partial t} = R_p C_4 f_{ON} a_{nc} + k_{diss} \theta_{diss}^{T-20} C_{14} - k_{\min} \theta_{\min}^{T-20} \left(\frac{C_4}{K_{mpc} + C_4} \right) C_7 \qquad \textbf{(5.34)}$$

Ammonia Nitrogen

$$\frac{\partial C_1}{\partial t} = (R_p + D_p) C_4 \left(1 - f_{ON}\right) a_{nc} + k_{\min} \theta_{\min}^{T-20} \left(\frac{C_4}{k_{mpC} + C_4} \right) C_7 - k_{12} \theta_{12}^{T-20} \left(\frac{C_6}{K_{nit} + C_6} \right) C_1 - G_p \, a_{nc} \, P_{NH3} \, C_4 \quad \textbf{(5.35)}$$

Nitrate Nitrogen

$$\frac{\partial C_2}{\partial t} = k_{12} \theta_{12}^{T-20} \left(\frac{C_6}{K_{nit} + C_6} \right) C_1 - G_p a_{nc} C_4 \left(1 - P_{NH_3}\right) - k_{2D} \theta_{2D}^{T-20} \left(\frac{k_{NO_3}}{k_{NO_3} + C_6} \right) C_2 \quad \textbf{(5.36)}$$

Ammonia preference factor is calculated accordingly;

$$P_{NH_3} = \frac{NH_4 NO_3}{\left(K_{mN} + NH_4\right)\left(K_{mN} + NO_3\right)} + \frac{NH_4 K_{mN}}{\left(NH_4 + NO_3\right)\left(K_{mN} + NO_3\right)} \quad \textbf{(5.37)}$$

Dissolved inorganic nitrogen (NH_3, NO_3^-) is taken up and incorporated into biomass by phytoplankton during growth. a_{NC} mg of inorganic nitrogen is taken up for every mg of phytoplankton carbon produced. Ammonia and nitrate are utilized for uptake and use in cell growth by phytoplankton, but ammonia is preferred for physiological reasons. Ammonia preference factor is given by equation (5.37). The behavior of this equation is most sensitive at low values of ammonia or nitrate. For a given concentration of ammonia, the available nitrate approximately increases above the Michaelis limitation, thus, the preference for ammonia reaches an asymptote.

Viable organic material is recycled to non-living organic and inorganic matter during phytoplankton respiration and death. a_{NC} mg of nitrogen is released for every mg of phytoplankton carbon consumed or lost. During phytoplankton respiration and death, a fraction of the cellular nitrogen f_{on} is organic, while (1 - f_{on}) is in the inorganic form of ammonia nitrogen. Particulate detrital nitrogen may settle out at the same velocity as organic matter (ν_{s3}). Particulate detrital nitrogen dissolves to dissolved organic nitrogen (DON) and DON mineralizes to ammonia nitrogen.

Non-viable organic nitrogen must be converted to ammonia nitrogen through mineralization or bacterial decomposition to be utilized by phytoplankton.

Nitrification in natural waters is a complex process, depending on dissolved oxygen, pH, and flow conditions, which in turn leads to spatially and temporally varying rates of nitrification.

The kinetic expression for nitrification in EUTRO contains three terms; a first order rate constant, a temperature correction term, and a low DO correction term. The first two terms are standard. The third term represents the decline of the nitrification rate as DO levels approach 0. The user may specify the half-saturation constant K_{NIT}, which represents the DO level at which the nitrification rate is reduced by half. The default value is zero, which allows this reaction to fully proceed even under anaerobic conditions.

Denitrification is included in the modeling framework simply as a sink of nitrate. The kinetic expression for denitrification in EUTRO contains three terms; a first order rate constant, a temperature correction term, and a DO correction term. The first two terms are standard. The third term represents the decline of the denitrification rate as DO levels rise above 0. The user may specify the half-saturation constant K_{NO3}, which represents the DO level at which the denitrification rate is reduced by half. The default value is zero, which prevents this reaction at all DO levels. Denitrification is assumed to occur in the sediment layer under anaerobic conditions.

5.6.1.3 Phosphorus Cycle

PO_4^{3-}, organic phosphorus, and detrital phosphorus state variables are modeled within EUTRO. The phosphorus cycle state variables and processes taken into consideration by EUTRO are given in Figure 5.9.

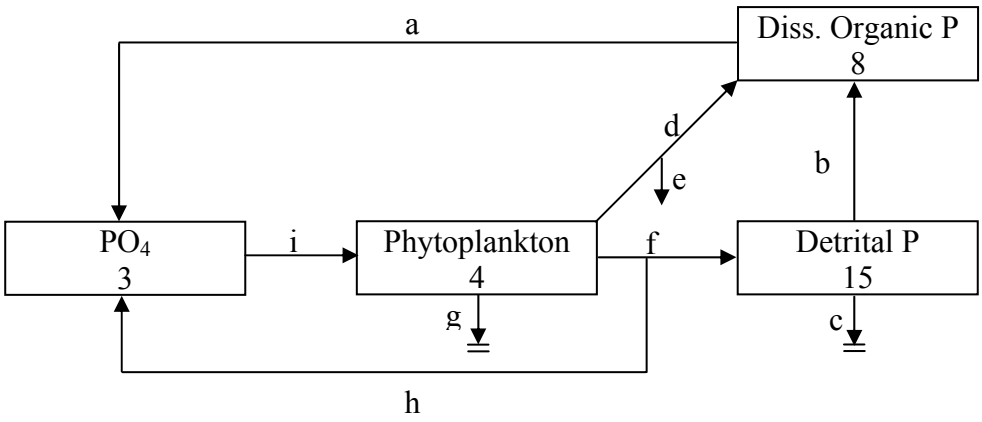

Figure 5.9: Phosphorus Cycle of EUTRO

The processes represented by letters in Figure 5.9 are described as follows:

(a): Mineralization, $k_{\min}\,\theta_{\min}^{T-20}\left(\frac{C_4}{K_{mpc}+C_4}\right)C_8$ (**5.38**)

(b): Dissolution, $k_{diss}\,\theta_{diss}^{T-20}\,C_{15}$ (**5.39**)

(c): Settling, $\frac{v_{s15}}{H}$ (**5.40**)

(d): Respiration, $R_p C_4 f_{OP} a_{PC}$ (**5.41**)

(e): Respiration, $R_p C_4 (1-f_{OP}) a_{PC}$ (**5.42**)

(f): Death, $D_p\,C_4 f_{OP}\,a_{pc}$ (**5.43**)

(g): Settling, $\frac{v_{s4}}{H} C_4 a_{pc}$ (**5.44**)

(h): Respiration, $R_p\,C_4(1-f_{OP})\,a_{pc}$ + Death, $D_p C_4 (1-f_{op}) a_{pc}$ (**5.45**)

(i): Growth (Uptake), $G_p C_4 a_{pc}$ (**5.46**)

where,

C_4 : phytoplankton carbon concentration, mg C/L

k_{min} : mineralization rate at 20°C, day^{-1}

Θ_{min} : temperature coefficient for mineralization, dimensionless

K_{mpc} : half saturation constant for phytoplankton recycled to the phosphorus pool, mg C/L

k_{diss} : dissolution rate at 20°C, day^{-1}

Θ_{diss} : temperature coefficient for dissolution, dimensionless

ν_{S15} : detritus settling velocity, m/day

H : depth, m

a_{pc} : phosphorus to carbon ratio, mg P/mg C

f_{OP} : fraction of dead and respired phytoplankton recycled to the organic phosphorus pool, dimensionless

$1 - f_{OP}$: fraction of dead and respired phytoplankton recycled to the phosphate phosphorus pool, dimensionless

ν_{S4} : phytoplankton settling velocity, m/day

G_p : phytoplankton growth rate, day^{-1}

R_p : phytoplankton respiration rate, day^{-1}

D_p : phytoplankton death rate, day^{-1}

The phosphorus cycle equations used by EUTRO are:

Phytoplankton Phosphorus

$$\frac{\partial C_4 a_{pc}}{\partial t} = \left(G_p - R_p - D_p - \frac{v_{s4}}{H} \right) C_4 a_{pc} \qquad \textbf{(5.47)}$$

Detrital Phosphorus

$$\frac{\partial C_{15}}{\partial t} = D_p C_4 f_{OP} a_{pc} - k_{diss} \theta_{diss}^{T-20} C_{15} - \frac{v_{s15}}{H} \qquad \textbf{(5.48)}$$

Dissolved Organic Phosphorus

$$\frac{\partial C_8}{\partial t} = R_p C_4 f_{OP} a_{PC} + k_{diss} \theta_{diss}^{T-20} C_{15} - k_{\min} \theta_{\min}^{T-20} \left(\frac{C_4}{K_{mpc} + C_4} \right) C_8 \qquad \textbf{(5.49)}$$

Inorganic Phosphorus (Orthophosphate)

$$\frac{\partial C_3}{\partial t} = (R_P + D_P) C_4 (1 - f_{OP}) a_{PC} + k_{\min} \theta_{\min}^{T-20} \frac{C_4}{K_{mpc} + C_4} C_8 - G_P C_4 a_{pc} - \frac{v_{s3}(1 - f_{d3})}{H} C_3 \qquad \textbf{(5.50)}$$

Dissolved inorganic phosphorus (orthophosphate) is taken up, stored and incorporated into biomass by phytoplankton during growth. a_{PC} mg of inorganic phosphorus is taken up for every mg of phytoplankton carbon produced.

Biomass is recycled to non-viable organic and inorganic matter during phytoplankton respiration and death. a_{PC} mg of phosphorus is released for every mg of phytoplankton carbon consumed or lost. A fraction f_{op} is organic, while (1 - f_{op}) is in the inorganic form and readily available for uptake by other viable algal cells.

Non-viable organic phosphorus must be converted to inorganic phosphorus through mineralization or bacterial decomposition to be utilized by phytoplankton. EUTRO uses a saturating recycle mechanism, a compromise between conventional first-order kinetics and a second-order recycle mechanism wherein the recycle rate is directly

proportional to the phytoplankton biomass present, as had been indicated in pure culture, bacteria-seeded, laboratory studies (Jewell and McCarty, 1971).

Saturating recycle permits second-order dependency at low phytoplankton concentrations, when Pc << K_{mPc}, where K_{mPc} is the half-saturation constant for recycle, and permits first-order recycle when the phytoplankton highly exceed the half-saturation constant. Basically, this mechanism slows the recycle rate if the phytoplankton population is small, but does not allow the rate to increase continuously as phytoplankton increases. The assumption is that at higher population levels, recycle kinetics proceed at the maximum first order rate. The default value for K_{mPc} is 0, which causes mineralization to precede at its first-order rate at all phytoplankton levels.

Dissolved inorganic phosphorus and suspended particulate matter interacts through adsorption–desorption mechanism in the water column. The subsequent settling of suspended solids together with the sorbed inorganic phosphorus can act as a significant loss mechanism in the water column, and is a source of phosphorus to the sediment. An equilibrium assumption can be made since the rates of reaction for adsorption–desorption are in the order of minutes whereas the reaction rates for the biological kinetics are in the order of days. This equilibrium reaction implies that the dissolved and particulate phosphorus phases “instantaneously” react to any discharge sources of phosphorus or runoff or shoreline erosion of solids so as to redistribute the phosphorus to its “equilibrium” dissolved and solids phase concentrations.

Particulate organic and inorganic phosphorus settle according to user-specified velocities and particulate fractions.

5.6.1.4 Dissolved Oxygen Balance

EUTRO program simulates the dissolved oxygen and the associated variables. The transport and interaction among the nutrients, phytoplankton, carbonaceous material, and dissolved oxygen in the aquatic environment could be affected by numerous physical and chemical processes. The principal kinetic interactions for the nutrient cycles, dissolved oxygen as well as the dissolved oxygen balance processes are given in Figure 5.10 and Figure 5.11, respectively.

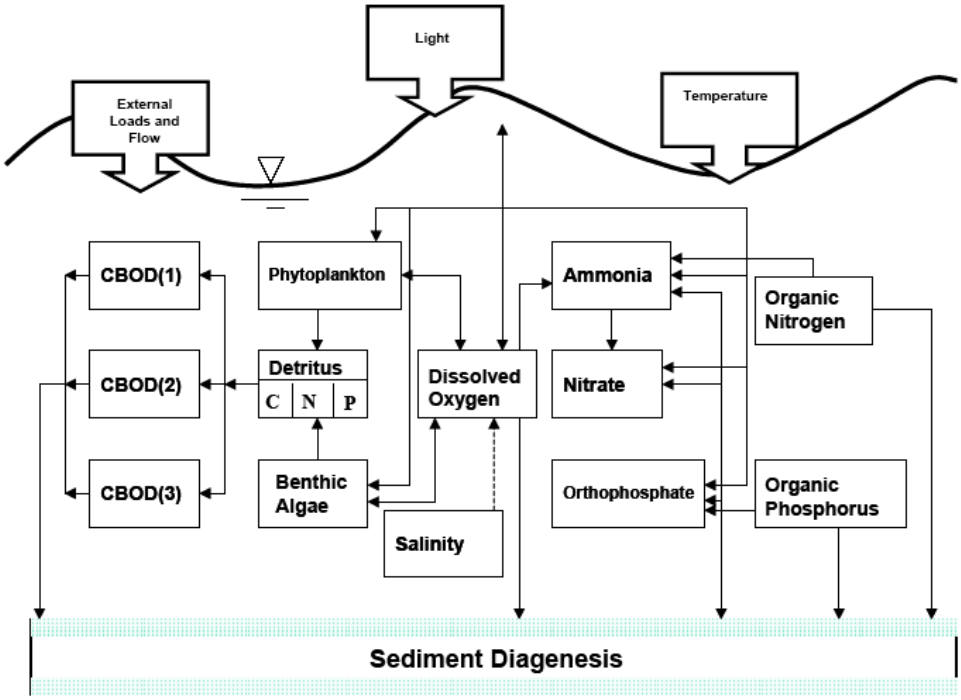

Figure 5.10: Eutrophication Dissolved Oxygen Interactions

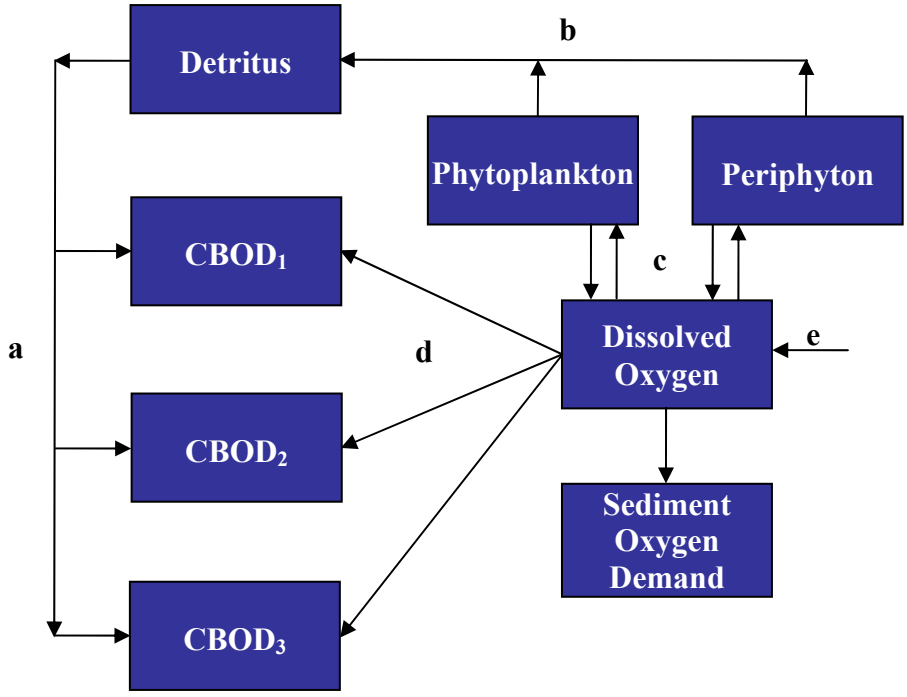

Figure 5.11: Dissolved Oxygen Balance Processes

The processes represented by letters in Figure 5.11 are described below as follows;

(a): Dissolution

(b): Death

(c): Photosynthesis and respiration

(d): Organic Decay

(e): Reaeration

Phytoplankton carbon, ammonia, nitrate, carbonaceous biochemical oxygen demand (CBOD), and dissolved oxygen (DO) are the EUTRO state variables, which can participate directly in the dissolved oxygen balance. As a consequence of the aerobic respiratory processes in the water column and the anaerobic processes in the underlying sediments, the dissolved oxygen is reduced. It is important to formulate their kinetics explicitly since these processes can contribute significantly.

Carbonaceous Biochemical Oxygen Demand

$$\frac{\partial C_5}{\partial t} = a_{OC} k_{1d} C_4 - k_D \theta_D^{T-20} \frac{C_6}{k_{BOD} + C_6} C_5 - \frac{\nu_{s3}(1 - f_{d5})}{D} C_5 - \frac{5}{4}\frac{32}{14} k_{2D} \theta_{2D}^{T-20} \left(\frac{k_{NO_3}}{k_{NO_3} + C_6} \right) C_2 \quad \textbf{(5.51)}$$

where,

a_{OC} : oxygen to carbon ratio, mg O_2/ mg C

k_{1d} : death and respiration constant for phytoplankton, day^{-1}

k_D : deoxygenation rate at 20°C, day^{-1}

Θ_D : temperature coefficient for decay, dimensionless

k_{BOD} : half saturation constant for oxygen limitation, mg O_2/L

ν_{S3} : organic matter settling velocity, m/day

f_{d5} : fraction dissolved CBOD, dimensionless

k_{2D} : denitrification rate at 20°C, day^{-1}

Θ_{2D} : temperature coefficient for denitrification, dimensionless

k_{NO3} : half saturation constant for oxygen limitation, mg N/L

While the first term represents death, the others represent oxidation, settling and denitrification, respectively.

Dissolved Oxygen

$$\frac{\partial C_6}{\partial t} = k_2(C_s - C_6) - k_D\theta_D^{T-20}\frac{C_6}{k_{BOD}+C_6}C_5 - \frac{64}{14}k_{12}\theta_{12}^{T-20}\frac{C_6}{k_{NIT}+C_6}C_1 - \frac{SOD}{D}\theta_s^{T-20} + G_p\left(\frac{32}{12}+\frac{48}{14}a_{nc}(1-P_{NH_3})\right)C_4 - \frac{32}{12}k_{1R}\theta_{1R}^{T-20}C_4 \quad (\mathbf{5.52})$$

where,

C_4 : phytoplankton carbon concentration, mg C/L

k_2 : reaeration rate at 20°C, day^{-1}

C_s : dissolved oxygen saturation constant, mg O_2/L

k_D : deoxygenation rate at 20°C, day^{-1}

Θ_D : temperature coefficient, dimensionless

k_{BOD} : half saturation constant for oxygen limitation, mg O_2/L

k_{12} : nitrification rate at 20°C, day^{-1}

Θ_{12} : temperature coefficient for nitrificaton, dimensionless

k_{nit} : half saturation constant for oxygen limitation, mg N/L

SOD : sediment oxygen demand, g/m^2 – day

Θ_S : sediment oxygen demand temperature coefficient, dimensionless

a_{nc} : phytoplankton nitrogen–carbon ratio, mg N/ mg C

P_{NH3} : preference for ammonia uptake term, dimensionless

k_{1R} : phytoplankton respiration rate at 20°C, day^{-1}

Θ_{1R} : phytoplankton respiration rate temperature coefficient, dimensionless

While the first term represents reaeration; the others in turn represent oxidation, nitrification, sediment oxygen demand, phytoplankton growth and respiration.

Reaeration

Waters with oxygen deficiency are replenished through atmospheric reaeration. Average water velocity, depth, wind, and temperature are the factors that affect the reaeration rate coefficient. In EUTRO, a single reaeration rate constant (global reaeration), spatially – variable reaeration rate constant (segment specific) may be specified or the model may be allowed to calculate variable reaeration rates based upon flow or wind. Covar, O'Connor – Dobbins, Owens, Churchill or Tsivoglou are the available methods to be selected for the model calculated reaeration option. The selected reaeration formulation is used under all conditions. If any particular option or reaeration rate is not specified the model will calculate reaeration as function of depth and water velocity using Covar method. Covar method calculates reaeration as a function of velocity and depth by one of three formulas; O'Connor – Dobbins, Owens, Churchill. Dam reaeration is the last reaeration option that allows specifying low–head dams/spillways where oxygen would be added to the riverine system as a function of water quality condition and dam type. Calculated reaeration will follow either the flow–induced rate or the wind–induced rate, whichever is larger.

O'Connor – Dobbins

$$k_a = 3.93\frac{U^{0.5}}{H^{1.5}} \quad \textbf{(5.53)}$$

Churchill

$$k_a = 5.026\frac{U}{H^{1.67}} \quad \textbf{(5.54)}$$

Owens

$$k_a = 5.32\frac{U^{0.67}}{H^{1.85}} \quad \textbf{(5.55)}$$

where,

U : velocity, m/s

H : depth, m

k_a : reaeration rate coefficient, day^{-1}

Dam Reaeration

$$r = 1 + 0.38abH(1 - 0.11H)(1 + 0.046T) \quad \textbf{(5.56)}$$

where,

r : ratio of deficit above and below the dam

H : difference in water elevation, m

T : water temperature, °C

a : water quality coefficient

b : dam-type coefficient (Chapra, 1997)

Carbonaceous Oxidation

Biochemical oxygen demand (BOD) is used as the primary parameter for measuring the quantity of oxygen demanding material whereas its oxidation rate is used as the controlling kinetic reaction. The classical BOD reaction is used for the oxidation of carbonaceous material. Ultimate carbonaceous biochemical oxygen demand (CBOD) is used as the indicator of equivalent oxygen demand for the carbonaceous material by the model internally.

WASP7 can simulate up to three carbonaceous BOD state variables. One or all of them can be simulated according to the nature of the problem. The parameterization and use of BOD state variables in the simulation are controlled by the user. The BOD state variables can be used as fast, medium, and slow reactions. They can be used for source analysis where one can be used for boundary CBOD, one for municipal wastewater, and the last for industrial or biotic components. Individual decay rates, f–ratios for loading the model, and temperature correction term can be specified. Loads and boundaries for each of the state variables selected to be used should be defined. The pathway of algal and periphyton death in which the carbonaceous component of the cells is placed must be provided by the user. The primary loss mechanism associated with CBOD is oxidation.

Nitrification

Nitrification causes additional significant oxygen loss.

$$NH_4^+ + 2O_2 \rightarrow NO_3^- + H_2O + 2H^+ \qquad \textbf{(5.57)}$$

According to the stoichiometry 2 (32/14) mg of oxygen are consumed for every mg of ammonia nitrogen oxidized. The kinetic expression for nitrification in EUTRO contains a first-order rate constant, a temperature correction term, and a low DO correction term. The first two are standard. The third represents the decline of the nitrification rate as DO levels approach 0. The half-saturation constant, k_{NIT}, may be specified, which represents the DO level at which the nitrification rate is reduced by half.

Denitrification

The denitrification reaction occurs under low DO conditions, which provides a sink for CBOD:

$$5\,CH_2O + 5\,H_2O + 4\,NO_3^- + 4\,H^+ \rightarrow 5\,CO_2 + 2\,N_2 + 12\,H_2O \qquad \textbf{(5.58)}$$

According to the stoichiometry 5/4 (12/14) mg of carbon are consumed for each mg of nitrate nitrogen reduced, which reduces CBOD by 5/4 (12/14) (32/12) mg. Denitrification is not a significant loss in the water column, but can be important when simulating anaerobic benthic conditions.

The kinetic expression for denitrification in EUTRO contains a first-order rate constant, a temperature correction term, and a DO correction term. The first two are standard. The third represents the decline of the denitrification rate as DO levels rise above 0. The half–saturation constant, k_{NO3}, may be specified which represents the DO level at which the denitrification rate is reduced by half.

Settling

The particulate fraction of CBOD can settle downwards through the water column and deposit on the bottom under quiescent flow conditions. In water bodies, this can reduce carbonaceous deoxygenation in the water column significantly. However, the deposition of CBOD and phytoplankton can increase sediment oxygen demand in the benthic sediment. Particulate CBOD from the bed can be re-suspended under high flow conditions.

The kinetic expression for settling in EUTRO is driven by the user-specified particulate settling velocity, v_{s3}, and the CBOD particulate fraction, $(1 - f_{D5})$, where f_{D5} is the dissolved fraction. Settling velocities that vary with time and segment can be input as part of the advective transport field. Re-suspension can also be input using a separate velocity time function. Segment–variable dissolved fractions are also input data with initial conditions.

Phytoplankton Growth

Dissolved oxygen production is a by-product of photosynthetic carbon fixation. The rate of oxygen production and nutrient uptake is proportional to the growth rate of the phytoplankton as its stoichiometry is fixed. According to the stoichiometry 32/12 mg of O_2 are produced for each mg of phytoplankton carbon produced by growth. When the available ammonia nutrient source is used up, the phytoplankton begins to utilize the available nitrate which provides an additional source of oxygen from phytoplankton growth. For nitrate uptake the initial step is a reduction to ammonia that produces oxygen:

$$2NO_3 + 6H^+ \rightarrow 2NH_3 + 3O_2 \qquad \textbf{(5.59)}$$

According to the stoichiometry, a_{NC} mg of phytoplankton nitrogen is reduced, and (48/14) a_{NC} mg of O_2 is produced for each mg of phytoplankton carbon produced by growth using nitrate.

Oxygen is reduced in the water column as a result of phytoplankton respiration, which is basically the reverse process of photosynthesis.

$$C + O_2 \rightarrow CO_2 \qquad \textbf{(5.60)}$$

where C is phytoplankton carbon, in mg/L. According to the stoichiometry, for every mg of phytoplankton carbon consumed by respiration, 32/12 mg of oxygen is also consumed.

Phytoplankton Death

The death of phytoplankton provides organic carbon, which can be oxidized. The kinetic expression in EUTRO recycles phytoplankton carbon to CBOD using a first order death rate and the stoichiometric oxygen to carbon ratio 32/12.

Sediment Oxygen Demand

The degradation of organic material in benthic sediment can have intensive effects on the oxygen concentrations in the overlying waters. Oxygen demand increases at

the sediment-water interface due to the degradation of organic material. As a result, the fluxes from the sediment can be considerable and oxygen sinks to the overlying water column.

Descriptive input and predictive calculations are the oxygen flux options provided by EUTRO. The first option is used for networks composed of only water column segments. Observed sediment oxygen demand fluxes must be specified for water segments in contact with the benthic layer. Sediment oxygen demand (SOD) can be affected by seasonal changes in water temperature through the temperature coefficient.

WASP7 allows a more detailed parameterization of settling into the benthos that includes not only a downward settling velocity but an upward re-suspension velocity as well. The difference between the downward settling flux and the upward resuspension flux gives the net particulate flux to the sediment.

The first step is to determine the benthic layer depth. Two factors should be considered to determine the benthic layer depth. The depth must satisfactorily reflect the thickness of the active layer, the depth to which the sediment is influenced by exchange with the overlying water column, and the model must reflect a reasonable time history in the sediment layer. If the layer is very thin, the benthos will be influenced by deposition of material that would have occurred only within the last year or two of the period being analyzed. If the layer is very thick, the model will average too long a history, which is not reflecting substantial reductions resulting from reduced discharges from sewage treatment plants. The choice of sediment thickness is further complicated by spatially variable sedimentation rates.

Anaerobic degradation of the phytoplankton carbon and the anaerobic breakdown of the benthic organic carbon are the degradation reactions driving the component mass balance equations. Both reactions are sinks of oxygen, and rapidly drive its concentration to negative, which indicates that the sediment is reduced rather than oxidized. The computed negative concentrations can be explained as the oxygen equivalents of the reduced end products produced by the chains of redox reactions occurring in the sediment.

6. DATA ANALYSES AND WATER QUALITY MODELING STUDIES WITH WASP

The data collected by Gürel (2000) during the water quality monitoring studies of Köyceğiz–Dalyan Lagoon, were used in the water quality modeling studies. Five cruises were realized to the pilot area between June 1998 and March 2000. Samples were collected from 14 stations in the first cruise. Two more stations were added starting from the second cruise, and monitoring studies were carried out with 16 stations in the Lagoon system.

6.1 Water Quality Input Data Gathering

A strategy of data collection and parameterization were planned by Gürel (2000) to provide utilizable information to eutrophication modelers during monitoring system design.

Gürel (2000) determined the locations of monitoring stations considering the following factors;

- Channel systems and lakes comprise the Köyceğiz – Dalyan Lagoon. Thus, monitoring stations are required to analyze the interaction between channel systems and lakes.
- Stations are required to represent the lake systems.
- Stations along the channels are required to detect spatial variations in channel systems.
- Stations are required close to the pollution sources to determine their effects.
- Stations are required to represent the boundary conditions for the system.

The locations of monitoring stations determined according to the above listed factors are given in Figure 6.1.

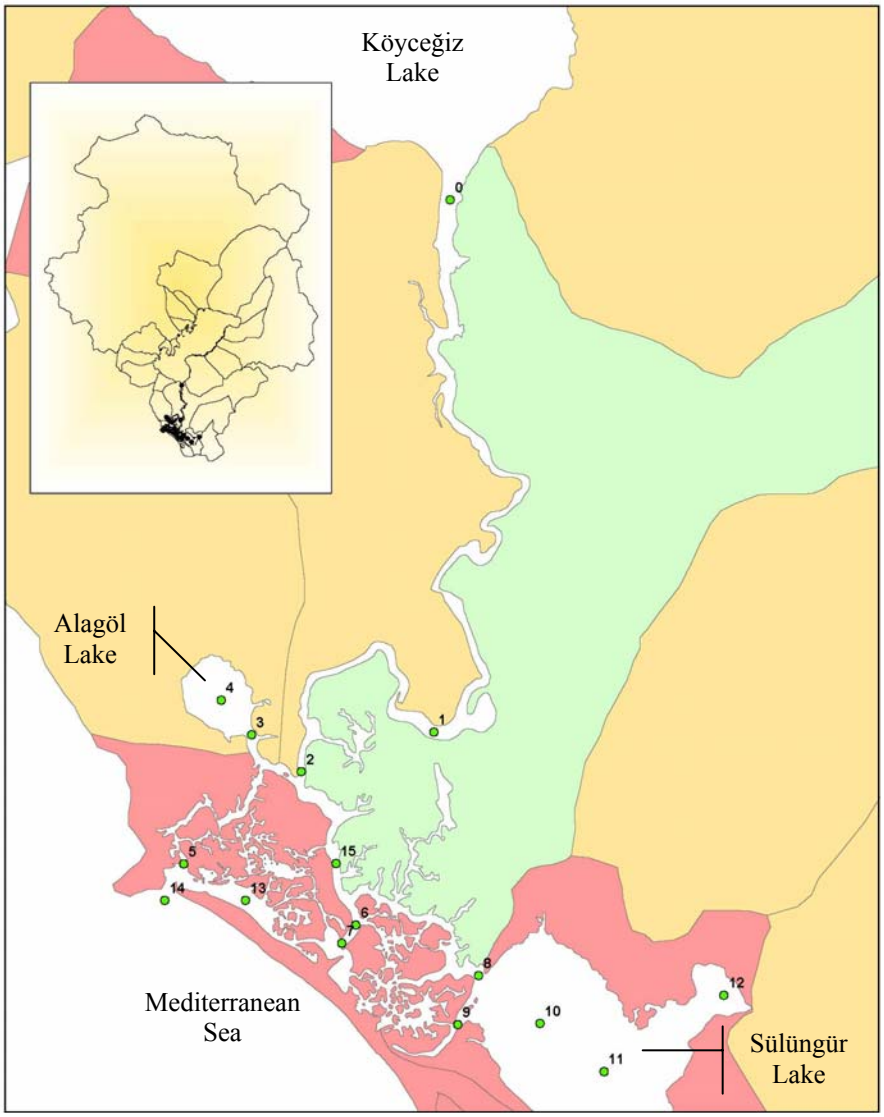

Figure 6.1: The Locations of Monitoring Stations (Karagöz, 2003)

Station 0: Represents the entrance from Köyceğiz Lake to the main channel (boundary condition),

Station 3: Represents the entrance to the Alagöl Lake,

Station 4: Station in the Alagöl Lake,

Station 8 and Station 9: Represent the entrance to the Sülüngür Lake,

Stations 10, 11, 12: Stations inside the Sülüngür Lake,

Station 1: After Dalyan Town, on the main channel,

Stations 2, 15, 6, 7, 13, 5: Stations on the channels

Station 14: Represents the sea, constituting one of the boundary conditions between the sea and the lagoon system.

As horizontal and vertical salinity gradients are observed throughout the cruises, surface and bottom water samples were collected at each station. Surface water samples were collected from 0.5 m depth from the surface. Bottom water sampling depths were selected according to the depth of the stations and vertical salinity gradients (Gürel, 2000).

6.1.1 Monitoring Parameters

The measured and calculated parameters during these five cruises are given in Table 6.1.

6.1.2 Sampling Period

The sampling period determined by Gürel (2000) is as follows;

The first Cruise to Köyceğiz – Dalyan Lagoon was realized in July 1998 (Cruise 1). The following Cruises were carried out in April 1999 (Cruise 2) and in August 1999 (Cruise 3). Cruise 1 and Cruise 3 were conducted in summer representing the dry season, Cruise 2 and Cruise 5 (March 2000) were conducted in spring and Cruise 4 (November 1999) in autumn representing the wet season.

Monitoring study is such a challenging task which requires multidisciplinary group work. The cruises to Köyceğiz – Dalyan Lagoon were conducted in cooperation with the İstanbul University Institute of Marine Sciences and Management. Each cruise had a preparation period of 15 days and a sampling period of 4 or 5 days. Most of the sampling and storage equipment and reagents were transported from İstanbul with trucks. Some of the measurements were done on – site, however most of the experiments were carried out at the laboratories of İstanbul University Institute of Marine Sciences and Management.

Table 6.1: Measured and Calculated Parameters through Cruises 1–5

Parameter	Cruise 1 (June 30-July 1, 1998)	Cruise 2 (April 19-21, 1999)	Cruise 3 (August 17-19, 1999)	Cruise 4 (November 21-23, 1999)	Cruise 5 (March 28-30, 2000)
Salinity (‰)	✓	✓	✓	✓	✓
Temperature (°C)	✓	✓	✓	✓	✓
Depth (m)	✓	✓	✓	✓	✓
Secchi Depth (m)	✓	✓	✓	✓	✓
Light (µEinstein $m^{-2}sec^{-1}$)	-	✓	-	✓	-
pH (-)	✓	✓	✓	✓	✓
TSS (mg/L)	✓	✓	✓	✓	✓
DO (mg/L)	✓	✓	✓	✓	✓
BOD_5 (mg/L)	✓	✓	✓	✓	✓
Alkalinity (mg/L $CaCO_3$)	✓	✓	✓	✓	✓
NO_3+NO_2 (µM)	✓	✓	✓	✓	✓
NO_2 (µM)	✓	✓	✓	✓	✓
NO_3 (µM)*	✓	✓	✓	✓	✓
NH_4 (µM)	-	✓	✓	✓	✓
DIN (µM)*	-	✓	✓	✓	✓
PON (µM)	✓	✓	-	✓	✓
DON (µM)*	-	✓	-	✓	✓
TN (µM)	✓	✓	-	✓	✓
DRP (µM)	-	✓	✓	✓	-
TRP (µM)	✓	-	✓	✓	-
TDP (µM)	-	✓	✓	✓	✓
PP (µM)*	-	-	✓	✓	✓
PIP (µM)*	-	-	✓	✓	-
POP (µM)*	-	-	✓	✓	-
TP (µM)	✓	-	✓	✓	✓
Si (µM)	✓	✓	✓	✓	✓
Chl-a (µg/L)	✓	✓	✓	✓	✓
POC (µM)	✓	✓	-	✓	✓

✓: Available Data
- : Data not available
*: calculated as follows
DON = TN - PON - DIN
DIN = NO^-_3-N + NO^-_2-N + NH_4^+-N
NO^-_3-N = (NO^-_3-N +NO^-_2-N) - NO^-_2-N
PP = TP - TDP
PIP = TRP - DRP
POP = PP – PIP

6.2 Generation of Input Data

6.2.1 Initial Concentrations

As mentioned in Chapter 5, the physical configuration of the water body is represented by the model network, which is a group of expanded control volumes, or "segments". Köyceğiz–Dalyan Lagoon is divided into segments for modeling with WASP. The system is divided into 49 segments. Since there are horizontal and vertical salinity gradients in the system, each segment is divided into two, as upper and bottom segments; therefore, the total number of segments representing the system is 98. The WASP segments are given in Figure 6.2, and the segment properties are given in Table 6.2.

The numbers between 1 and 49 represent the upper layers of the segments. When 49 is added to the segment number of a upper layer, the number that corresponds to the bottom layer of that segment is calculated.

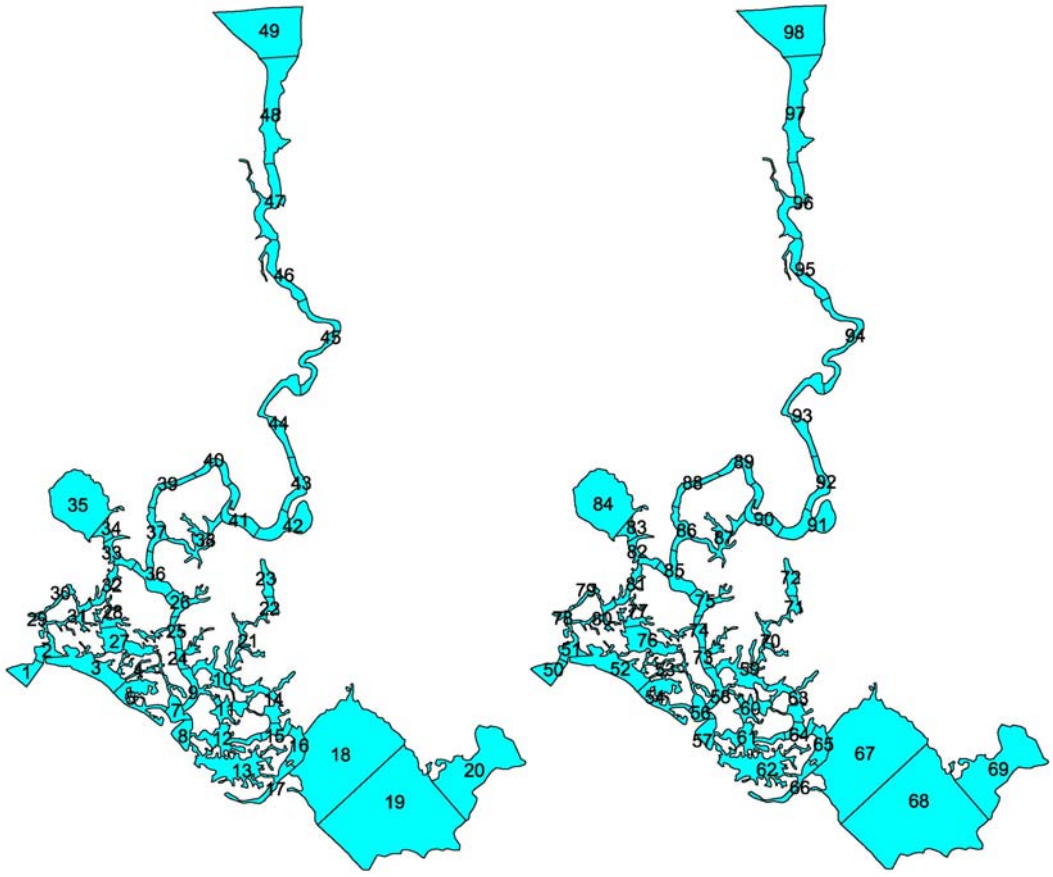

Figure 6.2: WASP Segments

Table 6.2: Properties of WASP Segments

WASP Segment No		Segment Area	Average Upper	Average Bottom	Upper Volume	Bottom Volume
Upper	Bottom	(m^2)	Depth (m)	Depth (m)	(m^3)	(m^3)
1	50	160000	0.5	1.7	80000	271660
2	51	97970	0.5	1.6	48985	166356
3	52	219938	0.5	1.6	109969	340904
4	53	27094	0.5	2.0	13547	52833
5	54	98813	0.5	2.5	49407	247033
6	55	16543	0.5	2.5	8272	41358
7	56	58650	0.5	3.1	29325	181815
8	57	48609	0.5	2.2	24305	106940
9	58	131875	0.5	3.0	65938	392328
10	59	65344	0.5	2.5	32672	160093
11	60	102000	0.5	1.8	51000	181560
12	61	89250	0.5	1.7	44625	151725
13	62	153000	0.5	1.7	76500	260100
14	63	102000	0.5	1.8	51000	187000
15	64	31875	0.5	1.7	15938	52594
16	65	48609	0.5	2.0	24305	97218
17	66	61359	0.5	1.7	30680	104310
18	67	1055063	0.5	3.8	527532	4044408
19	68	1156266	0.5	5.8	578133	6706343
20	69	380109	0.5	4.3	190055	1634469
21	70	34266	0.5	1.3	17133	42833
22	71	22313	0.5	0.8	11157	16735
23	72	51797	0.5	0.5	25899	25899
24	73	61359	0.5	3.5	30680	214757
25	74	50203	0.5	3.8	25102	189098
26	75	62953	0.5	3.8	31477	239221
27	76	109969	0.5	2.4	54985	261176
28	77	41438	0.5	2.3	20719	95307
29	78	19922	0.5	1.4	9961	27227
30	79	16703	0.5	1.0	8352	16703
31	80	34266	0.5	1.1	17133	36550
32	81	24703	0.5	1.3	12352	30879
33	82	32672	0.5	1.7	16336	54453
34	83	22313	0.5	2.4	11157	52436
35	84	349031	0.5	3.0	174516	1047093
36	85	43669	0.5	3.0	23290	131007
37	86	67734	0.6	3.0	42898	200944
38	87	100088	0.8	1.9	75066	185163
39	88	51000	0.7	3.4	33150	170850
40	89	50203	0.8	3.3	37652	165670
41	90	83672	0.9	2.6	72516	214758
42	91	103953	1.1	2.8	114348	291068
43	92	61359	1.5	2.5	92039	153398
44	93	108375	1.7	2.2	178819	238425
45	94	105984	2.0	1.8	206669	190771
46	95	100406	2.6	1.4	261056	140568
47	96	149813	3.0	1.0	449439	149813
48	97	250000	3.4	0.7	837500	162500
49	98	250000	3.5	0.5	875000	125000

Initial and boundary concentrations of the simulated parameters must be defined to the model for each segment. There are 16 monitoring stations, so the initial concentrations are available for 32 segments. The initial concentrations for the remaining segments are calculated by means of interpolations. Since the start date of the simulation is designated as January 1, 1998 the monitoring data collected during Cruise 4 (November 21 – 23, 1999) is used for interpolation, which is considered to be the most representative date for January among all the cruise dates.

The measured and calculated initial concentrations and boundary concentrations are given in Annex A.

6.2.2 Boundary Conditions

6.2.2.1 Pollutant Loads

Diffuse nutrient loads calculated by Adalı (2004) using MONERIS (**MO**delling **N**utrient **E**missions in **RI**ver **S**ystems) model are used for WASP simulations. MONERIS is a steady state model developed by Behrendt et al. (1999), which roughly estimates the nutrient loads annually, so the loads calculated are in the units of ton/year. However, WASP requires load inputs in the units of kg/day, therefore the calculated values were converted according to the model needs with an assumption that the loads enter the system equally throughout the year. The domestic wastewater loads arising from septic tanks and other diffuse loads adapted from MONERIS estimations are given in Table 6.3. The loads in the table are given after the unit conversion.

The nutrient loads calculated by the MONERIS model are in terms of total nitrogen and total phosphorus. However, the nitrogen loads should be defined as ammonium nitrogen, nitrate nitrogen, organic nitrogen and detrital nitrogen, and the phosphorus loads should be defined as orthophosphate phosphorus, organic phosphorus and detrital phosphorus to the WASP model. It was assumed that the total nitrogen loads were distributed evenly between the referred nitrogen species, and the total phosphorus loads were distributed as 50% orthophosphate, 15% organic phosphorus and 35% detrital phosphorus.

The BOD and SS loads given in Table 3.4 are also converted according to the requirements of WASP. The converted BOD and SS loads are given in Table 6.4.

Table 6.3: The Domestic and Diffuse Loads Adapted from Adalı (2004)

Pollutant Source	Üçtepeler Subwatershed		Alagöl Subwatershed		Dalyan Subwatershed		Gerendüzü Subwatershed	
	N (kg/day)	P (kg/day)	N (kg/day)	P (kg/day)	N (kg/day)	P (kg/day)	N (kg/day)	P (kg/day)
Domestic Wastewater	0.000	0.000	3.274	0.982	159.431	47.829	0.000	0.000
Atmospheric Deposition	0.000	0.000	0.000	0.000	1.066	0.037	0.348	0.012
Surface Runoff	0.252	0.010	2.493	0.142	10.464	2.655	5.788	0.706
Erosion	0.000	0.000	0.004	0.001	1.130	0.193	0.025	0.016
Tile Drainage	0.247	0.027	5.863	0.247	66.192	3.260	0.164	0.011
Groundwater	0.001	0.003	0.011	0.017	0.769	1.070	0.029	0.115
Urban Areas	0.000	0.000	2.620	0.172	35.949	2.398	0.000	0.000

Pollutant Source	Gökbel Subwatershed		Kaunos Subwatershed		Sülüngür Lake Subwatershed		İztuzu Subwatershed	
	N (kg/day)	P (kg/day)	N (kg/day)	P (kg/day)	N (kg/day)	P (kg/day)	N (kg/day)	P (kg/day)
Domestic Wastewater	7.867	2.360	0.000	0.000	0.000	0.000	0.000	0.000
Atmospheric Deposition	0.106	0.004	0.000	0.000	0.973	0.034	0.272	0.010
Surface Runoff	2.990	0.141	2.625	0.234	1.209	0.118	0.705	0.055
Erosion	0.000	0.000	0.032	0.010	0.008	0.003	0.000	0.000
Tile Drainage	1.397	0.082	6.192	0.411	4.904	0.384	0.000	0.411
Groundwater	0.003	0.008	0.036	0.064	0.019	0.063	0.005	0.059
Urban Areas	13.967	0.917	0.000	0.000	0.000	0.000	0.000	0.000

Table 6.4: Estimated BOD and SS Loads of Septic Tank Effluent

Alagöl Subwatershed		Dalyan Subwatershed		Gökbel Subwatershed	
BOD (kg/day)	SS (kg/day)	BOD (kg/day)	SS (kg/day)	BOD (kg/day)	SS (kg/day)
10.915	7.859	531.436	382.634	26.223	18.880

The model segments which receive the pollutant loads from the subwatersheds are determined by checking the maps indicating the locations of the subwatersheds and the model segments. The distribution of pollutant loads through the segments is given in Table 6.5.

Table 6.5: The Distribution of Pollutant Loads through the Segments

Subwatershed	WASP Segment
Üçtepeler	2, 51
Alagöl	35, 84
Dalyan	44, 93
Gerendüzü	18, 67
Gökbel	20, 69
Kaunos	43, 92
Sülüngür	18, 19, 20, 67, 68, 69
İztuzu	3, 52

6.2.2.2 Water Temperature Function

The water temperature of each segment varies temporally, since 98 segments were specified to WASP for Köyceğiz–Dalyan Lagoon 98 temperature functions are required. However, WASP allows specifying 4 temperature functions, so calculations were made to estimate temperature functions.

In the first step, the measured temperature values were interpolated in the horizontal direction. The spatial temperature distribution in the system was carried out for each cruise conducted during the monitoring study conducted by Gürel (2000). The temporal variation of temperatures was generated by interpolating temperatures for each segment over time using a temporal resolution of one month.

The segments which have the closest temperature values were classified into 4 groups for the spatial and temporal distribution.

6.2.2.3 Air Temperature

The daily air temperature data obtained from the State Meteorological Services was used for the WASP simulations. The air temperature time series used for the WASP simulations are given in Figure 6.3. The details of this parameter are given in Chapter 3.

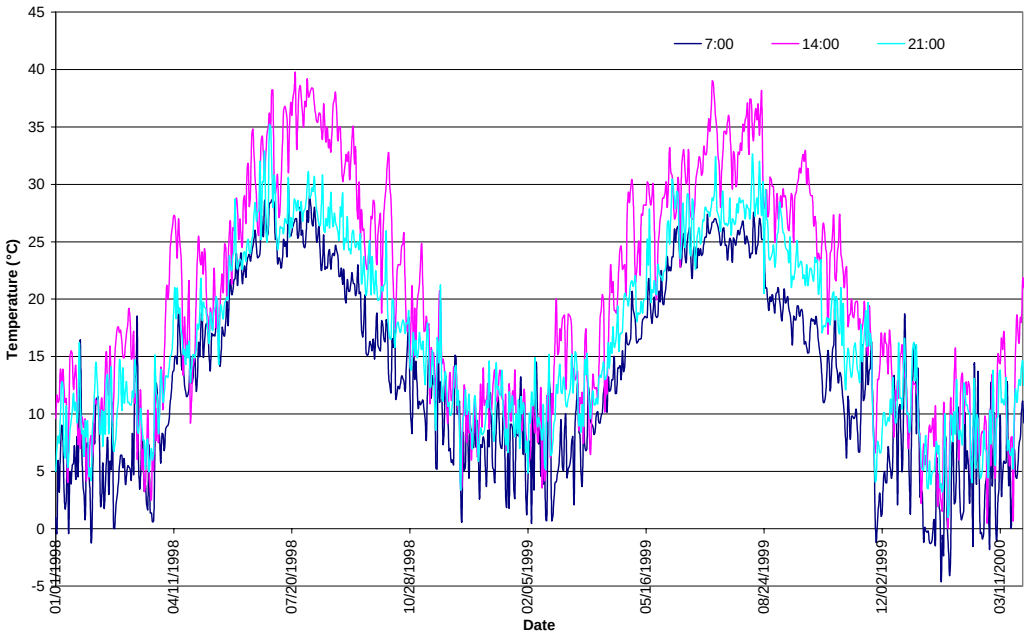

Figure 6.3: Air Temperature Time Series Data from 01/01/1998 to 30/03/2000

6.2.2.4 Daily Solar Radiation

Long term average monthly solar radiation data obtained from the State Meteorological Services was used for the WASP simulations. Fraction of daylight is calculated by using the duration of solar radiation in a day. The solar radiation intensity data used in the model is given in Figure 6.4. The details about this parameter are given in Chapter 3.

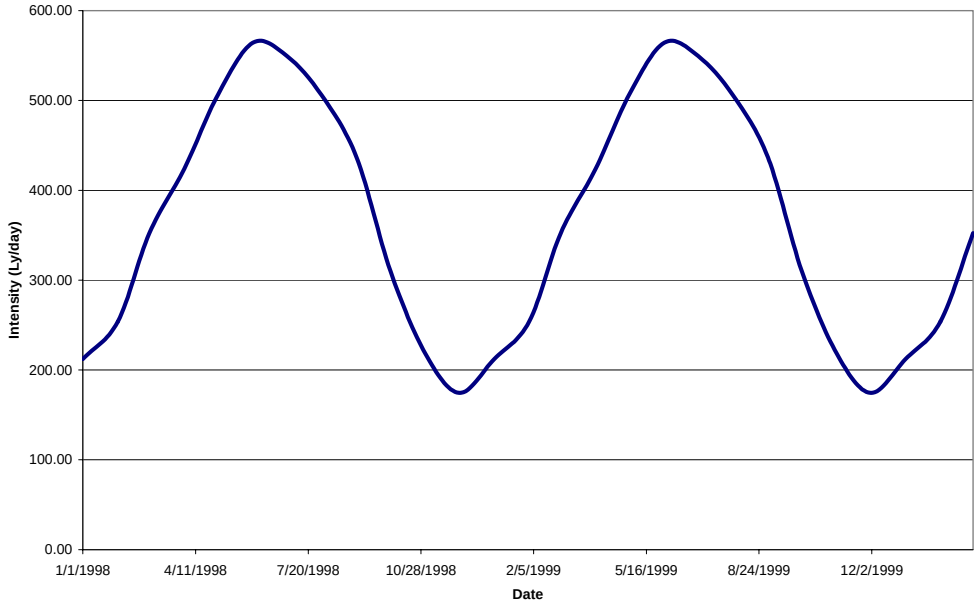

Figure 6.4: Solar Radiation Intensity Data Used in the Model

6.2.2.5 Wind Speed

The wind data obtained from the State Meteorological Services was used for the WASP simulations. The wind speed time series used for the WASP simulations are given in Figure 6.5. The details of this parameter are given in Chapter 3.

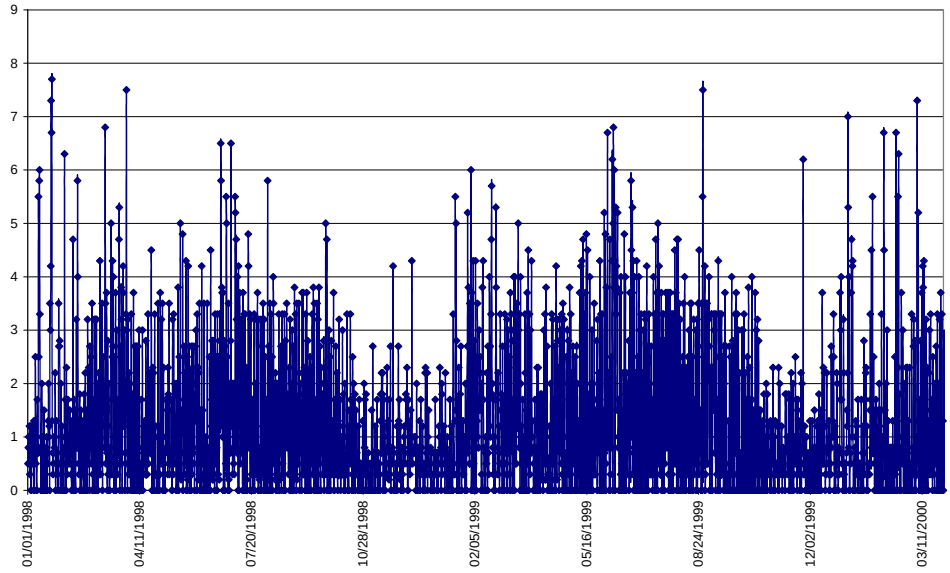

Figure 6.5: Wind Speed Time Series Data from 01/01/1998 to 30/03/2000

6.2.2.6 Flows and Exchanges

The complex geomorphological structure of the Lagoon caused problems in water budget calculations. Therefore, the water budget calculation studies were initiated with simplified systems and simple salinity mass balance approaches. The first model network developed consisted of 49 model segments and 63 links between them for each layer (Figure 6.2).

As mentioned in Chapter 3, Dalyan Lagoon has two boundary conditions, an upstream boundary connecting the Lagoon to the Lake, and a downstream boundary of the Mediterranean Sea. In the first step DYNHYD5 (Ambrose et al., 1993b) was used to conduct one-dimensional hydrodynamic calculations by Ertürk (2002). DYNHYD5 code was recompiled to run the model under Windows® operating system. The annual average surface elevations of Mediterranean Sea and Köyceğiz Lake were used as the boundary conditions. At the end of this study, one-dimensional steady state results for the channel network, which gives flow transmitting capacity of individual channels, were obtained. The model was calibrated by using Manning roughness coefficient and validated by utilizing the water budget calculations conducted for Köyceğiz Lake by Üstün (1998). Then, two dimensional vertical hydraulic calculations were carried out using DYNHYD5 results utilizing salinity profiles generated by Gürel (2000). The model coupled with

Lung O'Connor (Lung, 1992) method was used for these calculations. At the end of the study, two dimensional vertical (two layer) flow rate distribution for all channels were estimated. The flows were estimated with the salinity gradients in the system and the model was calibrated by changing the vertical eddy diffusion coefficients. The available salinity data at the boundaries were used to calculate salinity values for the entire system within this study. The estimated flows were checked using the field data obtained from another monitoring study. Modifications were made on an open source old version of WASP/EUTRO based on WASP 5.1 to enable salinity simulations. Then, the model was run with the estimated flow rates from DYNHYD5/Lung O'Connor method. The salinity results obtained from the modified EUTRO were compared with the field observations, and were found to be consistent. After this study, better meteorology and water surface elevation data were obtained, and inflows through the upper boundary were estimated using daily water budget calculations for the Köyceğiz Lake (Ekdal et al., 2003). The inflows from the Mediterranean Sea were updated using average salinity data and the verified flows are used in initial water quality simulations (Gönenç et al. 2004; Ekdal et al., 2005).

The following assumptions were made for the water budget calculation studies;

- Flow rate distribution ratios are the same for one dimensional and two dimensional calculations. This means that the flow rate distribution ratios are assumed to be the same for DYNHYD5 and Lung O'Connor studies. They are assumed to be constant over time and space. Although the flow originating from the Köyceğiz Lake varies temporally, the flow rate distribution ratios are assumed to be equal to the ones achieved with DYNHYD5 and Lung O'Connor.

- The vertical eddy diffusion coefficient was assumed to be constant over time and space.

- The inflow originating from the Mediterranean Sea was assumed to be constant over time and space, as there is no significant tidal or other affects causing fluctuations.

36 flow functions were defined to the model, the flow rates and their pathways used for the Köyceğiz–Dalyan Lagoon Water Quality Modeling study are given in Annex

B and Annex C, respectively. The constant flows entering to the system from the Mediterranean Sea through bottom layer are represented by Q_1–Q_{25}, and the dynamic flows entering the system from the Köyceğiz Lake through upper layer are represented by $Q_{26} - Q_{36}$. The dynamic flows originated from Köyceğiz Lake are given in Figure 6.6. The horizontal and vertical exchanges of the segments and eddy dispersion coefficients are given in Annex B.

All the surface and groundwater flows, and the pollutant loads originated from these sources were taken into consideration within polluting sources, which are mainly diffuse.

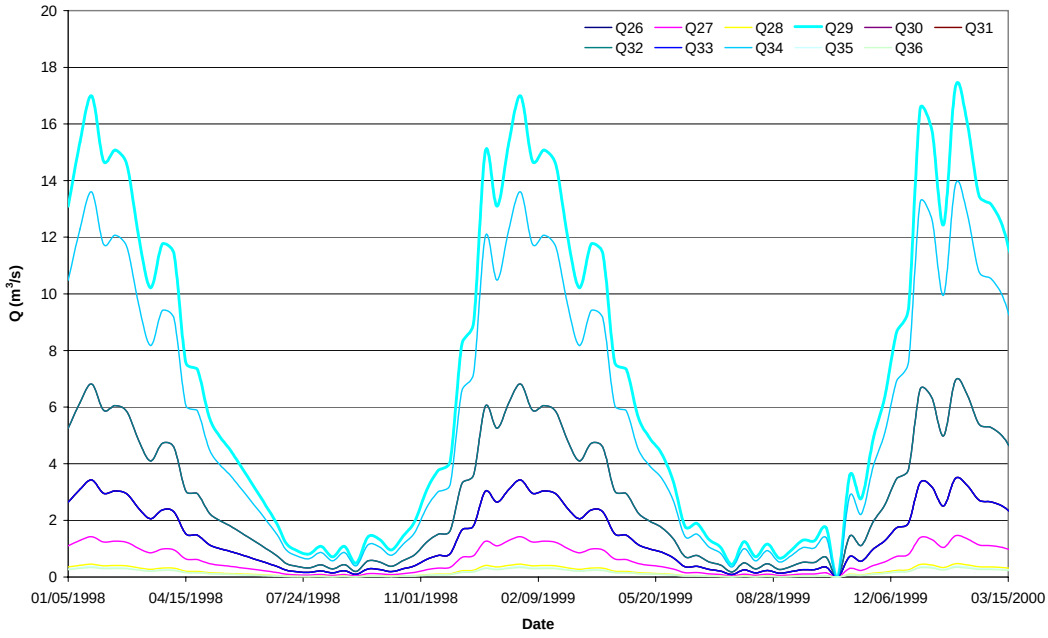

Figure 6.6: Flows Entering to the System from Köyceğiz Lake

6.3 Water Quality Modeling Studies with WASP

After WASP was selected as the appropriate surface water quality model for the Köyceğiz – Dalyan Lagoon the preliminary studies were started with WASP5 which was the available version running under DOS operating system at that time. EUTRO, the eutrophication module of WASP, was used for water quality modeling studies. WASP5 has strict rules in creating input files regarding FORTRAN programming features. While the preliminary studies were ongoing WASP6 the new version of the model, which runs under Windows operating system, was released. WASP6 was a

more user friendly version since it allows creating input files more easily, and it has the capability of interacting with spreadsheet applications. Another enhancement with WASP6 is the addition of a post processor to the program. The post processor helps the user to plot the model results and many model parameters easily, thus provides the evaluation of results faster and better when compared with the old versions. However, the state variables that the model simulates and kinetic mechanisms used in the model are the same for both versions. Therefore, it was decided to use the new version for the studies. When WASP6.1 released salinity was added as a new state variable to the model. However, the number of flows was limited to 25. If the number of flows defined for a system was higher than this, the users were encouraged to couple the Environmental Fluid Dynamics Code (EFDC) hydrodynamic model with WASP. As given in Chapter 6.2.2.6 the number flows defined for the Köyceğiz – Dalyan Lagoon is 36, which exceeds the limit. Unfortunately, due to technical restrictions of EFDC model in grid generation for Köyceğiz – Dalyan Lagoon, it was not possible to couple these two models and since the model was not running with flow numbers exceeding 25 the studies were halted. After negotiations with the developers of the model it was decided to continue the Köyceğiz – Dalyan Lagoon Water Quality Modeling Studies at the United States Environmental Protection Agency, National Exposure Research Laboratory, Ecosystems Research Division, which is located in Athens, Georgia. The simulation results given in this chapter were obtained during the studies conducted in Athens, Georgia between February 25, 2005 and February 25, 2006 under the supervision of Mr. Robert B. Ambrose, Jr, who is one of the principal developers of the model. Upon the arrival to Athens, the latest version of WASP was released to public domain, which simulates more state variables than the older versions and has some improvements in kinetic mechanisms, was used in the studies. The details of WASP7 are given in Chapter 5.

During the water quality modeling studies, the simulations were conducted from the simplest complexity level to higher complexity levels in order to better understand the processes and mechanisms that occur in the system. Therefore, the simulations were carried out in 5 steps. One or more state variables were added in each simulation step. Since the field data obtained by Gürel (2000) were used to generate

input files and for model calibration, the simulation period is selected as January 1, 1998 – March 30, 2000 for all simulations.

6.3.1 Simulation Step 1

In Simulation Step 1, salinity simulations were conducted for analyzing the flows and exchanges defined to the model. The simulation results were compared with the salinity data collected during the field studies. The model was calibrated by changing horizontal and vertical eddy diffusion coefficients. 60 salinity simulations were conducted in this step to get the best salinity calibration fit.

6.3.2 Simulation Step 2

In Simulation Step 2, all the nitrogen state variables (NH_3 – N, NO_3^- – N, Organic Nitrogen and Detrital Nitrogen) available in WASP and phytoplankton were simulated. The model was calibrated through changing the parameters and coefficients affecting the phytoplankton kinetics such as; maximum growth rate, death rate constant (non-zooplankton), phytoplankton settling, detrital settling, endogenous respiration rate and phytoplankton half-saturation constant for nitrogen uptake. The other calibration components are related to nitrogen conversion reactions included in the nitrogen cycle, which are nitrification and detritus dissolution rate constants. 62 simulations were conducted to get the best calibration fit for nitrogen species and phytoplankton concentrations.

6.3.3 Simulation Step 3

In Simulation Step 3, phosphorus species were added to the simulations. All the available state variables of WASP regarding nitrogen (NH_3 – N, NO_3^- – N, Organic Nitrogen and Detrital Nitrogen), phosphorus (PO_4^{3-} – P, Organic Phosphorus and Detrital Phosphorus) and phytoplankton are simulated together. The model was calibrated through changing the parameters and coefficients affecting the phytoplankton kinetics such as; maximum growth rate, death rate constant (non-zooplankton), phytoplankton settling, detrital settling, endogenous respiration rate, phytoplankton half saturation constant for nitrogen uptake and phytoplankton half saturation constant for phosphorus uptake. 26 simulations were conducted to get the

best calibration fit for nitrogen species, phosphorus species and phytoplankton concentrations.

6.3.4 Simulation Step 4

In Simulation Step 4, dissolved oxygen, $CBOD_1$, detrital carbon and salinity parameters were added to Simulation Step 3. Thus, a total number of 12 state variables were simulated. The model was calibrated through changing the parameters and coefficients affecting the phytoplankton kinetics such as; maximum growth rate, phytoplankton settling, detrital settling, phytoplankton half saturation constant for phosphorus uptake. Vertical eddy dispersion coefficients of some segments were also changed for calibration. 42 simulations were conducted to get the best calibration for 12 simulated state variables.

6.3.5 Simulation Step 5

In order to analyze the effects of point and diffuse pollutant loads on the system, load scenarios were developed. In the first load scenario, all the ammonia nitrogen, nitrate nitrogen, organic nitrogen, orthophosphate phosphorus, organic phosphorus, $CBOD_1$, detrital nitrogen and detrital phosphorus loads are increased by 50%. In the second scenario, the loads of the same state variables were increased by 100%, and in the last scenario these loads were decreased by 50%. The results of the simulations are referred and discussed in Chapter 7.

7. RESULTS AND DISCUSSION

The simulation results of Köyceğiz – Dalyan Lagoon water quality modeling studies with WASP model are given and discussed in detail in this chapter. Brief information about the studies conducted on current water quality assessment criteria of marine water and coastal lagoons is also provided.

As previously mentioned in Chapter 6, the simulations were conducted from the simplest complexity level to higher complexity levels in four steps to better understand the processes and mechanisms occurring in the system. As the final step of the simulations, three load scenarios were developed for predicting the response of the system to different loads.

For easier and better evaluation of the model runs, simulation results were plotted for each segment existing in the system and for each state variable simulated. As the simulation results were plotted on the same graph for upper and bottom layers of a segment, 49 graphs were obtained for each state variable simulated for each run. The water quality monitoring data is available for two different depths of each of the 16 monitoring stations representing the upper and bottom layers of a segment. Thus, it was possible to make a comparison between the simulation results and field data just for 32 segments out of 98, during the calibration process.

The plots of the simulation results, which give the best calibration fit for each simulation step, are given in Annex D, E and F. However, only the plots of the segments representing the boundary conditions are provided in these annexes. On the other hand, the discussions in this chapter are conducted on the selected segments 48, 97, 42, 91, 35, 84, 19, 68, 2 and 51. The location of selected segments in the system is marked in Figure 7.1. The reasons for selecting these segments are as follows:

- 48 and 97 represent the upper and bottom layers of the Köyceğiz Lake boundary condition,

- 42 and 91 represent the upper and bottom layers of the segment just after the Dalyan Town,
- 35 and 84 represent the upper and bottom layers of the Alagöl Lake,
- 19 and 68 represent the upper and bottom layers of the Sülüngür Lake,
- 2 and 51 represent the upper and bottom layers of the Mediterranean Sea boundary condition.

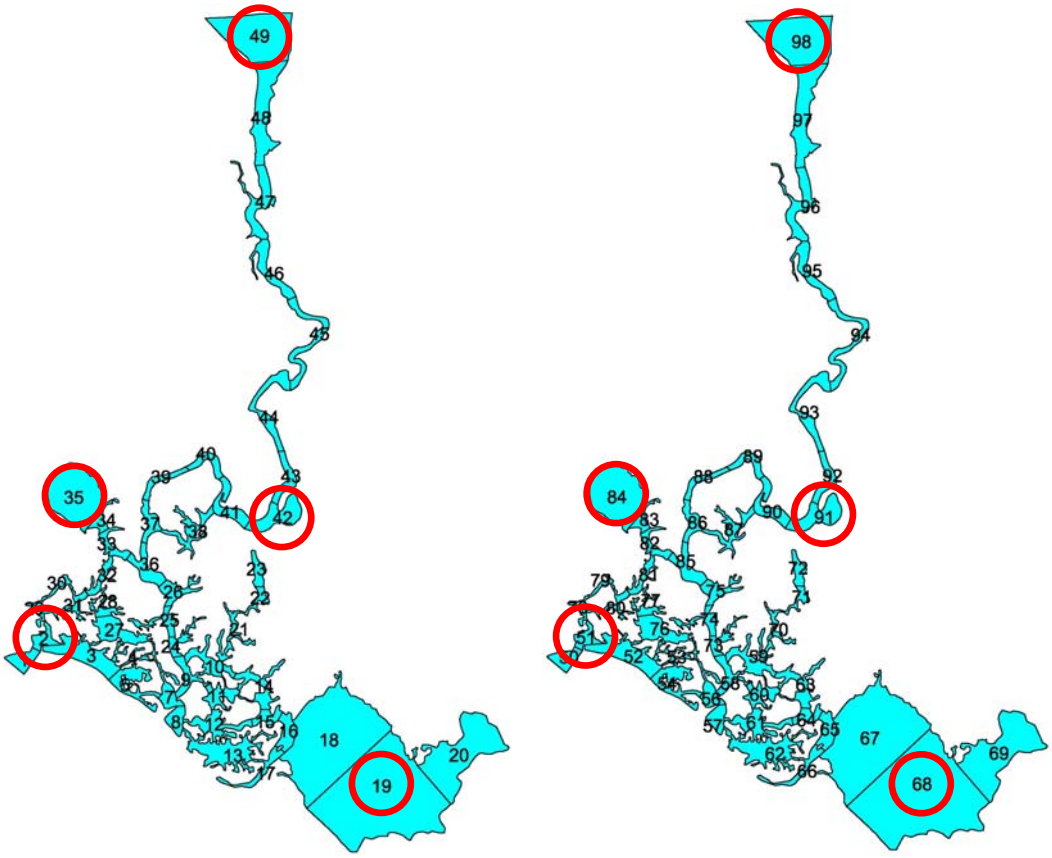

Figure 7.1: The Location of Selected Segments in the System

In the presentation of the simulation results the monitoring data are given as points on the plots, whereas the model predictions are given as curves. The simulation time is 819 days for every parameter simulated, which covers the period of available water quality data used for the model.

7.1 Current Water Quality Assessment Criteria

Eutrophication criteria related to freshwater eutrophication have already been established, whereas the criteria to satisfy the assessment needs of the coastal marine environment have not been fully developed yet; however, the studies on this issue have recently been accelerated within the last years. Such assessments nowadays form an integral part of the national, regional and global programs aiming to protect the coastal environments. Assessments support reviewing the effectiveness of current measures to prevent deterioration of such systems. It is particularly important for countries like Turkey, which has a long coastline with no concrete assessment criteria for marine water quality, to follow the studies on this issue and to benefit from the experience (Gurel et al., 2005b).

Since the response to nutrient enrichment and the significance of related changes in ecosystem dynamics vary considerably regionally, it is quite difficult to recommend single national/international criteria applicable to all coastal waters with different geographical and climatic conditions. Even in some specific cases, multiple criteria may be required for large systems with extended physical gradients, pointing out the fact that regional differences must also be considered during the development of nutrient criteria (Gurel et al., 2005b).

There exists neither an EU nor a national surface water quality standard to discuss and evaluate the state of the general quality conditions of the surface water of Köyceğiz – Dalyan Lagoon.

On the other hand, different approaches have started to be developed for assessing the marine water quality. With this new approach, it is recommended to determine the species one by one in the ecosystem and follow the changes of species related to the changes in nutrient concentrations by ecologists.

Stimulation of primary production usually occurs with small amounts of nutrients. This does not mean that a linear increase of the entire production of the ecosystem is expected, however, generally biological structure and functioning of the overall ecosystem is changed. As a result, sea grasses and slow-growing macro algae are replaced by fast-growing macro algae and phytoplankton, with a final dominance of

phytoplankton at high nutrient loads (Duarte, 1995; Cloern, 2001). One of the important processes is the competition of primary producers, but it is not the only one. The other factors that support shifts in the dominant plant communities are change in water turbidity, changes in the hydraulic conditions resulting in modifications of water residence time and a decline of grazing pressure. During eutrophication these changes in submerged vegetation appear to occur as a step process, with sudden shifts in submerged vegetation. However, they are not directly coupled to increased nutrient loading alone, but many indirect and feedback mechanisms cause their occurrence (Duarte, 1995).

Since the primary producers are the basis of the food web, the changes in the primary producers' structure affect secondary producers. Hydrodynamics, which determine the residence time of nutrients in the lagoon, is as important as the nutrient load for the trophic status of a coastal lagoon. For example, discharging the same amount of nutrients into a leaky lagoon with strong tidal currents will not have the same local effects as will a similar discharge into a choked lagoon with a low water exchange (Gamito et al., 2005).

Eutrophication process can be defined in four sequential phases of oligotrophic, mesotrophic, eutrophic, and hypertrophic. The oligotrophic state of coastal lagoons is generally characterized with abundant sea grasses and transparent water at relatively low nutrient concentrations. Moderate nutrient concentrations, presence of benthic macro algae at the bottom level and some higher phytoplankton concentration in the water column characterize the mesotrophic state. Complex interactions among these primary producers (macro algae and phytoplankton) and with primary consumers (grazers) lead to, in some systems, cycles of alternate dominance by either submerged vegetation or phytoplankton during this phase. These cycles can be relatively stable. However, a large disturbance, with the ability to affect different parts of the ecosystem, can prevail the self-stabilizing capacities, causing a shift from a benthic to a planktonic dominated system (Nienhuis, 1992; Scheffer, 1998).

When high nutrient concentrations exist in the water column, a lagoon is considered eutrophic. The biomass and production of phytoplankton communities that are greatly stimulated with nutrients produce highly turbid waters until the point that the phytoplankton biomass becomes dense enough to limit light access to the bottom,

thus preventing growth of benthic vegetation sea grasses (Nixon and Pelson, 1983). Benthic vegetation is then restricted to shallower areas, mostly disappearing in the deepest zones. Oxygen consumption from degradation of produced organic material increases, especially in the sediment, thus causes anoxic periods. The lack of oxygen and production of toxic gasses, such as hydrogen sulphide, due to the anaerobic condition in the sediment, has detrimental effects on the bottom-living fauna and in the recruitment of species (mainly fishes and crustaceans) that enter into the lagoon as larvae and juvenile stages. Hyper-eutrophy is generally considered an extreme case of eutrophy in which the above-mentioned characteristics are heavily enhanced (Gamito et al., 2005). An idealized sequence of the main features of the eutrophication processes is summarized in Figure 7.2.

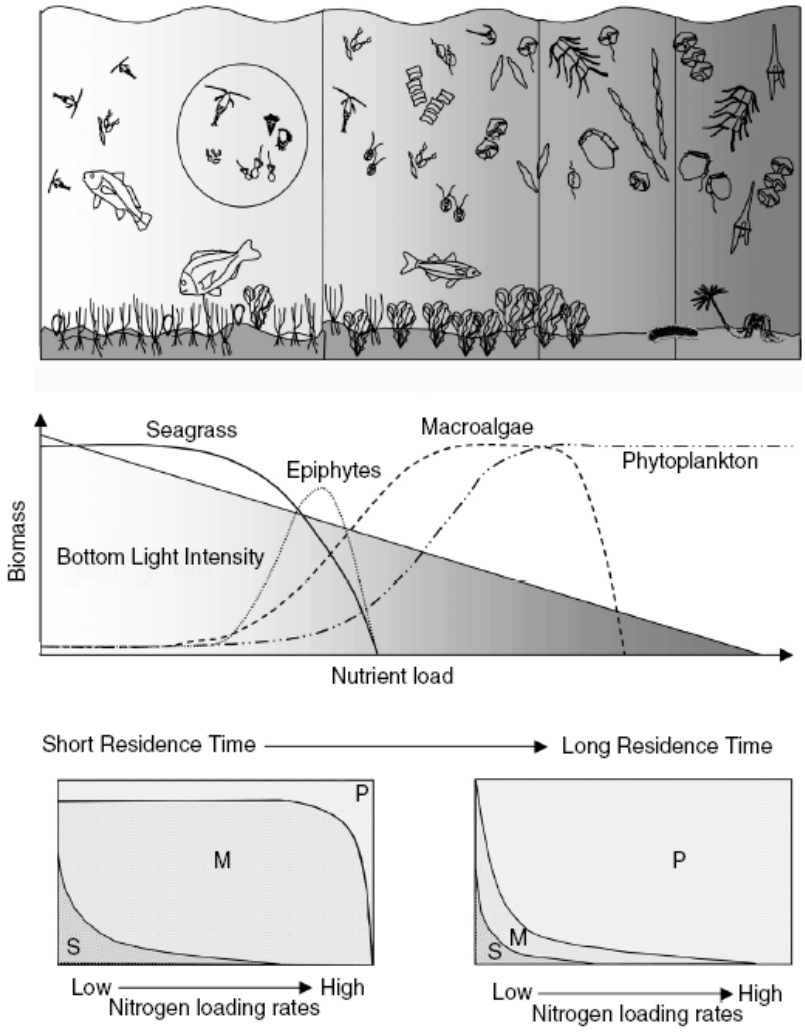

Figure 7.2: Representation of Changes in the Lagoon Ecosystem with Increasing Nutrient Loads (Gamito et al., 2005)

Since there is no adequate data to determine the changes in the biological structure of Köyceğiz – Dalyan Lagoon, it is not possible to utilize this approach for the water quality assessment of the system.

7.2 Simulation Step 1 Results

As mentioned previously in Chapter 6, in Simulation Step 1, salinity simulations were conducted for analyzing the flows and exchanges defined to the model. The simulation results were compared with the salinity data collected during the field studies. The model was calibrated by changing horizontal and vertical eddy diffusion coefficients. 60 salinity simulations were conducted in this step to achieve the best salinity calibration fit.

Köyceğiz Lake boundary condition (Segments 48 and 97) gives the best fit for the salinity simulations result, and its plot is given in Figure 7.3. The model predicts that the salinity concentrations for these segments will vary between 1.2 ppt and 3.6 ppt for the simulation period. Since they represent the boundary condition for Köyceğiz Lake, it is expected that this part of the lagoon is under the effect of the lake throughout the year and the simulation results confirm with this fact.

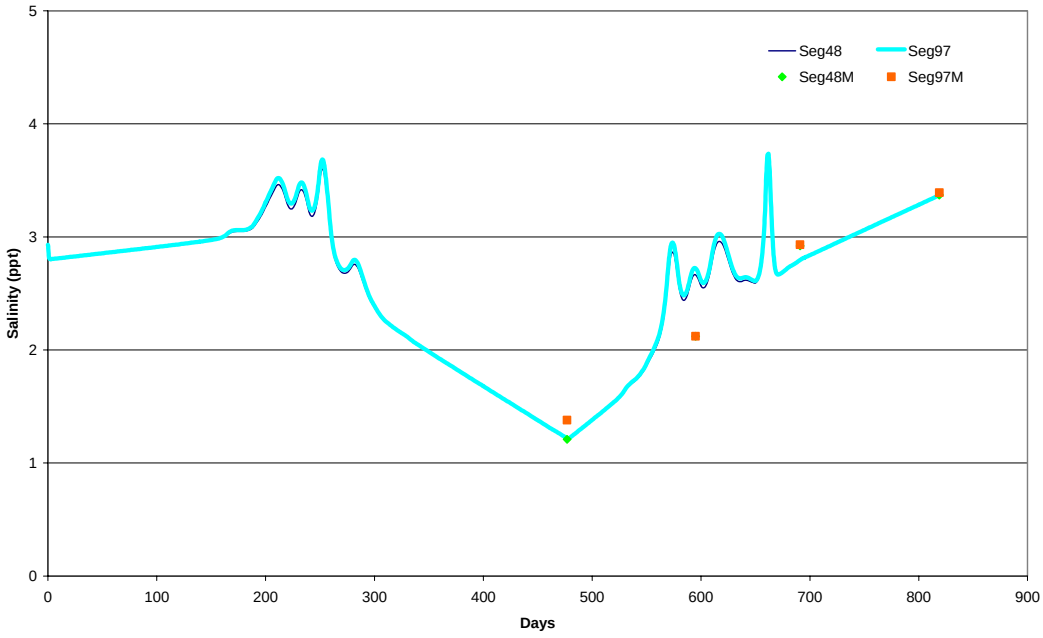

Figure 7.3: Simulation Results and Measured Concentrations of Salinity for the Köyceğiz Lake Boundary Condition

As can be seen from Figure 7.4, the salinity simulation results for the upper layer of Dalyan Town change between 3 ppt and 28 ppt. The model predicts that the effective boundary condition on the lagoon might either be Köyceğiz Lake or the Mediterranean Sea. The dominant boundary condition is the Mediterranean Sea during summer and autumn seasons, whereas the Köyceğiz Lake is dominant for the rest of the year. The simulation results of the bottom layer vary between 15 ppt and 34 ppt. These results indicate that the Mediterranean Sea is the dominant boundary condition for the bottom layer throughout the year. It is clearly observed from the salinity data and simulation results given in Figure 7.4 that throughout the main channel, there is a dual layer flow. The salinity trend of the upper and bottom layers are similar indicating that they are parallel to each other.

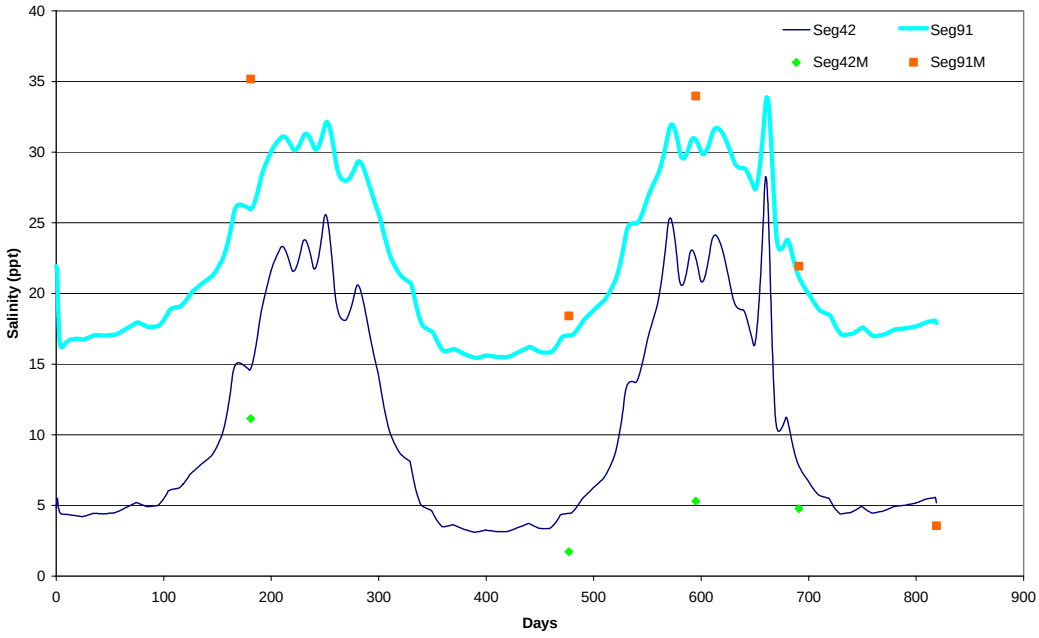

Figure 7.4: Simulation Results and Measured Concentrations of Salinity for Dalyan Town

Figure 7.5 gives the salinity simulation results for Alagöl Lake. The model predictions indicate that the salinity concentrations might change between 6 ppt and 32 ppt for the upper layer of Alagöl Lake. The predicted salinity concentrations are mostly higher than 10 ppt showing that the Mediterranean Sea boundary condition is more dominant than the Köyceğiz Lake boundary condition. The salinity simulations results for the bottom layer of Alagöl Lake vary between 35 ppt and 39 ppt. These results state that the bottom layer is prevailed by the Mediterranean Sea boundary condition throughout the year.

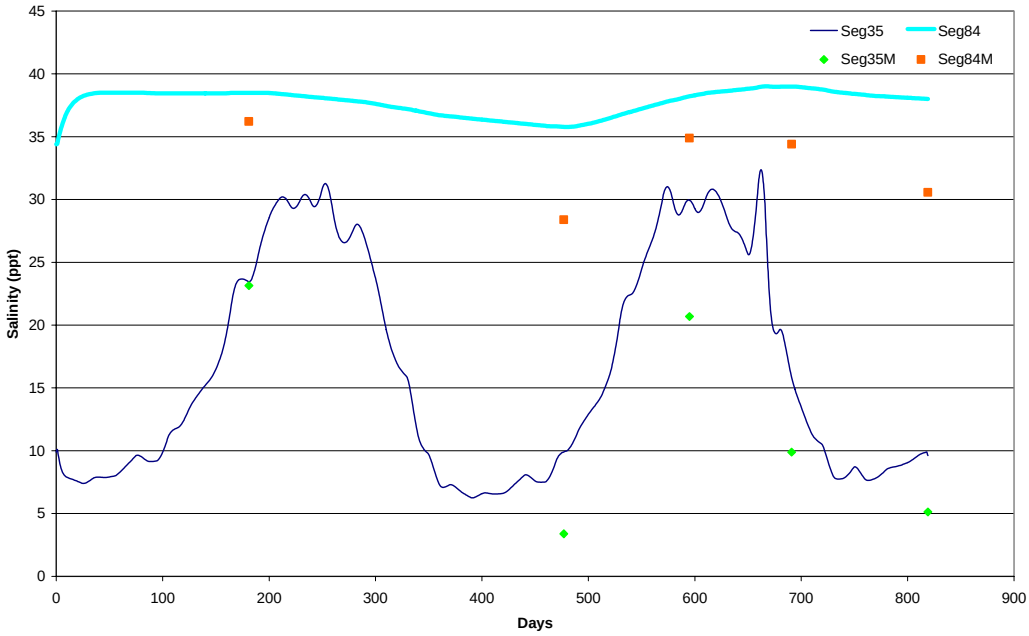

Figure 7.5: Simulation Results and Measured Concentrations of Salinity for Alagöl Lake

The plot of salinity simulation result which give the best calibration fit for Sülüngür Lake is given in Figure 7.6. Sülüngür Lake has the same pattern with Alagöl Lake. The salinity simulation results vary between 7 ppt and 30 ppt for the upper layer of Sülüngür Lake, and 28 ppt and 37 ppt for the bottom layer. Therefore, it can be concluded that the upper layer is dominated by the Köyceğiz Lake for a short period of time, and the bottom layer is always prevailed by the Mediterranean Sea.

As can be seen from Figure 7.7, the model predictions for the upper layer of the Mediterranean Sea boundary condition vary between 9 ppt and 35 ppt. The Köyceğiz Lake has a little effect for a short period of time for this segment. Since the upper layer the Mediterranean Sea boundary condition is the only exit of the system, the fluctuations that last in short period of times are due to the flows originated from the Köyceğiz Lake. The salinity simulations results fit perfectly for the bottom layer.

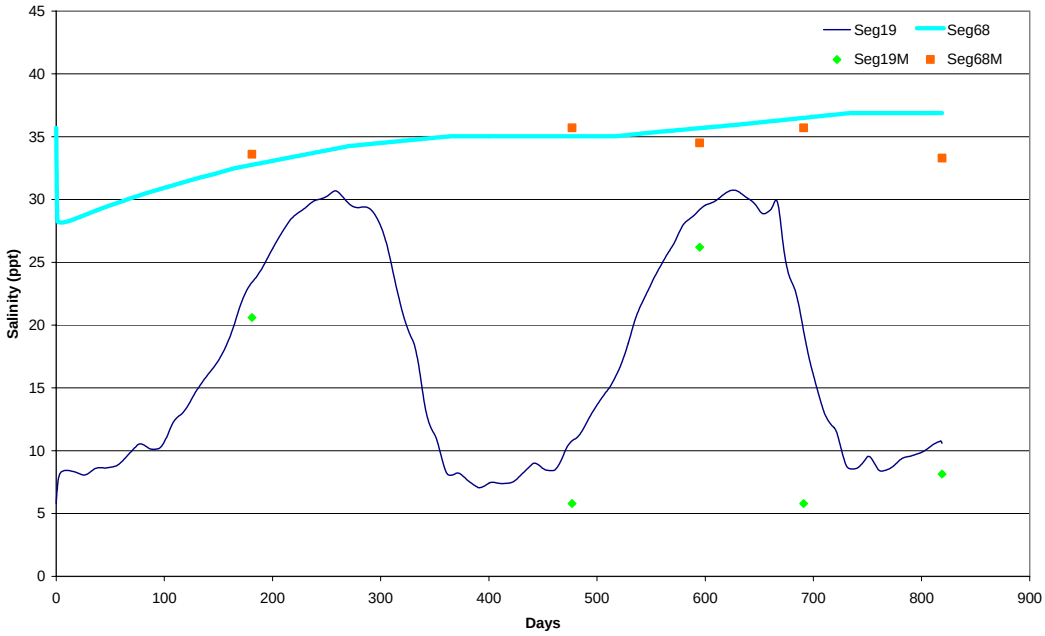

Figure 7.6: Simulation Results and Measured Concentrations of Salinity for Sülüngür Lake

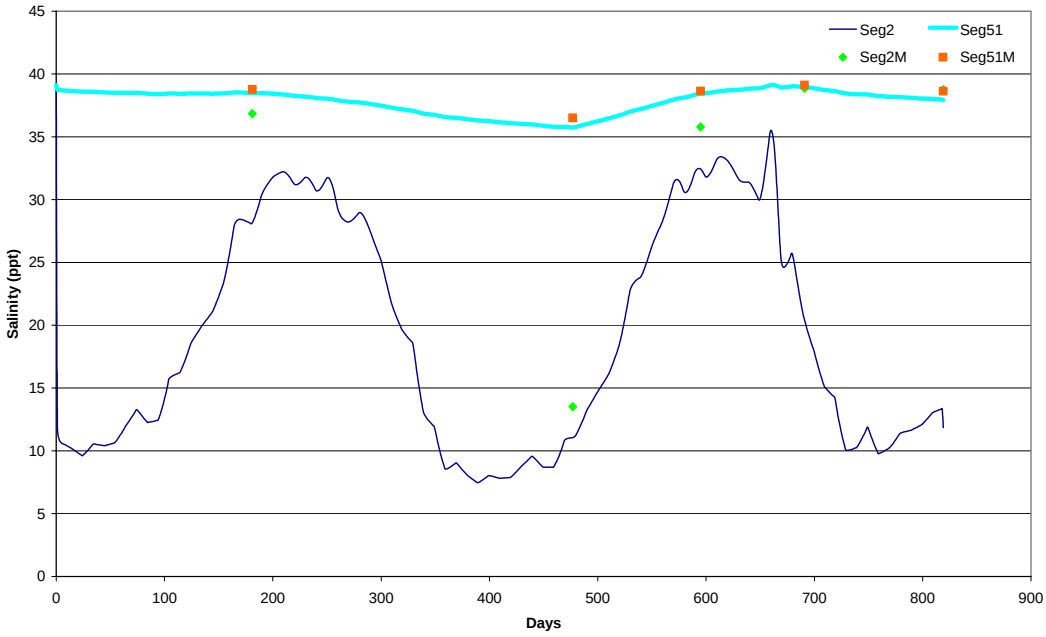

Figure 7.7: Simulation Results and Measured Concentrations of Salinity for the Mediterranean Sea Boundary Condition

When the salinity simulation plots are analyzed for the selected segments referred in this chapter, most of them comply with the monitoring data. However, the simulation results for Alagöl Lake are higher than the monitoring data; this might be due to the assumption that the flow enters to these segments only through horizontal dispersion.

In general, the simulation results indicate that the flow rates, pathways, exchanges and exchange coefficients, are estimated satisfactorily to run the water quality simulations.

7.3 Simulation Step 2 Results

In Simulation Step 2, all the nitrogen state variables (NH_3-N, NO_3^--N, organic nitrogen and detrital nitrogen) available in WASP and phytoplankton were simulated. The model was calibrated through changing the parameters and coefficients affecting the phytoplankton kinetics such as; maximum growth rate, death rate constant (non-zooplankton), phytoplankton settling, detrital settling, endogenous respiration rate and phytoplankton half saturation constant for nitrogen uptake. The other calibration components are related to nitrogen conversion reactions included in the nitrogen cycle, which are nitrification rate constant and detritus dissolution rate. 62 simulations were conducted to get the best calibration fit for nitrogen species and phytoplankton concentrations. The constants and their values used for the best calibration fit are given in Table 7.1. The plots of simulation results of Simulation Step 2 for the segments representing the boundary conditions are given in Annex D for ammonia nitrogen, nitrate nitrogen, and chlorophyll-a. The results for organic nitrogen and detrital nitrogen are not given in Annex D, as they do not affect the phytoplankton growth directly.

7.3.1 Simulation Step 2 NH_3 – N Results

According to the NH_3-N simulation results, the bottom layer of Mediterranean Sea boundary condition has the best calibration fit when compared with the other parts of the system. Simulation results for the upper layer of Mediterranean Sea boundary condition show low instability for a short period of time in summer. The results for the Alagöl Lake are in low compliance with the monitoring data. There exist two field data for the bottom layer of Sülüngür Lake and one measurement has an extreme value when compared with all other measurements, so it is hard to make an evaluation about this segment. The simulation results for the upper layer of Sülüngür Lake are higher than the field data; however, the results indicate the same trend with the measurements. The results for Köyceğiz Lake boundary condition have good

Table 7.1: Simulation Step 2 Calibration Parameters and Their Values

State Variable / Parameter	Constant	Unit	Value
Ammonia	Nitrification Rate Constant at 20°C	day^{-1}	0.1
	Nitrification Temperature Coefficient	-	1.08
Nitrate	Denitrification Rate Constant at 20°C	day^{-1}	0.01
	Denitrification Temperature Coefficient	-	1.08
Organic Nitrogen	Dissolved Organic Nitrogen Mineralization Rate Constant at 20°C	day^{-1}	0.075
	Dissolved Organic Nitrogen Mineralization Temperature Coefficient	-	1.08
Phytoplankton	Phytoplankton Maximum Growth Rate at 20°C	day^{-1}	2
	Phytoplankton Growth Temperature Coefficient	-	1.06
	Phytoplankton Carbon to Chlorophyll Ratio	-	50
	Phytoplankton Half Saturation Constant for Nitrogen Uptake	mg N/L	0.005
	Phytoplankton Half Saturation Constant for Phosphorus Uptake	mg P/L	0.001
	Phytoplankton Endogenous Respiration Rate Constant at 20°C	day^{-1}	0.05
	Phytoplankton Respiration Temperature Coefficient	-	1.045
	Phytoplankton Death Rate Constant (Non-Zooplankton Predation)	day^{-1}	0.04
	Phytoplankton Decay Rate Constant in Sediments	day^{-1}	0.02
	Phytoplankton Phosphorus to Carbon Ratio	-	0.025
	Phytoplankton Nitrogen to Carbon Ratio	-	0.25
Light	Phytoplankton Optimal Light Saturation	langleys/day	350
Detritus	Detritus Dissolution Rate	day^{-1}	0.02

calibration fit except for Cruise 4 whereas the upper layer of Dalyan Town has better calibration fit when compared with its bottom layer.

The plot of the best calibration fit is given in Figure 7.8, and the plots indicating the NH_3-N simulation results of the segments representing the boundary conditions are given in Annex D.

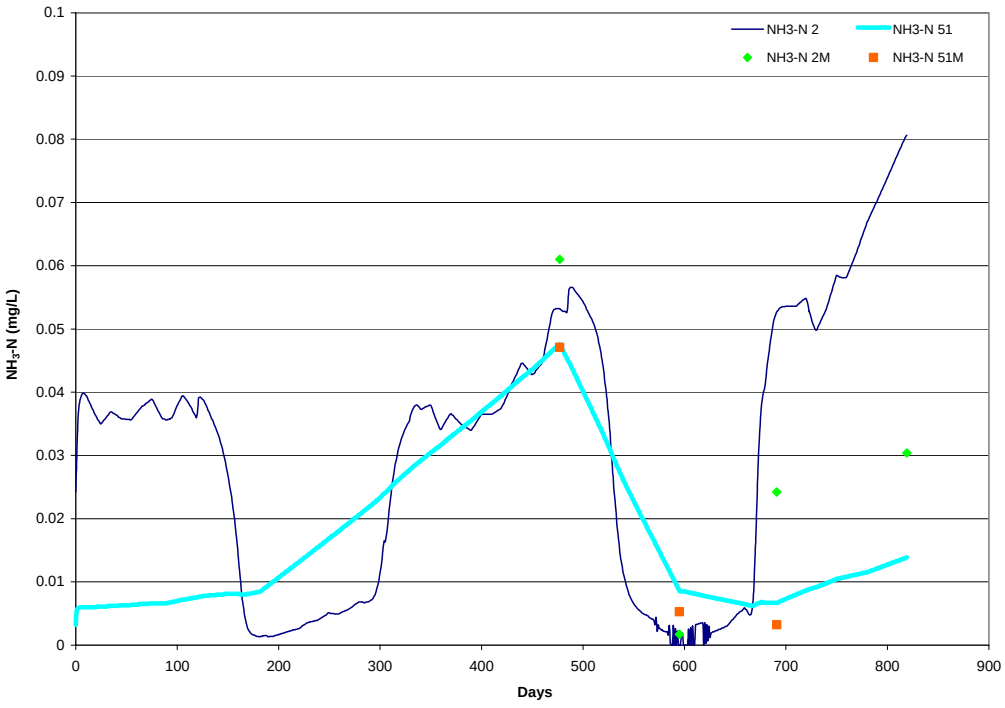

Figure 7.8: Simulation Results and Measured Concentrations of Ammonia Nitrogen for the Mediterranean Sea Boundary Condition

7.3.2 Simulation Step 2 NO_3^- – N Results

When NO_3^--N simulation result plots are analyzed, the best calibration fit is obtained for the Köyceğiz Lake boundary condition. The simulation results for the segments representing the Mediterranean Sea boundary condition, Sülüngür Lake and Alagöl Lake are also in compliance with the monitoring data. Although the time step is calculated by the model itself, the upper layer of the Mediterranean Sea boundary condition has a very low instability for a short period of time in summer. The results obtained especially for the upper layer of Dalyan Town have high differences with the monitoring data when compared with other segments; however, the simulation results have the same trend with the field data.

The NO_3^--N concentrations are higher during spring cruises (cruise 2 and cruise 5), which is also confirmed with the model simulations.

The plot of the best calibration fit is given in Figure 7.9, and the plots indicating the NO_3^--N simulation results of the segments representing the boundary conditions are given in Annex D.

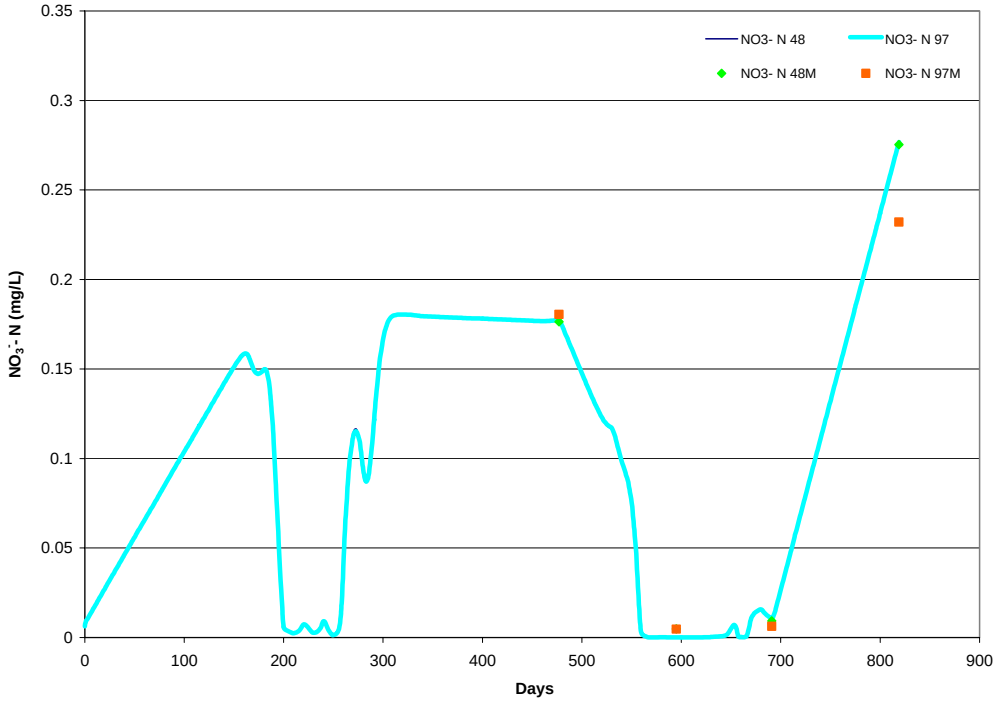

Figure 7.9: Simulation Results and Measured Concentrations of Nitrate Nitrogen for the Köyceğiz Lake Boundary Condition

7.3.3 Simulation Step 2 Organic Nitrogen Results

As the simulation results of organic nitrogen are compared with the monitoring data, the bottom layer of the Mediterranean Sea boundary condition has the best fit for all cruises. The results for the upper layer of this region are also in good agreement with the measured data except for cruise 5. The upper layer results for Sülüngür Lake have better fit when compared with its bottom layer. The results obtained for Alagöl Lake are in low compliance with the monitoring data. The results for Dalyan Town and Köyceğiz Lake boundary condition indicate moderate calibration fit. The plot of the best calibration fit is given in Figure 7.10.

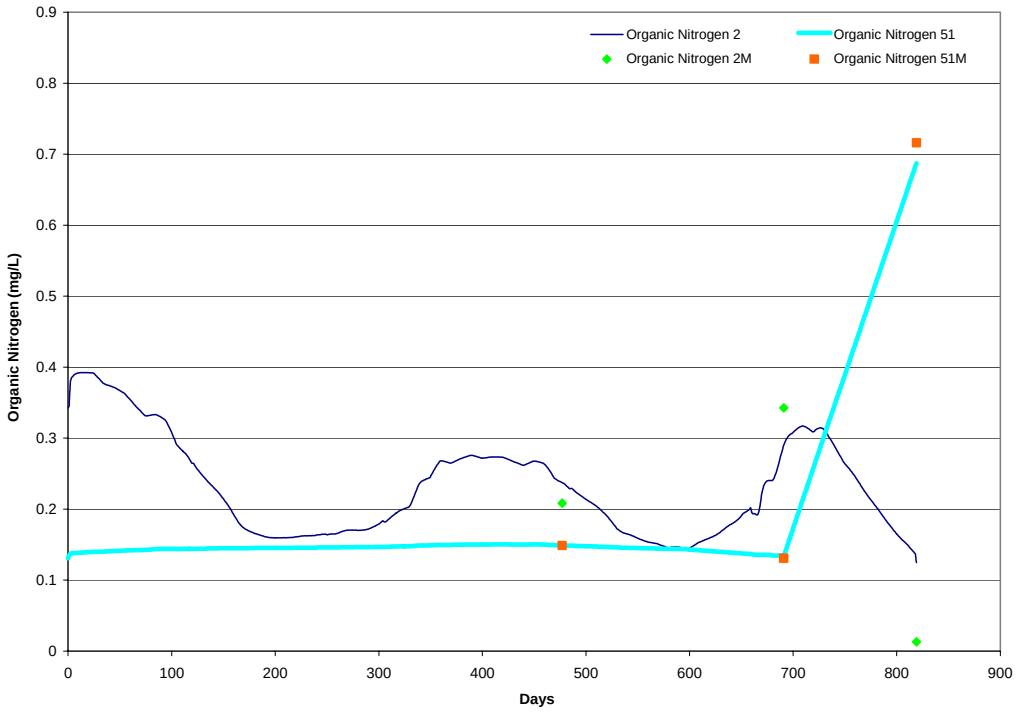

Figure 7.10: Simulation Results and Measured Concentrations of Organic Nitrogen for the Mediterranean Sea Boundary Condition

7.3.4 Simulation Step 2 Detrital Nitrogen Results

The detrital nitrogen simulation result plots indicate that most of them are in compliance with the monitoring data. Köyceğiz Lake boundary condition has the best calibration fit, whereas the upper layer of Mediterranean Sea boundary condition, and Dalyan Town simulation results have the lowest calibration fit when compared with other segments. However, the general trend of simulation results for the upper layer of Mediterranean Sea boundary condition is similar with the field data. The plot of the best calibration fit is given in Figure 7.11.

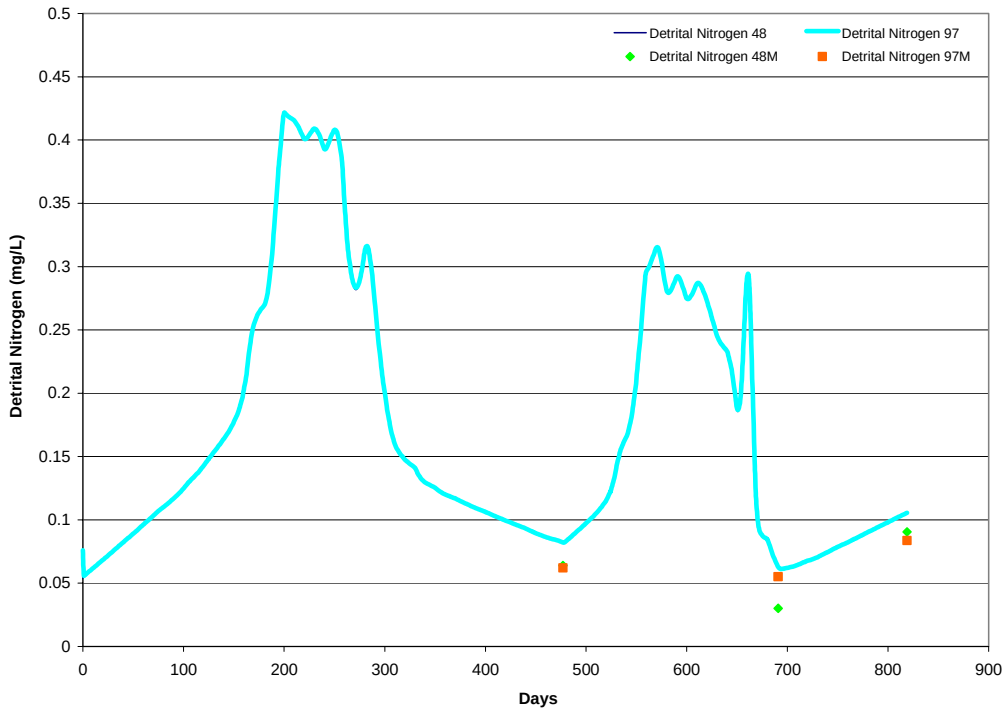

Figure 7.11: Simulation Results and Measured Concentrations of Detrital Nitrogen for the Köyceğiz Lake Boundary Condition

7.3.5 Simulation Step 2 Chlorophyll – a Results

According to the total chlorophyll-a plots the bottom layer of the Mediterranean Sea boundary condition has the best calibration fit when compared with other segments. The simulation results for the upper layer of Mediterranean Sea boundary condition provided good agreement with the monitoring data except for two cruises (Cruise 1 and Cruise 3) conducted in summer. The same pattern is observed for the Köyceğiz Lake boundary condition. Simulation results have the lowest calibration fit for Cruise 3. However, since the monitoring station located at the Köyceğiz Lake boundary is added during Cruise 2 there is no monitoring data available for these segments regarding the first summer cruise. One remarkable conclusion is that the simulation results for summer period are considerably higher than the monitoring data for all segments except for the bottom layer of the Mediterranean Sea boundary condition.

The plot of the best calibration fit is given in Figure 7.12, and the plots indicating the total chlorophyll-a simulation results of the segments representing the boundary conditions are given in Annex D.

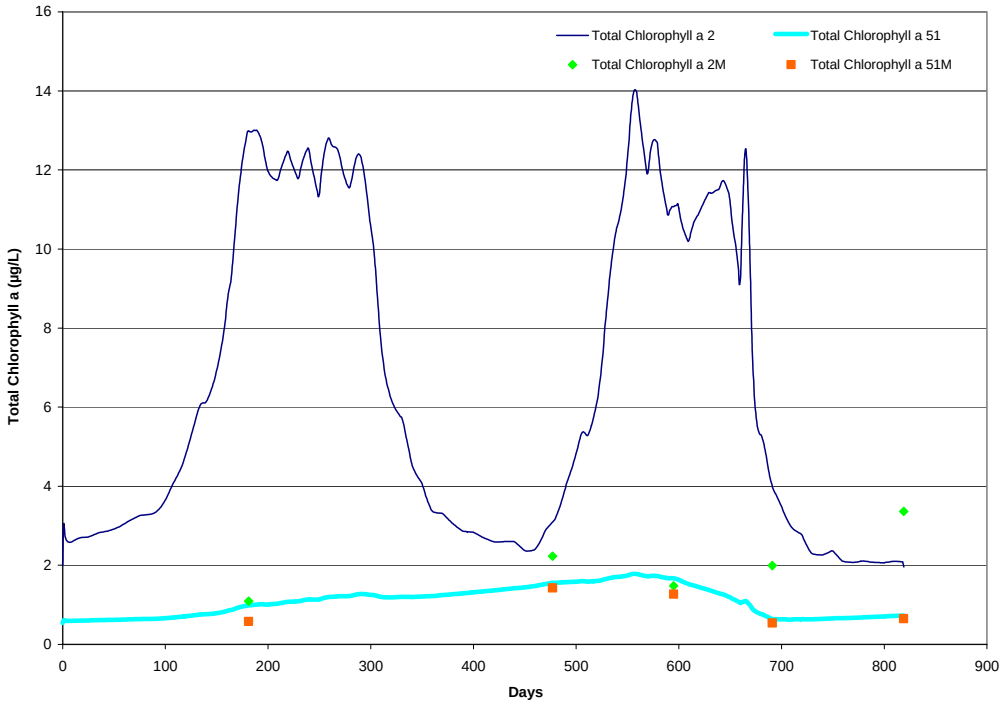

Figure 7.12: Simulation Results and Measured Concentrations of Total Chlorophyll – a for the Mediterranean Sea Boundary Condition

7.4 Simulation Step 3 Results

In Simulation Step 3, phosphorus species were added to the simulations. All the available state variables of WASP regarding nitrogen (NH_3-N, NO_3^--N, organic nitrogen and detrital nitrogen), phosphorus (PO_4^{3-}-P, organic phosphorus and detrital phosphorus) and phytoplankton are simulated together. The model was calibrated through changing the parameters and coefficients affecting the phytoplankton kinetics such as; maximum growth rate, death rate constant (non-zooplankton), phytoplankton settling, detrital settling, endogenous respiration rate, phytoplankton half saturation constant for nitrogen uptake and phytoplankton half-saturation constant for phosphorus uptake. 26 simulations were conducted to get the best calibration fit for nitrogen species, phosphorus species and phytoplankton concentrations. The constants and their values used for the best calibration fit are given in Table 7.2. The plots of simulation results of Simulation Step 3 for the segments representing the boundary conditions are given in Annex E for ammonia nitrogen, nitrate nitrogen, orthophosphate phosphorus and chlorophyll-a.

Table 7.2: Simulation Step 3 Calibration Parameters and Their Values

State Variable / Parameter	Constant	Unit	Value
Ammonia	Nitrification Rate Constant at 20°C	day^{-1}	0.1
	Nitrification Temperature Coefficient	-	1.08
Nitrate	Denitrification Rate Constant at 20°C	day^{-1}	0.01
	Denitrification Temperature Coefficient	-	1.08
Organic Nitrogen	Dissolved Organic Nitrogen Mineralization Rate Constant at 20°C	day^{-1}	0.075
	Dissolved Organic Nitrogen Mineralization Temperature Coefficient	-	1.08
Organic Phosphorus	Dissolved Organic Phosphorus Mineralization Rate Constant at 20°C	day^{-1}	0.22
	Dissolved Organic Nitrogen Mineralization Temperature Coefficient	-	1.08
Phytoplankton	Phytoplankton Maximum Growth Rate at 20°C	day^{-1}	1.5
	Phytoplankton Growth Temperature Coefficient	-	1.06
	Phytoplankton Carbon to Chlorophyll Ratio	-	50
	Phytoplankton Half Saturation Constant for Nitrogen Uptake	mg N/L	0.05
	Phytoplankton Half Saturation Constant for Phosphorus Uptake	mg P/L	0.02
	Phytoplankton Endogenous Respiration Rate Constant at 20°C	day^{-1}	0.05
	Phytoplankton Respiration Temperature Coefficient	-	1.045
	Phytoplankton Death Rate Constant (Non-Zooplankton Predation)	day^{-1}	0.04
	Phytoplankton Decay Rate Constant in Sediments	day^{-1}	0.02
	Phytoplankton Phosphorus to Carbon Ratio	-	0.025
	Phytoplankton Nitrogen to Carbon Ratio	-	0.25
Light	Phytoplankton Optimal Light Saturation	langleys/day	350
Detritus	Detritus Dissolution Rate	day^{-1}	0.02

The results for organic nitrogen, detrital nitrogen, organic phosphorus and detrital phosphorus are not given in Annex D, as they do not affect the phytoplankton growth directly.

7.4.1 Simulation Step 3 NH_3 - N Results

According to the NH_3-N simulation results for the bottom layer of the Mediterranean Sea boundary condition has the best calibration fit among the other segments. The results for Alagöl and Sülüngür Lakes are in poor agreement with the monitoring data. Köyceğiz Lake boundary condition has good calibration fit just for Cruise 5. Dalyan Town also has poor calibration fit.

The plot of the best calibration fit is given in Figure 7.13, and the plots indicating the NH_3-N simulation results of the segments representing the boundary conditions are given in Annex E.

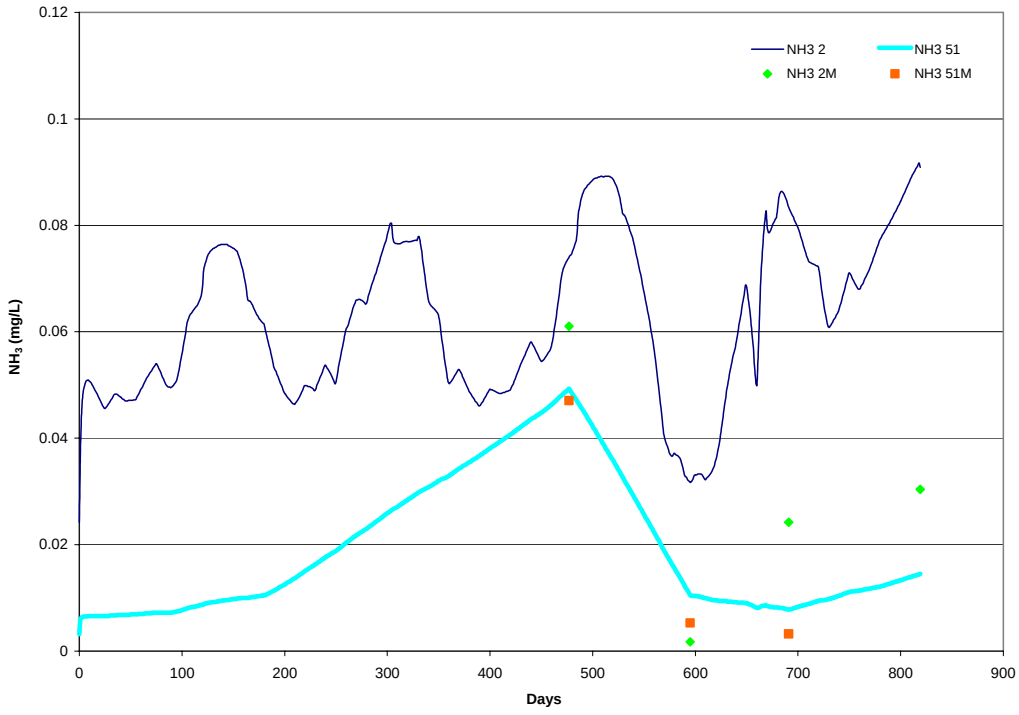

Figure 7.13: Simulation Results and Measured Concentrations of Ammonia Nitrogen for the Mediterranean Sea Boundary Condition

As the phosphorus species were included into the simulations in Simulation Step 3, the NH_3-N concentrations were increased when compared with Simulation Step 2

results. However, the bottom layer of the Mediterranean Sea boundary condition did not indicate any change. The low instability observed at the upper layer of this boundary condition is removed during this simulation step.

7.4.2 Simulation Step 3 NO_3^- - N Results

When NO_3^--N simulation results are analyzed, the bottom layer of the Mediterranean Sea boundary condition has the best calibration fit for all cruises. The second best calibration fit for NO_3^--N simulation is provided for the Köyceğiz Lake boundary condition. Cruise 3, which is the summer cruise, have the lowest fit for these segments. The model generally calculated higher concentrations than the monitoring data for the other plotted segments.

The plot of the best calibration fit is given in Figure 7.14, and the plots indicating the NO_3^--N simulation results of the segments representing the boundary conditions are given in Annex E.

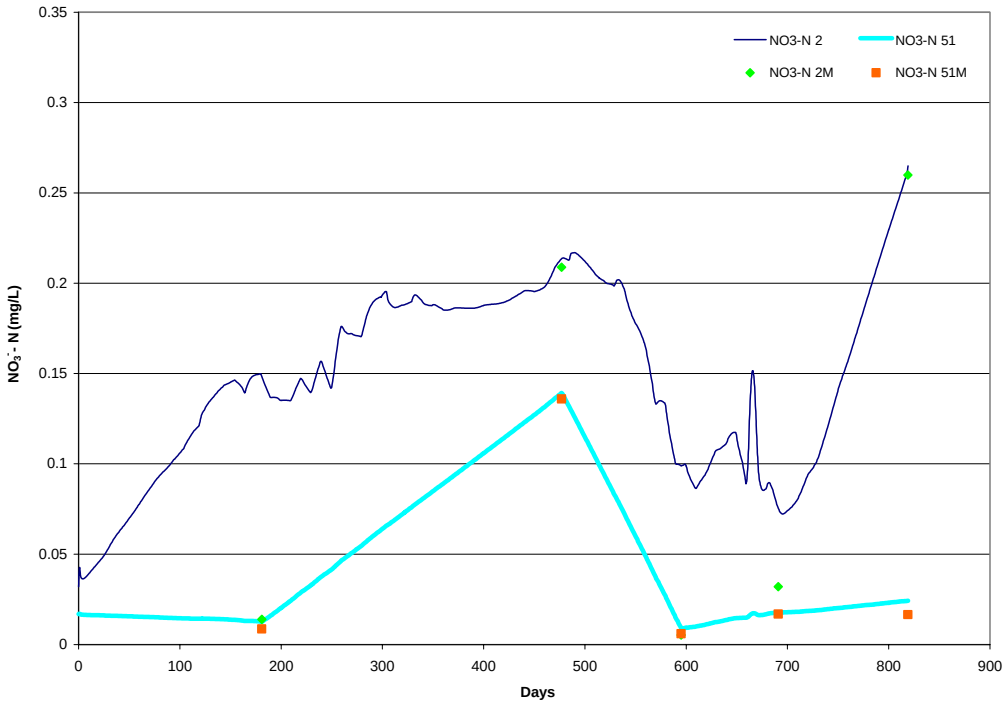

Figure 7.14: Simulation Results and Measured Concentrations of Nitrate Nitrogen for the Mediterranean Sea Boundary Condition

When the NO_3^--N simulation results of Simulation Step 3 are compared with the previous simulation results, it is seen that the NO_3^--N concentrations increased with

the addition of phosphorus species into the simulations. As is the case with the NH_3-N simulation results of Step 3, the bottom layer of the Mediterranean Sea boundary condition did not indicate any change, and the low instability in the concentration of the upper layer of the same boundary condition was removed. Another remarkable result is the increase observed in the NO_3^--N concentration for the bottom layer of Sülüngür Lake.

7.4.3 Simulation Step 3 Organic Nitrogen Results

As the simulation results of organic nitrogen are compared with the monitoring data the bottom layer of the Mediterranean Sea boundary condition has the best fit for all cruises. The results for the upper layer of this boundary condition are also in good agreement with the measured data except for cruise 5. The upper layer results for Sülüngür Lake have better fit when compared with its bottom layer. The results for Alagöl Lake are in poor agreement with the monitoring data. Dalyan Town and Köyceğiz Lake boundary condition indicate moderate calibration fit. The plot of the best calibration fit is given in Figure 7.15.

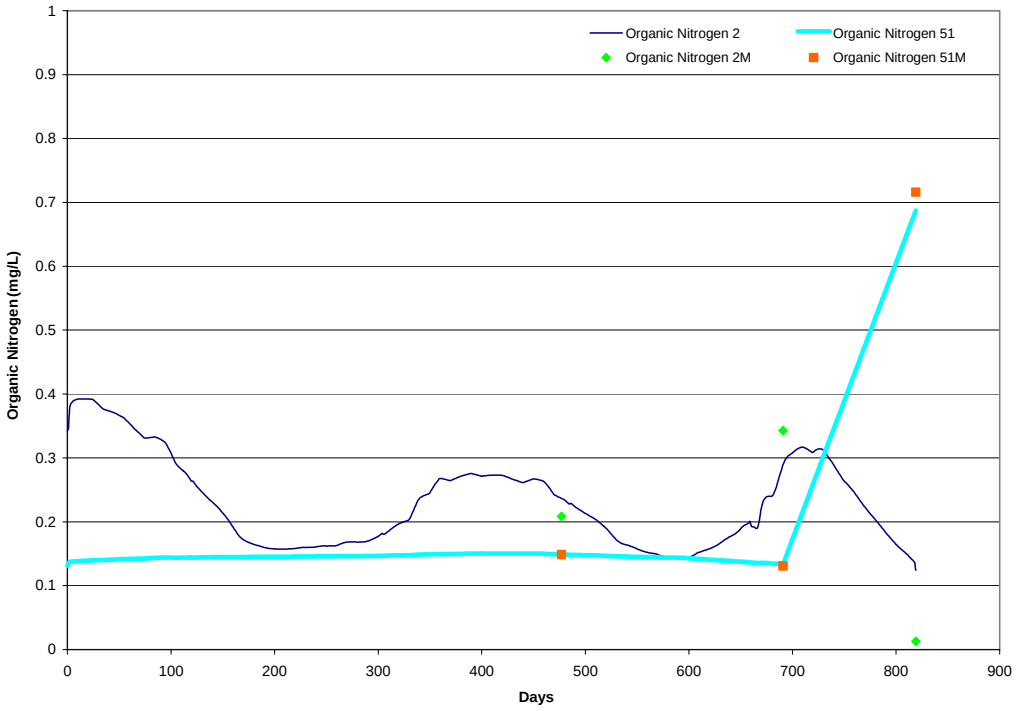

Figure 7.15: Simulation Results and Measured Concentrations of Organic Nitrogen for the Mediterranean Sea Boundary Condition

The organic nitrogen simulation results of step 3 did not show any considerable change when compared with step 2 results. However, a change was observed for the upper layer of the Mediterranean Sea boundary condition, which does not seem to be a significant one. This indicates that including phosphorus species into the simulations did not affect organic nitrogen concentrations.

7.4.4 Simulation Step 3 Detrital Nitrogen Results

When detrital nitrogen simulation results are analyzed, the bottom layer of the Mediterranean Sea boundary condition has the best calibration fit when compared with other segments. Köyceğiz Lake boundary condition has also good calibration fit for this parameter. The field data of the Sülüngür and Alagöl Lakes are generally higher than the model results. However, the model results have the same trend with the field data for these segments. The plot of the best calibration fit is given in Figure 7.16.

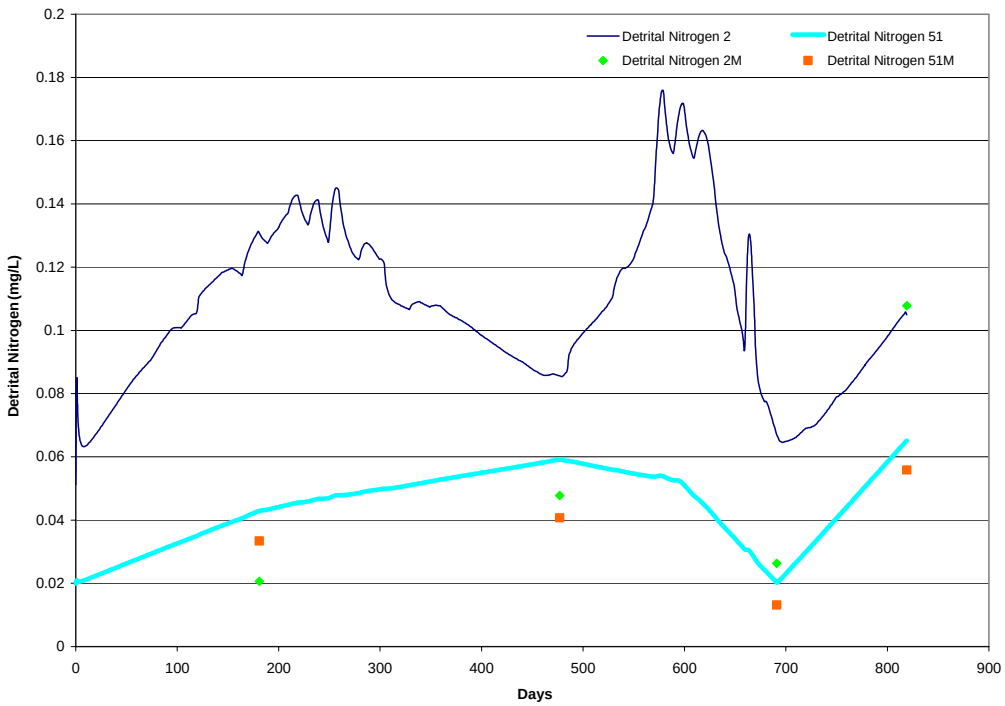

Figure 7.16: Simulation Results and Measured Concentrations of Detrital Nitrogen for the Mediterranean Sea Boundary Condition

The detrital nitrogen concentrations decreased, when compared with step 2 simulation results for this parameter.

7.4.5 Simulation Step 3 Chlorophyll – a Results

According to total chlorophyll-a simulation results, the bottom layer of the Mediterranean Sea boundary condition has the best calibration fit for all cruises. Since the bottom layer of Köyceğiz Lake has just one monitoring data for total chlorophyll-a it is not reasonable to make a comparison with the simulation results for the calibration. The model simulation results are lower than the monitoring data for Sülüngür and Alagöl Lakes. One remarkable conclusion for all segments excluding the bottom layer of the Mediterranean Sea boundary condition is that the simulation results have fluctuations during summer and autumn.

The plot of the best calibration fit is given in Figure 7.17, and the plots indicating the total chlorophyll-a simulation results of the segments representing the boundary conditions are given in Annex E.

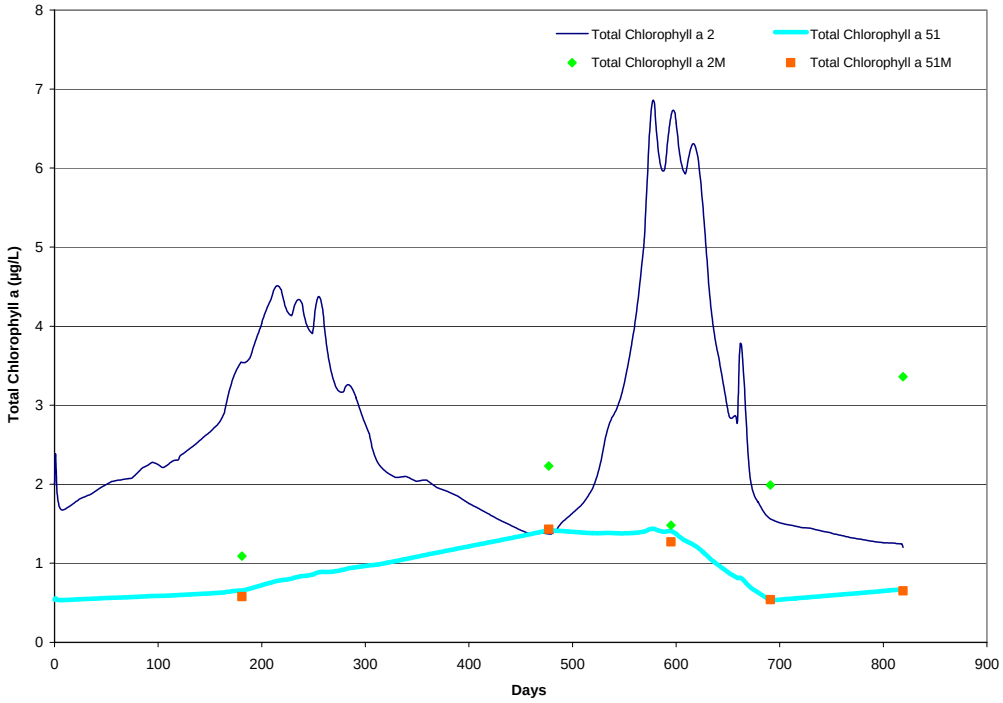

Figure 7.17: Simulation Results and Measured Concentrations of Total Chlorophyll a for Mediterranean Sea Boundary Condition

Simulation Step 3 total chlorophyll-a results are considerably lower than Simulation Step 2 results. This might be due to low phosphorus concentrations, which limits the primary production. Since phosphorus was not included in Simulation Step 2, there was no nutrient limitation related to phosphorus. The nitrogen concentration were

quite enough for primary production; therefore, the total chlorophyll-a concentrations were predicted higher for Simulation Step 2.

As a result, the low phosphorus concentrations decreased the primary production, thus the total chlorophyll-a concentrations were decreased. As the primary production reduced, the concentrations of available nitrogen species (NH_3 – N and NO_3^- – N) used for growth increased. Detrital nitrogen concentration, which is formed with the death of phytoplankton, decreased with less primary production.

7.4.6 Simulation Step 3 Orthophosphate Phosphorus Results

Orthophosphate phosphorus monitoring data is available for the last two cruises. Therefore, it is hard to make reasonable evaluations on the simulation results of this parameter.

7.4.7 Simulation Step 3 Organic Phosphorus Results

The simulation results of organic phosphorus are mostly lower than the monitoring data and only a few results indicate high compliance.

7.4.8 Simulation Step 3 Detrital Phosphorus Results

Detrital phosphorus data is limited; there is no data available for Cruises 1, 2 and 5 and for all cruises for Stations 0 and 14. Since there is lack of monitoring data it is hard to make reasonable evaluations on simulation results.

7.5 Simulation Step 4 Results

In Simulation Step 4, dissolved oxygen, $CBOD_1$, detrital carbon and salinity parameters were added to Simulation Step 3. Thus, a total number of 12 state variables were simulated. The model was calibrated through changing the parameters and coefficients affecting the phytoplankton kinetics such as; maximum growth rate, phytoplankton settling, detrital settling, phytoplankton half-saturation constant for phosphorus uptake. Vertical eddy dispersion coefficients of some segments were also changed for calibration. 42 simulations were conducted to get the best calibration for 12 simulated state variables. The constants and their values used for the best

calibration fit are given in Table 7.3. The plots of simulation results of Simulation Step 4 for the segments representing the boundary conditions are given in Annex F.

Considerable change was observed for Sülüngür Lake for all simulated state variables, due to addition of vertical dispersion between the segments representing the upper and bottom layers of the lake, which has a coefficient of 10^{-5} m^2/s.

7.5.1 Simulation Step 4 NH_3 - N Results

According to the NH_3-N simulation results, the bottom layer of the Mediterranean Sea boundary condition has the best calibration fit among the other segments. The results for Alagöl and Sülüngür Lakes are in low compliance with the monitoring data. Köyceğiz Lake has good calibration fit just for Cruise 2 and Cruise 5. Dalyan Town has also better calibration fit for Cruises 2 and 5.

The plots of the best and worst calibration fits are given in Figure 7.18 and Figure 7.19, respectively. The plots indicating the NH_3-N simulation results of the segments representing the boundary conditions are given in Annex F.

The NH_3-N concentrations predicted for step 4 is almost the same with step 3 results. Slight decrease was observed in the concentration for the upper layer of the Mediterranean Sea boundary condition, which is still higher than Simulation Step 3 result.

Table 7.3: Simulation Step 4 Calibration Parameters and Their Values

State Variable / Parameter	Constant	Unit	Value
Ammonia	Nitrification Rate Constant at 20°C	day^{-1}	0.1
	Nitrification Temperature Coefficient	-	1.08
Nitrate	Denitrification Rate Constant at 20°C	day^{-1}	0.01
	Denitrification Temperature Coefficient	-	1.08
Organic Nitrogen	Dissolved Organic Nitrogen Mineralization Rate Constant at 20°C	day^{-1}	0.075
	Dissolved Organic Nitrogen Mineralization Temperature Coefficient	-	1.08
Organic Phosphorus	Dissolved Organic Phosphorus Mineralization Rate Constant at 20°C	day^{-1}	0.22
	Dissolved Organic Nitrogen Mineralization Temperature Coefficient	-	1.08
Phytoplankton	Phytoplankton Maximum Growth Rate at 20°C	day^{-1}	2
	Phytoplankton Growth Temperature Coefficient	-	1.06
	Phytoplankton Carbon to Chlorophyll Ratio	-	50
	Phytoplankton Half Saturation Constant for Nitrogen Uptake	mg N/L	0.05
	Phytoplankton Half Saturation Constant for Phosphorus Uptake	mg P/L	0.02
	Phytoplankton Endogenous Respiration Rate Constant at 20°C	day^{-1}	0.05
	Phytoplankton Respiration Temperature Coefficient	-	1.045
	Phytoplankton Death Rate Constant (Non-Zooplankton Predation)	day^{-1}	0.04
	Phytoplankton Decay Rate Constant in Sediments	day^{-1}	0.02
	Phytoplankton Phosphorus to Carbon Ratio	-	0.025
	Phytoplankton Nitrogen to Carbon Ratio	-	0.25
Light	Phytoplankton Optimal Light Saturation	langleys/day	350
Dissolved Oxygen	Θ – Reaeration Temperature Correction	-	1.026
	Oxygen to Carbon Stoichiometric Ratio	-	2.67
CBOD (1)	BOD (1) Decay Rate Constant at 20°C	day^{-1}	0.07
	BOD (1) Decay Rate Constant at 20°C	-	1.05
	Fraction of Detritus Dissolution to BOD (1)	-	1
Detritus	Detritus Dissolution Rate	day^{-1}	0.02

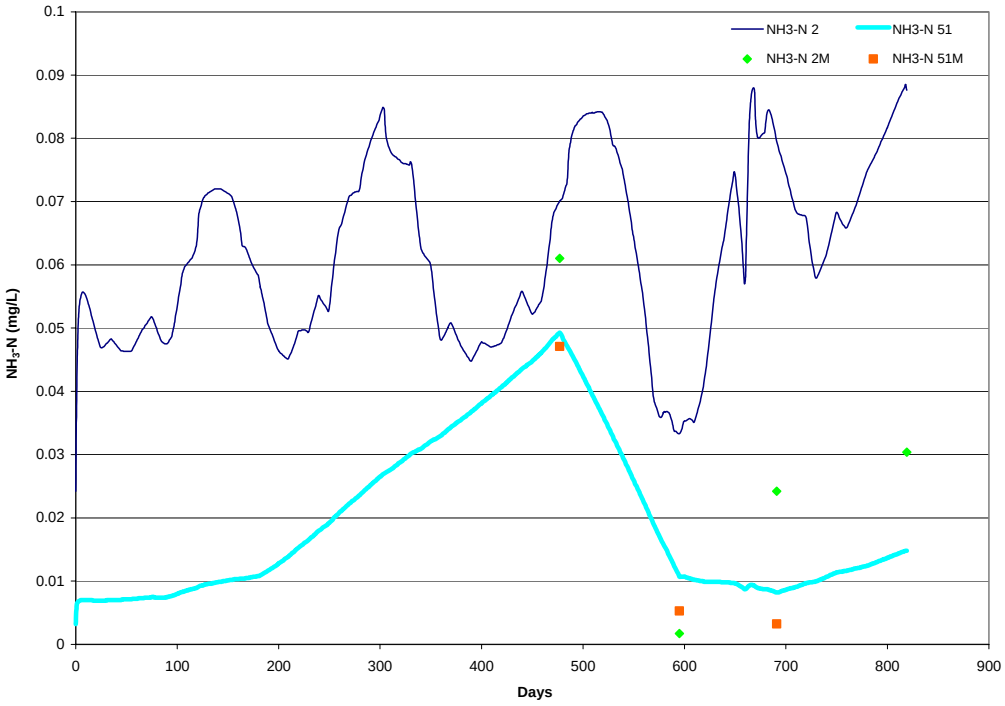

Figure 7.18: Simulation Results and Measured Concentrations of Ammonia Nitrogen for the Mediterranean Sea Boundary Condition

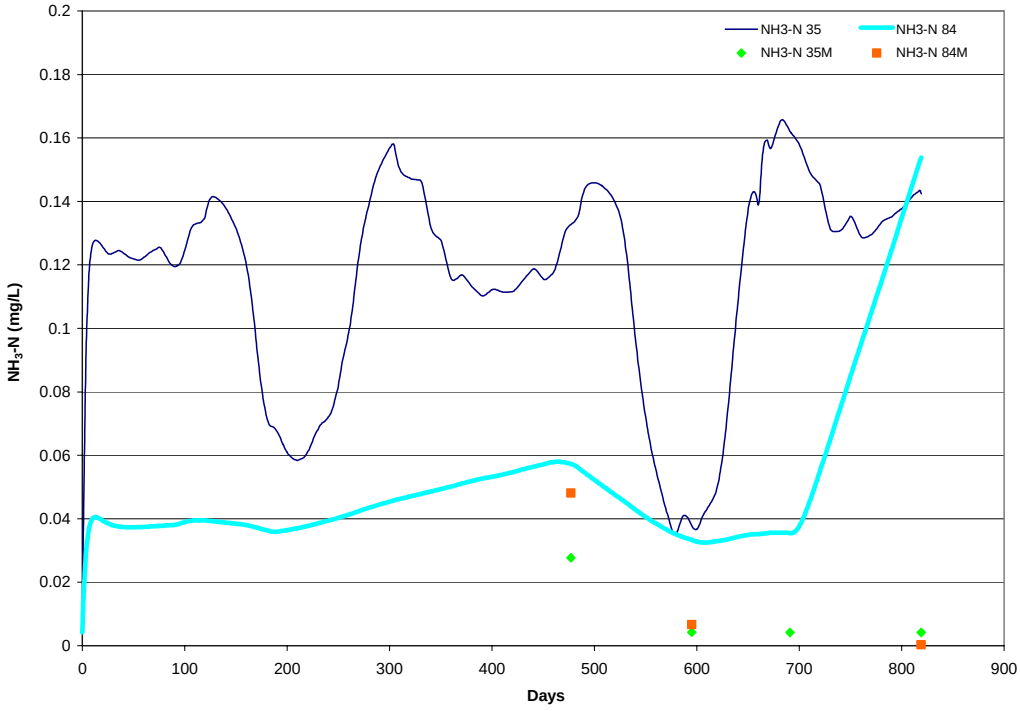

Figure 7.19: Simulation Results and Measured Concentrations of Ammonia Nitrogen for Alagöl Lake

7.5.2 Simulation Step 4 NO_3^- - N Results

When NO_3^--N simulation results are analyzed, the bottom layer of the Mediterranean Sea boundary condition has the best calibration fit for all cruises. The second best calibration fit for NO_3^--N simulation is provided for the Köyceğiz Lake boundary condition. Cruise 3, which represents the summer conditions, has the lowest fit for these segments.

The plots of the best and worst calibration fits are given in Figure 7.20 and Figure 7.21, respectively. The plots indicating the NO_3^--N simulation results of the segments representing the boundary conditions are given in Annex F.

When the NO_3^--N concentrations predicted for step 4 compared with step 3 results, it is seen that the concentrations are almost the same. The NO_3^--N concentration for the upper layer of the Mediterranean Sea boundary condition was slightly increased.

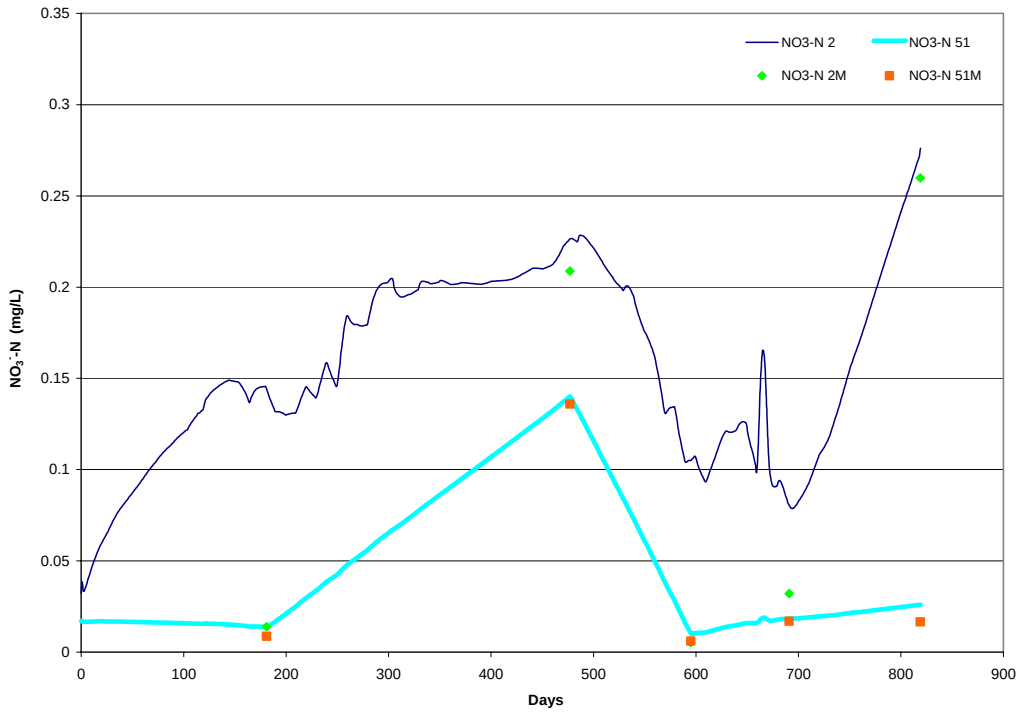

Figure 7.20: Simulation Results and Measured Concentrations of Nitrate Nitrogen for the Mediterranean Sea Boundary Condition

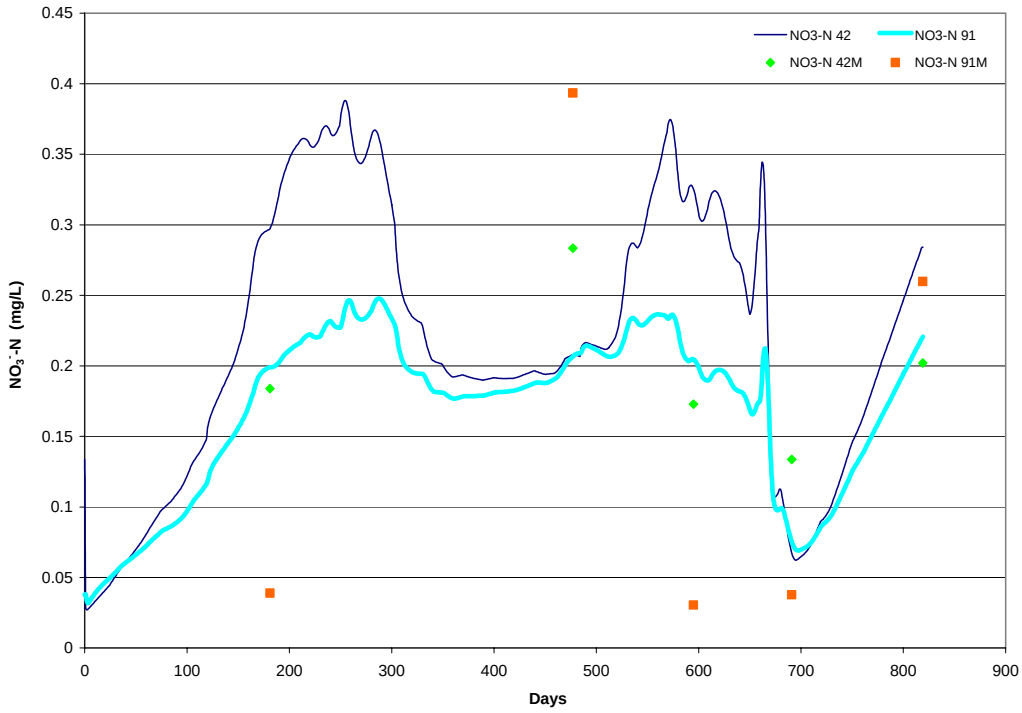

Figure 7.21: Simulation Results and Measured Concentrations of Nitrate Nitrogen for Dalyan Town

7.5.3 Simulation Step 4 Organic Nitrogen Results

According to organic nitrogen simulation results the best calibration fit is provided for the bottom layer of the Mediterranean Sea boundary condition. The upper layer of this boundary condition has also good agreement with the monitoring data except for Cruise 5. Only a few results indicate good agreement with the monitoring data for the other segments.

The plots of the best and worst calibration fits are given in Figure 7.22 and Figure 7.23, respectively. The plots indicating the organic nitrogen simulation results of the segments representing the boundary conditions are given in Annex F.

As the organic nitrogen concentrations predicted for this step compared with step 3 no significant difference between the concentrations was observed except for the upper layer of Sülüngür Lake.

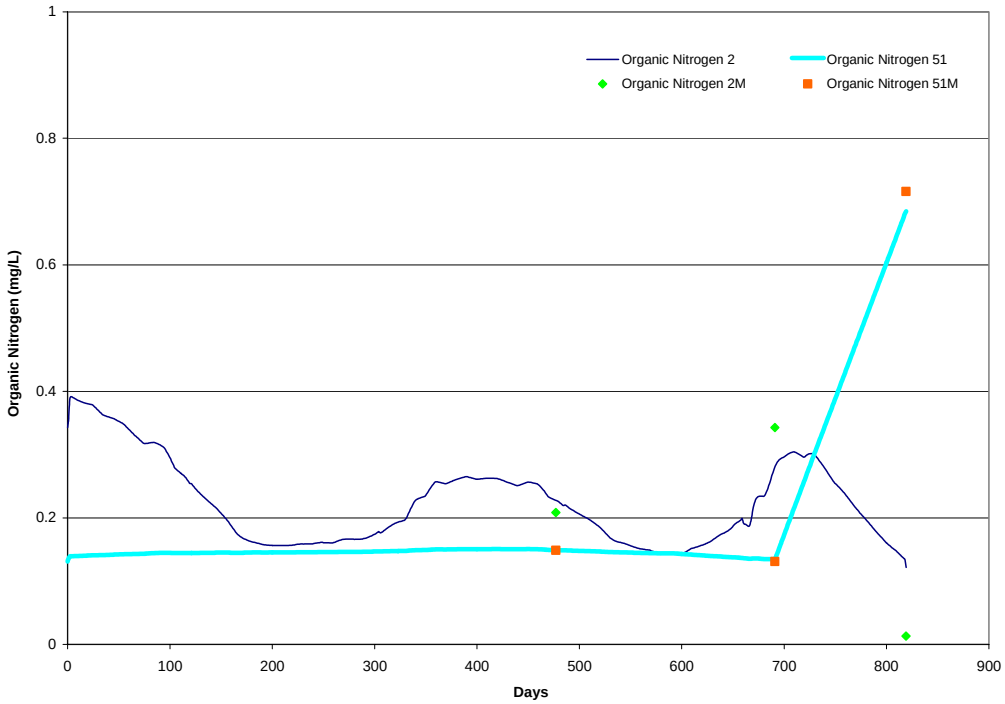

Figure 7.22: Simulation Results and Measured Concentrations of Organic Nitrogen for the Mediterranean Sea Boundary Condition

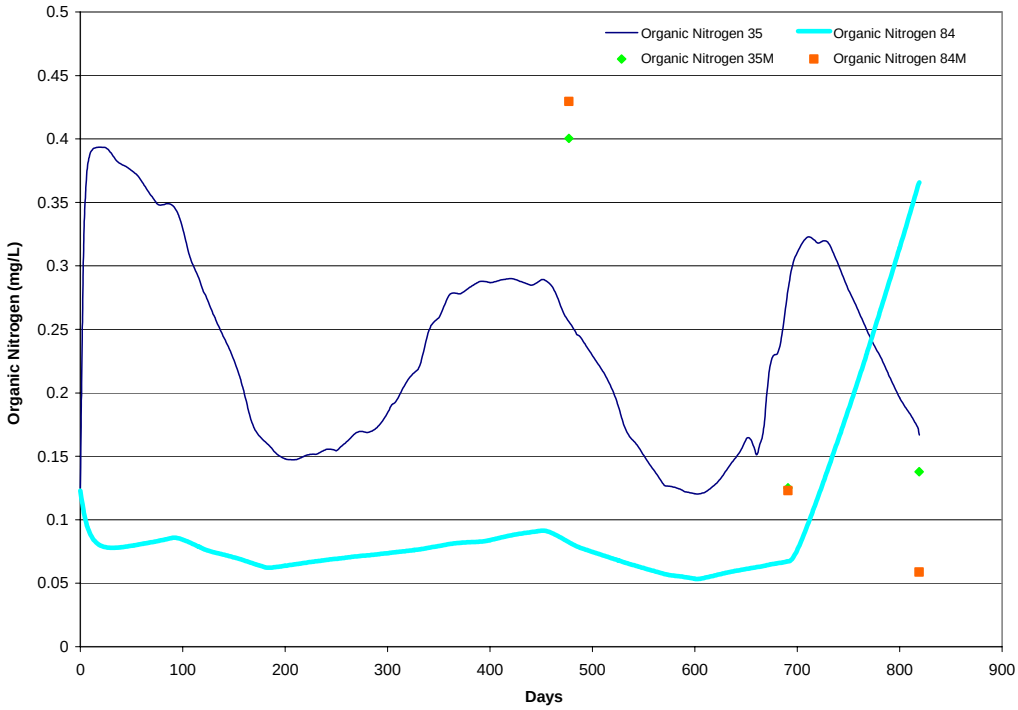

Figure 7.23: Simulation Results and Measured Concentrations of Organic Nitrogen for Alagöl Lake

7.5.4 Simulation Step 4 Detrital Nitrogen Results

The bottom layer of the Mediterranean Sea boundary condition has reasonably good calibration fit for detrital nitrogen when compared with other segments. The simulation results for the upper layer of Sülüngür Lake are also in good agreement with the monitoring data, whereas the simulations results of its bottom layer are considerably lower than the detrital nitrogen measurements. Köyceğiz Lake boundary condition has a certain degree of agreement with the data.

The plots of the best and worst calibration fits are given in Figure 7.24 and Figure 7.25, respectively. The plots indicating the detrital nitrogen simulation results of the segments representing the boundary conditions are given in Annex F.

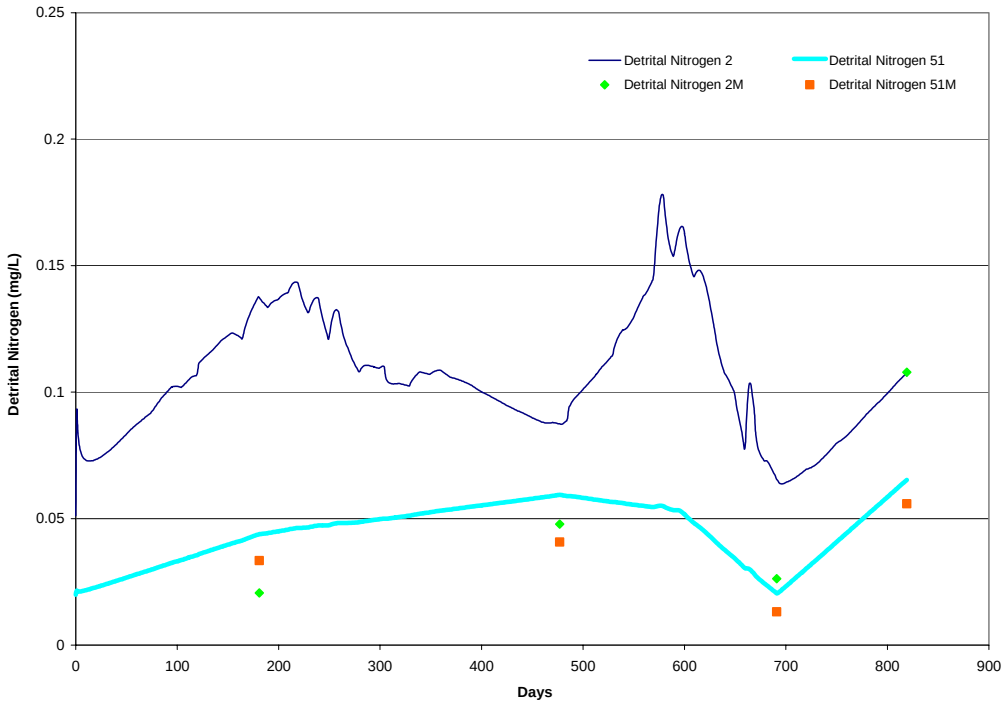

Figure 7.24: Simulation Results and Measured Concentrations of Detrital Nitrogen for the Mediterranean Sea Boundary Condition

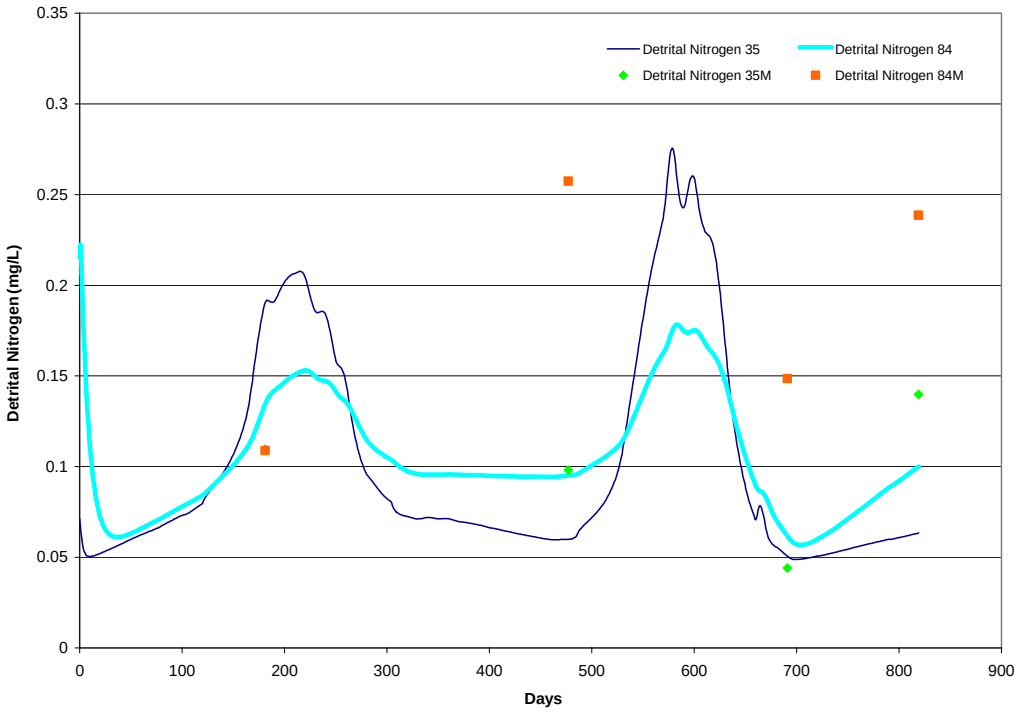

Figure 7.25: Simulation Results and Measured Concentrations of Detrital Nitrogen for Alagöl Lake

7.5.5 Simulation Step 4 Chlorophyll – a Results

When total chlorophyll-a simulation results are analyzed, the bottom layer of the Mediterranean Sea boundary condition has the best calibration fit for all cruises. The simulation results for the upper layer of Sülüngür Lake have reasonably good agreement with the monitoring data. Köyceğiz Lake boundary condition has high degree of calibration fit except one value. The bottom layer of Dalyan Town has the poorest fit when compared with other segments. Since the bottom layer of Köyceğiz Lake has just one monitoring data for total chlorophyll-a, it is not possible to make a reasonable evaluation.

The plots of the best and worst calibration fits are given in Figure 7.26 and Figure 7.27, respectively. The plots indicating the total chlorophyll-a simulation results of the segments representing the boundary conditions are given in Annex F.

Figure 7.26: Simulation Results and Measured Concentrations of Total Chlorophyll a for the Köyceğiz Lake Boundary Condition

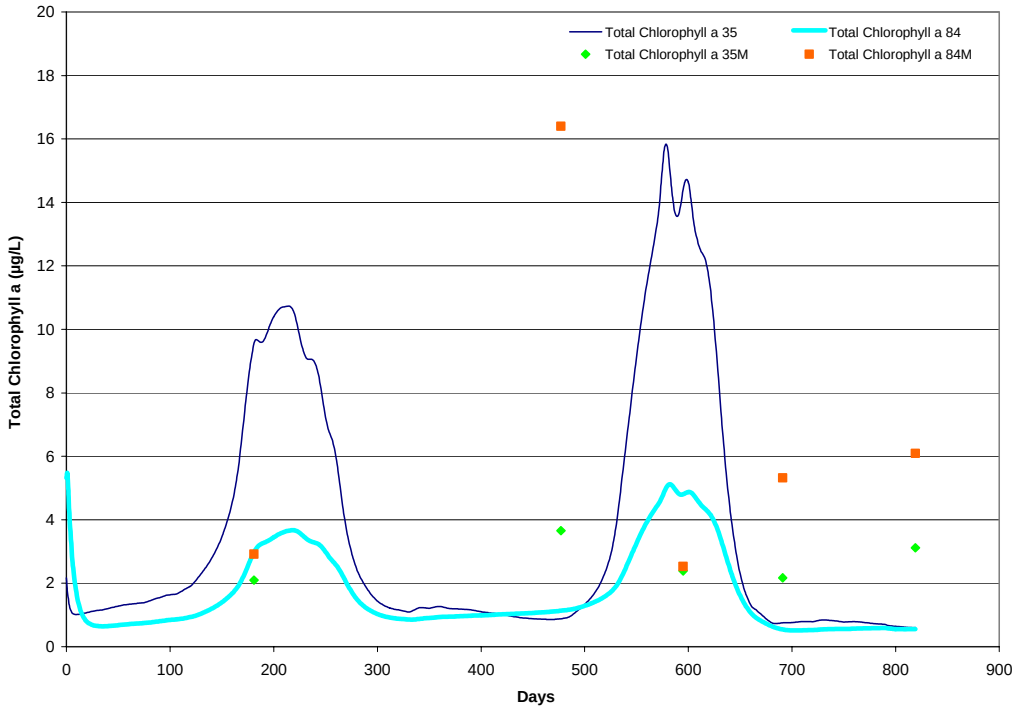

Figure 7.27: Simulation Results and Measured Concentrations of Total Chlorophyll a for Alagöl Lake

7.5.6 Simulation Step 4 Orthophosphate Phosphorus Results

Orthophosphate phosphorus monitoring data is available for the last two cruises. Therefore, it is hard to make reasonable evaluations on the simulation results of this parameter.

The orthophosphate phosphorus simulations results of step 4 are mostly higher than step 3.

7.5.7 Simulation Step 4 Organic Phosphorus Results

The simulation results of organic phosphorus are mostly lower than the monitoring data and only a few results indicate good agreement.

No significant change was observed in organic phosphorus concentrations, when compared with step 3 results.

7.5.8 Simulation Step 4 Detrital Phosphorus Results

Detrital phosphorus data is limited; there is no data available for Cruises 1, 2 and 5 and for all cruises for Stations 0 and 14. Since there is lack of monitoring data, it is hard to make reasonable evaluations on simulation results.

7.5.9 Simulation Step 4 Dissolved Oxygen Results

When dissolved oxygen simulation results analyzed a perfect calibration fit is obtained for the Mediterranean Sea boundary condition. The simulation results for the Köyceğiz Lake boundary condition have good agreement with the monitoring data except for Cruise 3. The upper layer of Alagöl Lake has also calibration fit for dissolved oxygen. Dalyan Town simulation results indicate reasonable agreement with the data excluding Cruise 3.

The plots of the best and worst calibration fits are given in Figure 7.28 and Figure 7.29, respectively. The plots indicating the dissolved oxygen simulation results of the segments representing the boundary conditions are given in Annex F.

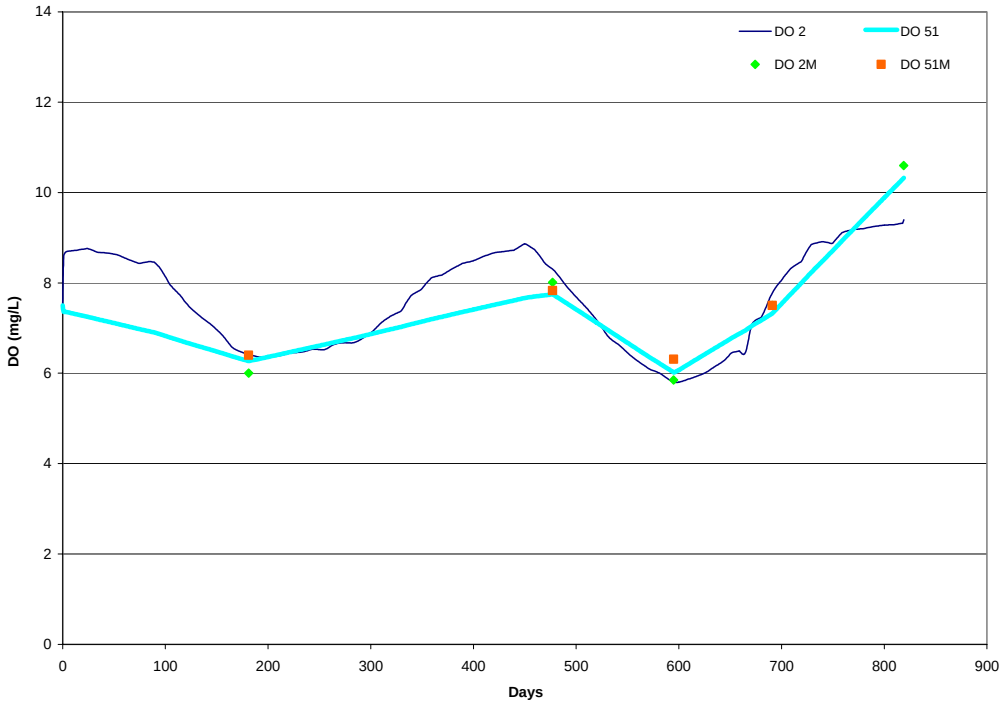

Figure 7.28: Simulation Results and Measured Concentrations of Dissolved Oxygen for the Mediterranean Sea Boundary Condition

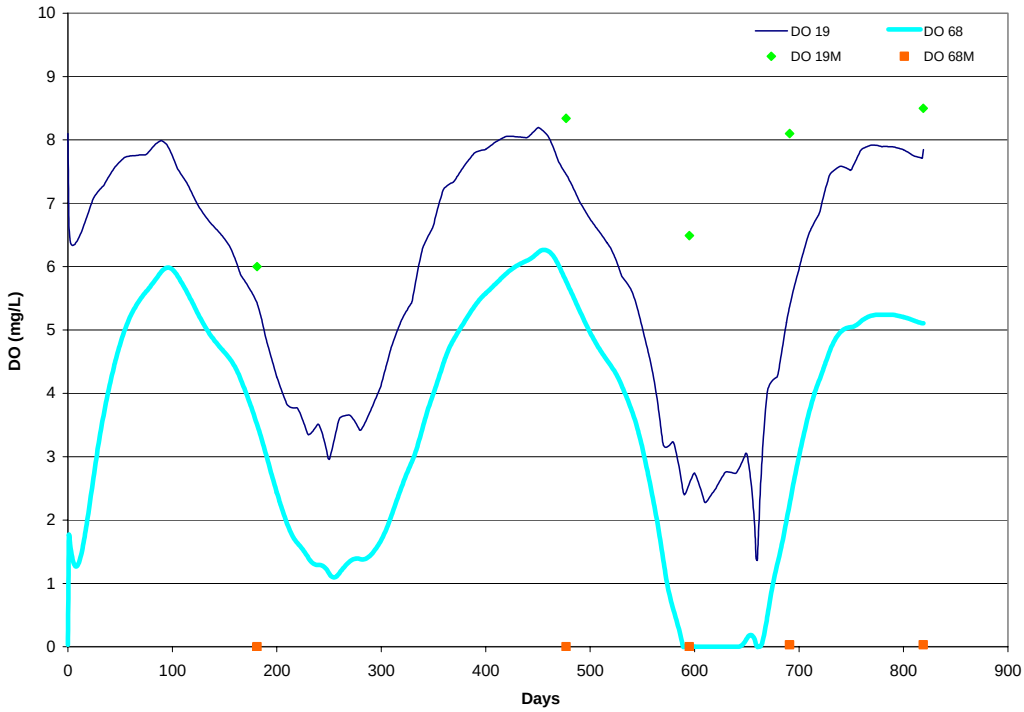

Figure 7.29: Simulation Results and Measured Concentrations of Dissolved Oxygen for Sülüngür Lake

7.5.10 Simulation Step 4 $CBOD_1$ Results

The bottom layer of the Mediterranean Sea boundary condition has the best calibration fit for $CBOD_1$ parameter. Köyceğiz Lake boundary condition simulation results are in good agreement with the monitoring data except for Cruise 3. The simulation results for Dalyan Town and Alagöl Lake indicate high calibration fit for Cruises 1, 2 and 5.

The plots of the best and worst calibration fits are given in Figure 7.30 and Figure 7.31, respectively. The plots indicating the $CBOD_1$ simulation results of the segments representing the boundary conditions are given in Annex F.

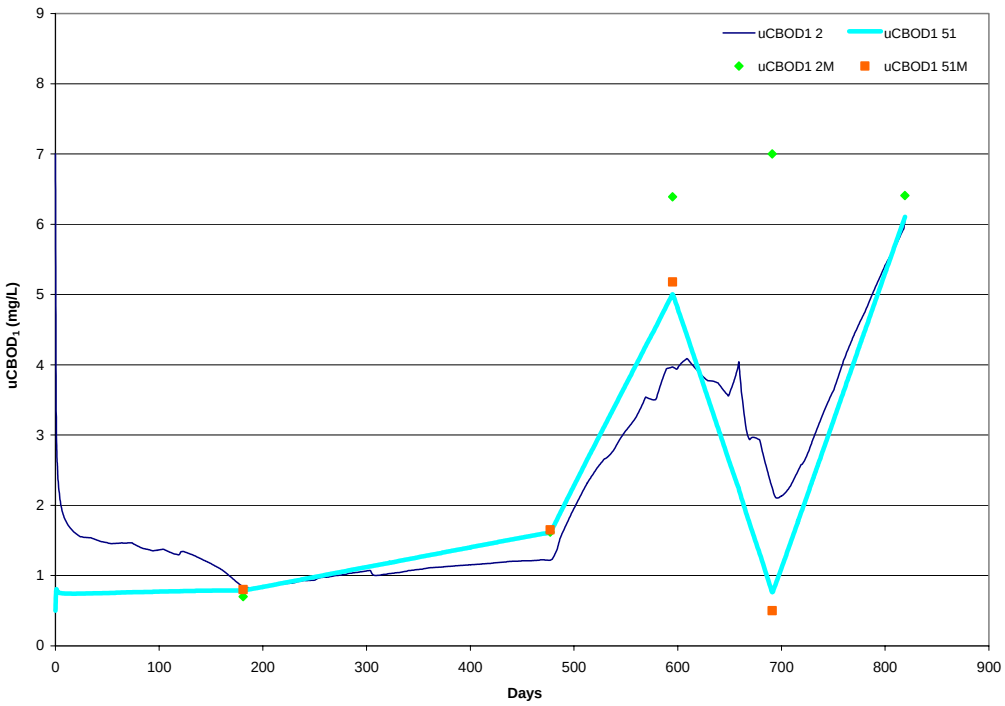

Figure 7.30: Simulation Results and Measured Concentrations of $CBOD_1$ for the Mediterranean Sea Boundary Condition

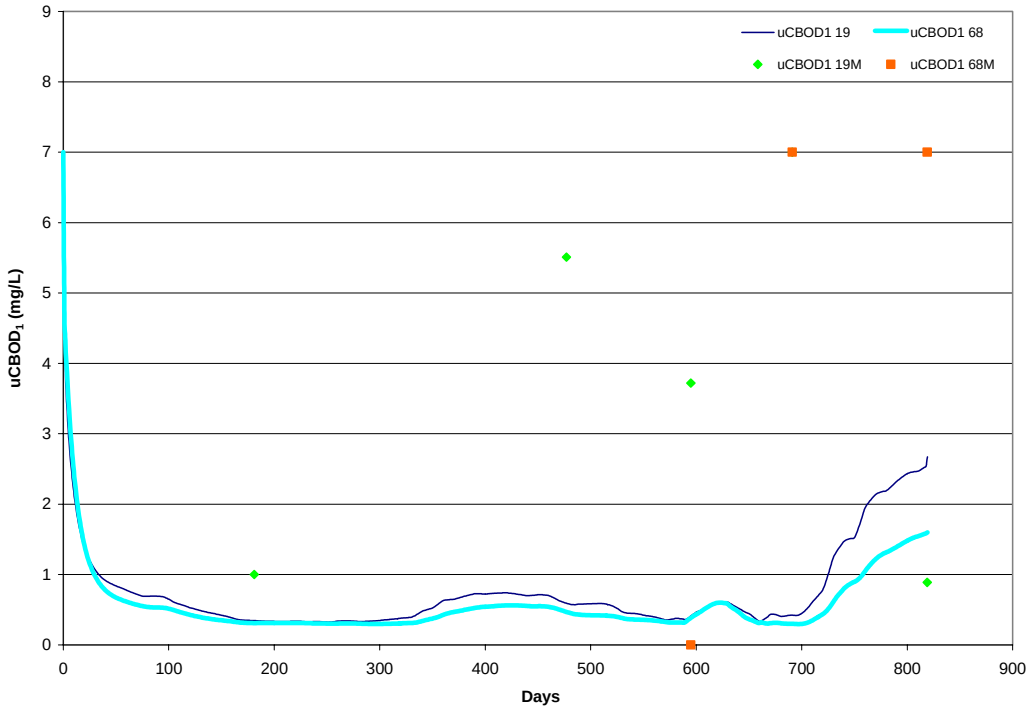

Figure 7.31: Simulation Results and Measured Concentrations of $CBOD_1$ for Sülüngür Lake

7.5.11 Simulation Step 4 Detrital Carbon Results

Detrital carbon simulation results indicate a similar pattern starting from the mid summer of 1999 until the mid autumn of 1999. Detrital carbon concentrations are calculated as 0 mg/L for this period almost for all segments. Sülüngür Lake have this pattern for a much shorter period than the other segments. The best calibration fit for detrital carbon is provided by the upper layer of Sülüngür Lake and the bottom layer of Alagöl Lake.

The plots of the best calibration fit are given in Figure 7.32 and Figure 7.33, and the worst calibration fit is given in Figure 7.34. The plots indicating the $CBOD_1$ simulation results of the segments representing the boundary conditions are given in Annex F.

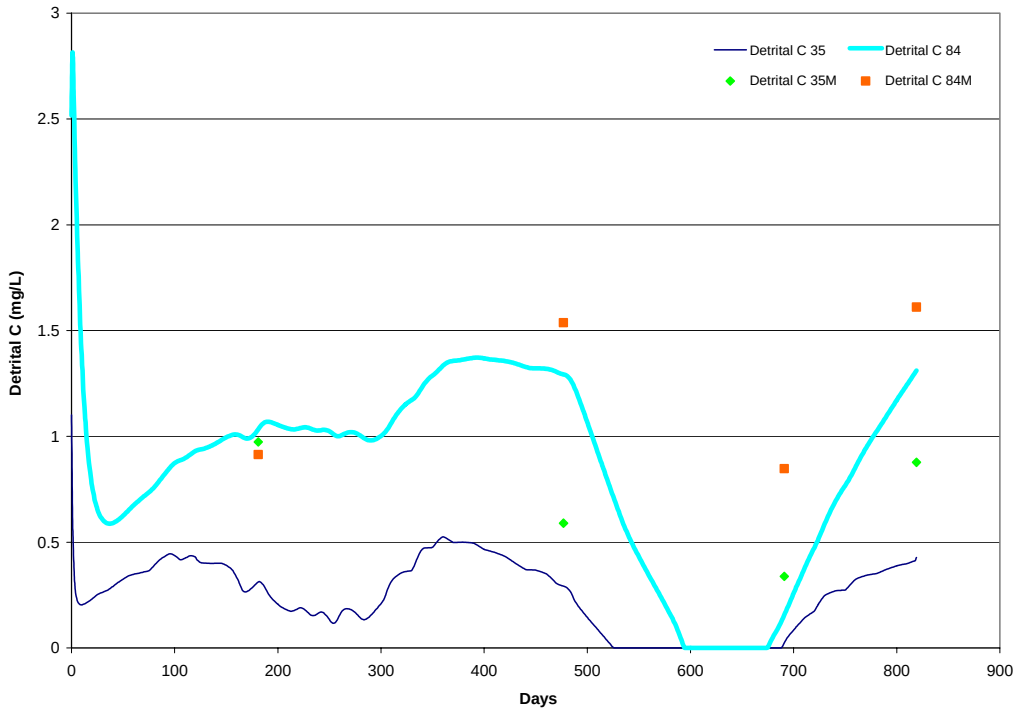

Figure 7.32: Simulation Results and Measured Concentrations of Detrital Carbon for Alagöl Lake

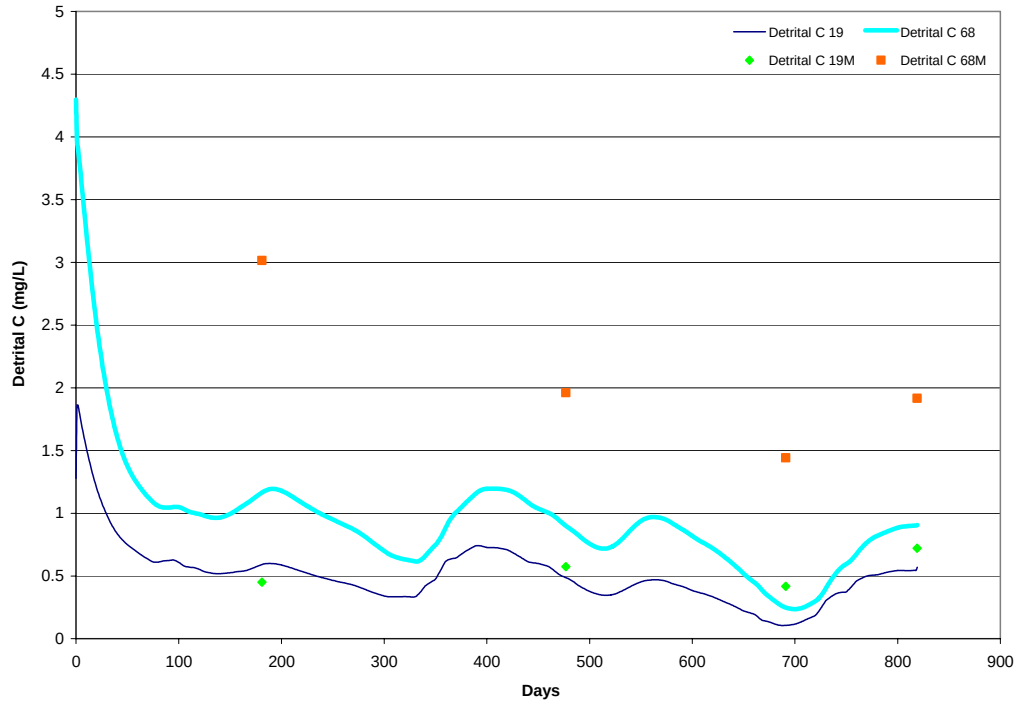

Figure 7.33: Simulation Results and Measured Concentrations of Detrital Carbon for Sülüngür Lake

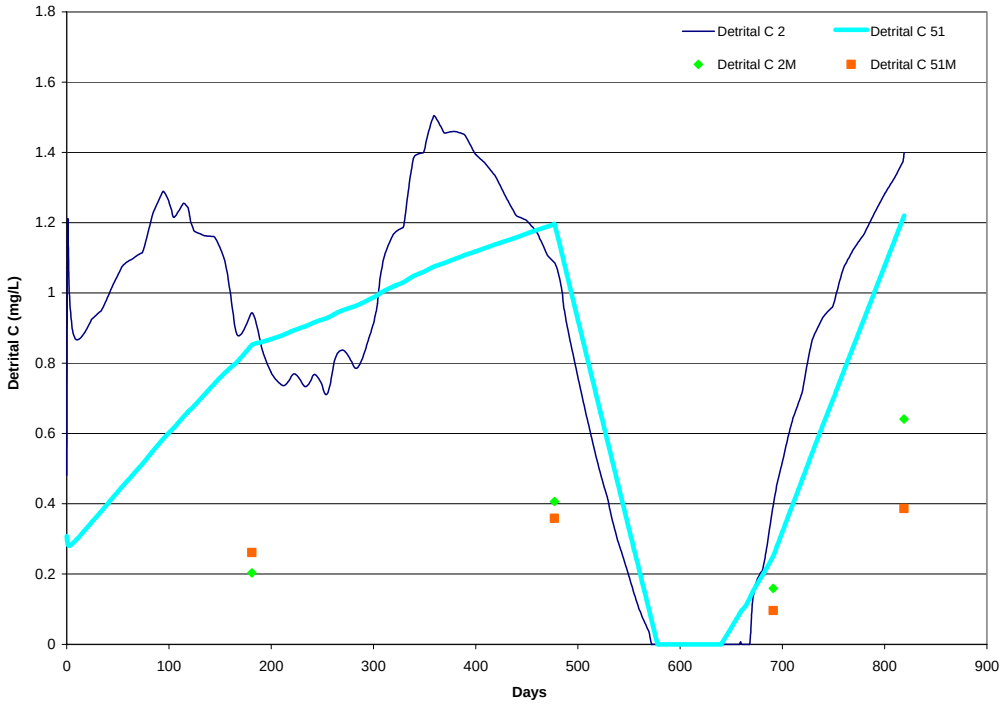

Figure 7.34: Simulation Results and Measured Concentrations of Detrital Carbon for the Mediterranean Sea Boundary Condition

7.5.12 Simulation Step 4 Salinity Results

When the salinity simulation plots are analyzed for the selected segments referred in this chapter, it is observed that the simulation results are the same with simulation step 1 results except for Sülüngür Lake. The reason for the change in the salinity concentrations of this part is the vertical dispersion coefficient defined between them in simulation step 4.

7.5.13 Compatibility of Simulation Results with the Monitoring Data

The compatibility of simulation results of step 4 with the monitoring data is evaluated by forming a matrix, which is given in Table 7.4. The matrix includes the selected segments, which are discussed in this chapter, and all the state variables simulated during step 4. The compatibility of simulation results with the monitoring data is evaluated as low, intermediate or high. It is assumed that if the simulation results fit well with 4 or 5 field data, this corresponds to high compatibility; when the simulation results fit well with 2 or 3 field data, it corresponds to intermediate compatibility, and if only one field data fits well it corresponds to low compatibility.

Table 7.4: Compatibility of Simulation Results with the Monitoring Data

	Köyceğiz Lake Boundary Condition[i]	Dalyan Town[ii]	Alagöl Lake[iii]	Sülüngür Lake[iv]	Mediterranean Sea Boundary Condition[v]
Ammonia Nitrogen	U: Inter. B: Inter.	U: Inter. B: Inter.	U: Low B: Low	U: Low B: One Data	U: Low B: High
Nitrate Nitrogen	U: High B: High	U: Low B: Low	U: Low B: Low	U: Low B: Low	U: Low B: High
Organic Nitrogen	U: High B: Low	U: Inter. B: Low	U: Low B: Low	U: Inter. B: One Data	U: Inter. B: High
Detrital Nitrogen	U: Inter. B: High	U: Low B: Inter.	U: Low B: Low	U: High B: Low	U: Low B: High
Total Chl-a	U: High B: High	U: Inter. B: Low	U: Low B: Low	U: Low B: One Data	U: Inter. B: High
Orthophosphate Phosphorus	U: Two Data B: Two Data	U: Two Data B: Two Data	U: Two Data B: Two Data	U: Two Data B: Two Data	U: Two Data B: Two Data
Organic Phosphorus	U: Low B: One Data	U: Low B: Low	U: High B: Low	U: High B: Low	U: Low B: High
Detrital Phosphorus	U: Data NA B: Data NA	U: One Data B: Two Data	U: Two Data B: Two Data	U: Two Data B: Data NA	U: Data NA B: Data NA
Dissolved Oxygen	U: High B: High	U: High B: High	U: High B: Low	U: Inter. B: Low	U: High B: High
CBOD	U: High B: High	U: Inter. B: Inter.	U: High B: Inter.	U: Low B: Low	U: High B: High
Detrital Carbon	U: Low B: Low	U: Inter. B: Low	U: Inter. B: High	U: High B: Low	U: Low B: Low
Salinity	U: High B: High	U: High B: High	U: High B: High	U: High B: Low	U: High B: High

U: Upper Layer, B: Bottom Layer, Inter.: Intermediate, NA: Not Available

[i] : Evaluations made for these segments are also valid for segments; 47-96 and 46-95

[ii] : Evaluations made for these segments are also valid for segments; 43-92, 41-90, 40-89, 39-88, 38-87 and 37-86

[iii] : Evaluations made for these segments are also valid for segments; 34-83

[iv] : Evaluations made for these segments are also valid for segments; 20-69, 18-67, 17-66 and 16-65

[v] : Evaluations made for these segments are also valid for segments; 31-80, 30-79, 29-78, 3-52 and 1-50

As mentioned previously in Chapter 6, monitoring data is collected seasonally with 5 cruises. Unfortunately, 5 data is not available for all the parameters included in the matrix. Orthophosphate phosphorus and detrital phosphorus data are available just for two cruises, and for some segments there is only one data as can be seen from the matrix. Therefore, it is not possible to make reasonable evaluations for these parameters and segments.

When the matrix is analyzed in terms of simulated parameters, it can be stated that salinity parameter has the highest compatibility with the monitoring data; for the bottom layer of Sülüngür Lake being the only exception for this parameter. Salinity parameter gives an idea about the physical state of the system like the flows and exchanges. Therefore, it is possible to say that the flows and exchanges are well defined to the model, and the model has a high capability in simulating this parameter.

The second highest compatibility is provided by the dissolved oxygen parameter in general. However, the bottom layers of Alagöl and Sülüngür Lakes represent the lowest compatibility for dissolved oxygen. Regarding the monitoring study measurements, the bottom layer of Sülüngür Lake is anoxic for all cruises, but the model predicted anoxic conditions just for a short period of time in summer, which complies only with the August 1999 measurement results. It is known that fishing activities are conducted within this lake; therefore, the bottom layer is always anoxic because of these activities. The reason of low compatibility for this layer might be that the affect of fishing activities is not well defined to the model while the generation of input data. Thus, care must be taken into consideration for this part of the system in the future studies.

$CBOD_1$ has the third highest compatibility with the monitoring data. Sülüngür Lake is the only part of the system, which has the lowest compatibility. The predictions of the model are mostly lower than the measured values. Dissolved oxygen is a parameter used in the calculation of CBOD by the model. Since the compatibility of dissolved oxygen for Sülüngür Lake is not very satisfactory, this also affects the simulation results of CBOD parameter. Another parameter used as a function in CBOD calculation is phytoplankton. It is thought that, when the simulation results of dissolved oxygen and phytoplankton are improved, the model results for CBOD will also improve.

The compatibility of total chlorophyll-a, ammonia nitrogen, detrital nitrogen and organic nitrogen is almost at the same level. 50% of the results comply with the monitoring data at high and intermediate level. Nitrate nitrogen, organic phosphorus and detrital carbon have the lowest compatibility when compared with the other simulated parameters. Ammonia nitrogen and nitrate nitrogen have direct roles in phytoplankton growth kinetics; thus, the changes in these parameters affect phytoplankton directly. However, detrital nitrogen and organic nitrogen have roles in the nitrogen cycle; therefore, change in the concentrations of them affect ammonia nitrogen and nitrate nitrogen concentrations, which also affects the phytoplankton kinetics. On the other hand, phytoplankton increases dissolved organic nitrogen and detrital nitrogen concentration by respiration and death, respectively. It is thought that, more emphasis should be given to these parameters in the future studies, since they have interactions with each other, which makes the study more complicated and

challenging. When the nutrient loads are calculated by means of a watershed model, at least monthly, the compatibility of the simulation results for these parameters will also improve. Besides, solar radiation data, which has an important effect on phytoplankton growth, is available only between 1987 and 1990 for the study area; and the water quality monitoring data used in the model is available between 1998 and 2000. This situation of having short term values rather than long term and continuous data also causes problems for phytoplankton concentration predictions. This leads to the fact that, well-designed, systematic and continuous monitoring is of utmost importance for making more reliable model predictions.

When the matrix is analyzed in terms of segments, the bottom layer of Mediterranean Sea boundary condition has the highest compatibility. Detrial carbon is the only parameter, which has low compatibility, for this segment. As mentioned previously in section 6.2.2.6, since there are no significant tidal and other effects causing fluctuations, a stable hydrodynamic character is observed at this boundary condition, it was assumed that the flow going into the lagoon from this segment is constant throughout the simulation period. Therefore, this stable hydrodynamic character of this segment provided high compatibility with the simulation results. On the other hand, the compatibility of the upper layer of Mediterranean Sea boundary is not as high as its bottom layer. It is known that, this layer is the only flow exit from the system, and it has a dynamic character. Therefore, this dynamic character might be the cause of low compatibility.

The second highest compatibility is provided by the Köyceğiz Lake boundary condition. Detrital carbon is the only parameter, which has low compatibility, for both of the layers of this boundary condition.

The upper layer of Dalyan Town shows higher compatibility than its bottom layer. Dissolved oxygen and salinity parameters have high compatibility for both layers, whereas nitrate nitrogen and organic phosphorus have low compatibility.

Salinity is the only parameter, which has high compatibility for both layers of Alagöl Lake. All nitrogen species and total chlorophyll-a parameters have low compatibility for this lake. Emphasis should be given to improve these parameters in the future studies.

The bottom layer of Sülüngür Lake has no compatibility for any of the simulated parameters. As mentioned previously, fishing activities are conducted in this lake. The effect of these activities should be represented better in the future studies to get better model predictions.

7.6 Simulation Step 5 Results

In order to analyze the effects of point and diffuse pollution loads on the system, load scenarios were developed. In the first load scenario, all the ammonia, nitrate, organic nitrogen, orthophosphate, organic phosphorus, $CBOD_1$, detrital nitrogen and detrital phosphorus loads are increased by 50%. In the second scenario, the loads of the same state variables were increased by 100% and in the last scenario these loads were decreased by 50%. The plots of simulation results for Scenario 1, Scenario 2 and Scenario 3 are given in Annex G, Annex H and Annex I, respectively.

As the simulation results of all three load scenarios are considered, it is seen that the scenario results mostly have similar trends with the original simulation results for all simulated parameters.

It is assumed that there is no nutrient loading prior to or into segments representing the Köyceğiz Lake boundary condition; thus, the simulation results of these segments do not indicate any change when the nutrient loads entering into the system are altered. The bottom layer of Mediterranean Sea boundary condition and the bottom layer of Alagöl Lake also have the same response with the Köyceğiz Lake boundary condition, due to very low nutrient loads going into these segments. The predictions for the other selected segments increase with the increased nutrient load, and decrease with the decreased nutrient load, as expected.

The nitrogen species (NH_3 – N, NO_3^- – N, organic N and detrital N) show similar trends with the original simulation. The response of nitrogen species to load changes were as expected, the predicted concentrations increased as the loads were increased and vice versa. However, the level of response to load changes was different for different nitrogen species. For example, the difference between the minimum and maximum concentrations for NO_3^- – N seems more considerable as the load increases.

On the other hand, organic nitrogen does not show too much variation with the changes in load. Detrital nitrogen also indicates considerable response to load changes.

Total chlorophyll-a concentrations increase with increasing loads, and decrease with decreasing loads. However, this statement seems to be valid for summer months, since total chlorophyll-a concentrations do not show any response to changing loads for the rest of the year. Another remarkable result is the slight changes observed in the total chlorophyll-a concentrations of the Köyceğiz Lake boundary condition.

The phosphorus species (PO_4^{3-} – P, organic P and detrital P) show similar trends with the original simulation. The response of phosphorus species to load changes were as expected, the predicted concentrations increased as the loads were increased and vice versa. One remarkable result about the phosphorus species is the slight changes observed in the PO_4^{3-} – P concentrations of Köyceğiz Lake boundary condition, which might be due to the changes observed in the total chlorophyll-a concentrations in summer.

Detrital carbon shows a different trend when compared with other parameters. Its concentrations increase with decreasing load, and vice versa during summer months.

Dissolved oxygen and $CBOD_1$ parameters did not show any response to changes in load.

8. CONCLUSIONS AND RECOMMENDATIONS

In this study, Water Quality Simulation Analysis Program (WASP) is applied to Köyceğiz – Dalyan Lagoon, which is situated in the southwestern part of Turkey along the Mediterranean Sea coast. The model network was developed and the system was divided into 49 segments to define the system to the model. The data utilized for the generation input files was analyzed. The field data that has been previously collected from the 16 monitoring stations and from two different depths representing the characteristics of the dual layer flow are used in the study. Following the definition of the flows and exchanges to the model, the simulations were conducted from the simplest complexity level to higher complexity levels in order to better understand the processes and mechanisms that occur in the system. The simulations were carried out in 5 steps. One or more state variables were added in each simulation step. In the most complex simulation step 12 parameters were simulated.

Within the first 4 simulations, preliminary and preparatory analysis has been conducted to better evaluate the behavior of certain parameters on the outputs of modeling. The first simulation covers the only the salinity term to represent the physical conditions of the system. The second simulation included only nitrogen species and phytoplankton, covering 5 parameters. The third one added phosphorous species involving 8 parameters, whereas the forth one included dissolved oxygen, CBOD, detrital carbon and salinity indicating the 12 parameters of concern.

When the 12 parameters simulated in the most complex step are analyzed, salinity indicated the best results complying with the monitoring data. According to the salinity simulation results of the selected segments, the predicted concentrations for the segments which represent the bottom layers are always higher than 10 ppt which indicates the dominant effect of the Mediterranean Sea in these parts, except for the Köyceğiz Lake boundary condition. However, as the predicted salinity concentrations of the segments which represent the upper layers are sometimes lower

than 10 ppt during winter months, this leads to the conclusion that Köyceğiz Lake is dominant for this time of the year. The salinity simulation results confirmed that there is a dual layer flow except the Köyceğiz Lake boundary condition. In general, the simulation results indicate that the flow rates, pathways, exchanges and exchange coefficients, are estimated satisfactorily to run the water quality simulations, and the model has a high capability in simulating this parameter.

The simulation results of CBOD and dissolved oxygen parameters also indicated high compliance with the monitoring data, except for the bottom layers of Alagöl and Sülüngür Lakes. The anoxic conditions observed in the bottom layer of Sülüngür Lake at all cruises, were able to be simulated by the model just for one cruise. The effect of fishing activities in the lake should be better defined to the model in order to obtain better simulation results in the future studies. Besides, the improvement in the dissolved oxygen and total chlorophyll-a simulation results will contribute to the improvement of CBOD results.

Almost 50% of the total chlorophyll-a, ammonia nitrogen, detrital nitrogen and organic nitrogen simulation results have high or intermediate compliance with the measurements. The compliance of the simulation results of nitrate nitrogen, organic phosphorus and detrital carbon are lower among the other simulated parameters. These parameters have direct or indirect roles in phytoplankton kinetics; therefore the interactions between these parameters make the study more complicated and challenging. If the nutrient loads are better estimated by using a watershed load model at least monthly, it will be possible to have better simulation results for these parameters.

When the simulation results are analyzed in terms of segments, it is observed that the simulation results of the segments representing the Köyceğiz Lake and Mediterranean Sea boundary conditions are in high compliance with the monitoring data. The stable hydrodynamic character of the Mediterranean Sea provided to get better simulation results for its bottom layer. The simulation results for Alagöl and Sülüngür Lakes are not in high compliance with the monitoring data. Emphasis should be given to these parts to improve the simulation results.

As a modeler one of the most important problems faced is the change observed in a parameter due to the boundary conditions. Therefore, it is not possible to say that the parameters indicate constant behavior which makes the study even more challenging. The other problem is based directly on the hydrological and hydrodynamic behavior of the system that needs to be monitored quite frequently to understand the effective and prevailing processes that direct the behavior of the system. For example, it is thought that the presence of reeds along the channel and its branches cause uncertainties in the processes taking place in the lagoon. Moreover, lack of data on groundwater resources might be an other source for causing additional uncertainties in the system.

The following recommendations are mentioned to be considered in the future studies, which will be conducted to better understand similar aquatic systems, and to help generating information for the sustainable management of the region of concern.

- More monitoring data is required in order to better calibrate the water quality model. Especially lack of data in phosphorus species did not allow making enhanced evaluations about these state variables. Since monitoring study is such a challenging and expensive task which requires multidisciplinary team work, projects with high budgets should be conducted to collect data. When short term monitoring data is available rather than long term continuous data, this causes problems in having reliable model predictions. Therefore, well-designed, systematic and continuous monitoring is of utmost importance for better model predictions. At least, seasonal monitoring studies should be carried out for five years for a modeling study.

- A watershed load modeling should be conducted to better estimate the pollutant loads arising from the watershed. The model should estimate the loads at least monthly. Also it should be taken into account that the model should make predictions in terms of different nitrogen and phosphorus species. As the land-based sources of pollutants need to be determined in detail, the land-use activities prevailing at the watershed must be investigated together with the types of polluting sources. Emphasis on the entire watershed must be given to lead to better and more precise load estimations.

- 3 dimensional hydrodynamic modeling studies should be conducted in order to better estimate the flow and exchanges in the system. It should be considered that the hydrodynamic modeling results should be compatible with the water quality model for incorporating the models easily.

- As mentioned in Chapter 7, since the response to nutrient enrichment and the significance of related changes in ecosystem dynamics vary considerably regionally, it is quite difficult to recommend single national/international criteria applicable to all coastal waters with different geographical and climatic conditions. The new approach among ecologists is to determine the species one by one in the system. Thus, ecological studies should be conducted in the region in order to estimate the trophic level of the system. Classifications based on the present species composition, should be made for the systems having such dynamic character.

- Sediments can be important as internal nutrient sources. Thus, sediment sampling and modeling should also be performed.

- Models and simulations allow the rapid evaluation of pollution in terms of cause and effect relationships. Models are required for forecasting the impact of eutrophication on aquatic ecosystems. Water quality models attempt to describe the major spatial and temporal changes of constituents of concern. The main advantage is that they enable analyses of different future scenarios. The models are also useful since they allow making more objective and reliable assessments, and predictions. Surface water quality models are used both in research as well as in designing and assessing the water quality management measures. Therefore, mathematical models are useful tools, not only for saving time and money, but also for solving ecological problems easier and for helping the decision-makers to choose an appropriate management alternative for sustainable management.

- Since WASP has not been effectively applied in Turkey yet, this study is considered to be a leading one, where the model is applied to a lagoon system. One of the main advantages of WASP for developing countries like Turkey is that, it is free of charge and can be downloaded easily from the

internet. Basic WASP structure and kinetics has a unique flexibility. The model can be structured as one, two, and three dimensional. Time – variable exchange coefficients, advective flows, waste loads and water quality boundary conditions can be specified to the model. Taking into account all these advantages, it is thought that the use of WASP will increase in Turkey and this study will form a basis and act as a guide in the application of the model for similar studies in future.

- Better models are needed to avoid the severe economic penalties associated with wrong decisions.

- In particular, graphical user interfaces and decision-support systems are being developed that facilitate the generation and visualization of model output.

- Two and three dimensional models with highly mechanistic kinetics can be simulated at a reasonable cost.

- It should be kept in mind that widespread and easy use of models could lead to their being applied without insight as “black boxes”. Models must be applied with insight and with regard to their underlying assumptions.

REFERENCES

Adalı, İ. N., 2004. Modelling of nutrient emissions in Köyceğiz Lake-Dalyan Lagoon Watershed – Application of the MONERIS Model, *MSc. Thesis*, ITU Institute of Science and Technology, İstanbul.

Alongi, D. M., 1998. Coastal Ecosystem Processes, CRC Press, Boca Raton, FL.

Ambrose, R. B., 1987. Modeling volatile organics in the Delaware Estuary, *Am. Soc. Civil Eng. J. Environ. Eng*., **113**, 703–721.

Ambrose, R. B., Wool, T. A., Connolly, J. P. and Schanz, R.W., 1988**.** WASP4, A hydrodynamic and water quality model - model theory, user's manual, and programmer's guide, **EPA/600/3-87-039**, U.S. Environmental Protection Agency, Environmental Research Laboratory, Athens, GA.

Ambrose, R. B., Wool, T. and Martin, J.L., 1993a. WASP5, User's manual, **EPA/600/3-87-039**, U.S. Environmental Protection Agency, Environmental Research Laboratory, Athens, GA.

Ambrose, R. B., Wool, T. and Martin, J. L. 1993b. The dynamic estuary model hydrodynamics program, DYNHYD5 model documentation and user's manual, U.S. Environmental Protection Agency, Environmental Research Laboratory, Athens, GA.

Anderson, D. M., 1994. Red tides, *Scientific American*, **271**, 62-68.

Anderson, D. **M. and Garrison, D. J.,** 1997. The ecology and oceanography of harmful algal blooms, *Limnology and Ocenanography,* **42**, 1009-1305.

Beck, M. **B.,** 1983. A procedure for modeling, in *Mathematical Modeling Of Water Quality: Streams, Lakes, and Reservoirs*, pp. 11 – 41, Ed: Orlob, G. T., John Wiley and Sons, Chichester.

Behrendt, H., Huber, P., Kornmilch, M., Opitz, D., Schmoll, O., Scholz, G. and Uebe, R., 1999. Nutrient Emmisions into River Basins of Germany, Institute of Freshwater Ecology and Inland Fisheries.

Bierman, Jr., V. J., Hinz, S. C., Zhu, D. W., Wiseman, Jr., W. J., Rabalais, N. N. and Turner, R.E., 1994. A preliminary mass balance model of primary productivity and dissolved oxygen in the Mississippi River Plume/Inner Gulf Shelf Region, *Estuaries*, **17**(4), 886–899.

Biggs, B. J. F., 1996. Patterns in benthic algae in streams, in *Algal Ecology*, pp. 31–56, Eds. Stevenson, R. J., Bothwell, M. L., Lowe, R. L., Academic Press, San Diego.

Bilecik, N., Ezer, N., Buhan, E., Morkan, Y., Erol, G., Topgül, M., Zünbülcan, F., Özdemir, G., Yılmaz, H. and Diçer, S., 1994. Köyceğiz Dalyan regional environmental protection fisheries project, Final Report, Republic of Turkey, Ministry of Environment and Forestry, Environmental Protection Agency for Special Areas.

Canale, R. P., De Palma, L. M. and Vogel, A. H., 1976. A plankton – based food web model for Lake Michigan, in *Modeling Biochemical Processes in Aquatic Ecosystems*, p.33, Ed. Canale, R. P., Ann Arbor Science, Ann Arbor, MI.

Canale, R. P., Hineman, D. F. and Nachippan, S., 1974. A biological production model for Grand Traverse Bay, *University of Michigan Sea Grant Program Techinical Report No. 37*, Ann Arbor.

Carpenter, S. R., Caraco, N. F., Correll, D. L., Howarth, R. W., Sharpley, A. N. and Smith, V. H., 1998. Nonpoint pollution of surface waters with phosphorus and nitrogen, *Ecological Applications*, **8**(3), 559-568.

Castel, J., Caumette, P. and Herbert, R., 1996. Eutrophication gradients in coastal lagoons as exemplified by the Bassin d'Arcachon and the Étang du Prévost, *Hydrobiologia*, 329, 9-28.

Cerco, C. F. and Cole, T., 1994. Three dimensional eutrophication model of Chesapeake Bay; Volume 1, *Main Report*, **Technical Report EL 94-4**, U.S. Army Corps of Engineers Waterways Experiment Station, Vicksburg, MS**.**

Cerco, C. F. and Cole, T., 1995. User's guide to the CE-QUAL-ICM three dimensional eutrophication model, Release Version 1.0, **Technical Report EL-95-15**, U.S. Army Corps of Engineers Waterways Experiment Station, Vicksburg, MS.

Chapra, S. C., 1997. Surface Water Quality Modeling, McGraw-Hill Inc.

Chapra, S. C. and Reckhow, K. H., 1983. Engineering Approaches for Lake Management, Vol. 2: Mechanistic Modeling, Butterworth, Woburn, MA.

Chen, C. W., 1970. Concepts and utilities of ecological models, *J. San. Engr. Div.*, ASCE, **96**(SA5), 1085 – 1086.

Chen, C. W., and Orlob, G. T., 1975. Ecological simulation for aquatic environments, in *Systems Analysis and Simulation in Ecology Vol. III*, Ed. Patton, B. C., Academic, New York.

Clark, J. R., 1998. Coastal Seas: The Conservation Challenge, Blackwell Science, Oxford, UK.

Cloern, J.E., 2001. Our evolving conceptual model of the coastal eutrophication problem, *Mar. Ecol. Prog. Ser.*, 210 – 223.

Cole, T.M. and Wells, S.A., 2002. CE-QUAL-W2 A two dimensional, laterally averaged, hydrodynamic and water quality model, Version 3.1, **Instruction Report EL-2002-1**, U.S. Army Engineering and Research Development Center, Vicksburg, MS.

Connolly, J. P. and Winfield, R., 1984. A user's guide for WASTOX, a framework for modeling the fate of toxic chemicals in aquatic environments, Part 1: Exposure Concentration, **EPA-600/3-84-077**, U.S. Environmental Protection Agency, Gulf Breeze, FL.

Decamps, H., Capblanc, J. and Tourenq, J. N., 1984. In *Ecology, of European Rivers*, pp. 207–235, Ed. Whitton, B. A., Blackwell Scientific Publications.

de Jonge, V. N., Elliott, M. and Orive, E., 2002. Causes, historical development, effects and future challenges of a common environmental problem: eutrophication, *Hydrobiologia*, **475/476**, 1-19.

Deininger, R. A., 1965. Water quality management – The planning of economically optimal control systems, *Proceedings of the First Annual Meeting of the American Water Resources Association*, USA.

Di Toro, D. M. and Connolly, J. P., 1980. Mathematical models of water quality in large lakes, Part 2: Lake Erie, **EPA-600/3-80-065**, pp. 90–101.

Di Toro, D. M., Fitzpatrick, J. J. and Thomann, R. V., 1983. Water Quality Analysis Simulation Program (WASP) and Model Verification Program (MVP) - Documentation. Hydroscience, Inc., Westwood, NY, for U.S. EPA, Duluth, MN, Contract No. 68-01-3872.

Di Toro, D. M., O'Connor, D. J. and Thomann., R. V., 1971. A dynamic model of the phytoplankton population in the Sacramento San Joaquin Delta, in *Advances in Chemistry Series 106: Nonequilibrium Systems in Natural Water Chemistry*, pp. 131-180, Ed. Gould, R. F., American Chemical Society, Washington, DC.

Donigian, A. S., Imhoff, J. C., Bicknell, B. R. and Kittle, J. L., 1984. Application guide for the hydrologic simulation program – FORTRAN, **EPA 600/3-84-066**, U.S. Environmental Protection Agency, Athens, GA.

Duarte, C. M., 1995. Submerged aquatic vegetation in relation to different nutrient regimes,Ophelia, 41 – 87.

Ekdal, A., Erturk, A., Gurel, M., Yuceil, K. and Tanik, A., 2003. Developing a computational framework for estimating inflows to a coastal lagoon from its basin, *Proceedings of Sixth International Symposium & Exhibition on Environmental Contamination in Central & Eastern Europe and the Commonwealth of Independent States*, Prague, Czech Republic, September 1 – 4, 2003 (on CD ROM).

Ekdal, A., Gurel, M., Erturk A. and Tanik, A., 2005. Hydrodynamic and water quality modeling approach for a dynamic lagoon system, *Proceedings of the Environmental Hydraulics and Sustainable Water Management*, Eds: Lee & Lam, Hong Kong, People Republic of China, December 15-18 2004, 621-627.

Environmental Laboratory, 1995. CE-QUAL-R1: A numerical one dimensional model of reservoir water quality; user's manual, *Revised Edition*, **Instruction Report E-82-1**, U.S. Army Corps of Engineers Waterways Experiment Station, Vicksburg, MS.

EPA, 1996. Environmental indicators of water quality in the United States, **EPA 841-R-96-002**, U.S. Environmental Protection Agency, Office of Water, (4503F), Washington, DC.

EPA, 2001. Nutrient criteria technical guidance manual, estuarine and coastal marine waters, **EPA-822-B-01-003,** United States Environmental Protection Agency.

Ertürk, A., 2002. Köyceğiz – Dalyan Lagün Sistemi'nin hidrolik modellenmesi, *MSc. Thesis*, ITU Institute of Science and Technology, İstanbul.

Erturk, A., Ekdal, A., Gurel, M., Yuceil, K. and Tanik, A., 2004. Use of mathematical models to estimate the effects of nutrient loadings on small streams, *Fresenius Environmental Bulletin*, **13**(11b), 1350-1359.

Gamito, S., Gilabert, J., Diego, C. M. and Pérez-Ruzafa, A., 2005. Effects of changing environmental conditions on lagoon ecology, in *Coastal Lagoons: Ecosystem Processes and Modeling for Sustainable Use and Development*, pp. 193-229, Eds. Gonenc, I. E. and Wolflin, J., CRC Press.

Gertsev, V. I. and Gertseva, V. V., 2004. Classification of mathematical models in ecology, *Ecol Model*, **178**, 329 – 334.

Gönenç, E., Baykal, B. B., Çakır, A., Bederli, A. and Kabdaşlı, N. I., 1990. Göllerde su kalitesi yönetimi için bir model – EGÖLEM, İnşaat Fakültesi Bilgisayar Kullanımı II.

Gönenç, İ. E., Tanık, A., Şeker, D. Z., Gürel, M., Ertürk, A., Ekdal, A., Yüceil, K., Köse, C., Beyazgül, M. and Bilir, Z. L., 2004. Ecosystem modeling for the sustainable management of lagoons, Final Report, TÜBİTAK, Project No: YDABAG – 100Y047 (in Turkish).

Gönenç, I. E. and Wolflin, J. P., 2005. Coastal Lagoons: Ecosystem Processes and Modeling for Sustainable Use and Development, pp. 1-5, Eds. Gonenc, I. E. and Wolflin, J., CRC Press.

Gualtieri, C. and Rotondo, G., 1996a. Water quality modeling of Speed River, Part One: Model calibration, *Ingegneria Sanitaria*, **2**, March/April (in Italian).

Gualtieri, C. and Rotondo, G., 1996b.Water quality modeling of Speed River, Part Two: Model validation and application, *Ingegneria Sanitaria*, **5-6**, November/December (in Italian).

Gurel, M., Tanik, A., Erturk, A., Dogan, E., Okus, E., Seker, D.Z., Ekdal, A., Yuceil, K., Bederli Tumay, A., Karakaya, N., Beler Baykal, B. and Gonenç, I. E., 2005a. Köyceğiz – Dalyan Lagoon: A case study for sustainable use and development, in *Coastal Lagoons: Ecosystem Processes and Modeling for Sustainable Use and Development*, pp. 440-474, Eds. Gonenc, I. E. and Wolflin, J., CRC Press.

Gurel, M., Ekdal, A., Erturk, A. and Tanik, A., 2005b. Efforts towards setting eutrophication assessment criteria for coastal marine ecosystems, *Int. J. Environment and Pollution*, Vol. 23, No. 3, pp.325–335.

Gürel, M., 2000. Nutrient dynamics in coastal lagoons: Dalyan Lagoon case study, *PhD. Thesis*, ITU Institute of Science and Technology, İstanbul.

Güvensoy, G., 2000. Fate of pesticides on soil and their impact on water environment, *MSc Thesis*, İTÜ Institute of Science and Technology, İstanbul.

Hamrick, J. M., 1992. A three dimensional Environmental Fluid Dynamics Computer Code: Theoretical and computational aspects, Special Report No. 327 in Applied Marine Science and Ocean Engineering , Virginia Institute of Marine Science School of Marine Science, The College of William and Mary Gloucester Point, 23062, VA.

Hamrick, J. M., 1996. User's manual for the Environmental Fluid Dynamics Computer code, Special Report No. 331 in Applied Marine Science and Ocean Engineering,Virginia Institute of Marine Science School of Marine Science, The College of William and Mary Gloucester Point, 23062, VA.

HEC, 1978. Generalized computer program, water quality for river-reservoir systems, The Hydrologic Engineering Center, U. S. Army Corps of Engineers.

Hossenipour, E. Z. and Martin J. L., 1990. The One-Dimensional Riverline Hydrodynamic Model, RIVMOD-H model documentation and user's manual, U.S. Environmental Protection Agency, Environmental Research Laboratory. Athens, GA.

Howarth, R. W., 1988. Nutrient limitation of net primary production in marine ecosystems, *Annual Review of Ecology and Systematics*, **19**(8), 98-110.

Howarth, R. W., Billen, G., Swaney, D., Townsend, A., Jaworski, N., Lajtha, K., Downing, J. A., Elmgren, R., Caraco, N., Jordan, T., Berendse, F., Freney, J., Kudeyarov, V., Murdoch, P. and Zhao-liang, Z., 1996. Regional nitrogen budgets and riverine inputs of N and P for the drainages to the North Atlantic Ocean: natural and human influences, *Biogeochemistry*, **35**, 75-139.

Jeppesen, E., Sondergaard, Ma., Sondergaard, Mo. and Christofferson, K. 1998. The Structuring Role of Submerged Macrophytes in Lakes, Springer-Verlag, New York, New York, USA.

Jewell, W. J. and McCarty, P. L., 1971. Aerobic decomposition of algae, *Environ Sci Technol*, **5** (10), 1023-1031.

Johanson, R. C., Imhoff, J. C., Kittle, J. L., Jr. and Donigian, A. S., Jr. 1984. Hydrological Simulation Program FORTRAN (HSPF): User's manual for Release 8.0, **EPA 600/3 84 066**, U.S. Environmental Protection Agency, Environmental Research Laboratory, Athens, GA

Jørgensen, S. E., 1988. Fundamentals of Ecological Modelling, Elsevier, Amsterdam.

JRB Inc., 1984. Development of heavy metal waste load allocations for the Deep River, North Carolina, JRB Associates, McLean, VA, for U.S. EPA Office of Water Enforcement and Permits, Washington, DC.

Karagöz, İ., 2003. Land assessment of Köyceğiz Lake – Dalyan Lagoon Watershed for integrated planning and management, *MSc Thesis*, İTÜ Institute of Science and Technology, İstanbul.

Karak, P., 2000. Kara kökenli kirletici kaynaklarda besi maddesi hareketlerinin incelenmesi, *MSc Thesis*, İTÜ Institute of Science and Technology, İstanbul.

Kjerfve, B., 1994. Coastal lagoon processes, in *Coastal Lagoon Processes*, pp.1-8, Ed. Kjerfve B.,. Elsevier Oceanography Series, 60, Elsevier Sicence Publishers, Amsterdam.

Lung, W., 1992. A water quality model for the Patuxent Estuary, Final Report submitted to Maryland Department of Environment, University of Virginia.

Lung, W. S. and Larson, C. E., 1994. Water quality modeling of the Upper Mississippi River and Lake Pepin, ASCE EED.

Lung, W. S., Martin, J. L. and McCutcheon, S. C., 1993. Eutrophication and mixing analysis of embayments in Prince William sound, Alaska, *ASCE J. Environ. Eng*., **119**(5), 811–824.

Luyten, P. J., Jones, J. H., Proctor, R., Tabor, A., Tett, P. and Wild-Allen, K., 1999. COHERENS – A Coupled Hydrodynamical – Ecological Model for Regional and Shelf Seas: user documentation, MUMM Report, Management Unit of the Mathematical Models of the North Sea.

Mainstone, C. P. and Parr, W., 2002. Phosphorus in rivers – ecology and management, *Sci Total Environ*, **282/283**, 25 – 47.

Nienhuis, P. H., 1992. Ecology of coastal lagoons in The Netherlands (Veerse Meer and Grevelingen), *Vie Milieu*, 42 – 59.

Nijboer, R. C. and Verdonschot, P. F. M., 2004. Variable selection for modelling effects of eutrophication on stream and river ecosystems, *Ecol Model*, **177**, 17-39.

Nixon, S. W., 1995. Coastal marine eutrophication: a definition, causes, and future concerns, *Ophelia*, **41**, 119-219.

Nixon, S. W., Ammerman, J. W., Atkinson, L. P., Berounsky, V. M., Bilen, G., Boicourt, W. C., Boynton, W. R., Church, T. M., Di Toro, D. M., Elmgren, R., Garber, J., Giblin, A. E., Jahnke, R. A., Owens, J. P., Pilson, M. E. Q. and Seitzinger, S. P., 1996. The fate of nitrogen and phosphorus at the land-sea margin of the North Atlantic Ocean, *Biogeochemistry*, **35**, 141-180.

Nixon, S. W. and Pilson, M. E. Q., 1983. Nitrogen in estuarine and coastal marine ecosystems, in *Nitrogen in the Marine Environment*, Chapte. 16, Eds. Carpenter, E.J. and Capone, D.G., Academic Press, New York.

Novotny, V. and Zheng, S., 1988. Impact of nonpoint pollution on a Great Lakes freshwater harbor estuary, *Proceedings of Special Group Seminar Water Quality Impact of Storm Sewage Overflows on Receiving Waters*, Ed. Ellis, J. B.,14th Biennial Conference, IAWPRC, Brighton, UK, 27–36.

NRC (National Research Council), 1993. Managing Wastewater in Coastal Urban Areas, National Academy Press, Washington, DC, USA.

O'Connor, D. J., 1960. Oxygen balance of an estuary, *J. San. Engr. Div.,* ASCE, **86**(SA3), 35 – 55.

O'Connor, D. J., 1962. The bacterial distribution in a lake in the vicinity of a sewage discharge, *Proceedings of the 2nd Purdue Industrial Waste Conference*, West Lafayette, IN.

O'Connor, D. J., 1967. The temporal and spatial distribution of dissolved oxygen in streams, *Water Resour. Res.*, **3**(1), 65 – 79.

O'Connor, D. J., 1988. Models of sorptive toxic substances in freshwater systems I: Basic equations, *J. Envir. Engr.*, **114**(3), 533 – 551.

O'Connor, D. J., Mueller, J.A. and Farley, K.J., 1983. Distribution of kepone in the James River Estuary, *J. Environ. Eng. Div*., ASCE, **109**(EE2), 396–413.

Pätsch, P., 2001. The long term run with the ecosystem model ERSEM: Technical Guidance for the PC Application.

Pickett, P. J., 1997. Pollutant loading capacity for the Black River, Chehalis River System, Washington, *JAWRA*, **33**(2), 465–480.

Postel, S. **L. and Carpenter, S. R.** 1997. Freshwater ecosystem services, in *Nature's Services*, pp. 195-214, Ed. Daily, G. C., Island Press, Washington, DC, USA.

Ravelle, C., Loucks, D. P. and Lynn, W. R., 1967. A management model for water quality control, *J. Water Poll. Control Fed.*, **39**(7), 1164 – 1183.

Reckhow, K. H. and Chapra, S. C., 1983. Engineering Approaches for Lake Management, Volume 1, Data Analysis and Empirical Modelling, Butterworth Publishers, Boston.

Sanders, H. L., 1968. Marine benthic diversity: a comparative study, *Am Nat*, **102**, 243.

Scheffer, M., 1998. Ecology of Shallow Lakes, Chapman & Hall, London.

Seehausen, O., van Alphen, J. J. M. and Witte, F., 1997. Cichlid fish diversity threatened by eutrophication that curbs sexual selection, *Science*, **277**, 1808-1811.

Sheng, Y. P., Eliason, D. E., Chen, X. J. and Choi, **J. K.** 1991. A three-dimensional numerical model of hydrodynamics and sediment transport in lakes and estuaries: theory, model development and documentation, U.S. Environmental Protection Agency, Athens, GA.

Shumway, S. E., 1990. A review of the effects of algal blooms on shellfish and aquaculture, *Journal of the World Aquaculture Society*, **21**, 65-104.

SIS, 2000. State Institute of Statistics under the Prime Ministry of Turkish Republic, item no: 48, Muğla.

Sladecek, V., 1973. System of water quality from the biological point of view, *Arch. Hydrobiol Suppl*, **7**, 1 – 218.

Smith, R. A., 1980. The theoretical basis for estimating phytoplankton production and specific growth rate from chlorophyll, light and temperature data, *Ecol Model,* **10**, 243-264.

Steele, J. H., 1962. Environmental control of photosynthesis in the sea, *Limnol. Oceanogr*, **7**, 137-150.

Stefan, H. G., Ambrose, R. B., Dortch, M.S., 1990. Surface water quality models: Modeler's Perspective, *Proceedings of the International Symposium on Water Quality Modeling of Agricultural Non-Point Sources*, *Part 1*, June 19-23 1988, Utah State University, Logan, Utah, Ed. De Coursey, D. G., 421.

Stevenson, R. J., 1984. How current on different sides of substrates in streams affects mechanisms of benthic algal accumulation, *Int. Rev. Hydrobiol.*, **69**, 241–262.

Streeter, H. W. and Phelps, E. B., 1925. A study of the pollution and natural purification of the Ohio River, III. Factors concerning the phenomena of Oxidation and reaeration, U.S. Public Health Service, Pub. Health Bulletin No. 146, February 1925, Reprinted by U.S., DHEW, PHA, 1958.

Tanik, A., Gurel, M. and Gonenc, I. E., 2002. Effect of irrigation on the Distribution of Surplus Fertilizer Loads on Land, *Proceedings of 13th International Symposium of the International Scientific Centre of Fertilizers (CIEC), Fertilizers in Context with Resource Management in Agriculture,* Gaziosmanpaşa University and CIEC, June 10-13, Tokat, Turkey, 187-196.

Tetratech, 2002. Draft user's manual for Environmental Fluid Dynamics Code Hyrdo Version (EFDC-Hydro), Release 1.00 for U.S. Environmental Protection Agency, Region 4, Atlanta, GA.

Thomann, R. V., 1975. Mathematical modeling of phytoplankton in Lake Ontario, 1. Model development and verification, **EPA-600/3-75-005**, U.S. Environmental Protection Agency, Corvallis, OR.

Thomann, R. V., 1981. Equilibrium model of fate of microcontaminants in diverse aquatic food chains, *Can. J. Fish. Aquat. Sci.*, **38**, 280 – 296.

Thomann, R. V. and Di Toro, D. M., 1983. Physicochemical model of toxic substances in the Great Lakes, *J. Great Lakes Res.*, **9**(4), 474 – 496.

Thomann, R. V. and Fitzpatrick, J. J., 1982. Calibration and verification of a mathematical model of the eutrophication of the Potomac Estuary, Prepared for Department of Environmental Services, Government of the District of Columbia, Washington, DC.

Thomann, R. V. and Mueller, J. A., 1987. Principles of Surface Water Quality Modelling and Control, Harper and Row Publishers, New York.

Thomann, R. V. and Sobel, M. J., 1964. Estuarine water quality management and forecasting, *J. San. Engr. Div.*, ASCE, **90**(SA5), 9 – 36.

Thomann, R. V., Winfield, R. P., Di Toro, D. M. and O'Connor, D.J., 1976. Mathematical modeling of phytoplankton in Lake Ontario, 2. Simulations Using LAKE 1 Model, **EPA-600/3-76-065**, U.S. Environmental Protection Agency, Grosse Ile, MI.

Thomann, R. V., Winfield, R. P. and Segna, J.J., 1979. Verification analysis of Lake Ontario and Rochester Embayment three dimensional eutrophication models, **EPA-600/3-79-094**, U.S. Environmental Protection Agency, Grosse Ile, MI.

Tufford, D. L. and McKellar, H.N., 1999. Spatial and temporal hydrodynamic and water quality models of a large reservoir on the South Carolina (USA) coastal plain, *Ecol. Modelling*, **114**(2/3), 137–173.

Tufford, D. L., McKellar, H. N., Flora, J. R. V. and Meadows, M. E., 1999. A reservoir model for use in regional water resources management, *Lake Reservoir Manage.*, **15**(3), 220–230.

UNESCO, 1981. Coastal lagoons research, present and future, *UNESCO Technical Papers in Marine Science*, 33, 51 – 79.

Üstün, T. T., 1998. Köyceğiz Gölü su kalitesi için EGÖLEM Modeli, *MSc Thesis*, İTÜ Institute of Science and Technology, İstanbul.

Velz, C. J., 1938. Deoxygenation and reoxygenation, *Proc. Am. Soc. Civ. Engr.*, **65**(4), 677 – 680.

Velz, C. J., 1947. Factors influencing self-purification and their relation in pollution abatement, *Sewage Works J.*, **19**(4), 629 – 644.

Vollenweider, R. A., 1968. Scientific fundamentals of the eutrophication of lakes and flowing waters, with particular reference to nitrogen and phosphorus as factors in eutrophication, **Technical Report DAS/CSI/68.27**, Environmental Directorate, Organization for Economic Cooperation and Development (OECD), Paris.

Wetzel, R. G. and Ward, A. K., 1992. Primary production, in *The Rivers Handbook*, Vol. 1, pp. 354–369, Eds. Calow, P. and Petts, G. E., Blackwell Scientific Publications, Oxford, UK.

Winterbourn, M.J., 1990. Interactions among nutrients, algae and invertebrates in a New Zealand mountain stream, *Freshwater Biol*, **23**, 463–474.

Wool, T. A., Ambrose, R. B., Martin, J. L. and Comer, E. A. 2001. Water Quality Analysis Simulation Program (WASP), Version 6.0.0.12, User's manual, United States Environmental Protection Agency, Athens, GA.

Wool, T. A., Davie, S. R. and Rodriguez, H. N., 2003. Development of three dimensional hydrodynamic and water quality model to support total maximum daily load decision process for the Neuse River Estuary, North Carolina, American Society of Civil Engineers, *J. Water Resources Planning Manage*., **129**(4), 295–306.

Yuceil, K., Tanik, A., Gurel, M., Seker, D. Z., Ekdal, A., Erturk, A. and Gonenc, I. E. 2007. Implementation of soil survey and analyses for promoting watershed modelling applications, *Environ Monit Assess*, **128**, 465-474.

ANNEXES

Annex A

Measured and Calculated Initial Concentrations

Table A.1: NH_4^+- N Initial Concentrations (mg/L)

Segment No*	Upper Layer	Bottom Layer
1	0.0220	0.0030
2 (Station 14)	0.0242	0.0032
3 (Station 13)	0.0141	0.0146
4	0.0177	0.0156
5	0.0172	0.0154
6	0.0165	0.0152
7 (Station 7)	0.0206	0.0164
8	0.0281	0.0335
9 (Station 6)	0.0136	0.0066
10	0.0269	0.0259
11	0.0319	0.0331
12	0.0387	0.0576
13	0.0452	0.0722
14	0.0399	0.0446
15	0.0556	0.0674
16 (Station 8)	0.0675	0.0846
17 (Station 9)	0.0589	0.1035
18 (Station 10)	0.0491	0.0940
19 (Station 11)	0.0253	0.103
20 (Station 12)	0.0315	0.123
21	0.025	0.0255
22	0.023	0.0253
23	0.02	0.025
24	0.0148	0.0056
25 (Station 15)	0.0154	0.0050
26	0.0164	0.0094
27	0.0148	0.0099
28	0.0145	0.0095
29 (Station 5)	0.0132	0.0028
30	0.0142	0.0055
31	0.0144	0.0059
32	0.0153	0.0084
33	0.0165	0.0115
34 (Station 3)	0.0110	0.0082
35 (Station 4)	0.0042	0.0042
36 (Station 2)	0.0182	0.0172
37	0.0167	0.0218
38	0.0156	0.0254
39	0.0163	0.0233
40	0.0149	0.0275
41	0.0142	0.0297
42 (Station 1)	0.0129	0.0339
43	0.0118	0.0308
44	0.0100	0.0261
45	0.0077	0.0197
46	0.0060	0.0153
47	0.0046	0.0114
48 (Station 0)	0.0021	0.0046
49	0.0020	0.004

*The segment numbers with Station IDs indicate the measured values

Table A.2: NO^{-}_{3} – N Initial Concentrations (mg/L)

Segment No*	Upper Layer	Bottom Layer
1	0.03	0.016
2 (Station 14)	0.0321	0.0169
3 (Station 13)	0.1027	0.0277
4	0.0979	0.0436
5	0.0986	0.0411
6	0.0995	0.0382
7 (Station 7)	0.0941	0.0563
8	0.1071	0.0595
9 (Station 6)	0.1124	0.0180
10	0.1185	0.0290
11	0.1207	0.0330
12	0.1254	0.0640
13	0.1365	0.0667
14	0.1243	0.0396
15	0.1314	0.0525
16 (Station 8)	0.1368	0.0622
17 (Station 9)	0.1603	0.0725
18 (Station 10)	0.1531	0.0401
19 (Station 11)	0.1772	0.0009
20 (Station 12)	0.1646	0.0306
21	0.115	0.027
22	0.113	0.025
23	0.11	0.023
24	0.1091	0.0177
25 (Station 15)	0.1073	0.0176
26	0.1078	0.0190
27	0.1050	0.0227
28	0.09	0.0225
29 (Station 5)	0.0456	0.0175
30	0.0638	0.0130
31	0.0662	0.0124
32	0.0825	0.0083
33	0.1032	0.0032
34 (Station 3)	0.1006	0.0083
35 (Station 4)	0.0974	0.0146
36 (Station 2)	0.1086	0.0215
37	0.1155	0.0260
38	0.1210	0.0295
39	0.1177	0.0274
40	0.1240	0.0314
41	0.1273	0.0336
42 (Station 1)	0.1336	0.0377
43	0.1206	0.0344
44	0.1006	0.0293
45	0.0735	0.0225
46	0.0548	0.0178
47	0.0379	0.0135
48 (Station 0)	0.0093	0.0063
49	0.009	0.006

*The segment numbers with Station IDs indicate the measured values

Table A.3: Organic Nitrogen Initial Concentrations (mg/L)

Segment No*	Upper Layer	Bottom Layer
1	0.33	0.132
2 (Station 14)	0.3427	0.1308
3 (Station 13)	0.0015	0.0000
4	0.2679	0.0377
5	0.2268	0.0319
6	0.1777	0.0250
7 (Station 7)	0.4828	0.0682
8	0.4330	0.1134
9 (Station 6)	0.2561	0.1046
10	0.2176	0.0852
11	0.2034	0.0780
12	0.3631	0.1771
13	0.3205	0.2158
14	0.1805	0.0664
15	0.1351	0.0435
16 (Station 8)	0.1010	0.0263
17 (Station 9)	0.2297	0.2985
18 (Station 10)	0.2209	0.0795
19 (Station 11)	0.2947	0.9425
20 (Station 12)	0.2505	0.1247
21	0.215	0.08
22	0.213	0.077
23	0.21	0.75
24	0.2212	0.1735
25 (Station 15)	0.2023	0.2108
26	0.2185	0.2886
27	0.1008	0.1043
28	0.09	0.1
29 (Station 5)	0.4113	0.3583
30	0.2814	0.2593
31	0.2638	0.2459
32	0.1475	0.1573
33	0.0000	0.0448
34 (Station 3)	0.0565	0.0801
35 (Station 4)	0.1252	0.1230
36 (Station 2)	0.2473	0.4263
37	0.2363	0.3187
38	0.2277	0.2345
39	0.2328	0.2848
40	0.2229	0.1877
41	0.2177	0.1363
42 (Station 1)	0.2077	0.0381
43	0.2379	0.0557
44	0.2846	0.0828
45	0.3475	0.1195
46	0.3912	0.1448
47	0.4305	0.1677
48 (Station 0)	0.4971	0.2065
49	0.49	0.21

*The segment numbers with Station IDs indicate the measured values

Table A.4: Orthophosphate Initial Concentrations (mg/L)

Segment No*	Upper Layer	Bottom Layer
1	0.0018	0.0018
2 (Station 14)	0.0016	0.0016
3 (Station 13)	0.0008	0.0008
4	0.0006	0.0006
5	0.0006	0.0006
6	0.0006	0.0006
7 (Station 7)	0.0004	0.0004
8	0.0036	0.0004
9 (Station 6)	0.0016	0.0022
10	0.0021	0.0020
11	0.0022	0.0020
12	0.0081	0.0003
13	0.0109	0.0003
14	0.0025	0.0019
15	0.0031	0.0018
16 (Station 8)	0.0035	0.0016
17 (Station 9)	0.0167	0.0002
18 (Station 10)	0.0024	0.0020
19 (Station 11)	0.0007	0.0288
20 (Station 12)	0.0007	0.004
21	0.0018	0.0017
22	0.0015	0.0015
23	0.0013	0.0013
24	0.0022	0.0016
25 (Station 15)	0.0026	0.0013
26	0.0022	0.0018
27	0.0017	0.0010
28	0.0015	0.001
29 (Station 5)	0.0012	0.0004
30	0.0010	0.0013
31	0.0010	0.0014
32	0.0008	0.0023
33	0.0006	0.0033
34 (Station 3)	0.0005	0.0024
35 (Station 4)	0.0004	0.0012
36 (Station 2)	0.0015	0.0028
37	0.0017	0.0029
38	0.0019	0.0030
39	0.0018	0.0029
40	0.0020	0.0031
41	0.0021	0.0031
42 (Station 1)	0.0024	0.0032
43	0.0024	0.0031
44	0.0025	0.0028
45	0.0026	0.0025
46	0.0026	0.0023
47	0.0027	0.0021
48 (Station 0)	0.0028	0.0017
49	0.0029	0.0018

*The segment numbers with Station IDs indicate the measured values

Table A.5: Organic Phosphorus Initial Concentrations (mg/L)

Segment No*	Upper Layer	Bottom Layer
1	0.0074	0.002
2 (Station 14)	0.0000	0.0000
3 (Station 13)	0.0002	0.0000
4	0.0003	0.0000
5	0.0003	0.0000
6	0.0003	0.0000
7 (Station 7)	0.0004	0.0000
8	0.0003	0.0000
9 (Station 6)	0.0029	0.0000
10	0.0022	0.0000
11	0.0019	0.0000
12	0.0002	0.0000
13	0.0001	0.0000
14	0.0015	0.0000
15	0.0006	0.0000
16 (Station 8)	0.0000	0.0000
17 (Station 9)	0.0000	0.0000
18 (Station 10)	0.0007	0.0000
19 (Station 11)	0.0023	0.024
20 (Station 12)	0.0012	0.0103
21	0.002	0.001
22	0.0018	0.0009
23	0.0015	0.0008
24	0.0017	0.0002
25 (Station 15)	0.0010	0.0003
26	0.0023	0.0026
27	0.0006	0.0002
28	0.0006	0.0002
29 (Station 5)	0.0027	0.0011
30	0.0032	0.0016
31	0.0032	0.0016
32	0.0036	0.0021
33	0.0041	0.0026
34 (Station 3)	0.0042	0.0029
35 (Station 4)	0.0044	0.0032
36 (Station 2)	0.0046	0.0068
37	0.0043	0.0050
38	0.0041	0.0036
39	0.0042	0.0044
40	0.0039	0.0028
41	0.0038	0.0019
42 (Station 1)	0.0035	0.0003
43	0.0032	0.0002
44	0.0026	0.0002
45	0.0018	0.0001
46	0.0013	0.0001
47	0.0008	0.0001
48 (Station 0)	0.0000	0.0000
49	0.0057	0.0044

*The segment numbers with Station IDs indicate the measured values

Table A.6: Chlorophyll-a Initial Concentrations (μg/L)

Segment No*	Upper Layer	Bottom Layer
1	1.95	0.5
2 (Station 14)	1.99	0.54
3 (Station 13)	1.74	0.91
4	1.89	1.67
5	1.87	1.56
6	1.84	1.42
7 (Station 7)	2.01	2.29
8	2.18	2.55
9 (Station 6)	2.27	2.49
10	2.54	2.68
11	2.64	2.76
12	2.43	2.90
13	2.58	3.12
14	2.81	2.87
15	3.13	3.10
16 (Station 8)	3.37	3.27
17 (Station 9)	2.90	3.59
18 (Station 10)	3.77	4.89
19 (Station 11)	4.14	15.97
20 (Station 12)	3.33	2.82
21	2.5	2.65
22	2.47	2.6
23	2.45	2.55
24	1.76	2.40
25 (Station 15)	1.48	2.35
26	1.59	2.71
27	1.61	1.62
28	1.55	1.5
29 (Station 5)	1.32	1.02
30	1.54	5.97
31	1.57	6.64
32	1.76	11.07
33	2.01	16.69
34 (Station 3)	2.08	11.56
35 (Station 4)	2.17	5.32
36 (Station 2)	1.78	3.34
37	1.76	3.95
38	1.74	4.42
39	1.75	4.14
40	1.72	4.69
41	1.71	4.98
42 (Station 1)	1.69	5.53
43	1.71	5.13
44	1.75	4.50
45	1.80	3.66
46	1.83	3.08
47	1.86	2.55
48 (Station 0)	1.91	1.66
49	1.8	1.6

*The segment numbers with Station IDs indicate the measured values

Table A.7: Dissolved Oxygen Initial Concentrations (mg/L)

Segment No*	Upper Layer	Bottom Layer
1	7.4	7.4
2 (Station 14)	7.50	7.50
3 (Station 13)	7.50	7.30
4	7.56	7.08
5	7.55	7.11
6	7.54	7.15
7 (Station 7)	7.60	6.90
8	7.56	6.70
9 (Station 6)	7.70	6.60
10	7.63	6.48
11	7.60	6.43
12	7.51	6.43
13	7.47	6.26
14	7.55	6.36
15	7.47	6.21
16 (Station 8)	7.40	6.10
17 (Station 9)	7.40	5.90
18 (Station 10)	7.94	4.55
19 (Station 11)	8.1	0.03
20 (Station 12)	8.5	2.9
21	7.55	6.45
22	7.45	6.43
23	7.3	6.4
24	8.09	6.92
25 (Station 15)	8.30	7.10
26	8.34	6.92
27	7.90	7.20
28	7.7	6.8
29 (Station 5)	7.10	7.20
30	7.48	6.69
31	7.53	6.63
32	7.87	6.17
33	8.30	5.60
34 (Station 3)	8.44	5.83
35 (Station 4)	8.60	6.10
36 (Station 2)	8.40	6.60
37	8.59	6.30
38	8.75	6.06
39	8.66	6.20
40	8.83	5.92
41	8.92	5.78
42 (Station 1)	9.10	5.50
43	9.22	5.95
44	9.39	6.64
45	9.63	7.58
46	9.80	8.23
47	9.95	8.81
48 (Station 0)	10.20	9.80
49	10.00	9.7

*The segment numbers with Station IDs indicate the measured values

Table A.8: CBOD Initial Concentrations (mg/L)

Segment No*	Upper Layer	Bottom Layer
1	7.1	0.7
2 (Station 14)	7.00	0.50
3 (Station 13)	1.00	1.40
4	4.32	0.90
5	3.81	0.98
6	3.20	1.07
7 (Station 7)	7.00	0.50
8	7.00	1.78
9 (Station 6)	7.00	7.00
10	5.44	5.41
11	4.86	4.82
12	7.00	3.57
13	7.00	4.67
14	3.93	3.88
15	2.09	2.01
16 (Station 8)	0.70	0.60
17 (Station 9)	7.00	7.00
18 (Station 10)	0.70	3.27
19 (Station 11)	7	7
20 (Station 12)	7	0.5
21	5.5	5.45
22	5.55	5.5
23	5.6	5.7
24	2.85	2.98
25 (Station 15)	0.60	0.80
26	2.54	2.31
27	0.80	1.10
28	1	5.76
29 (Station 5)	7.00	0.60
30	5.20	2.62
31	4.96	2.90
32	3.34	4.70
33	1.30	7.00
34 (Station 3)	1.03	7.00
35 (Station 4)	0.70	7.00
36 (Station 2)	0.60	7.00
37	2.37	7.00
38	6.48	5.98
39	6.35	5.72
40	6.61	6.22
41	6.74	6.49
42 (Station 1)	7.00	7.00
43	6.39	6.55
44	5.46	5.86
45	4.20	4.92
46	3.32	4.27
47	2.53	3.69
48 (Station 0)	1.20	2.70
49	1.4	2.8

*The segment numbers with Station IDs indicate the measured values

Table A.9: Detrital Carbon Initial Concentrations (mg/L)

Segment No*	Upper Layer	Bottom Layer
1	0.15	0.08
2 (Station 14)	0.16	0.10
3 (Station 13)	0.27	0.18
4	0.26	0.31
5	0.26	0.29
6	0.26	0.27
7 (Station 7)	0.25	0.41
8	0.31	0.53
9 (Station 6)	0.31	0.72
10	0.38	0.81
11	0.41	0.84
12	0.38	0.69
13	0.43	0.80
14	0.45	0.89
15	0.53	1.00
16 (Station 8)	0.59	1.07
17 (Station 9)	0.53	1.01
18 (Station 10)	0.64	1.07
19 (Station 11)	0.418	1.443
20 (Station 12)	0.629	1.61
21	0.38	0.77
22	0.37	0.75
23	0.35	0.73
24	0.34	0.52
25 (Station 15)	0.35	0.41
26	0.36	0.57
27	0.31	0.29
28	0.3	0.29
29 (Station 5)	0.24	0.25
30	0.25	0.89
31	0.26	0.98
32	0.27	1.55
33	0.28	2.29
34 (Station 3)	0.31	1.64
35 (Station 4)	0.34	0.85
36 (Station 2)	0.38	0.87
37	0.33	0.84
38	0.30	0.82
39	0.32	0.84
40	0.27	0.81
41	0.25	0.80
42 (Station 1)	0.21	0.77
43	0.21	0.73
44	0.22	0.67
45	0.23	0.58
46	0.24	0.52
47	0.25	0.47
48 (Station 0)	0.26	0.38
49	0.262	0.375

*The segment numbers with Station IDs indicate the measured values

Table A.10: Detrital Nitrogen Initial Concentrations (mg/L)

Segment No*	Upper Layer	Bottom Layer
1	0.025	0.0125
2 (Station 14)	0.0263	0.0131
3 (Station 13)	0.0471	0.0298
4	0.0455	0.0463
5	0.0457	0.0437
6	0.0460	0.0407
7 (Station 7)	0.0441	0.0596
8	0.0527	0.0710
9 (Station 6)	0.0493	0.0775
10	0.0580	0.0911
11	0.0612	0.0962
12	0.0649	0.0871
13	0.0723	0.0969
14	0.0664	0.1043
15	0.0767	0.1203
16 (Station 8)	0.0844	0.1324
17 (Station 9)	0.0881	0.1178
18 (Station 10)	0.0983	0.1593
19 (Station 11)	0.0673	0.2505
20 (Station 12)	0.1083	0.2719
21	0.056	0.087
22	0.053	0.085
23	0.051	0.082
24	0.0505	0.0606
25 (Station 15)	0.0511	0.0514
26	0.0512	0.0683
27	0.0491	0.0405
28	0.047	0.038
29 (Station 5)	0.0322	0.0265
30	0.0340	0.1053
31	0.0342	0.1160
32	0.0358	0.1865
33	0.0379	0.2760
34 (Station 3)	0.0407	0.2184
35 (Station 4)	0.0441	0.1485
36 (Station 2)	0.0514	0.0983
37	0.0452	0.0995
38	0.0404	0.1004
39	0.0433	0.0999
40	0.0378	0.1009
41	0.0348	0.1015
42 (Station 1)	0.0292	0.1025
43	0.0293	0.0976
44	0.0295	0.0899
45	0.0296	0.0796
46	0.0298	0.0725
47	0.0299	0.0660
48 (Station 0)	0.0301	0.0551
49	0.03	0.045

*The segment numbers with Station IDs indicate the measured values

Table A.11: Detrital Phosphorus Initial Concentrations (mg/L)

Segment No*	Upper Layer	Bottom Layer
1	0	0
2 (Station 14)	0.0000	0.0000
3 (Station 13)	0.0077	0.0041
4	0.0034	0.0067
5	0.0041	0.0063
6	0.0049	0.0058
7 (Station 7)	0.0000	0.0087
8	0.0000	0.0092
9 (Station 6)	0.0000	0.0000
10	0.0000	0.0024
11	0.0000	0.0033
12	0.0000	0.0099
13	0.0000	0.0103
14	0.0000	0.0047
15	0.0000	0.0076
16 (Station 8)	0.0000	0.0097
17 (Station 9)	0.0000	0.0111
18 (Station 10)	0.0035	0.0097
19 (Station 11)	0.0099	0.0087
20 (Station 12)	0.0056	0.0077
21	0.0025	0.002
22	0.0023	0.0018
23	0.0021	0.0016
24	0.0078	0.0035
25 (Station 15)	0.0120	0.0054
26	0.0110	0.0054
27	0.0099	0.0048
28	0.009	0.0045
29 (Station 5)	0.0000	0.0058
30	0.0000	0.0040
31	0.0000	0.0037
32	0.0000	0.0021
33	0.0000	0.0000
34 (Station 3)	0.0031	0.0014
35 (Station 4)	0.0069	0.0031
36 (Station 2)	0.0093	0.0053
37	0.0067	0.0062
38	0.0047	0.0068
39	0.0059	0.0064
40	0.0036	0.0072
41	0.0023	0.0076
42 (Station 1)	0.0000	0.0083
43	0.0000	0.0075
44	0.0000	0.0061
45	0.0000	0.0043
46	0.0000	0.0031
47	0.0000	0.0019
48 (Station 0)	0.0000	0.0000
49	0	0

*The segment numbers with Station IDs indicate the measured values

Table A.12: Salinity Initial Concentrations (ppt)

Segment No*	Upper Layer	Bottom Layer
1	39	39.5
2 (Station 14)	38.86	39.12
3 (Station 13)	24.83	36.51
4	17.97	34.70
5	19.03	34.98
6	20.29	35.31
7 (Station 7)	12.44	33.24
8	11.04	27.91
9 (Station 6)	13.16	34.39
10	11.34	27.36
11	10.66	24.74
12	9.06	20.43
13	7.86	15.87
14	9.58	20.56
15	7.43	12.26
16 (Station 8)	5.82	6.02
17 (Station 9)	5.30	6.14
18 (Station 10)	5.89	15.91
19 (Station 11)	5.8	35.7
20 (Station 12)	5.44	30.9
21	11.3	27
22	11.2	26.8
23	11	26.7
24	11.25	33.20
25 (Station 15)	10.22	32.55
26	9.26	33.23
27	17.60	34.55
28	17	34
29 (Station 5)	36.28	36.78
30	28.71	35.46
31	27.68	35.28
32	20.91	34.09
33	12.31	32.59
34 (Station 3)	11.21	33.41
35 (Station 4)	9.88	34.40
36 (Station 2)	7.56	34.42
37	6.79	30.96
38	6.19	28.25
39	6.55	29.87
40	5.85	26.75
41	5.48	25.09
42 (Station 1)	4.78	21.93
43	4.59	19.94
44	4.29	16.88
45	3.88	12.75
46	3.60	9.89
47	3.35	7.30
48 (Station 0)	2.92	2.93
49	2.8	2.8

*The segment numbers with Station IDs indicate the measured values

ANNEX B

The Flow Rates, Exchanges and Eddy Dispersion Coefficients

Table B1: Flows Q1 – Q13 from the Mediterranean Sea

Date	Time	Q1	Q2	Q3	Q4	Q5	Q6	Q7	Q8	Q9	Q10	Q11	Q12	Q13
01/05/1998	0:00:00	0.4	0.5	0.4	0.6	0.125	0.025	0.017	0.017	2.5	2.5	1	2.5	2.5
01/15/1998	0:00:00	0.4	0.5	0.4	0.6	0.125	0.025	0.017	0.017	2.5	2.5	1	2.5	2.5
01/25/1998	0:00:00	0.4	0.5	0.4	0.6	0.125	0.025	0.017	0.017	2.5	2.5	1	2.5	2.5
02/04/1998	0:00:00	0.4	0.5	0.4	0.6	0.125	0.025	0.017	0.017	2.5	2.5	1	2.5	2.5
02/14/1998	0:00:00	0.4	0.5	0.4	0.6	0.125	0.025	0.017	0.017	2.5	2.5	1	2.5	2.5
02/24/1998	0:00:00	0.4	0.5	0.4	0.6	0.125	0.025	0.017	0.017	2.5	2.5	1	2.5	2.5
03/06/1998	0:00:00	0.4	0.5	0.4	0.6	0.125	0.025	0.017	0.017	2.5	2.5	1	2.5	2.5
03/16/1998	0:00:00	0.4	0.5	0.4	0.6	0.125	0.025	0.017	0.017	2.5	2.5	1	2.5	2.5
03/26/1998	0:00:00	0.4	0.5	0.4	0.6	0.125	0.025	0.017	0.017	2.5	2.5	1	2.5	2.5
04/05/1998	0:00:00	0.4	0.5	0.4	0.6	0.125	0.025	0.017	0.017	2.5	2.5	1	2.5	2.5
04/15/1998	0:00:00	0.4	0.5	0.4	0.6	0.125	0.025	0.017	0.017	2.5	2.5	1	2.5	2.5
04/25/1998	0:00:00	0.4	0.5	0.4	0.6	0.125	0.025	0.017	0.017	2.5	2.5	1	2.5	2.5
05/05/1998	0:00:00	0.4	0.5	0.4	0.6	0.125	0.025	0.017	0.017	2.5	2.5	1	2.5	2.5
05/15/1998	0:00:00	0.4	0.5	0.4	0.6	0.125	0.025	0.017	0.017	2.5	2.5	1	2.5	2.5
05/25/1998	0:00:00	0.4	0.5	0.4	0.6	0.125	0.025	0.017	0.017	2.5	2.5	1	2.5	2.5
06/30/1998	0:00:00	0.4	0.5	0.4	0.6	0.125	0.025	0.017	0.017	2.5	2.5	1	2.5	2.5
07/09/1998	0:00:00	0.4	0.5	0.4	0.6	0.125	0.025	0.017	0.017	2.5	2.5	1	2.5	2.5
07/19/1998	0:00:00	0.4	0.5	0.4	0.6	0.125	0.025	0.017	0.017	2.5	2.5	1	2.5	2.5
07/29/1998	0:00:00	0.4	0.5	0.4	0.6	0.125	0.025	0.017	0.017	2.5	2.5	1	2.5	2.5
08/08/1998	0:00:00	0.4	0.5	0.4	0.6	0.125	0.025	0.017	0.017	2.5	2.5	1	2.5	2.5
08/18/1998	0:00:00	0.4	0.5	0.4	0.6	0.125	0.025	0.017	0.017	2.5	2.5	1	2.5	2.5
08/28/1998	0:00:00	0.4	0.5	0.4	0.6	0.125	0.025	0.017	0.017	2.5	2.5	1	2.5	2.5
09/07/1998	0:00:00	0.4	0.5	0.4	0.6	0.125	0.025	0.017	0.017	2.5	2.5	1	2.5	2.5
09/17/1998	0:00:00	0.4	0.5	0.4	0.6	0.125	0.025	0.017	0.017	2.5	2.5	1	2.5	2.5
09/27/1998	0:00:00	0.4	0.5	0.4	0.6	0.125	0.025	0.017	0.017	2.5	2.5	1	2.5	2.5
10/07/1998	0:00:00	0.4	0.5	0.4	0.6	0.125	0.025	0.017	0.017	2.5	2.5	1	2.5	2.5

Table B1: Flows Q1 – Q13 from the Mediterranean Sea (continued)

Date	Time	Q1	Q2	Q3	Q4	Q5	Q6	Q7	Q8	Q9	Q10	Q11	Q12	Q13
10/17/1998	0:00:00	0.4	0.5	0.4	0.6	0.125	0.025	0.017	0.017	2.5	2.5	1	2.5	2.5
10/27/1998	0:00:00	0.4	0.5	0.4	0.6	0.125	0.025	0.017	0.017	2.5	2.5	1	2.5	2.5
11/06/1998	0:00:00	0.4	0.5	0.4	0.6	0.125	0.025	0.017	0.017	2.5	2.5	1	2.5	2.5
11/16/1998	0:00:00	0.4	0.5	0.4	0.6	0.125	0.025	0.017	0.017	2.5	2.5	1	2.5	2.5
11/26/1998	0:00:00	0.4	0.5	0.4	0.6	0.125	0.025	0.017	0.017	2.5	2.5	1	2.5	2.5
12/06/1998	0:00:00	0.4	0.5	0.4	0.6	0.125	0.025	0.017	0.017	2.5	2.5	1	2.5	2.5
12/16/1998	0:00:00	0.4	0.5	0.4	0.6	0.125	0.025	0.017	0.017	2.5	2.5	1	2.5	2.5
12/26/1998	0:00:00	0.4	0.5	0.4	0.6	0.125	0.025	0.017	0.017	2.5	2.5	1	2.5	2.5
01/05/1999	0:00:00	0.4	0.5	0.4	0.6	0.125	0.025	0.017	0.017	2.5	2.5	1	2.5	2.5
01/15/1999	0:00:00	0.4	0.5	0.4	0.6	0.125	0.025	0.017	0.017	2.5	2.5	1	2.5	2.5
01/25/1999	0:00:00	0.4	0.5	0.4	0.6	0.125	0.025	0.017	0.017	2.5	2.5	1	2.5	2.5
02/04/1999	0:00:00	0.4	0.5	0.4	0.6	0.125	0.025	0.017	0.017	2.5	2.5	1	2.5	2.5
02/14/1999	0:00:00	0.4	0.5	0.4	0.6	0.125	0.025	0.017	0.017	2.5	2.5	1	2.5	2.5
02/24/1999	0:00:00	0.4	0.5	0.4	0.6	0.125	0.025	0.017	0.017	2.5	2.5	1	2.5	2.5
03/06/1999	0:00:00	0.4	0.5	0.4	0.6	0.125	0.025	0.017	0.017	2.5	2.5	1	2.5	2.5
03/16/1999	0:00:00	0.4	0.5	0.4	0.6	0.125	0.025	0.017	0.017	2.5	2.5	1	2.5	2.5
03/26/1999	0:00:00	0.4	0.5	0.4	0.6	0.125	0.025	0.017	0.017	2.5	2.5	1	2.5	2.5
04/05/1999	0:00:00	0.4	0.5	0.4	0.6	0.125	0.025	0.017	0.017	2.5	2.5	1	2.5	2.5
04/15/1999	0:00:00	0.4	0.5	0.4	0.6	0.125	0.025	0.017	0.017	2.5	2.5	1	2.5	2.5
04/25/1999	0:00:00	0.4	0.5	0.4	0.6	0.125	0.025	0.017	0.017	2.5	2.5	1	2.5	2.5
05/05/1999	0:00:00	0.4	0.5	0.4	0.6	0.125	0.025	0.017	0.017	2.5	2.5	1	2.5	2.5
05/15/1999	0:00:00	0.4	0.5	0.4	0.6	0.125	0.025	0.017	0.017	2.5	2.5	1	2.5	2.5
05/25/1999	0:00:00	0.4	0.5	0.4	0.6	0.125	0.025	0.017	0.017	2.5	2.5	1	2.5	2.5
06/04/1999	0:00:00	0.4	0.5	0.4	0.6	0.125	0.025	0.017	0.017	2.5	2.5	1	2.5	2.5
06/14/1999	0:00:00	0.4	0.5	0.4	0.6	0.125	0.025	0.017	0.017	2.5	2.5	1	2.5	2.5
06/24/1999	0:00:00	0.4	0.5	0.4	0.6	0.125	0.025	0.017	0.017	2.5	2.5	1	2.5	2.5
07/04/1999	0:00:00	0.4	0.5	0.4	0.6	0.125	0.025	0.017	0.017	2.5	2.5	1	2.5	2.5
07/14/1999	0:00:00	0.4	0.5	0.4	0.6	0.125	0.025	0.017	0.017	2.5	2.5	1	2.5	2.5

Table B1: Flows Q1 – Q13 from the Mediterranean Sea (continued)

Date	Time	Q1	Q2	Q3	Q4	Q5	Q6	Q7	Q8	Q9	Q10	Q11	Q12	Q13
07/24/1999	0:00:00	0.4	0.5	0.4	0.6	0.125	0.025	0.017	0.017	2.5	2.5	1	2.5	2.5
08/03/1999	0:00:00	0.4	0.5	0.4	0.6	0.125	0.025	0.017	0.017	2.5	2.5	1	2.5	2.5
08/13/1999	0:00:00	0.4	0.5	0.4	0.6	0.125	0.025	0.017	0.017	2.5	2.5	1	2.5	2.5
08/23/1999	0:00:00	0.4	0.5	0.4	0.6	0.125	0.025	0.017	0.017	2.5	2.5	1	2.5	2.5
09/02/1999	0:00:00	0.4	0.5	0.4	0.6	0.125	0.025	0.017	0.017	2.5	2.5	1	2.5	2.5
09/12/1999	0:00:00	0.4	0.5	0.4	0.6	0.125	0.025	0.017	0.017	2.5	2.5	1	2.5	2.5
09/22/1999	0:00:00	0.4	0.5	0.4	0.6	0.125	0.025	0.017	0.017	2.5	2.5	1	2.5	2.5
10/02/1999	0:00:00	0.4	0.5	0.4	0.6	0.125	0.025	0.017	0.017	2.5	2.5	1	2.5	2.5
10/12/1999	0:00:00	0.4	0.5	0.4	0.6	0.125	0.025	0.017	0.017	2.5	2.5	1	2.5	2.5
10/22/1999	0:00:00	0.4	0.5	0.4	0.6	0.125	0.025	0.017	0.017	2.5	2.5	1	2.5	2.5
11/01/1999	0:00:00	0.4	0.5	0.4	0.6	0.125	0.025	0.017	0.017	2.5	2.5	1	2.5	2.5
11/11/1999	0:00:00	0.4	0.5	0.4	0.6	0.125	0.025	0.017	0.017	2.5	2.5	1	2.5	2.5
11/21/1999	0:00:00	0.4	0.5	0.4	0.6	0.125	0.025	0.017	0.017	2.5	2.5	1	2.5	2.5
12/01/1999	0:00:00	0.4	0.5	0.4	0.6	0.125	0.025	0.017	0.017	2.5	2.5	1	2.5	2.5
12/11/1999	0:00:00	0.4	0.5	0.4	0.6	0.125	0.025	0.017	0.017	2.5	2.5	1	2.5	2.5
12/21/1999	0:00:00	0.4	0.5	0.4	0.6	0.125	0.025	0.017	0.017	2.5	2.5	1	2.5	2.5
12/31/1999	0:00:00	0.4	0.5	0.4	0.6	0.125	0.025	0.017	0.017	2.5	2.5	1	2.5	2.5
01/10/2000	0:00:00	0.4	0.5	0.4	0.6	0.125	0.025	0.017	0.017	2.5	2.5	1	2.5	2.5
01/20/2000	0:00:00	0.4	0.5	0.4	0.6	0.125	0.025	0.017	0.017	2.5	2.5	1	2.5	2.5
01/30/2000	0:00:00	0.4	0.5	0.4	0.6	0.125	0.025	0.017	0.017	2.5	2.5	1	2.5	2.5
02/09/2000	0:00:00	0.4	0.5	0.4	0.6	0.125	0.025	0.017	0.017	2.5	2.5	1	2.5	2.5
02/19/2000	0:00:00	0.4	0.5	0.4	0.6	0.125	0.025	0.017	0.017	2.5	2.5	1	2.5	2.5
02/29/2000	0:00:00	0.4	0.5	0.4	0.6	0.125	0.025	0.017	0.017	2.5	2.5	1	2.5	2.5
03/10/2000	0:00:00	0.4	0.5	0.4	0.6	0.125	0.025	0.017	0.017	2.5	2.5	1	2.5	2.5
03/20/2000	0:00:00	0.4	0.5	0.4	0.6	0.125	0.025	0.017	0.017	2.5	2.5	1	2.5	2.5
03/29/2000	0:00:00	0.4	0.5	0.4	0.6	0.125	0.025	0.017	0.017	2.5	2.5	1	2.5	2.5

Table B2: Flows Q14 – Q25 from the Mediterranean Sea

Date	Time	Q14	Q15	Q16	Q17	Q18	Q19	Q20	Q21	Q22	Q23	Q24	Q25
01/05/1998	0:00:00	1	1	3.03	1.25	0.536	1	0.5	0.2	0.1	0.1	0.1	0.1
01/15/1998	0:00:00	1	1	3.03	1.25	0.536	1	0.5	0.2	0.1	0.1	0.1	0.1
01/25/1998	0:00:00	1	1	3.03	1.25	0.536	1	0.5	0.2	0.1	0.1	0.1	0.1
02/04/1998	0:00:00	1	1	3.03	1.25	0.536	1	0.5	0.2	0.1	0.1	0.1	0.1
02/14/1998	0:00:00	1	1	3.03	1.25	0.536	1	0.5	0.2	0.1	0.1	0.1	0.1
02/24/1998	0:00:00	1	1	3.03	1.25	0.536	1	0.5	0.2	0.1	0.1	0.1	0.1
03/06/1998	0:00:00	1	1	3.03	1.25	0.536	1	0.5	0.2	0.1	0.1	0.1	0.1
03/16/1998	0:00:00	1	1	3.03	1.25	0.536	1	0.5	0.2	0.1	0.1	0.1	0.1
03/26/1998	0:00:00	1	1	3.03	1.25	0.536	1	0.5	0.2	0.1	0.1	0.1	0.1
04/05/1998	0:00:00	1	1	3.03	1.25	0.536	1	0.5	0.2	0.1	0.1	0.1	0.1
04/15/1998	0:00:00	1	1	3.03	1.25	0.536	1	0.5	0.2	0.1	0.1	0.1	0.1
04/25/1998	0:00:00	1	1	3.03	1.25	0.536	1	0.5	0.2	0.1	0.1	0.1	0.1
05/05/1998	0:00:00	1	1	3.03	1.25	0.536	1	0.5	0.2	0.1	0.1	0.1	0.1
05/15/1998	0:00:00	1	1	3.03	1.25	0.536	1	0.5	0.2	0.1	0.1	0.1	0.1
05/25/1998	0:00:00	1	1	3.03	1.25	0.536	1	0.5	0.2	0.1	0.1	0.1	0.1
06/30/1998	0:00:00	1	1	3.03	1.25	0.536	1	0.5	0.2	0.1	0.1	0.1	0.1
07/09/1998	0:00:00	1	1	3.03	1.25	0.536	1	0.5	0.2	0.1	0.1	0.1	0.1
07/19/1998	0:00:00	1	1	3.03	1.25	0.536	1	0.5	0.2	0.1	0.1	0.1	0.1
07/29/1998	0:00:00	1	1	3.03	1.25	0.536	1	0.5	0.2	0.1	0.1	0.1	0.1
08/08/1998	0:00:00	1	1	3.03	1.25	0.536	1	0.5	0.2	0.1	0.1	0.1	0.1
08/18/1998	0:00:00	1	1	3.03	1.25	0.536	1	0.5	0.2	0.1	0.1	0.1	0.1
08/28/1998	0:00:00	1	1	3.03	1.25	0.536	1	0.5	0.2	0.1	0.1	0.1	0.1
09/07/1998	0:00:00	1	1	3.03	1.25	0.536	1	0.5	0.2	0.1	0.1	0.1	0.1
09/17/1998	0:00:00	1	1	3.03	1.25	0.536	1	0.5	0.2	0.1	0.1	0.1	0.1
09/27/1998	0:00:00	1	1	3.03	1.25	0.536	1	0.5	0.2	0.1	0.1	0.1	0.1
10/07/1998	0:00:00	1	1	3.03	1.25	0.536	1	0.5	0.2	0.1	0.1	0.1	0.1
10/17/1998	0:00:00	1	1	3.03	1.25	0.536	1	0.5	0.2	0.1	0.1	0.1	0.1
10/27/1998	0:00:00	1	1	3.03	1.25	0.536	1	0.5	0.2	0.1	0.1	0.1	0.1

Table B2: Flows Q14 – Q25 from the Mediterranean Sea (continued)

Date	Time	Q14	Q15	Q16	Q17	Q18	Q19	Q20	Q21	Q22	Q23	Q24	Q25
11/06/1998	0:00:00	1	1	3.03	1.25	0.536	1	0.5	0.2	0.1	0.1	0.1	0.1
11/16/1998	0:00:00	1	1	3.03	1.25	0.536	1	0.5	0.2	0.1	0.1	0.1	0.1
11/26/1998	0:00:00	1	1	3.03	1.25	0.536	1	0.5	0.2	0.1	0.1	0.1	0.1
12/06/1998	0:00:00	1	1	3.03	1.25	0.536	1	0.5	0.2	0.1	0.1	0.1	0.1
12/16/1998	0:00:00	1	1	3.03	1.25	0.536	1	0.5	0.2	0.1	0.1	0.1	0.1
12/26/1998	0:00:00	1	1	3.03	1.25	0.536	1	0.5	0.2	0.1	0.1	0.1	0.1
01/05/1999	0:00:00	1	1	3.03	1.25	0.536	1	0.5	0.2	0.1	0.1	0.1	0.1
01/15/1999	0:00:00	1	1	3.03	1.25	0.536	1	0.5	0.2	0.1	0.1	0.1	0.1
01/25/1999	0:00:00	1	1	3.03	1.25	0.536	1	0.5	0.2	0.1	0.1	0.1	0.1
02/04/1999	0:00:00	1	1	3.03	1.25	0.536	1	0.5	0.2	0.1	0.1	0.1	0.1
02/14/1999	0:00:00	1	1	3.03	1.25	0.536	1	0.5	0.2	0.1	0.1	0.1	0.1
02/24/1999	0:00:00	1	1	3.03	1.25	0.536	1	0.5	0.2	0.1	0.1	0.1	0.1
03/06/1999	0:00:00	1	1	3.03	1.25	0.536	1	0.5	0.2	0.1	0.1	0.1	0.1
03/16/1999	0:00:00	1	1	3.03	1.25	0.536	1	0.5	0.2	0.1	0.1	0.1	0.1
03/26/1999	0:00:00	1	1	3.03	1.25	0.536	1	0.5	0.2	0.1	0.1	0.1	0.1
04/05/1999	0:00:00	1	1	3.03	1.25	0.536	1	0.5	0.2	0.1	0.1	0.1	0.1
04/15/1999	0:00:00	1	1	3.03	1.25	0.536	1	0.5	0.2	0.1	0.1	0.1	0.1
04/25/1999	0:00:00	1	1	3.03	1.25	0.536	1	0.5	0.2	0.1	0.1	0.1	0.1
05/05/1999	0:00:00	1	1	3.03	1.25	0.536	1	0.5	0.2	0.1	0.1	0.1	0.1
05/15/1999	0:00:00	1	1	3.03	1.25	0.536	1	0.5	0.2	0.1	0.1	0.1	0.1
05/25/1999	0:00:00	1	1	3.03	1.25	0.536	1	0.5	0.2	0.1	0.1	0.1	0.1
06/04/1999	0:00:00	1	1	3.03	1.25	0.536	1	0.5	0.2	0.1	0.1	0.1	0.1
06/14/1999	0:00:00	1	1	3.03	1.25	0.536	1	0.5	0.2	0.1	0.1	0.1	0.1
06/24/1999	0:00:00	1	1	3.03	1.25	0.536	1	0.5	0.2	0.1	0.1	0.1	0.1
07/04/1999	0:00:00	1	1	3.03	1.25	0.536	1	0.5	0.2	0.1	0.1	0.1	0.1
07/14/1999	0:00:00	1	1	3.03	1.25	0.536	1	0.5	0.2	0.1	0.1	0.1	0.1
07/24/1999	0:00:00	1	1	3.03	1.25	0.536	1	0.5	0.2	0.1	0.1	0.1	0.1
08/03/1999	0:00:00	1	1	3.03	1.25	0.536	1	0.5	0.2	0.1	0.1	0.1	0.1

Table B2: Flows Q14 – Q25 from the Mediterranean Sea (continued)

Date	Time	Q14	Q15	Q16	Q17	Q18	Q19	Q20	Q21	Q22	Q23	Q24	Q25
08/13/1999	0:00:00	1	1	3.03	1.25	0.536	1	0.5	0.2	0.1	0.1	0.1	0.1
08/23/1999	0:00:00	1	1	3.03	1.25	0.536	1	0.5	0.2	0.1	0.1	0.1	0.1
09/02/1999	0:00:00	1	1	3.03	1.25	0.536	1	0.5	0.2	0.1	0.1	0.1	0.1
09/12/1999	0:00:00	1	1	3.03	1.25	0.536	1	0.5	0.2	0.1	0.1	0.1	0.1
09/22/1999	0:00:00	1	1	3.03	1.25	0.536	1	0.5	0.2	0.1	0.1	0.1	0.1
10/02/1999	0:00:00	1	1	3.03	1.25	0.536	1	0.5	0.2	0.1	0.1	0.1	0.1
10/12/1999	0:00:00	1	1	3.03	1.25	0.536	1	0.5	0.2	0.1	0.1	0.1	0.1
10/22/1999	0:00:00	1	1	3.03	1.25	0.536	1	0.5	0.2	0.1	0.1	0.1	0.1
11/01/1999	0:00:00	1	1	3.03	1.25	0.536	1	0.5	0.2	0.1	0.1	0.1	0.1
11/11/1999	0:00:00	1	1	3.03	1.25	0.536	1	0.5	0.2	0.1	0.1	0.1	0.1
11/21/1999	0:00:00	1	1	3.03	1.25	0.536	1	0.5	0.2	0.1	0.1	0.1	0.1
12/01/1999	0:00:00	1	1	3.03	1.25	0.536	1	0.5	0.2	0.1	0.1	0.1	0.1
12/11/1999	0:00:00	1	1	3.03	1.25	0.536	1	0.5	0.2	0.1	0.1	0.1	0.1
12/21/1999	0:00:00	1	1	3.03	1.25	0.536	1	0.5	0.2	0.1	0.1	0.1	0.1
12/31/1999	0:00:00	1	1	3.03	1.25	0.536	1	0.5	0.2	0.1	0.1	0.1	0.1
01/10/2000	0:00:00	1	1	3.03	1.25	0.536	1	0.5	0.2	0.1	0.1	0.1	0.1
01/20/2000	0:00:00	1	1	3.03	1.25	0.536	1	0.5	0.2	0.1	0.1	0.1	0.1
01/30/2000	0:00:00	1	1	3.03	1.25	0.536	1	0.5	0.2	0.1	0.1	0.1	0.1
02/09/2000	0:00:00	1	1	3.03	1.25	0.536	1	0.5	0.2	0.1	0.1	0.1	0.1
02/19/2000	0:00:00	1	1	3.03	1.25	0.536	1	0.5	0.2	0.1	0.1	0.1	0.1
02/29/2000	0:00:00	1	1	3.03	1.25	0.536	1	0.5	0.2	0.1	0.1	0.1	0.1
03/10/2000	0:00:00	1	1	3.03	1.25	0.536	1	0.5	0.2	0.1	0.1	0.1	0.1
03/20/2000	0:00:00	1	1	3.03	1.25	0.536	1	0.5	0.2	0.1	0.1	0.1	0.1
03/29/2000	0:00:00	1	1	3.03	1.25	0.536	1	0.5	0.2	0.1	0.1	0.1	0.1

Table B3: Flows Q26 – Q36 from the Köyceğiz Lake

Date	Time	Q26	Q27	Q28	Q29	Q30	Q31	Q32	Q33	Q34	Q35	Q36
01/05/1998	0:00:00	2.6401	1.1001	0.3531	13.0951	5.2531	2.6401	5.2531	2.6401	10.4811	0.2871	0.261
01/15/1998	0:00:00	3.0967	1.2907	0.4137	15.3607	6.1627	3.0967	6.1627	3.0967	12.2947	0.3377	0.307
01/25/1998	0:00:00	3.4259	1.4279	0.4579	16.9929	6.8179	3.4259	6.8179	3.4259	13.6019	0.3729	0.339
02/04/1998	0:00:00	2.9613	1.2343	0.3953	14.6893	5.8933	2.9613	5.8933	2.9613	11.7573	0.3223	0.293
02/14/1998	0:00:00	3.0401	1.2671	0.4061	15.0801	6.0501	3.0401	6.0501	3.0401	12.0701	0.3311	0.301
02/24/1998	0:00:00	2.933	1.223	0.392	14.55	5.837	2.933	5.837	2.933	11.646	0.319	0.29
03/06/1998	0:00:00	2.426	1.011	0.324	12.034	4.828	2.426	4.828	2.426	9.632	0.264	0.24
03/16/1998	0:00:00	2.0584	0.8584	0.2754	10.2124	4.0974	2.0584	4.0974	2.0584	8.1744	0.2244	0.204
03/26/1998	0:00:00	2.3705	0.9885	0.3165	11.7595	4.7185	2.3705	4.7185	2.3705	9.4125	0.2585	0.235
04/05/1998	0:00:00	2.3018	0.9598	0.3078	11.4178	4.5808	2.3018	4.5808	2.3018	9.1388	0.2508	0.228
04/15/1998	0:00:00	1.5281	0.6371	0.2041	7.5821	3.0421	1.5281	3.0421	1.5281	6.0691	0.1661	0.151
04/25/1998	0:00:00	1.4786	0.6166	0.1976	7.3336	2.9426	1.4786	2.9426	1.4786	5.8706	0.1606	0.146
05/05/1998	0:00:00	1.1383	0.4743	0.1523	5.6453	2.2653	1.1383	2.2653	1.1383	4.5183	0.1243	0.113
05/15/1998	0:00:00	0.9888	0.4118	0.1318	4.9048	1.9678	0.9888	1.9678	0.9888	3.9258	0.1078	0.098
05/25/1998	0:00:00	0.8787	0.3667	0.1177	4.3597	1.7497	0.8787	1.7497	0.8787	3.4897	0.0957	0.087
06/30/1998	0:00:00	0.402	0.168	0.054	1.995	0.8	0.402	0.8	0.402	1.597	0.044	0.04
07/09/1998	0:00:00	0.2454	0.1024	0.0324	1.2154	0.4874	0.2454	0.4874	0.2454	0.9734	0.0264	0.024
07/19/1998	0:00:00	0.1858	0.0778	0.0248	0.9228	0.3708	0.1858	0.3708	0.1858	0.7388	0.0198	0.018
07/29/1998	0:00:00	0.1636	0.0676	0.0216	0.8096	0.3246	0.1636	0.3246	0.1636	0.6486	0.0176	0.016
08/08/1998	0:00:00	0.2182	0.0912	0.0292	1.0812	0.4332	0.2182	0.4332	0.2182	0.8652	0.0242	0.022
08/18/1998	0:00:00	0.1434	0.0594	0.0194	0.7124	0.2854	0.1434	0.2854	0.1434	0.5694	0.0154	0.014
08/28/1998	0:00:00	0.2192	0.0912	0.0292	1.0852	0.4352	0.2192	0.4352	0.2192	0.8692	0.0242	0.022
09/07/1998	0:00:00	0.098	0.041	0.013	0.488	0.196	0.098	0.196	0.098	0.391	0.011	0.01
09/17/1998	0:00:00	0.2858	0.1188	0.0378	1.4158	0.5678	0.2858	0.5678	0.2858	1.1328	0.0308	0.028
09/27/1998	0:00:00	0.2687	0.1117	0.0357	1.3317	0.5347	0.2687	0.5347	0.2687	1.0657	0.0297	0.027
10/07/1998	0:00:00	0.1919	0.0799	0.0259	0.9539	0.3829	0.1919	0.3829	0.1919	0.7639	0.0209	0.019
10/17/1998	0:00:00	0.2919	0.1219	0.0389	1.4459	0.5799	0.2919	0.5799	0.2919	1.1569	0.0319	0.029
10/27/1998	0:00:00	0.3969	0.1659	0.0529	1.9709	0.7909	0.3969	0.7909	0.3969	1.5779	0.0429	0.039

Table B3: Flows Q26 – Q36 from the Köyceğiz Lake (continued)

Date	Time	Q26	Q27	Q28	Q29	Q30	Q31	Q32	Q33	Q34	Q35	Q36
11/06/1998	0:00:00	0.6181	0.2571	0.0821	3.0641	1.2291	0.6181	1.2291	0.6181	2.4531	0.0671	0.061
11/16/1998	0:00:00	0.7595	0.3165	0.1015	3.7675	1.5115	0.7595	1.5115	0.7595	3.0155	0.0825	0.075
11/26/1998	0:00:00	0.8221	0.3431	0.1101	4.0781	1.6361	0.8221	1.6361	0.8221	3.2641	0.0891	0.081
12/06/1998	0:00:00	1.6554	0.6904	0.2214	8.2134	3.2954	1.6554	3.2954	1.6554	6.5744	0.1804	0.164
12/16/1998	0:00:00	1.8119	0.7549	0.2419	8.9869	3.6059	1.8119	3.6059	1.8119	7.1929	0.1969	0.179
12/26/1998	0:00:00	3.028	1.262	0.405	15.021	6.026	3.028	6.026	3.028	12.023	0.33	0.3
01/05/1999	0:00:00	2.6401	1.1001	0.3531	13.0951	5.2531	2.6401	5.2531	2.6401	10.4811	0.2871	0.261
01/15/1999	0:00:00	3.0967	1.2907	0.4137	15.3607	6.1627	3.0967	6.1627	3.0967	12.2947	0.3377	0.307
01/25/1999	0:00:00	3.4259	1.4279	0.4579	16.9929	6.8179	3.4259	6.8179	3.4259	13.6019	0.3729	0.339
02/04/1999	0:00:00	2.9613	1.2343	0.3953	14.6893	5.8933	2.9613	5.8933	2.9613	11.7573	0.3223	0.293
02/14/1999	0:00:00	3.0401	1.2671	0.4061	15.0801	6.0501	3.0401	6.0501	3.0401	12.0701	0.3311	0.301
02/24/1999	0:00:00	2.933	1.223	0.392	14.55	5.837	2.933	5.837	2.933	11.646	0.319	0.29
03/06/1999	0:00:00	2.426	1.011	0.324	12.034	4.828	2.426	4.828	2.426	9.632	0.264	0.24
03/16/1999	0:00:00	2.0584	0.8584	0.2754	10.2124	4.0974	2.0584	4.0974	2.0584	8.1744	0.2244	0.204
03/26/1999	0:00:00	2.3705	0.9885	0.3165	11.7595	4.7185	2.3705	4.7185	2.3705	9.4125	0.2585	0.235
04/05/1999	0:00:00	2.3018	0.9598	0.3078	11.4178	4.5808	2.3018	4.5808	2.3018	9.1388	0.2508	0.228
04/15/1999	0:00:00	1.5281	0.6371	0.2041	7.5821	3.0421	1.5281	3.0421	1.5281	6.0691	0.1661	0.151
04/25/1999	0:00:00	1.4786	0.6166	0.1976	7.3336	2.9426	1.4786	2.9426	1.4786	5.8706	0.1606	0.146
05/05/1999	0:00:00	1.1383	0.4743	0.1523	5.6453	2.2653	1.1383	2.2653	1.1383	4.5183	0.1243	0.113
05/15/1999	0:00:00	0.9888	0.4118	0.1318	4.9048	1.9678	0.9888	1.9678	0.9888	3.9258	0.1078	0.098
05/25/1999	0:00:00	0.8787	0.3667	0.1177	4.3597	1.7497	0.8787	1.7497	0.8787	3.4897	0.0957	0.087
06/04/1999	0:00:00	0.6797	0.2837	0.0907	3.3717	1.3527	0.6797	1.3527	0.6797	2.6987	0.0737	0.067
06/14/1999	0:00:00	0.3596	0.1496	0.0476	1.7816	0.7146	0.3596	0.7146	0.3596	1.4256	0.0396	0.036
06/24/1999	0:00:00	0.3818	0.1588	0.0508	1.8938	0.7598	0.3818	0.7598	0.3818	1.5158	0.0418	0.038
07/04/1999	0:00:00	0.2697	0.1127	0.0357	1.3357	0.5357	0.2697	0.5357	0.2697	1.0697	0.0297	0.027
07/14/1999	0:00:00	0.2121	0.0881	0.0281	1.0531	0.4221	0.2121	0.4221	0.2121	0.8431	0.0231	0.021
07/24/1999	0:00:00	0.0899	0.0379	0.0119	0.4449	0.1789	0.0899	0.1789	0.0899	0.3559	0.0099	0.009
08/03/1999	0:00:00	0.2515	0.1045	0.0335	1.2485	0.5015	0.2515	0.5015	0.2515	0.9995	0.0275	0.025

Table B3: Flows Q26 – Q36 from the Köyceğiz Lake (continued)

Date	Time	Q26	Q27	Q28	Q29	Q30	Q31	Q32	Q33	Q34	Q35	Q36
08/13/1999	0:00:00	0.1434	0.0604	0.0194	0.7134	0.2864	0.1434	0.2864	0.1434	0.5704	0.0154	0.014
08/23/1999	0:00:00	0.2353	0.0983	0.0313	1.1653	0.4673	0.2353	0.4673	0.2353	0.9333	0.0253	0.023
09/02/1999	0:00:00	0.1343	0.0563	0.0183	0.6673	0.2673	0.1343	0.2673	0.1343	0.5343	0.0143	0.013
09/12/1999	0:00:00	0.1879	0.0789	0.0249	0.9329	0.3739	0.1879	0.3739	0.1879	0.7469	0.0209	0.019
09/22/1999	0:00:00	0.2626	0.1096	0.0346	1.3016	0.5226	0.2626	0.5226	0.2626	1.0416	0.0286	0.026
10/02/1999	0:00:00	0.2586	0.1076	0.0346	1.2826	0.5146	0.2586	0.5146	0.2586	1.0266	0.0286	0.026
10/12/1999	0:00:00	0.3495	0.1455	0.0465	1.7345	0.6955	0.3495	0.6955	0.3495	1.3885	0.0385	0.035
10/22/1999	0:00:00	0.002	0.001	0	0.011	0.005	0.002	0.005	0.002	0.009	0	0
11/01/1999	0:00:00	0.7222	0.3012	0.0962	3.5832	1.4372	0.7222	1.4372	0.7222	2.8672	0.0792	0.072
11/11/1999	0:00:00	0.5605	0.2335	0.0745	2.7785	1.1145	0.5605	1.1145	0.5605	2.2235	0.0605	0.055
11/21/1999	0:00:00	0.9817	0.4087	0.1307	4.8687	1.9537	0.9817	1.9537	0.9817	3.8977	0.1067	0.097
12/01/1999	0:00:00	1.2878	0.5368	0.1718	6.3888	2.5628	1.2878	2.5628	1.2878	5.1138	0.1408	0.128
12/11/1999	0:00:00	1.7453	0.7273	0.2333	8.6573	3.4733	1.7453	3.4733	1.7453	6.9293	0.1903	0.173
12/21/1999	0:00:00	1.9099	0.7959	0.2549	9.4729	3.8009	1.9099	3.8009	1.9099	7.5829	0.2079	0.189
12/31/1999	0:00:00	3.331	1.388	0.445	16.522	6.629	3.331	6.629	3.331	13.224	0.363	0.33
01/10/2000	0:00:00	3.1795	1.3255	0.4255	15.7725	6.3275	3.1795	6.3275	3.1795	12.6245	0.3465	0.315
01/20/2000	0:00:00	2.5078	1.0448	0.3348	12.4378	4.9898	2.5078	4.9898	2.5078	9.9548	0.2728	0.248
01/30/2000	0:00:00	3.4885	1.4545	0.4665	17.3045	6.9425	3.4885	6.9425	3.4885	13.8505	0.3795	0.345
02/09/2000	0:00:00	3.232	1.347	0.432	16.034	6.433	3.232	6.433	3.232	12.833	0.352	0.32
02/19/2000	0:00:00	2.7169	1.1329	0.3629	13.4769	5.4069	2.7169	5.4069	2.7169	10.7869	0.2959	0.269
02/29/2000	0:00:00	2.6553	1.1073	0.3553	13.1723	5.2843	2.6553	5.2843	2.6553	10.5433	0.2893	0.263
03/10/2000	0:00:00	2.5008	1.0428	0.3338	12.4048	4.9768	2.5008	4.9768	2.5008	9.9288	0.2728	0.248
03/20/2000	0:00:00	2.2119	0.9219	0.2959	10.9739	4.4029	2.2119	4.4029	2.2119	8.7839	0.2409	0.219
03/29/2000	0:00:00	2.1392	0.8912	0.2862	10.6092	4.2562	2.1392	4.2562	2.1392	8.4912	0.2332	0.212

Table B4: Exchanges and Eddy Dispersion Coefficients

Segment No		Surface Area (m^2)	Mixing Length (m)	Eddy Dispersion Coefficient (m^2/s)
37	86	67734	1.80	$6.0*10^{-5}$
38	87	100088	1.35	$6.0*10^{-5}$
39	88	51000	2.05	$4.0*10^{-5}$
40	89	50203	2.05	$4.0*10^{-5}$
41	90	83672	1.75	$1.0*10^{-6}$
42	91	103953	1.95	$1.0*10^{-5}$
43	92	61359	2.00	$2.0*10^{-5}$
44	93	108375	1.90	$2.5*10^{-4}$
45	94	105984	1.90	$2.5*10^{-4}$
46	95	100406	2.00	$2.5*10^{-4}$
47	96	149813	2.00	$2.5*10^{-4}$
48	97	250000	2.05	$2.5*10^{-4}$
33	34	44	363	$1.0*10^{1}$
82	83	150	363	$1.0*10^{1}$
34	35	241	413	$1.0*10^{1}$
83	84	1443	413	$1.0*10^{1}$
27	28	99	350	1.0
76	77	455	350	1.0
36	85	43669	1.75	$3.0*10^{-5}$
1	50	250000	1.10	$3.0*10^{-6}$
2	51	7969	1.05	$3.0*10^{-6}$
3	52	219938	1.05	$3.0*10^{-6}$
Boundary	1	219	438	$1.0*10^{2}$
Boundary	50	219	438	$1.0*10^{2}$
1	2	51	500	$1.0*10^{2}$
50	51	173	500	$1.0*10^{2}$
2	3	59	375	$1.0*10^{2}$
51	52	129	375	$1.0*10^{2}$
65	67	72	413	$2.0*10^{1}$
17	18	45	663	$2.0*10^{1}$
66	67	162	663	$2.0*10^{1}$
18	19	597	1200	$2.0*10^{1}$
67	68	8716	1200	$2.0*10^{1}$
19	20	276	988	$2.0*10^{1}$
68	69	2374	988	$2.0*10^{1}$
16	18	15	413	$5.0*10^{1}$
16	65	48609	1.25	$1.0*10^{-5}$
17	66	61359	1.10	$1.0*10^{-5}$
18	67	1055063	2.15	$1.0*10^{-5}$
19	68	1156266	3.15	$1.0*10^{-5}$
20	69	380109	2.40	$1.0*10^{-5}$

Annex C
The Flow Pathways for Köyceğiz - Dalyan Lagoon Water Quality Model

Table C1: Pathways for Flows Q1 – Q25 (Flows from Mediterranean Sea Boundary Condition)

Segment No	Q1	Q2	Q3	Q4	Q5	Q6	Q7	Q8	Q9	Q10	Q11	Q12	Q13	Q14	Q15	Q16	Q17	Q18	Q19	Q20	Q21	Q22	Q23	Q24	Q25
1	X	X	X	X	X	X	X	X	X	X	X	X	X	X	X	X	X	X	X	X	X	X	X	X	X
2	X	X	X	X	X	X	X	X	X	X	X	X	X	X	X	X	X	X	X	X	X	X	X	X	X
3					X	X	X	X	X	X	X	X	X	X	X	X	X	X	X	X	X	X	X	X	X
4																									
5					X	X	X	X	X	X	X	X	X	X	X	X	X	X	X	X	X	X	X	X	X
6					X	X	X	X								X	X	X		X	X		X	X	X
7					X	X	X	X	X	X	X	X	X	X	X	X	X	X	X	X	X	X	X	X	X
8																						X			
9									X	X	X	X	X	X	X				X						
10																									
11																									
12																									
13																						X			
14																									
15																									
16																									
17																						X			
18																						X			
19																						X			
20																						X			
21																									
22																									
23																									
24									X	X	X	X	X	X	X										
25					X	X	X	X	X	X	X	X	X	X	X	X	X	X	X	X	X		X	X	X
26					X	X	X	X	X	X	X		X	X	X	X	X	X	X	X	X		X	X	X
27					X	X	X	X								X	X	X	X	X	X		X	X	X
28																									
29	X	X	X	X																					
30	X	X																							
31	X	X	X	X																					
32	X	X	X	X																					
33	X	X	X	X																					
34																									
35																									
36	X	X	X	X	X	X	X	X	X	X	X	X	X	X	X	X	X	X	X	X	X		X	X	X
37	X	X	X	X	X	X	X	X	X	X	X	X	X	X	X	X	X	X	X	X	X		X	X	X
38				X		X					X		X	X	X		X	X	X	X	X		X	X	X
39	X		X				X	X	X	X		X				X									
40			X					X	X	X		X	X			X									
41									X	X	X	X	X	X	X	X	X	X	X	X	X		X	X	X
42									X	X	X	X	X	X	X		X	X	X	X	X		X	X	X
43									X	X	X	X	X	X	X				X	X	X		X	X	X
44									X	X		X	X	X	X					X					
45									X	X		X	X												
46										X		X	X												
47												X	X												
48													X												
49																									
50	X	X	X	X	X	X	X	X	X	X	X	X	X	X	X	X	X	X	X	X	X	X	X	X	X
51	X	X	X	X	X	X	X	X	X	X	X	X	X	X	X	X	X	X	X	X	X	X	X	X	X
52					X	X	X	X	X	X	X	X	X	X	X	X	X	X	X	X	X	X	X	X	X
53												X	X	X	X										
54					X	X	X	X								X	X	X	X	X	X	X	X	X	X
55												X	X	X	X				X						
56					X	X	X	X								X	X	X	X	X	X	X	X	X	X
57																				X	X	X	X	X	
58					X	X	X	X								X	X	X							
59																				X	X		X	X	X
60																				X	X		X	X	X
61																				X			X		
62																					X	X	X	X	
63																									
64																					X			X	
65																					X			X	
66																					X	X		X	
67																					X	X			
68																						X			
69																						X			
70																									
71																									
72																									
73					X	X	X	X								X	X	X		X	X		X	X	X
74					X	X	X	X	X	X	X	X	X	X	X	X	X	X	X	X	X		X	X	X
75						X	X	X	X	X	X	X	X	X	X	X	X	X	X	X	X		X	X	X
76									X	X	X	X	X	X	X				X						
77																									
78	X	X	X	X																					
79	X	X																							
80	X	X	X	X																					
81	X	X	X	X																					
82	X	X	X	X																					
83																									
84																									
85	X	X	X	X	X	X	X	X	X	X	X	X	X	X	X	X	X	X	X	X	X		X	X	X
86	X	X	X	X	X	X	X	X	X	X	X	X	X	X	X	X	X	X	X	X	X		X	X	X
87				X		X					X		X	X	X		X	X	X	X	X		X	X	X
88	X		X				X	X	X	X		X				X									
89			X					X	X	X		X				X									
90									X	X	X	X	X	X	X	X	X	X	X	X	X		X	X	X
91									X	X	X	X	X	X	X		X	X	X	X	X		X	X	X
92									X	X	X	X	X	X	X				X	X	X		X	X	X
93									X	X		X	X	X	X					X					
94									X	X		X	X												
95										X		X	X												
96												X	X												
97													X												
98																									

Table C2: Pathways for Flows Q26 – Q36 (Flows from Köyceğiz Lake Boundary Condition)

Segment No	Q26	Q27	Q28	Q29	Q30	Q31	Q32	Q33	Q34	Q35	Q36
1	X	X	X	X	X	X	X	X	X	X	X
2	X	X	X	X	X	X	X	X	X	X	X
3		X	X	X	X	X	X	X	X	X	X
4									X		
5		X	X		X	X	X	X		X	X
6		X	X						X		
7		X	X		X	X	X	X		X	X
8					X	X	X	X		X	X
9					X						
10					X	X	X	X		X	X
11					X		X				
12					X		X				
13						X		X		X	X
14						X		X		X	X
15						X		X		X	X
16						X		X		X	X
17						X		X		X	X
18						X		X		X	
19						X		X		X	
20						X		X		X	
21										X	X
22										X	X
23										X	X
24					X	X	X	X			
25		X	X	X	X	X	X	X	X		
26		X	X	X	X	X	X	X	X		
27		X	X	X					X		
28											
29	X										
30											
31	X										
32	X										
33	X										
34											
35											
36	X	X	X	X	X	X	X	X	X		
37	X	X	X	X	X	X	X	X	X		
38	X	X					X	X	X		
39			X	X	X	X					
40			X	X	X	X					
41	X	X	X	X	X	X	X	X	X		
42	X	X	X	X	X	X	X	X	X		
43	X	X	X	X	X	X	X	X	X		
44	X	X	X	X	X	X	X	X	X		
45	X	X	X	X	X	X	X	X	X		
46	X	X	X	X	X	X	X	X	X		
47	X	X	X	X	X	X	X	X	X		
48	X	X	X	X	X	X	X	X	X		
49	X	X	X	X	X	X	X	X	X		
50											X
51											X
52											X
53											
54											X
55											
56											X
57											X
58											
59											X
60											
61											
62											X
63											X
64											X
65											X
66											X
67											
68											
69											
70											X
71											X
72											X
73											
74											
75											
76											
77											
78											
79											
80											
81											
82											
83											
84											
85											
86											
87											
88											
89											
90											
91											
92											
93											
94											
95											
96											
97											
98											

Annex D
Simulation Results of Simulation Step 2

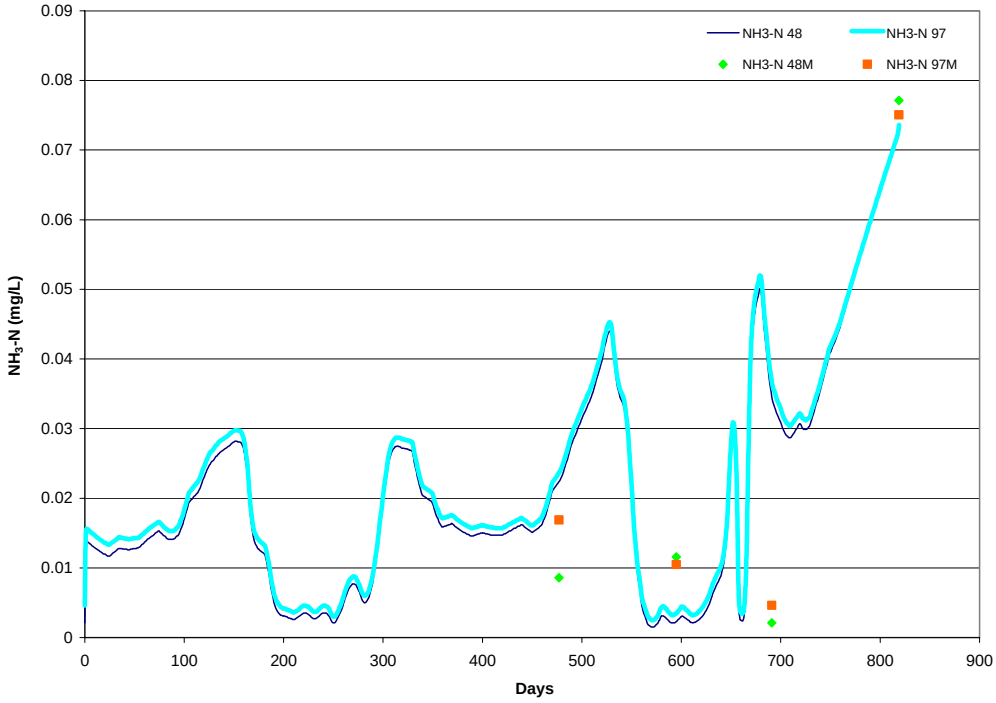

Figure D.1: Simulation Results and Measured Concentrations of Ammonia Nitrogen for the Köyceğiz Lake Boundary Condition

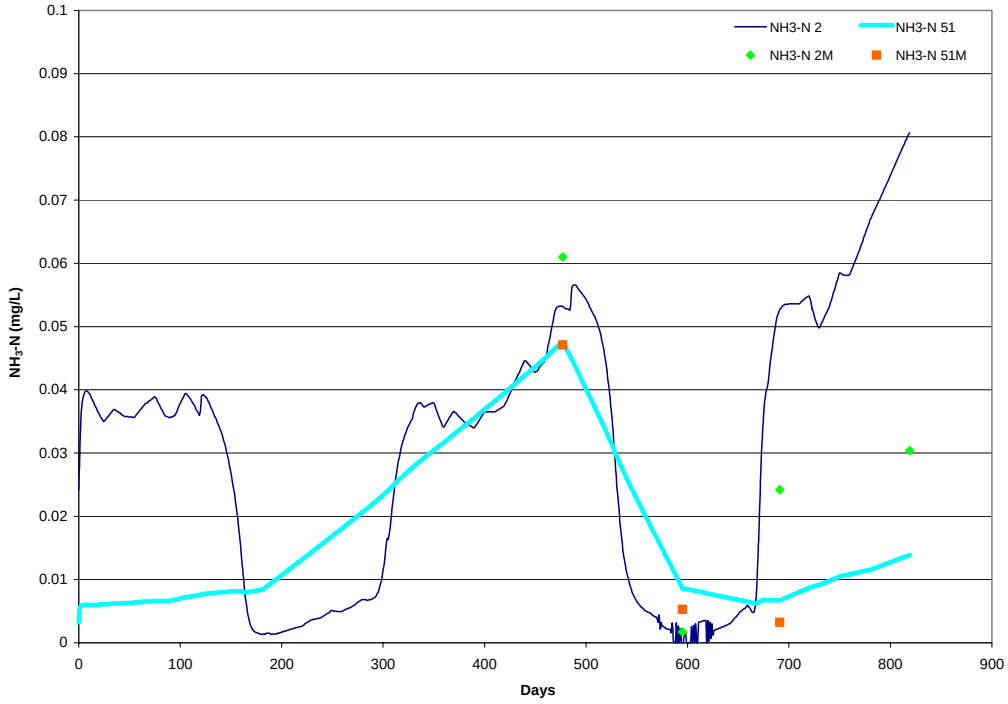

Figure D.2: Simulation Results and Measured Concentrations of Ammonia Nitrogen for the Mediterranean Sea Boundary Condition

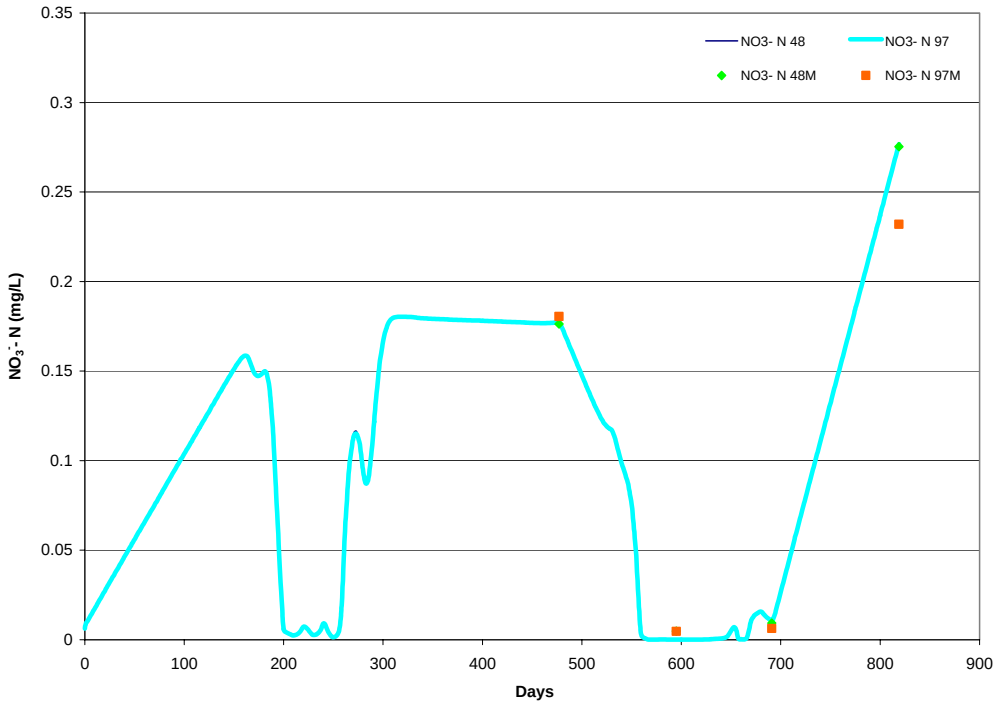

Figure D.3: Simulation Results and Measured Concentrations of Nitrate Nitrogen for the Köyceğiz Lake Boundary Condition

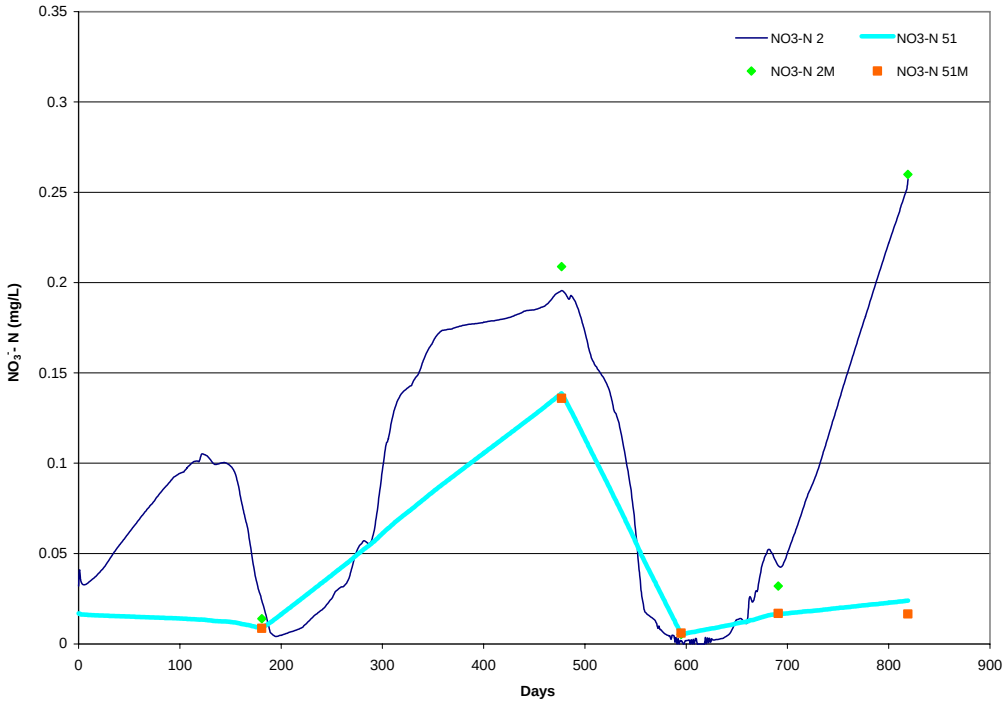

Figure D.4: Simulation Results and Measured Concentrations of Nitrate Nitrogen for the Mediterranean Sea Boundary Condition

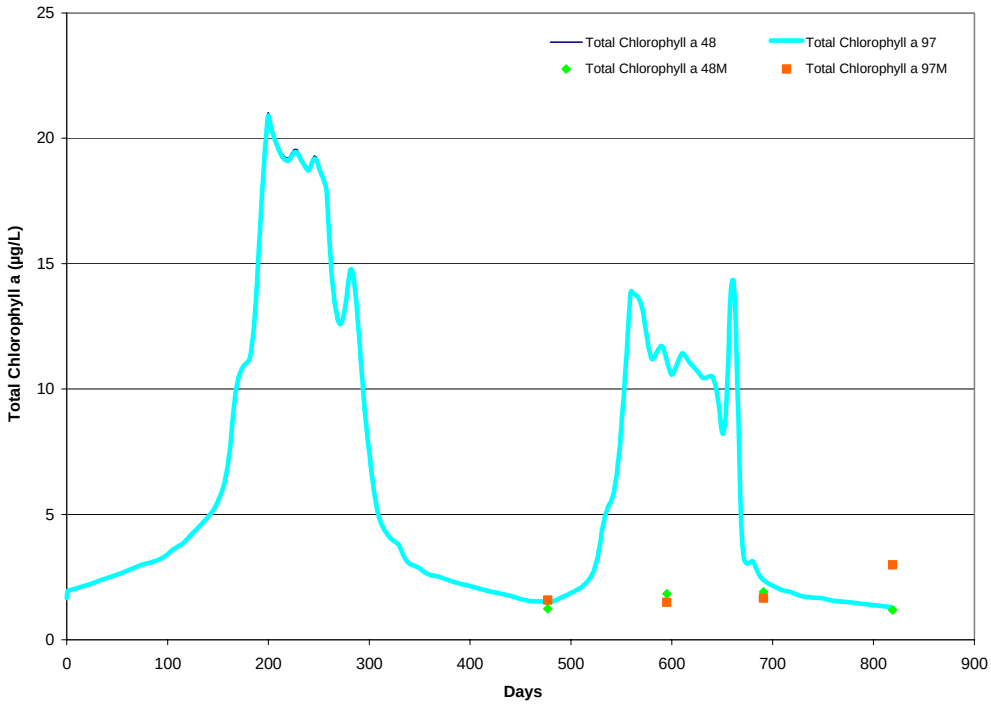

Figure D.5: Simulation Results and Measured Concentrations of Total Chlorophyll a for the Köyceğiz Lake Boundary Condition

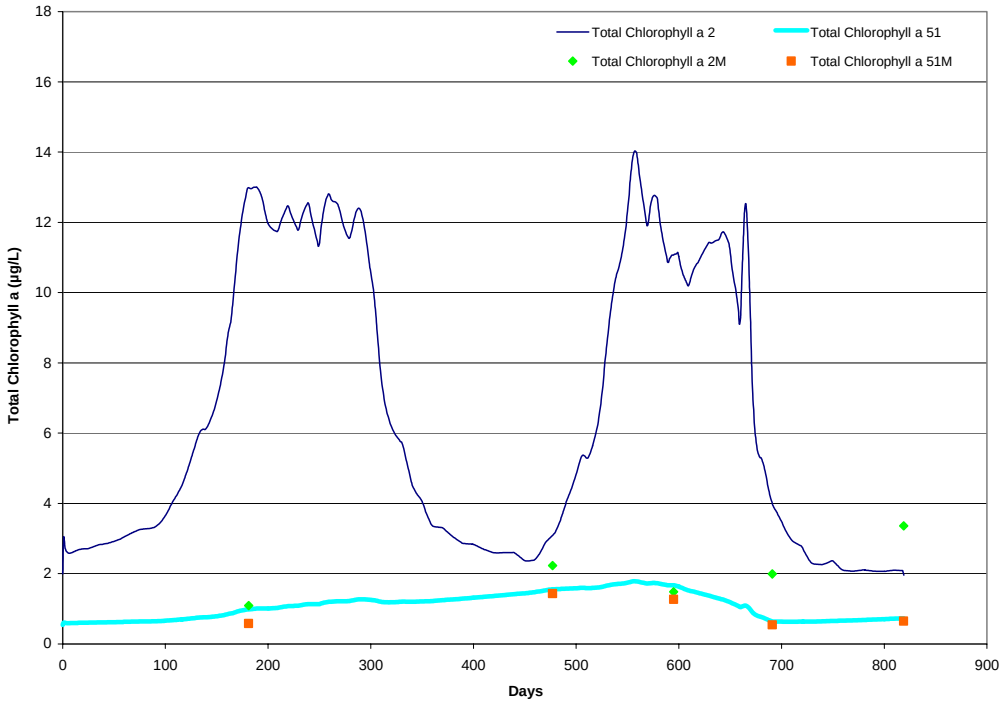

Figure D.6: Simulation Results and Measured Concentrations of Total Chlorophyll a for the Mediterranean Sea Boundary Condition

Annex E
Simulation Results of Simulation Step 3

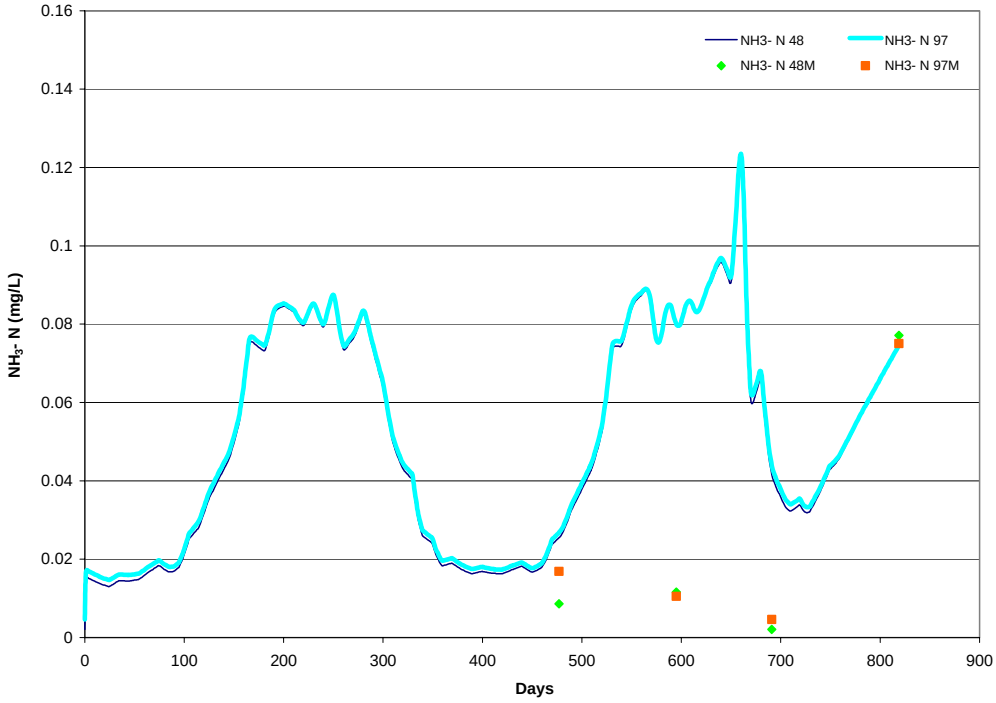

Figure E.1: Simulation Results and Measured Concentrations of Ammonia Nitrogen for the Köyceğiz Lake Boundary Condition

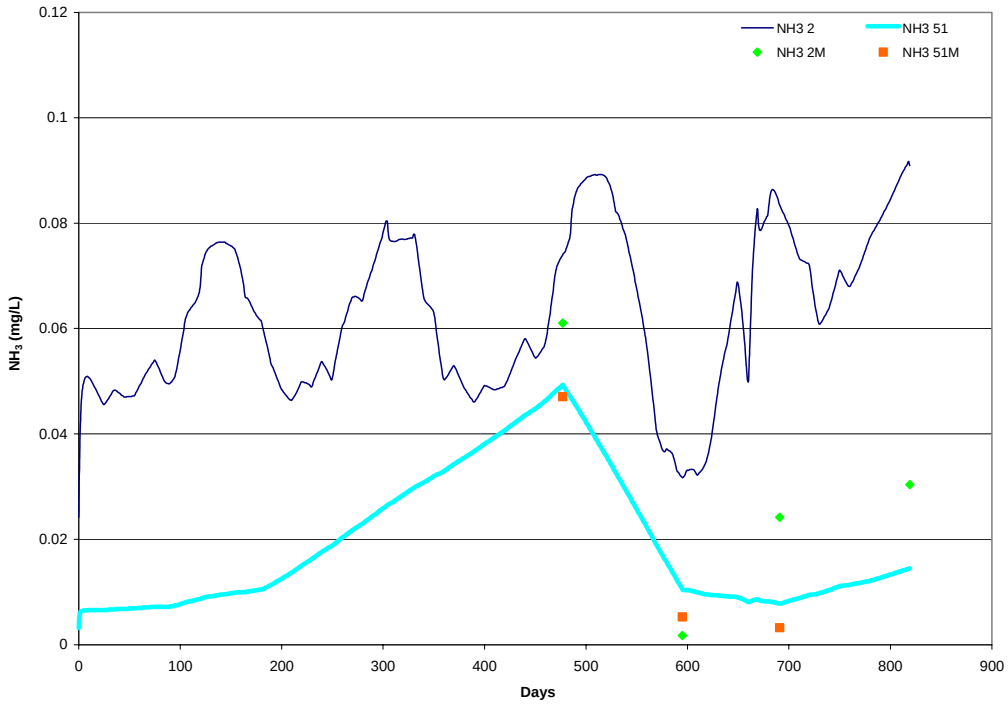

Figure E.2: Simulation Results and Measured Concentrations of Ammonia Nitrogen for the Mediterranean Sea Boundary Condition

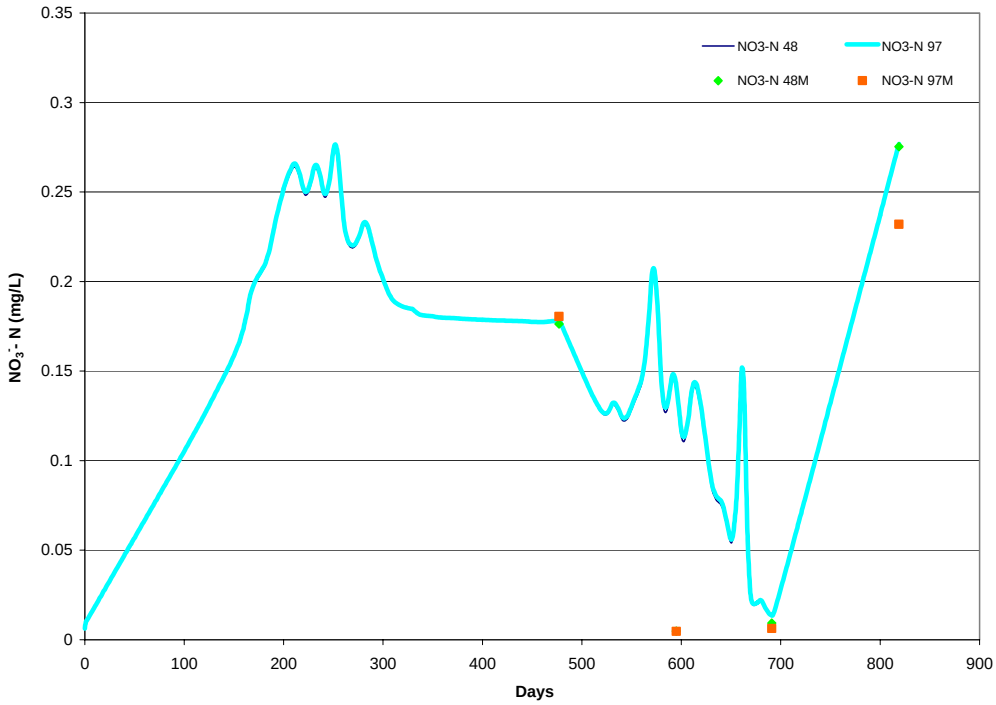

Figure E.3: Simulation Results and Measured Concentrations of Nitrate Nitrogen for the Köyceğiz Lake Boundary Condition

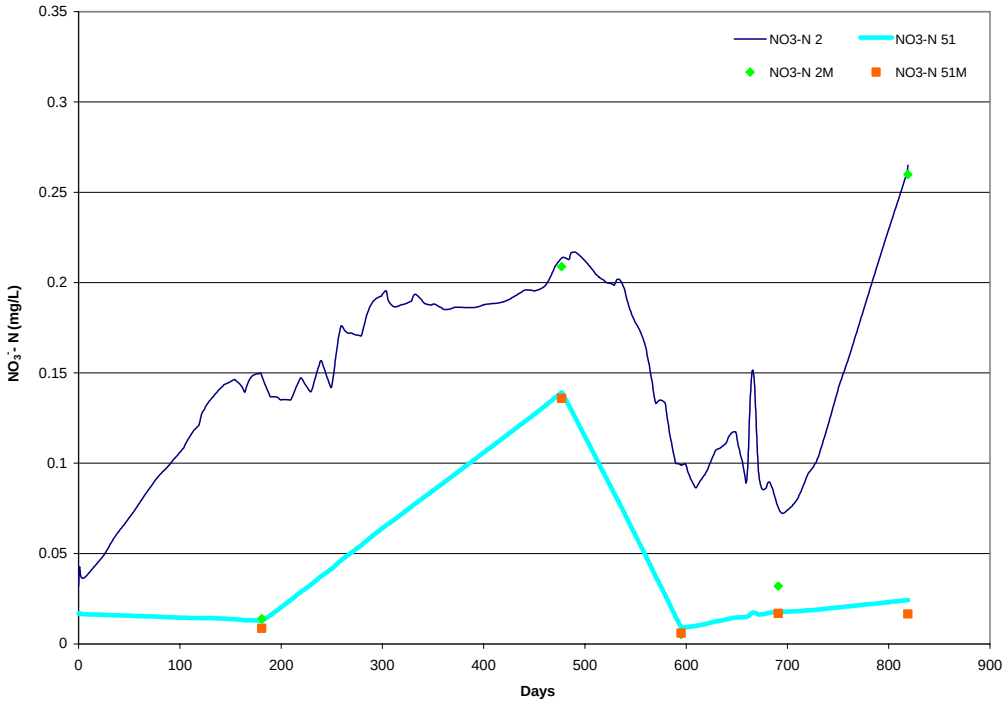

Figure E.4: Simulation Results and Measured Concentrations of Nitrate Nitrogen for the Mediterranean Sea Boundary Condition

Figure E.5: Simulation Results and Measured Concentrations of Total Chlorophyll a for the Köyceğiz Lake Boundary Condition

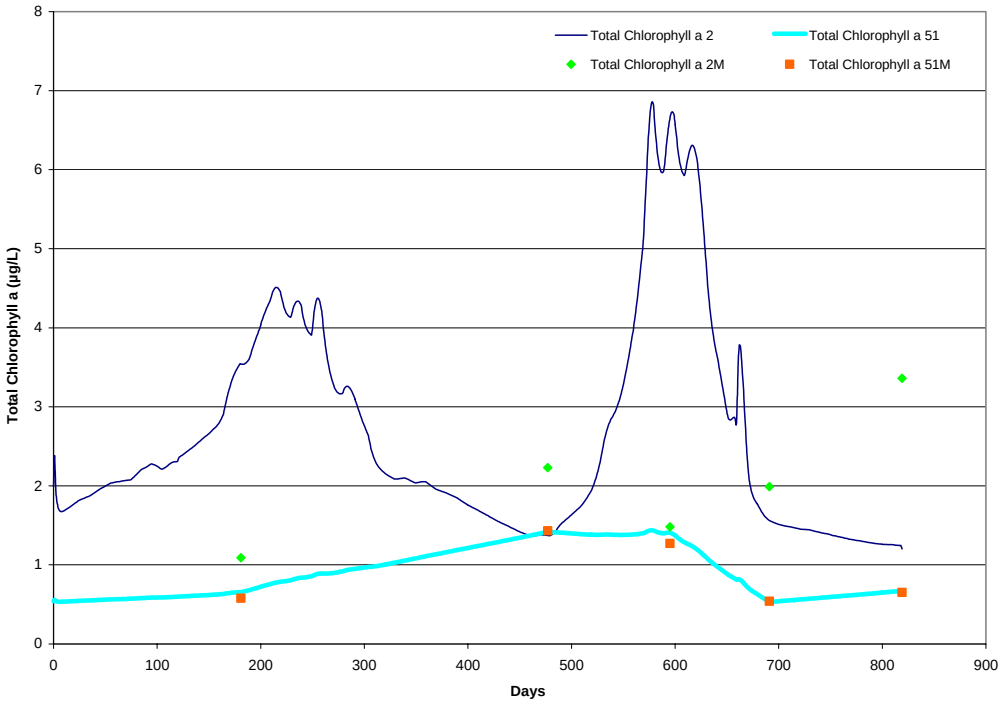

Figure E.6: Simulation Results and Measured Concentrations of Total Chlorophyll a for the Mediterranean Sea Boundary Condition

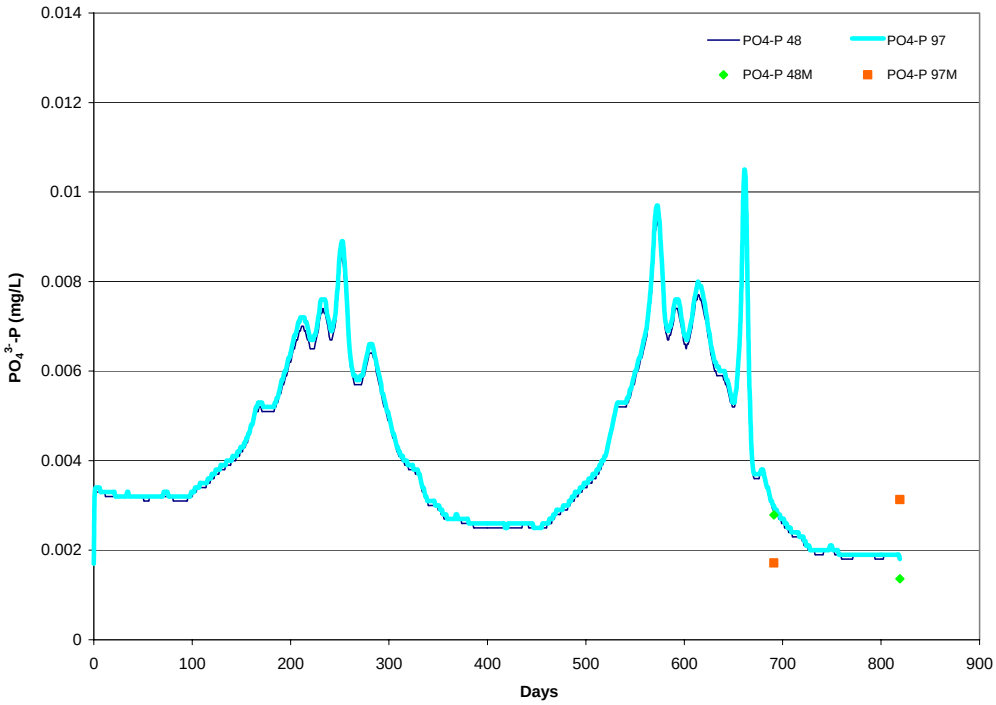

Figure E.7: Simulation Results and Measured Concentrations of Orthophosphate for the Köyceğiz Lake Boundary Condition

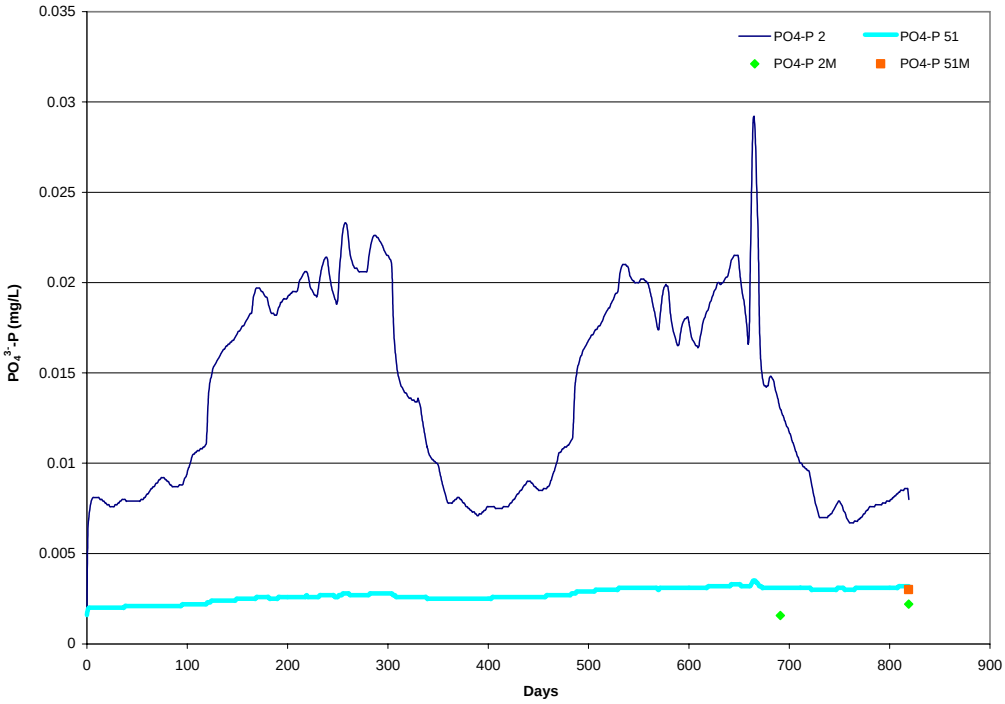

Figure E.8: Simulation Results and Measured Concentrations of Orthophosphate Phosphorus for the Mediterranean Sea Boundary Condition

Annex F
Simulation Results of Simulation Step 4

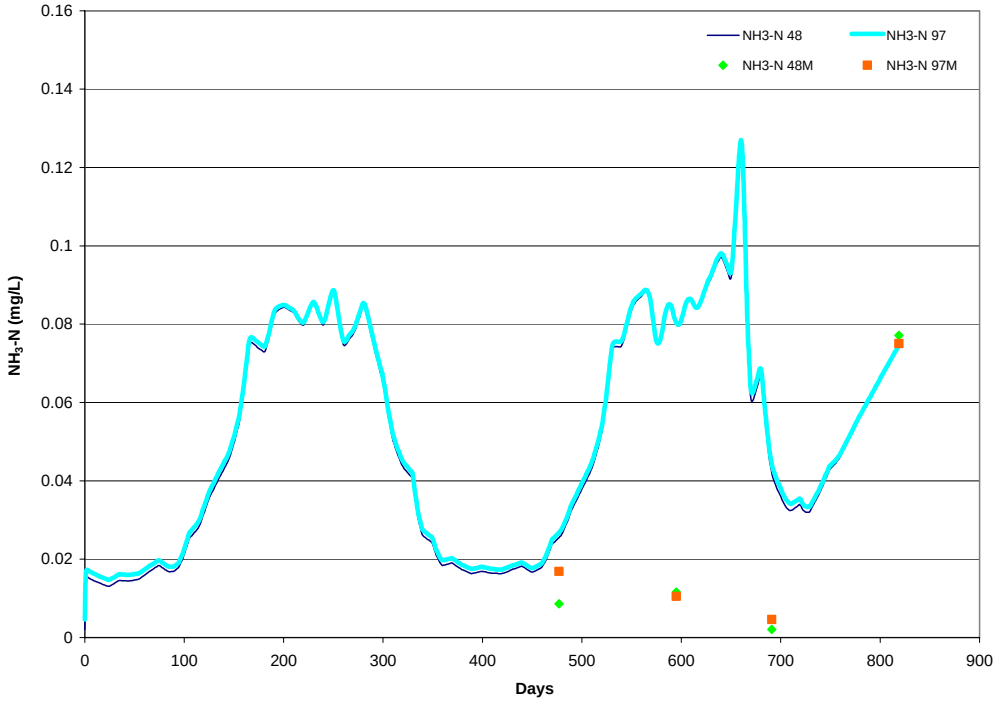

Figure F.1: Simulation Results and Measured Concentrations of Ammonia Nitrogen for the Köyceğiz Lake Boundary Condition

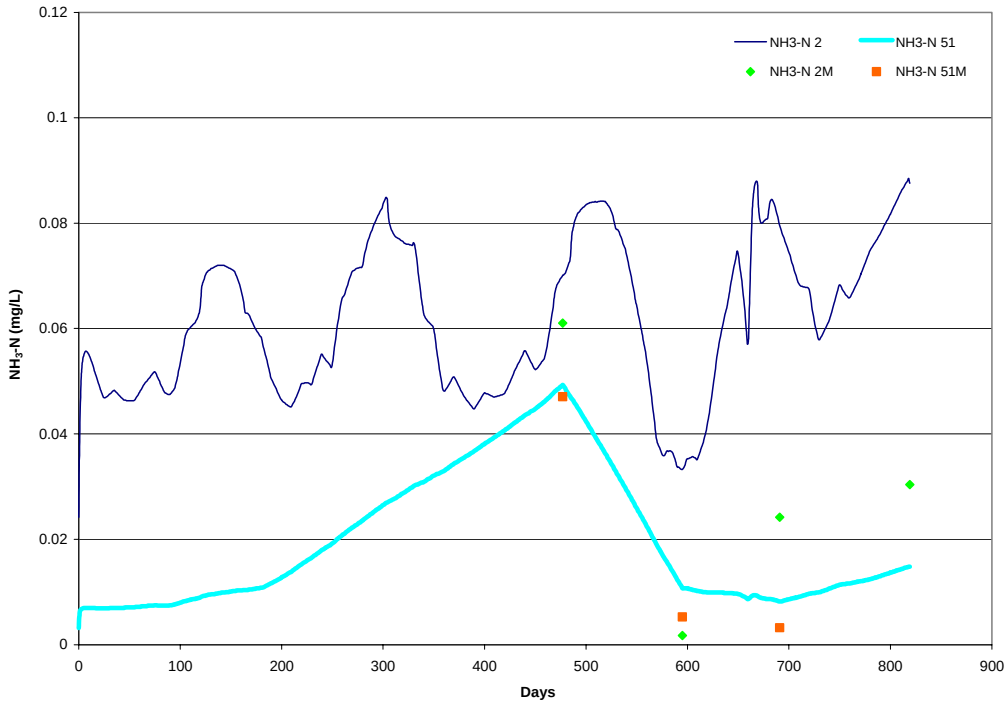

Figure F.2: Simulation Results and Measured Concentrations of Ammonia Nitrogen for the Mediterranean Sea Boundary Condition

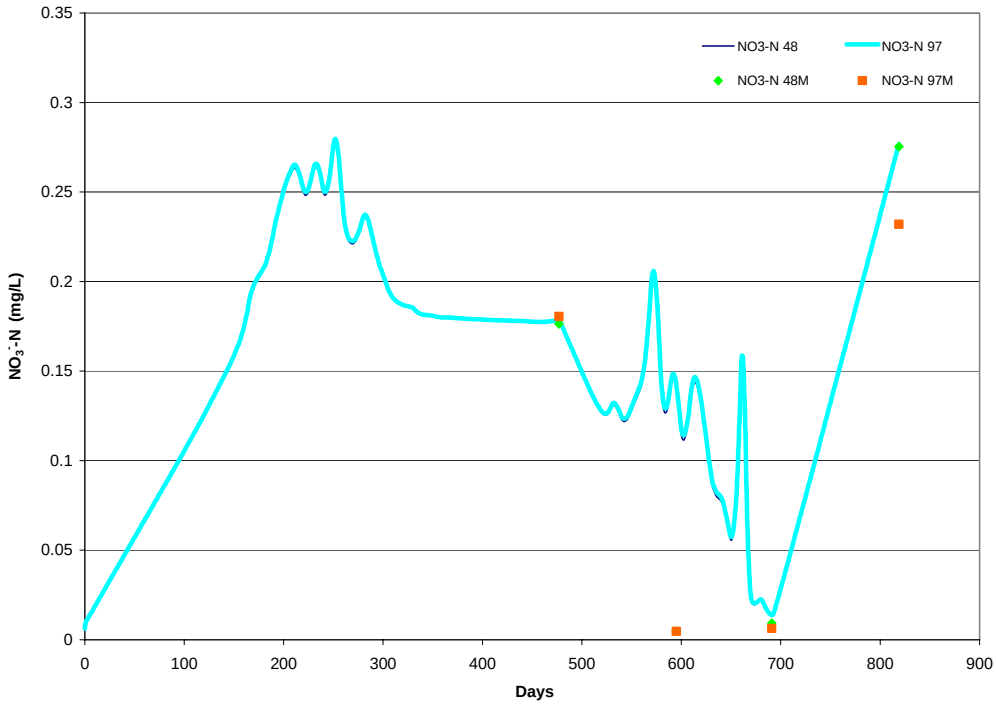

Figure F.3: Simulation Results and Measured Concentrations of Nitrate Nitrogen for the Köyceğiz Lake Boundary Condition

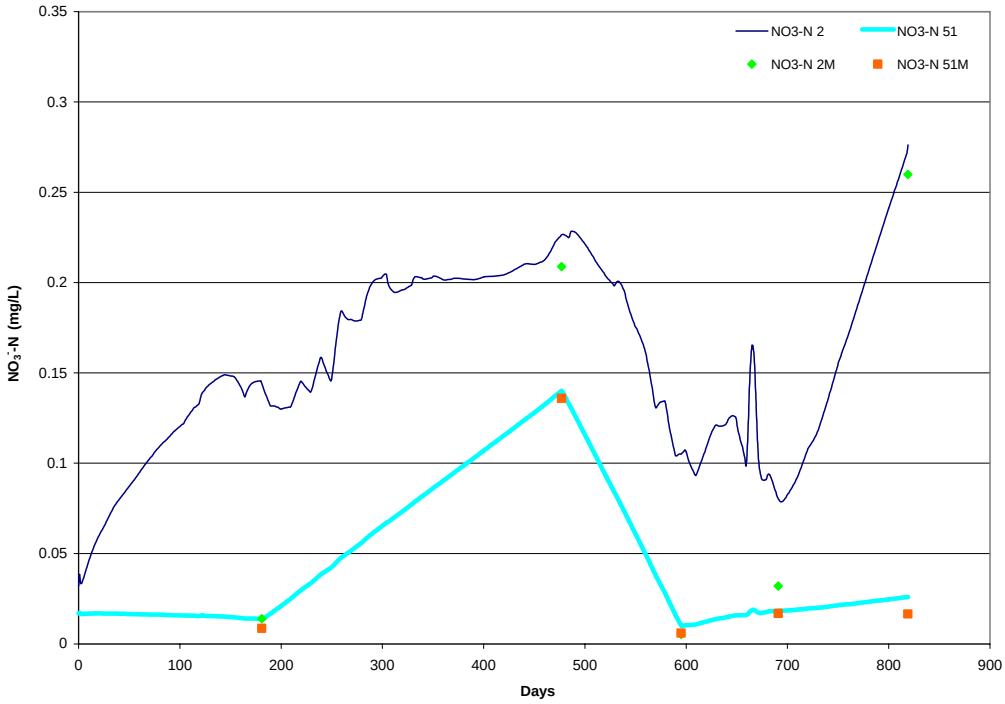

Figure F.4: Simulation Results and Measured Concentrations of Nitrate Nitrogen for the Mediterranean Sea Boundary Condition

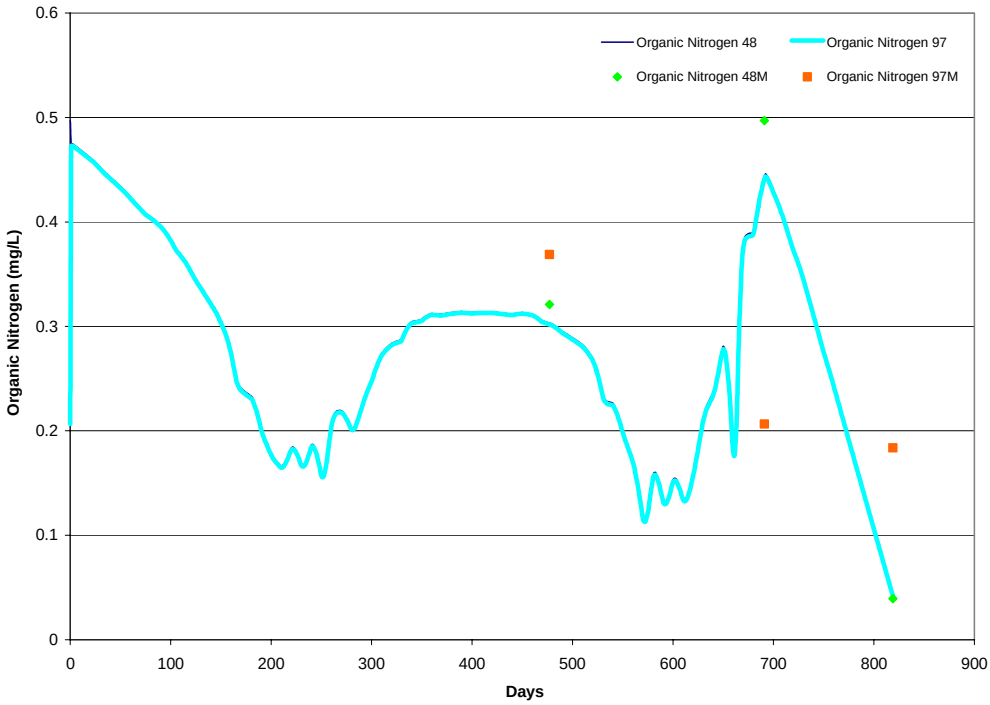

Figure F.5: Simulation Results and Measured Concentrations of Organic Nitrogen for the Köyceğiz Lake Boundary Condition

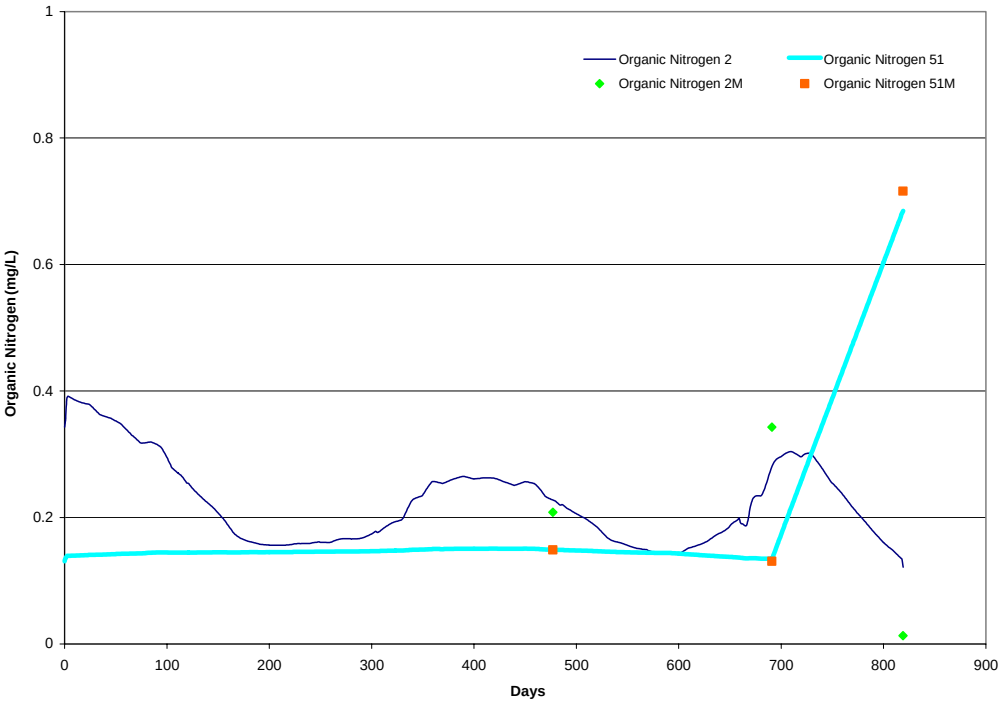

Figure F.6: Simulation Results and Measured Concentrations of Organic Nitrogen for the Mediterranean Sea Boundary Condition

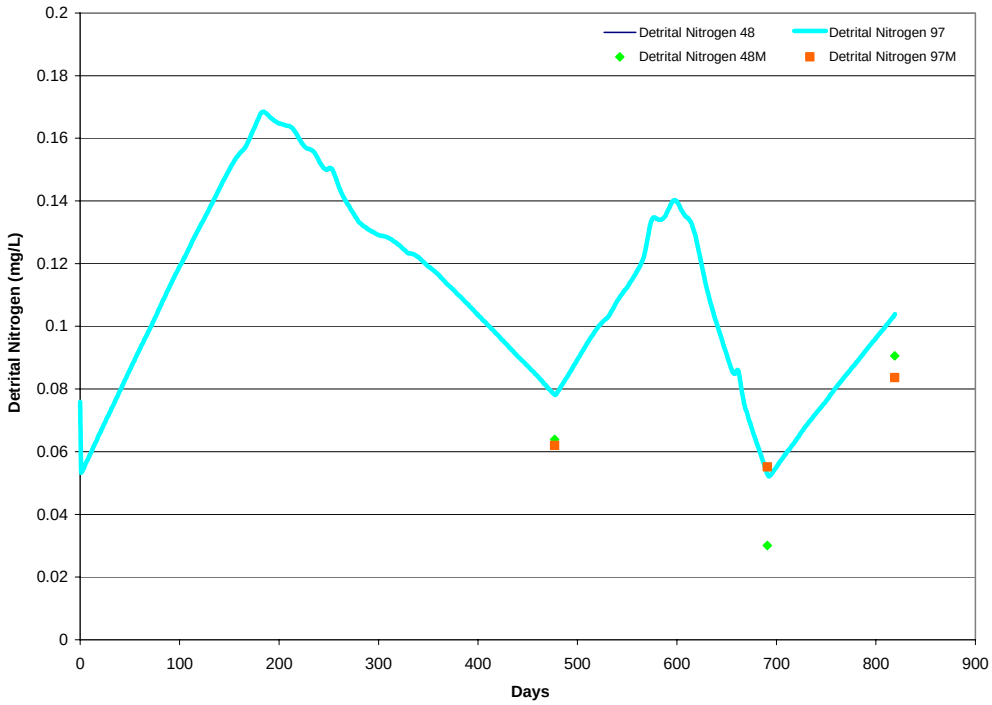

Figure F.7: Simulation Results and Measured Concentrations of Detrital Nitrogen for the Köyceğiz Lake Boundary Condition

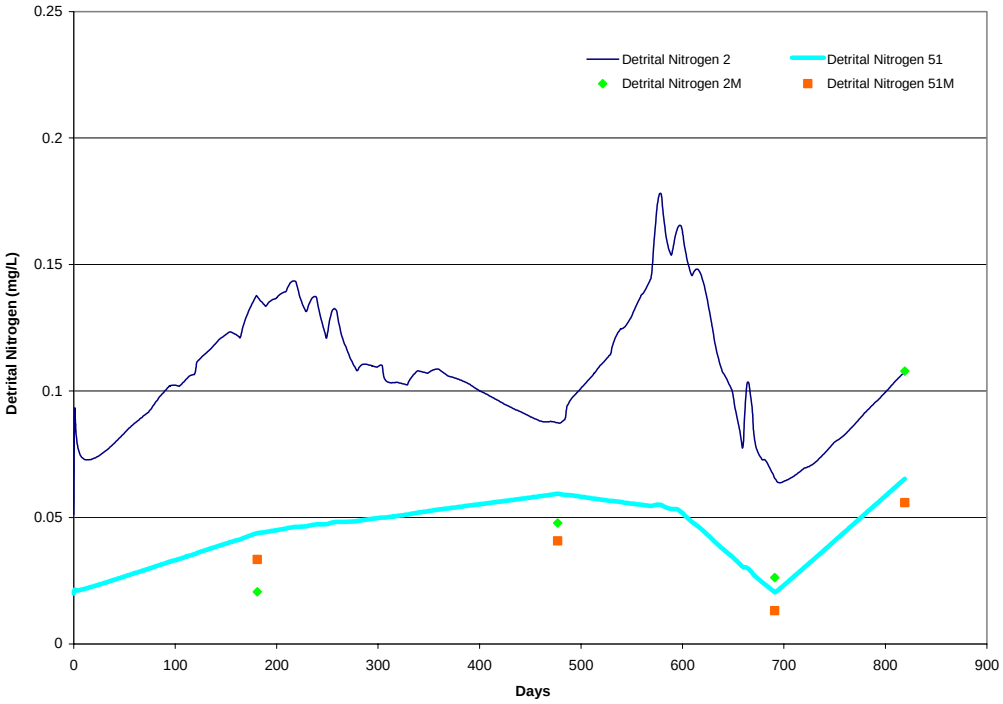

Figure F.8: Simulation Results and Measured Concentrations of Detrital Nitrogen for the Mediterranean Sea Boundary Condition

Figure F.9: Simulation Results and Measured Concentrations of Total Chlorophyll a for the Köyceğiz Lake Boundary Condition

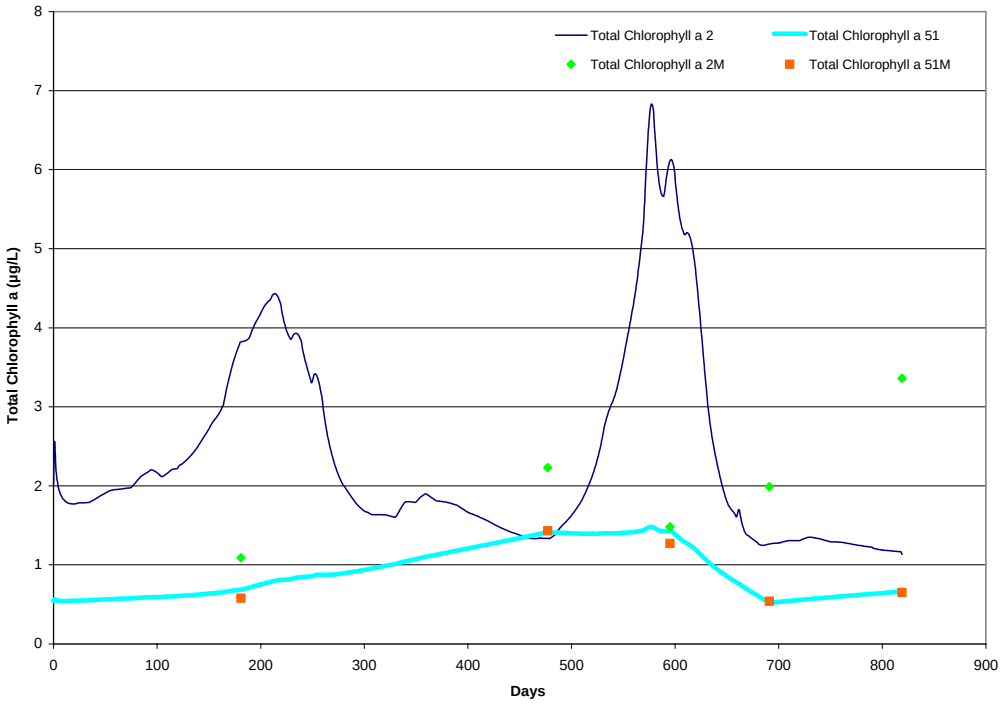

Figure F.10: Simulation Results and Measured Concentrations of Total Chlorophyll a for the Mediterranean Sea Boundary Condition

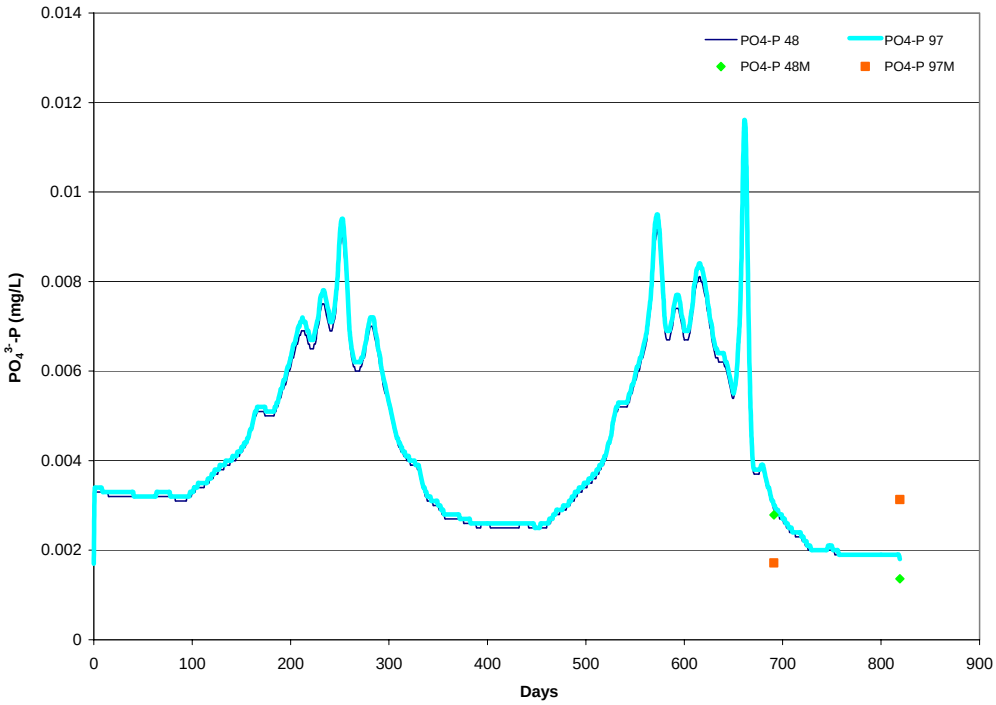

Figure F.11: Simulation Results and Measured Concentrations of Orthophosphate Phosphorus for the Köyceğiz Lake Boundary Condition

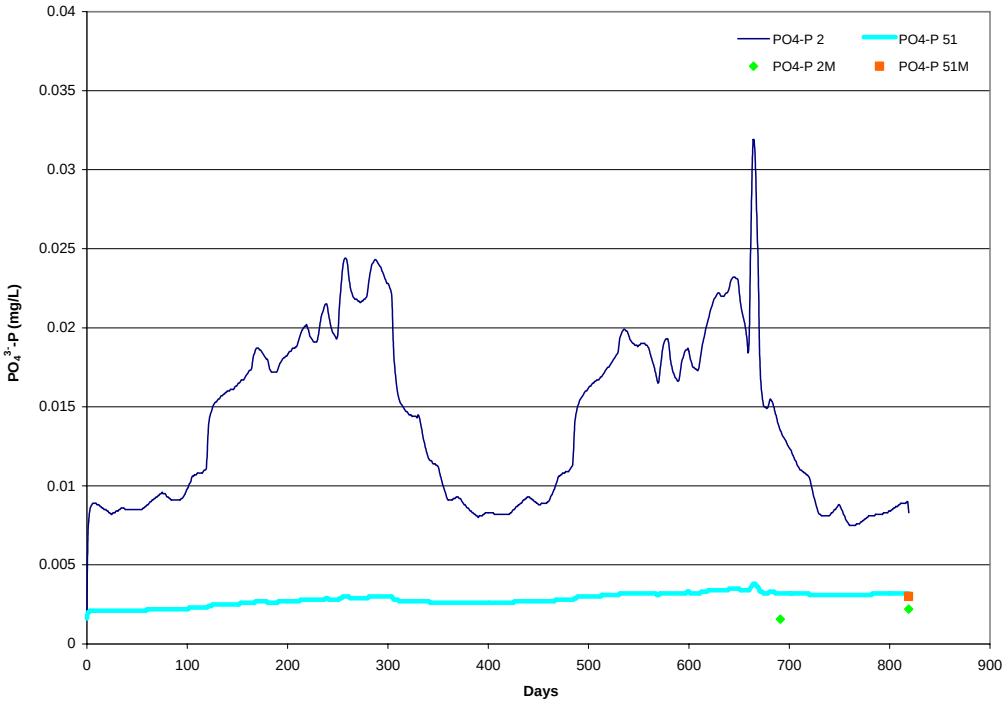

Figure F.12: Simulation Results and Measured Concentrations of Orthophosphate Phosphorus for the Mediterranean Sea Boundary Condition

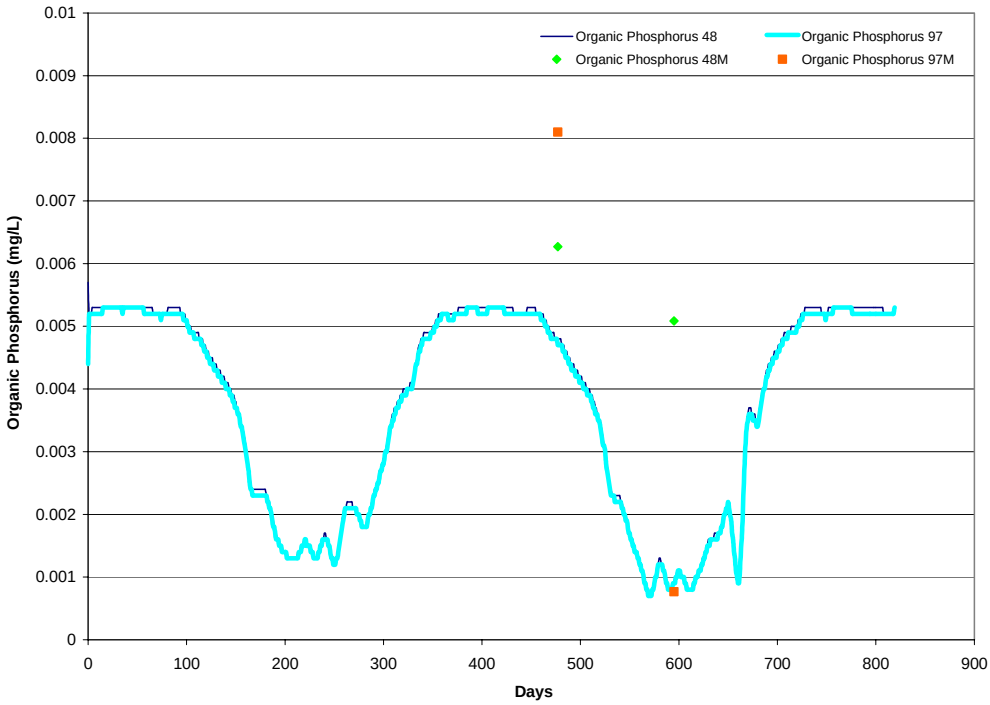

Figure F.13: Simulation Results and Measured Concentrations of Organic Phosphorus for the Köyceğiz Lake Boundary Condition

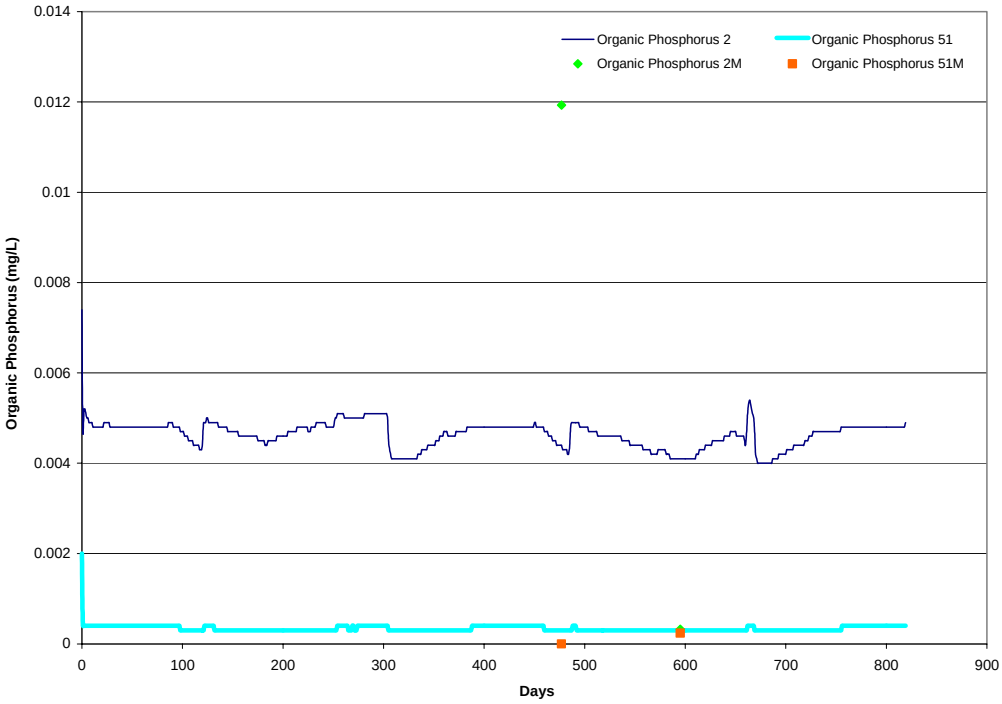

Figure F.14: Simulation Results and Measured Concentrations of Organic Phosphorus for the Mediterranean Sea Boundary Condition

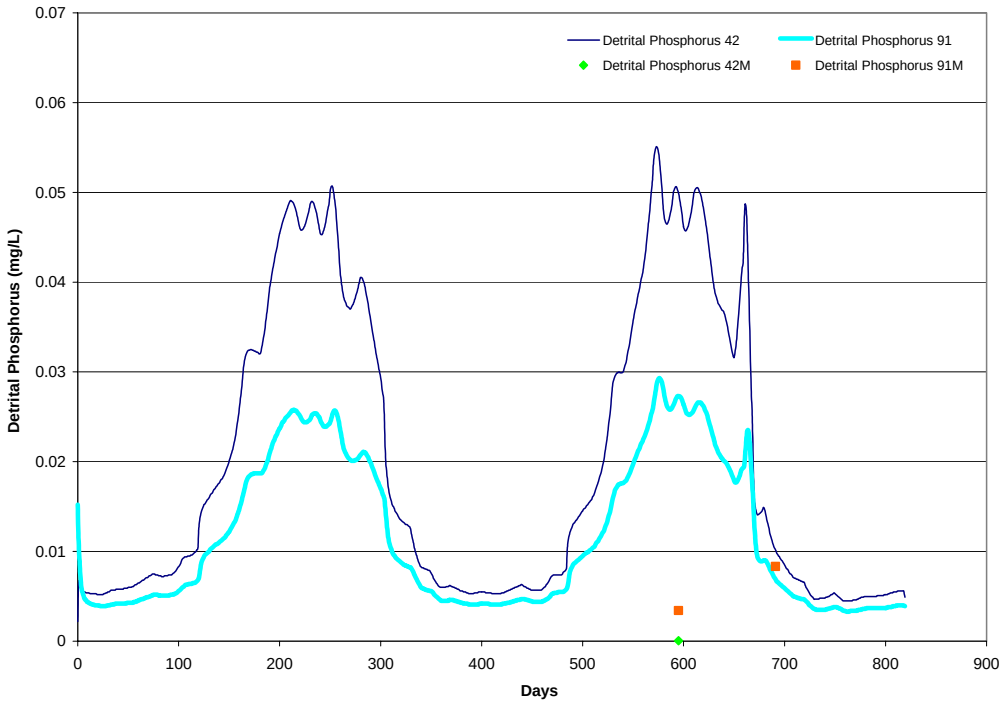

Figure F.15: Simulation Results and Measured Concentrations of Detrital Phosphorus for the Segments 42 and 91

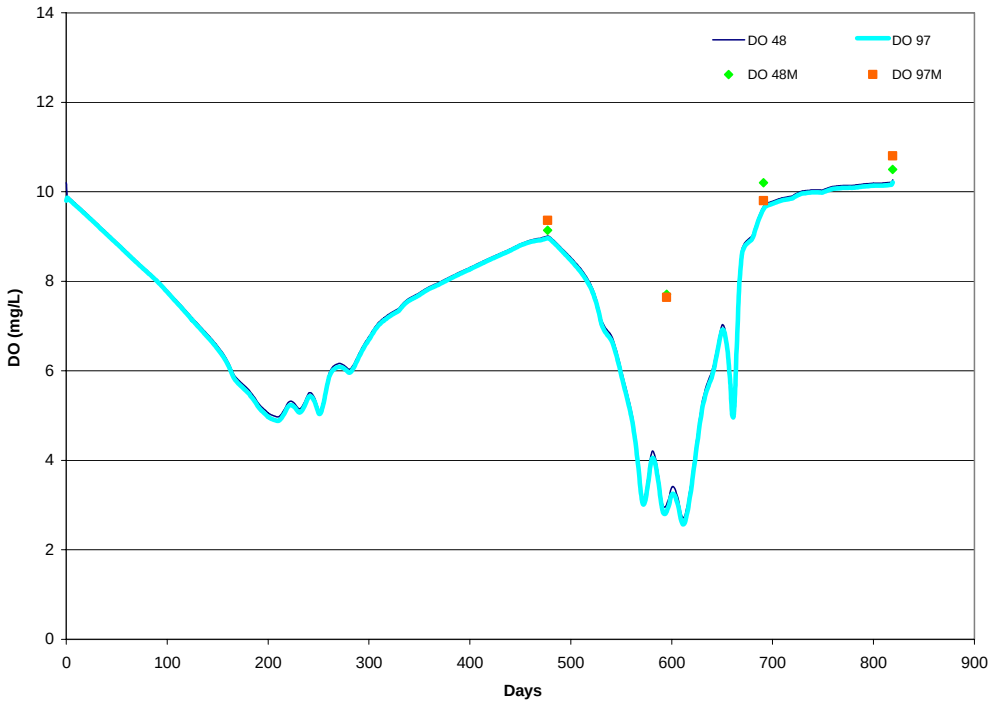

Figure F.16: Simulation Results and Measured Concentrations of Dissolved Oxygen for the Köyceğiz Lake Boundary Condition

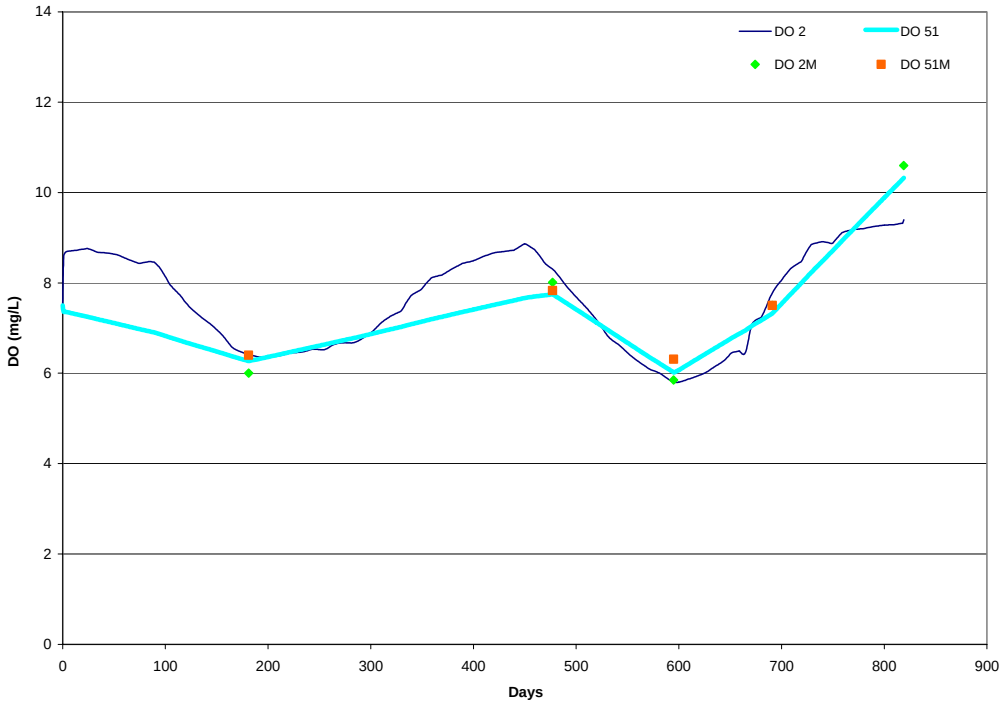

Figure F.17: Simulation Results and Measured Concentrations of Dissolved Oxygen for the Mediterranean Sea Boundary Condition

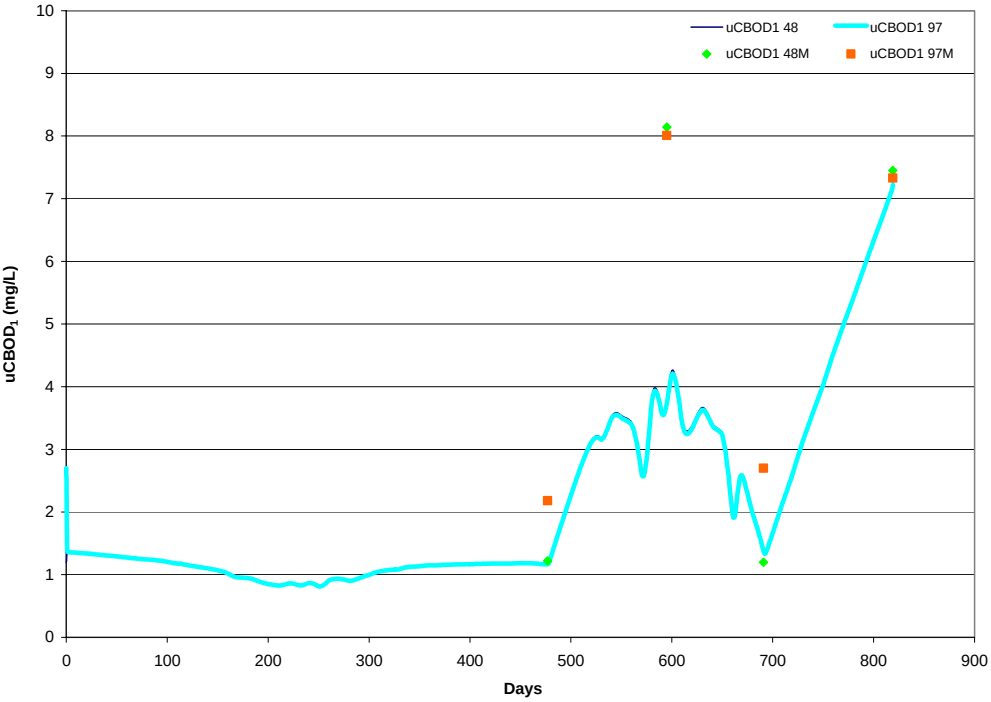

Figure F.18: Simulation Results and Measured Concentrations of $CBOD_1$ for the Köyceğiz Lake Boundary Condition

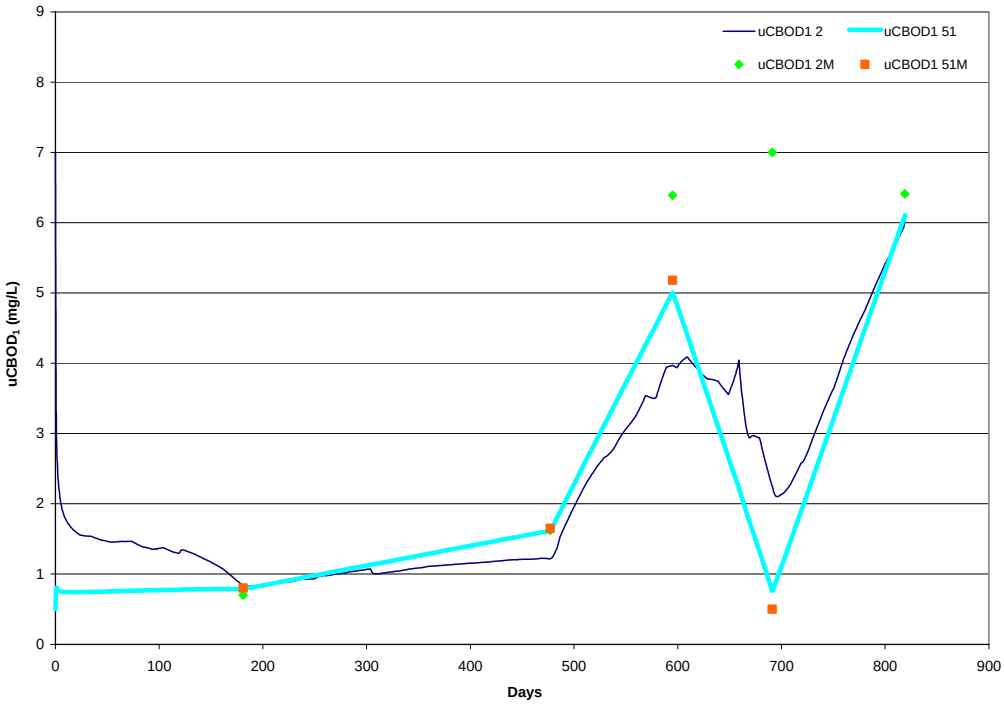

Figure F.19: Simulation Results and Measured Concentrations of $CBOD_1$ for the Mediterranean Sea Boundary Condition

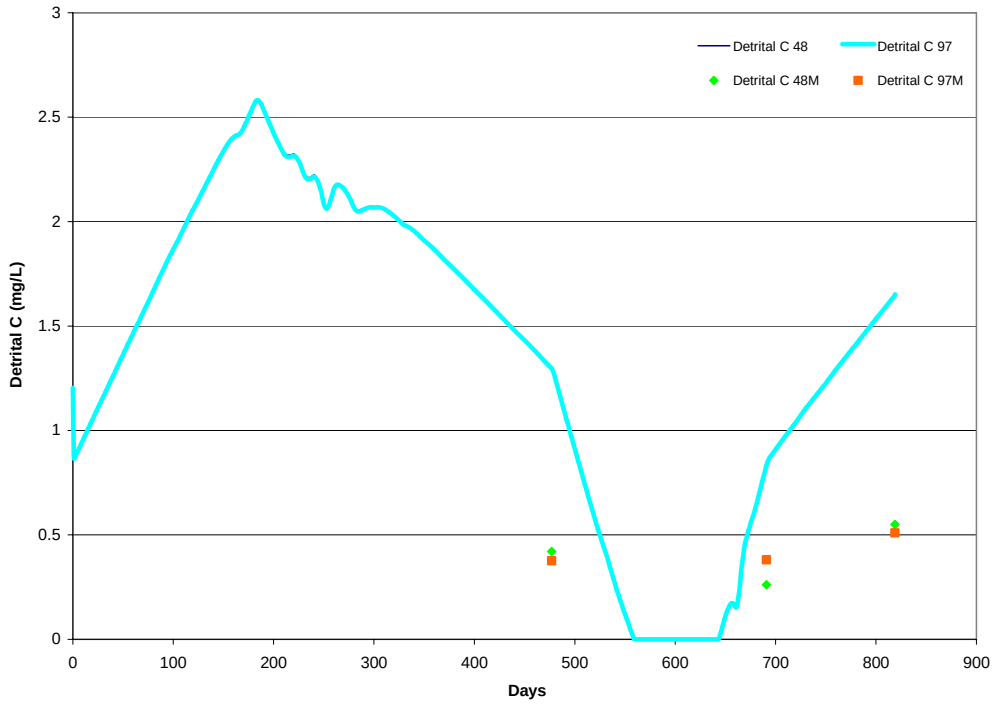

Figure F.20: Simulation Results and Measured Concentrations of Detrital Carbon for the Köyceğiz Lake Boundary Condition

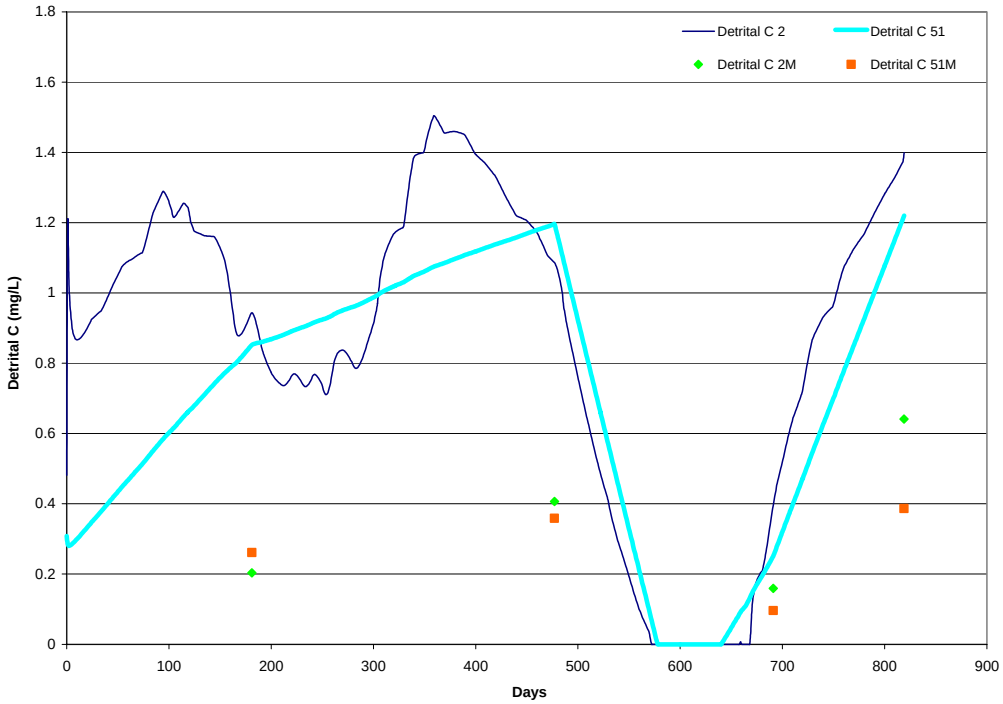

Figure F.21: Simulation Results and Measured Concentrations of Detrital Carbon for the Mediterranean Sea Boundary Condition

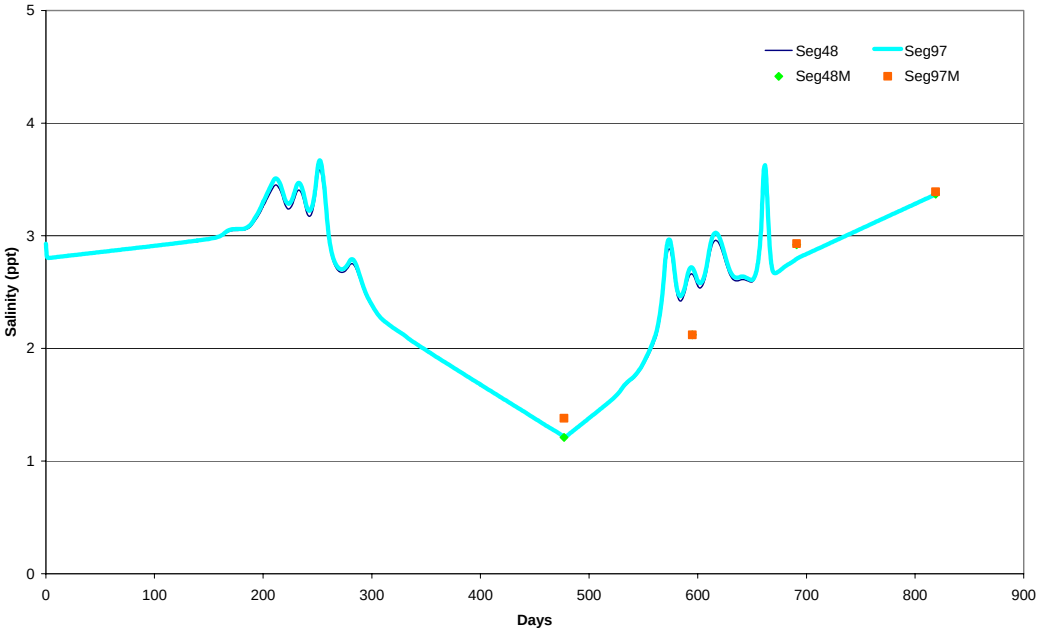

Figure F.22: Simulation Results and Measured Concentrations of Salinity for the Köyceğiz Lake Boundary Condition

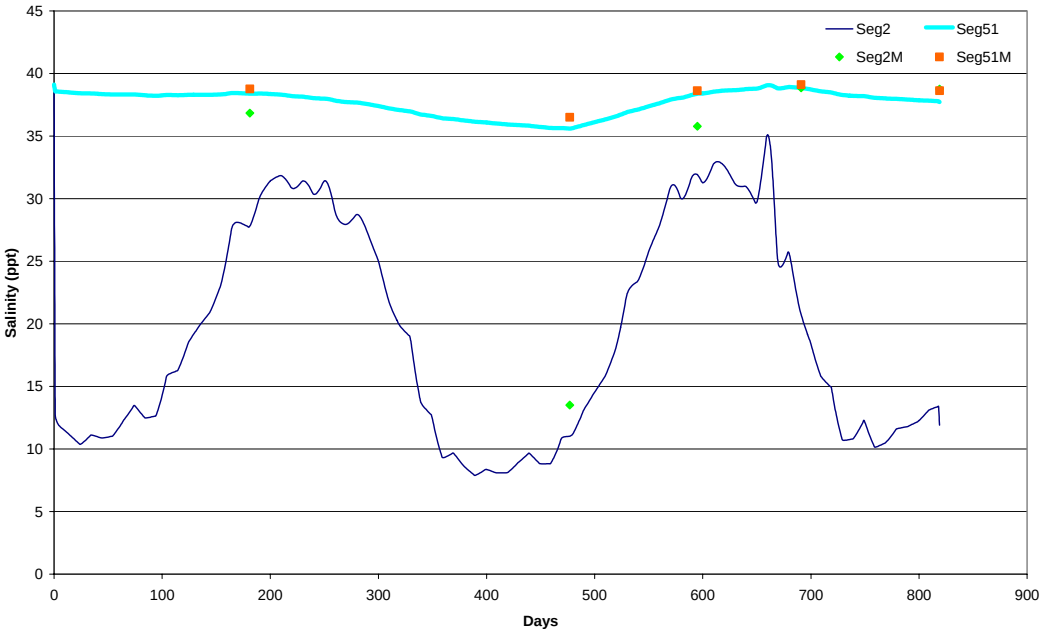

Figure F.23: Simulation Results and Measured Concentrations of Salinity for the Mediterranean Sea Boundary Condition

Annex G
Simulation Results of Load Scenario 1

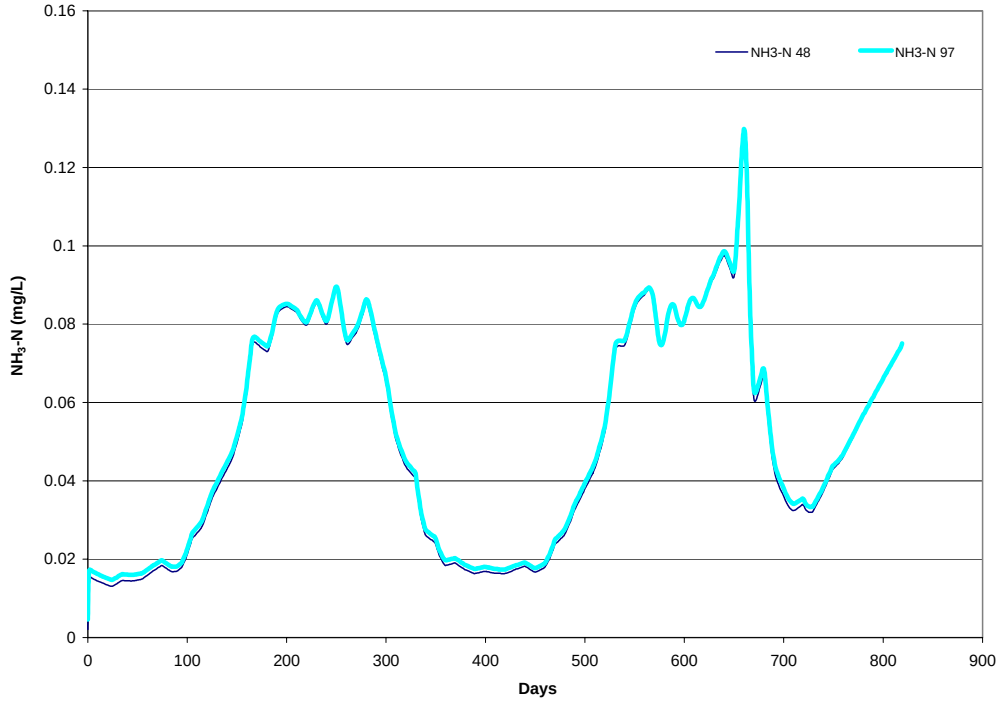

Figure G.1: Scenario 1 Simulation Results of Ammonia Nitrogen for the Köyceğiz Lake Boundary Condition

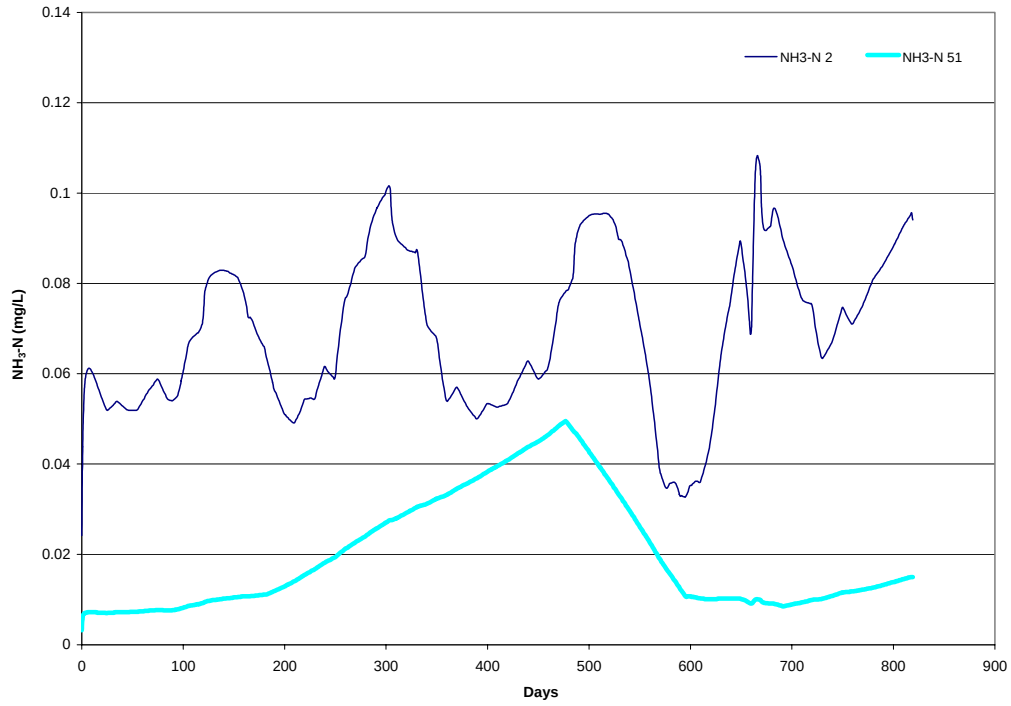

Figure G.2: Scenario 1 Simulation Results of Ammonia Nitrogen for the Mediterranean Sea Boundary Condition

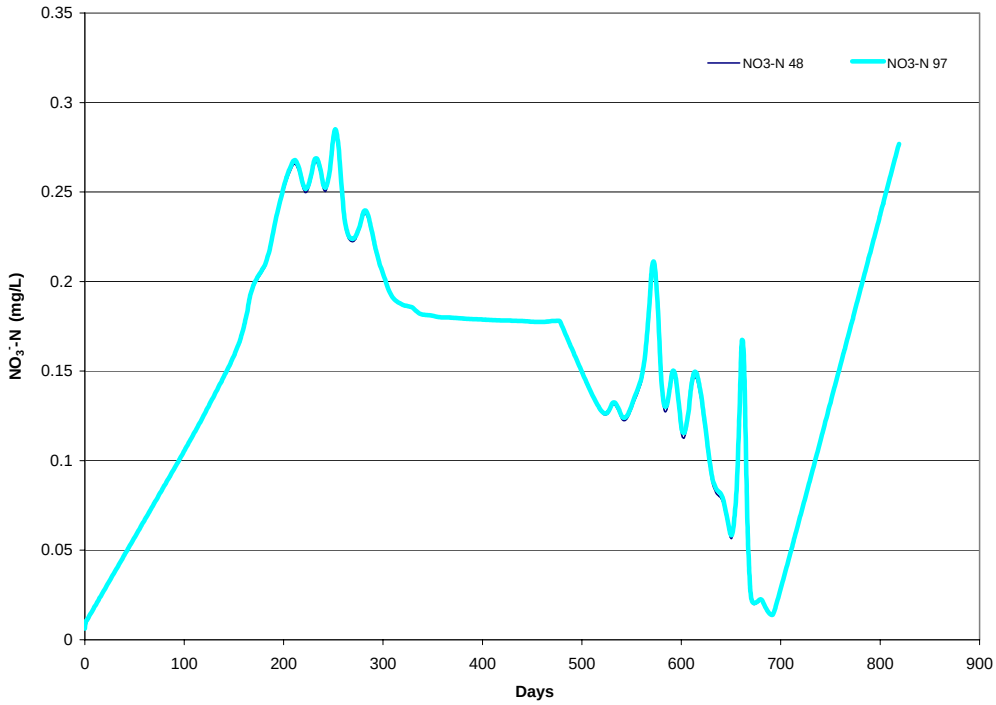

Figure G.3: Scenario 1 Simulation Results of Nitrate Nitrogen for the Köyceğiz Lake Boundary Condition

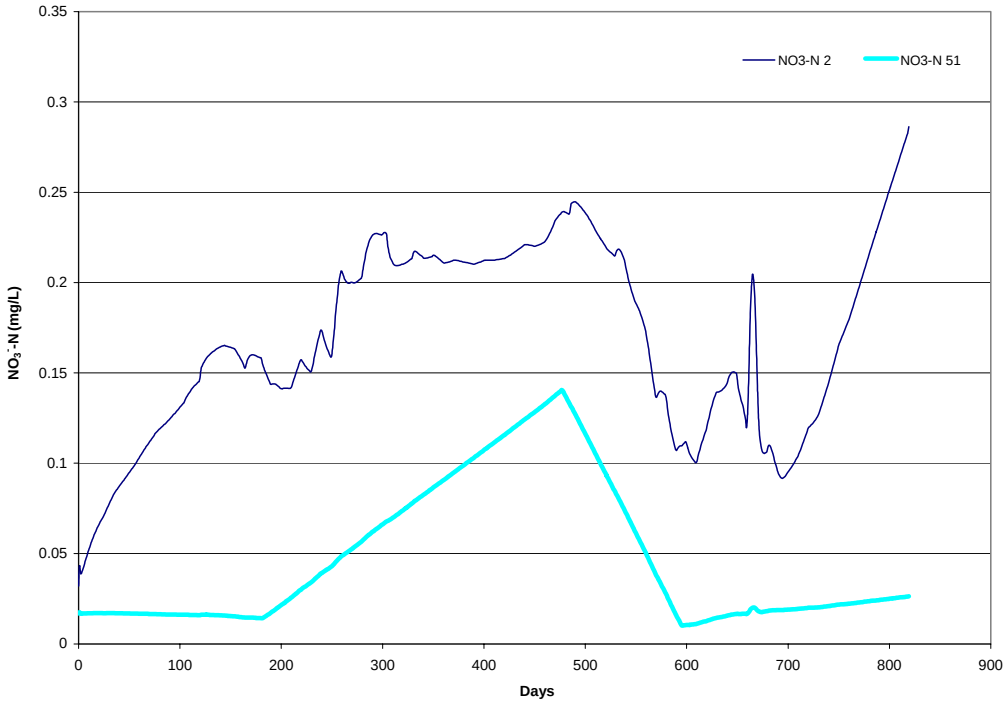

Figure G.4: Scenario 1 Simulation Results of Nitrate Nitrogen for the Mediterranean Sea Boundary Condition

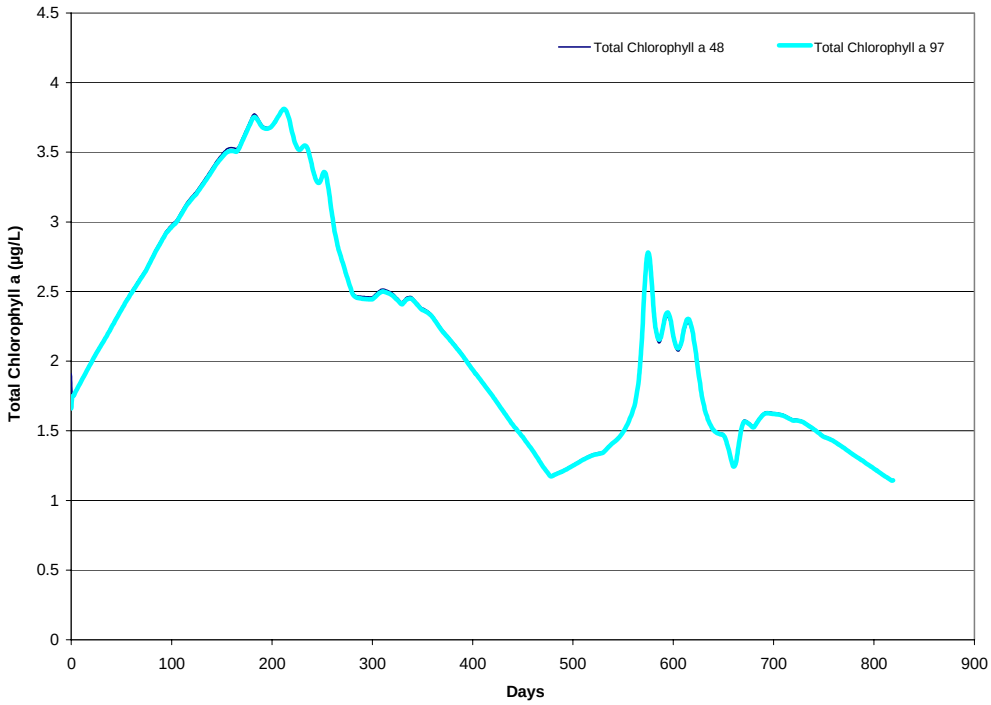

Figure G.5: Scenario 1 Simulation Results of Total Chlorophyll a for the Köyceğiz Lake Boundary Condition

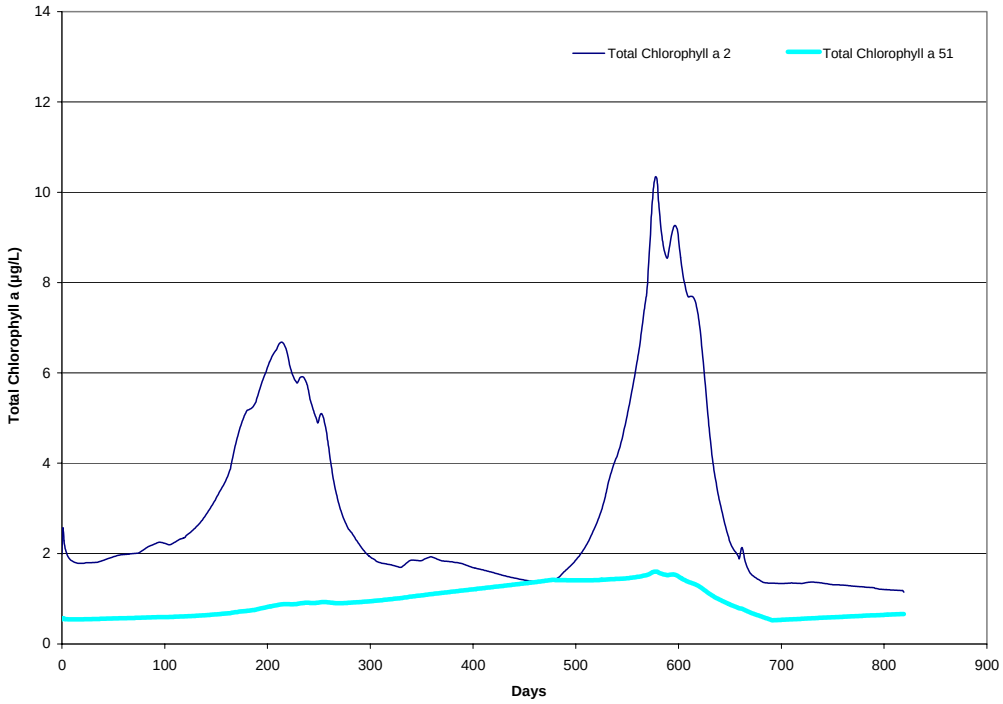

Figure G.6: Scenario 1 Simulation Results of Total Chlorophyll a for the Mediterranean Sea Boundary Condition

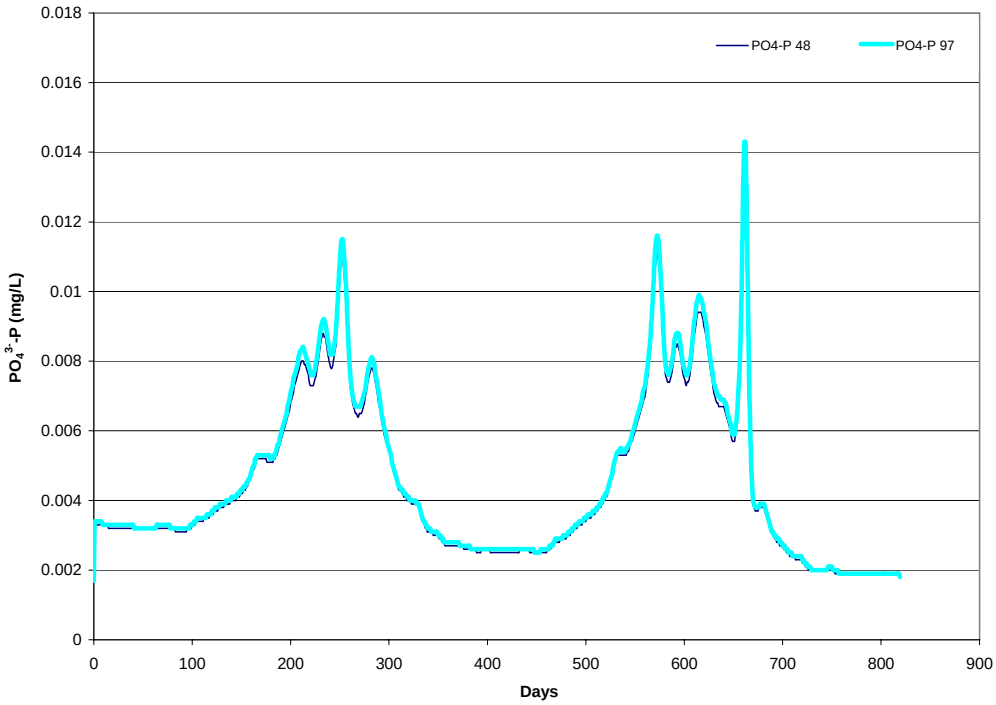

Figure G.7: Scenario 1 Simulation Results of Orthophosphate Phosphorus for the Köyceğiz Lake Boundary Condition

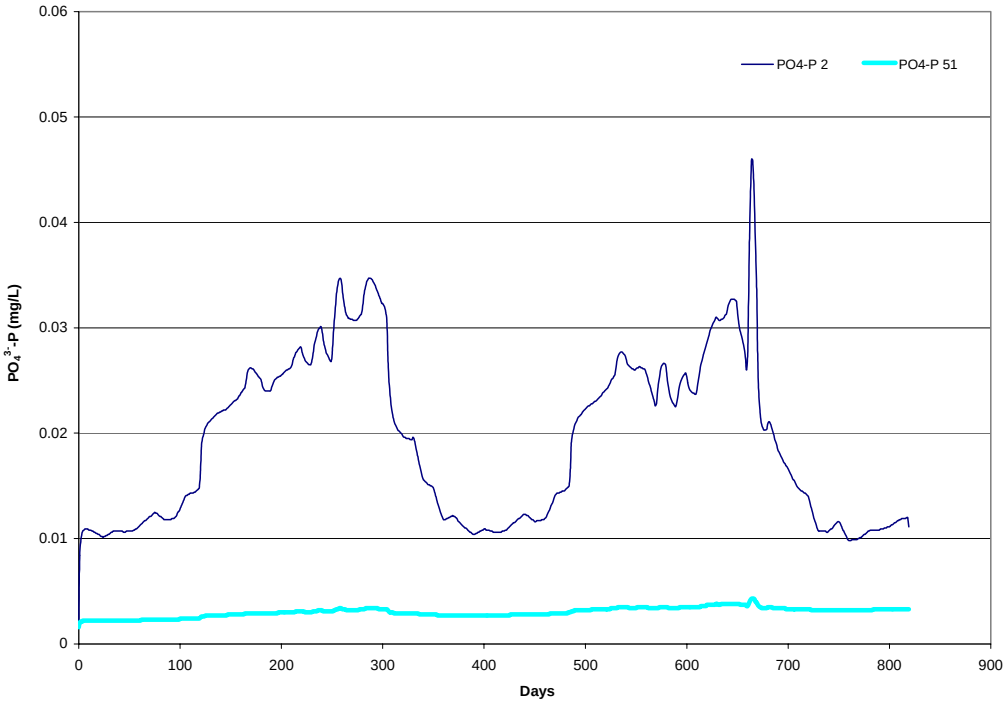

Figure G.8: Scenario 1 Simulation Results of Orthophosphate Phosphorus for the Mediterranean Sea Boundary Condition

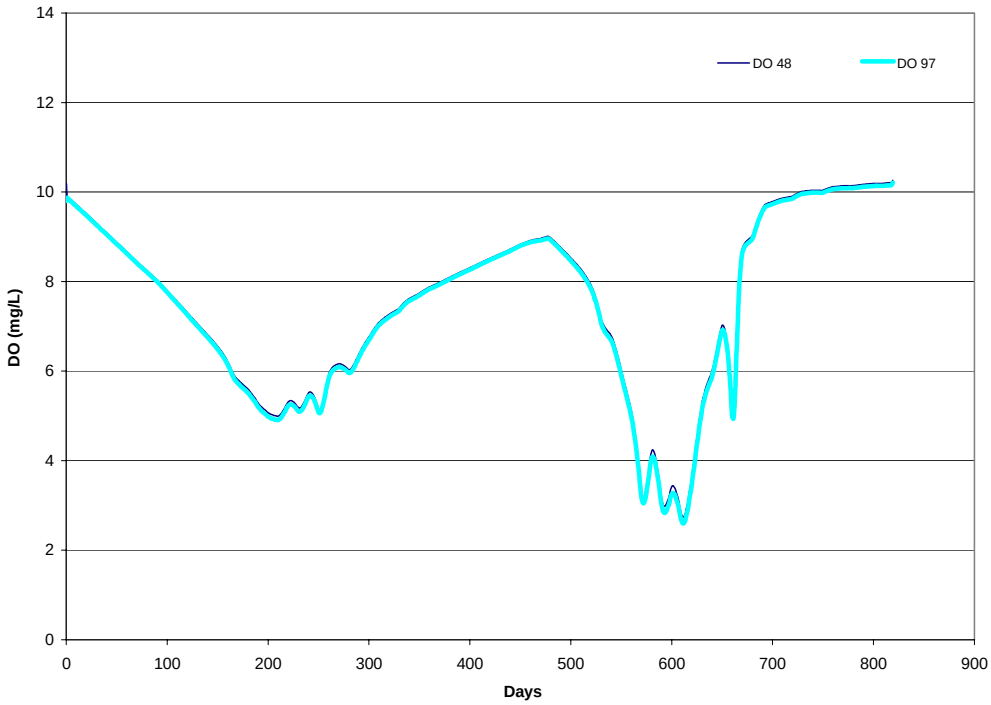

Figure G.9: Scenario 1 Simulation Results of Dissolved Oxygen for the Köyceğiz Lake Boundary Condition

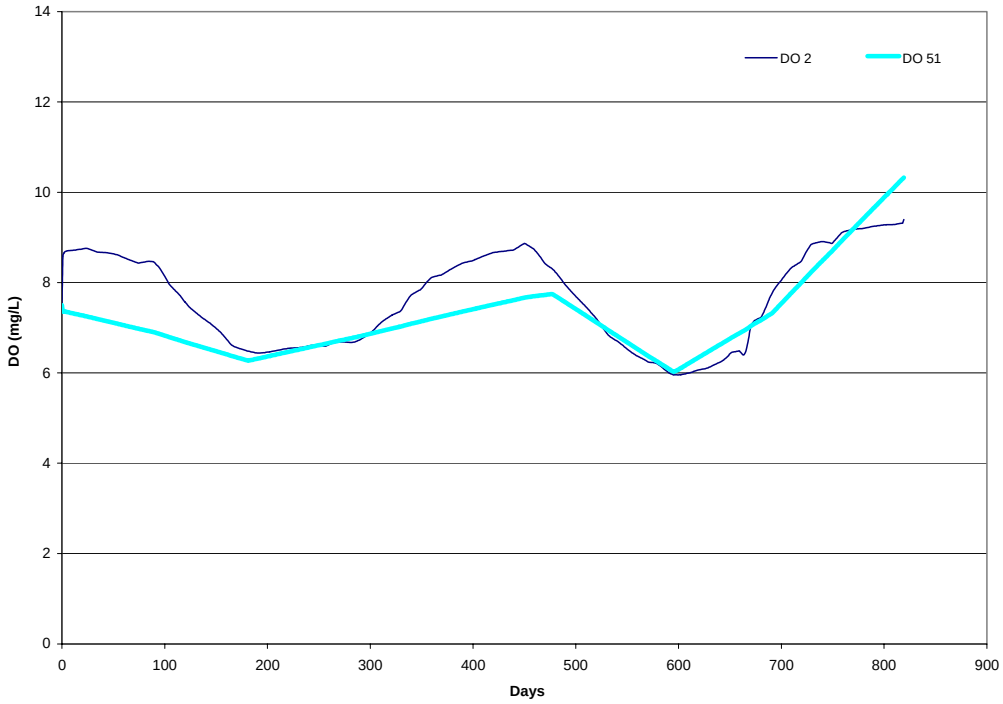

Figure G.10: Scenario 1 Simulation Results of Dissolved Oxygen for the Mediterranean Sea Boundary Condition

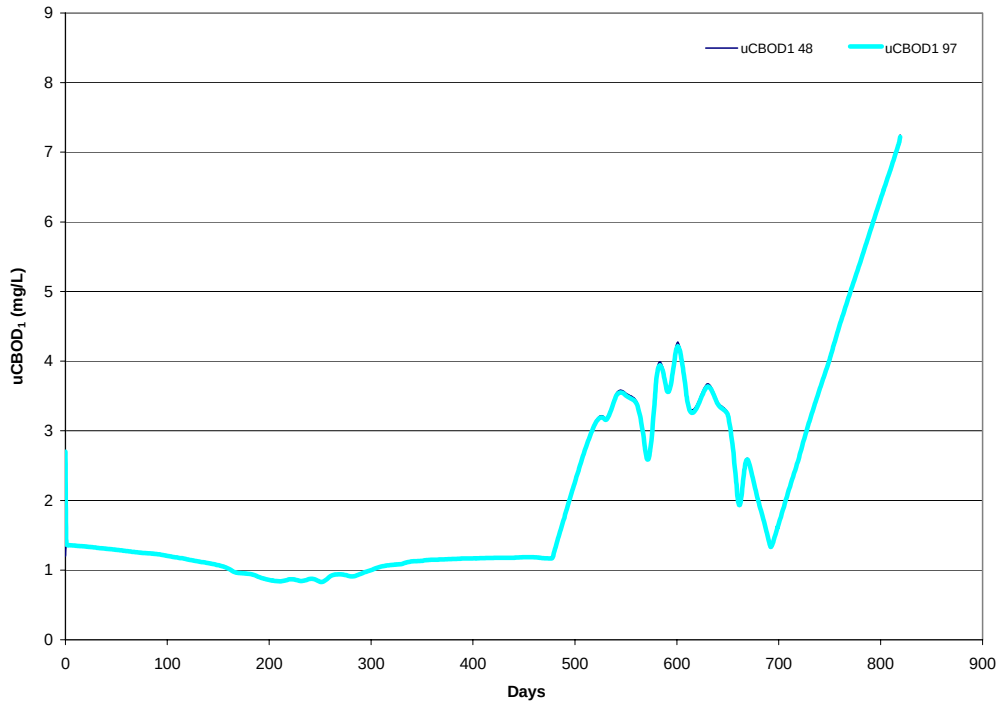

Figure G.11: Scenario 1 Simulation Results of $CBOD_1$ for the Köyceğiz Lake Boundary Condition

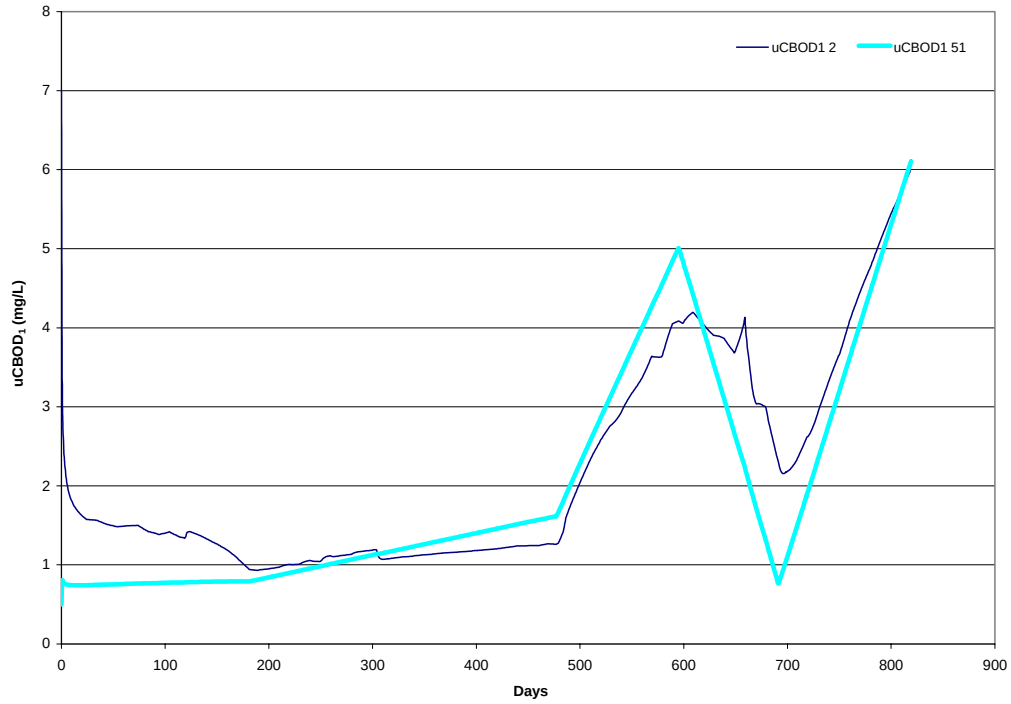

Figure G.12: Scenario 1 Simulation Results of $CBOD_1$ for the Mediterranean Sea Boundary Condition

Annex H
Simulation Results of Load Scenario 2

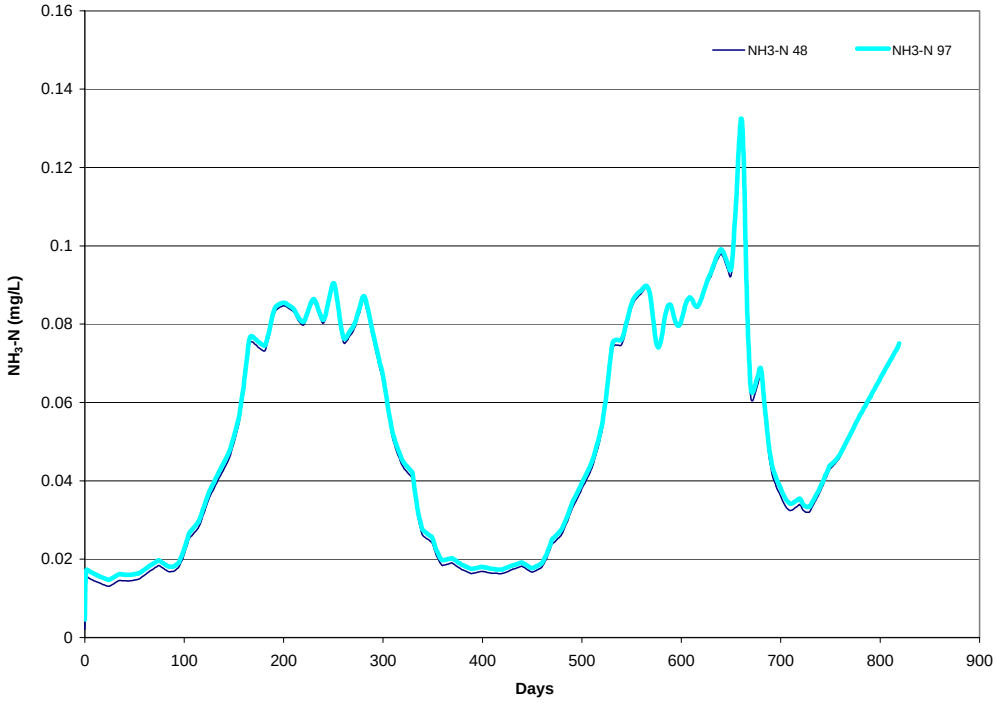

Figure H.1: Scenario 2 Simulation Results of Ammonia Nitrogen for the Köyceğiz Lake Boundary Condition

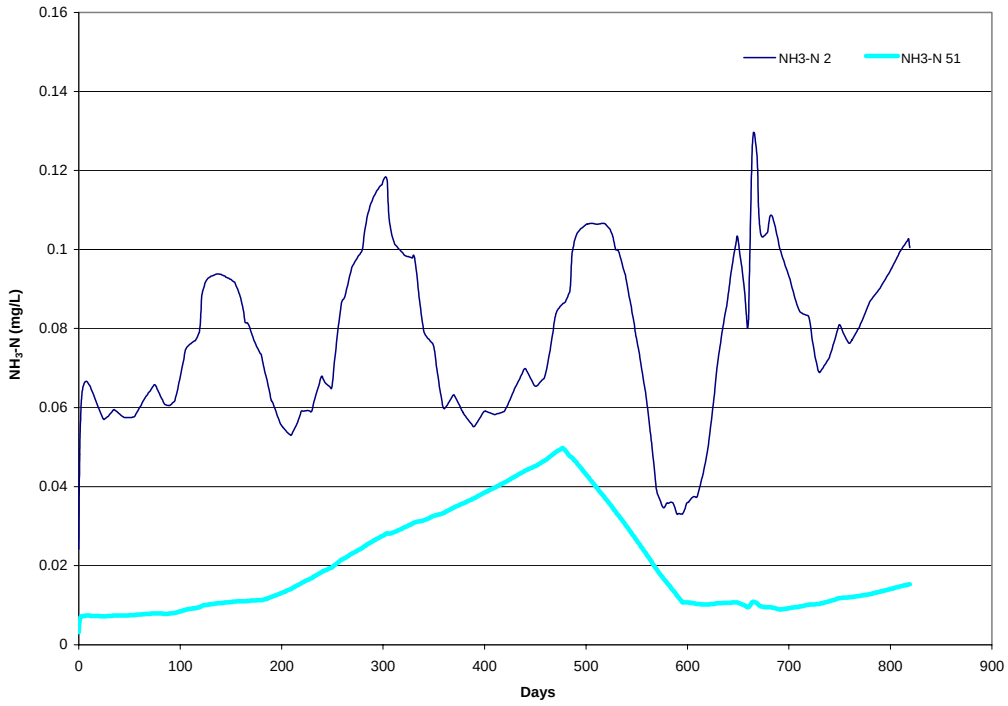

Figure H.2: Scenario 2 Simulation Results of Ammonia Nitrogen for the Mediterranean Sea Boundary Condition

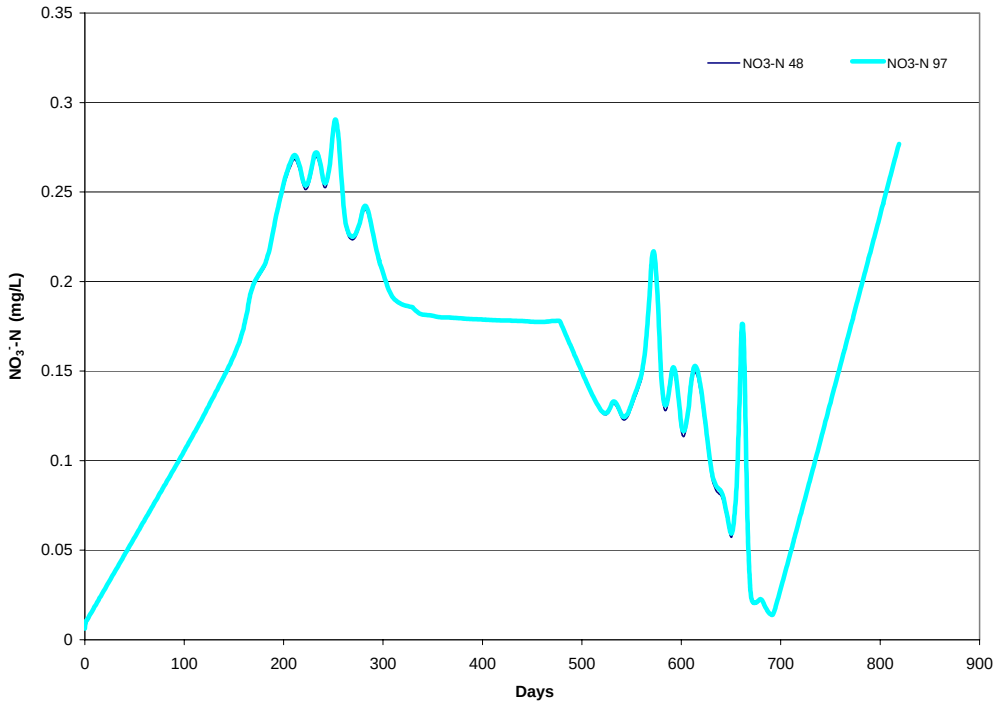

Figure H.3: Scenario 2 Simulation Results of Nitrate Nitrogen for the Köyceğiz Lake Boundary Condition

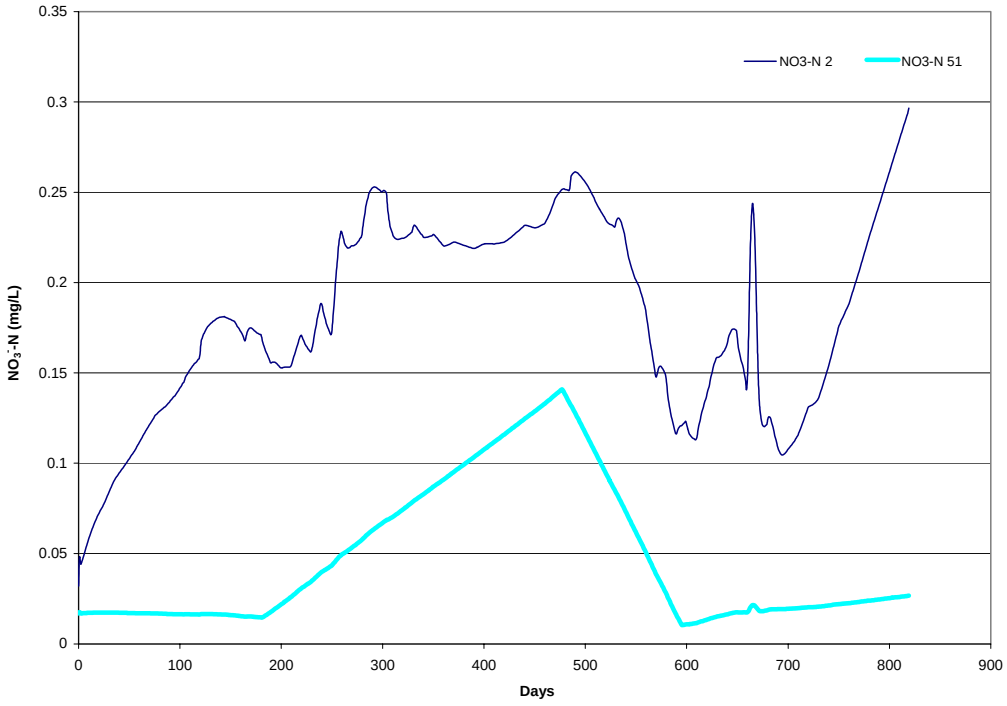

Figure H.4: Scenario 2 Simulation Results of Nitrate Nitrogen for the Mediterranean Sea Boundary Condition

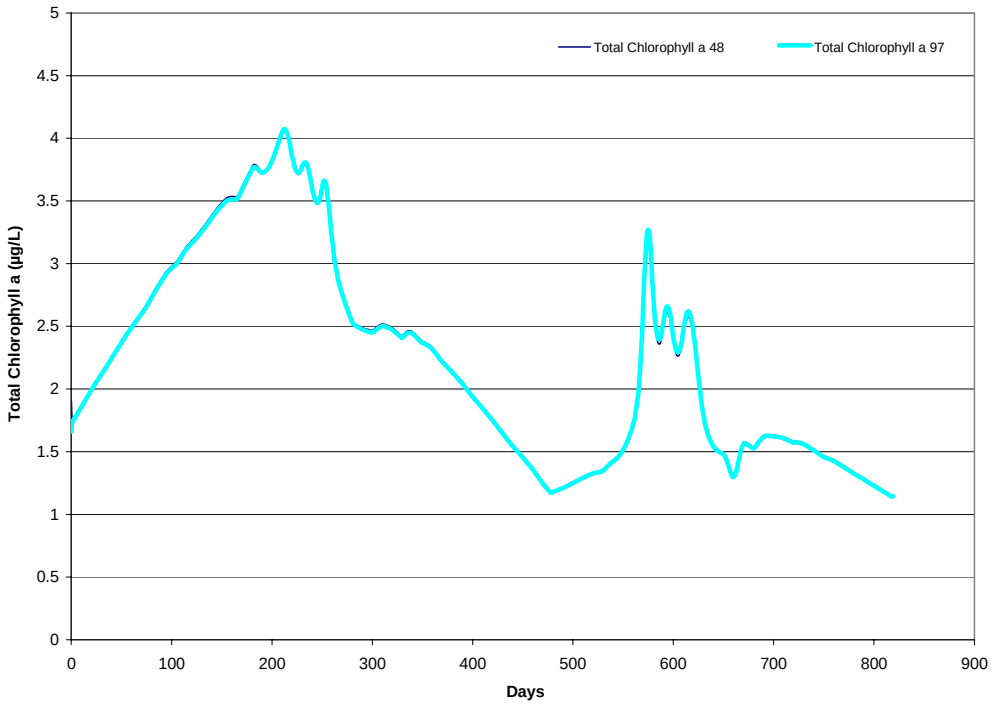

Figure H.5: Scenario 2 Simulation Results of Total Chlorophyll a for the Köyceğiz Lake Boundary Condition

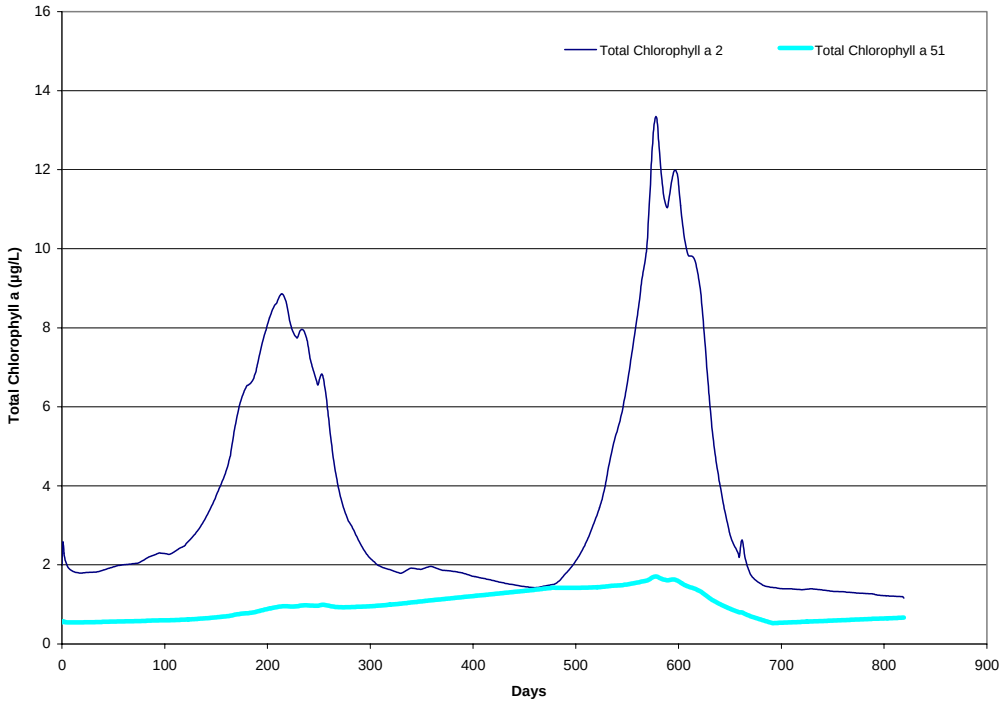

Figure H.6: Scenario 2 Simulation Results of Total Chlorophyll a for the Mediterranean Sea Boundary Condition

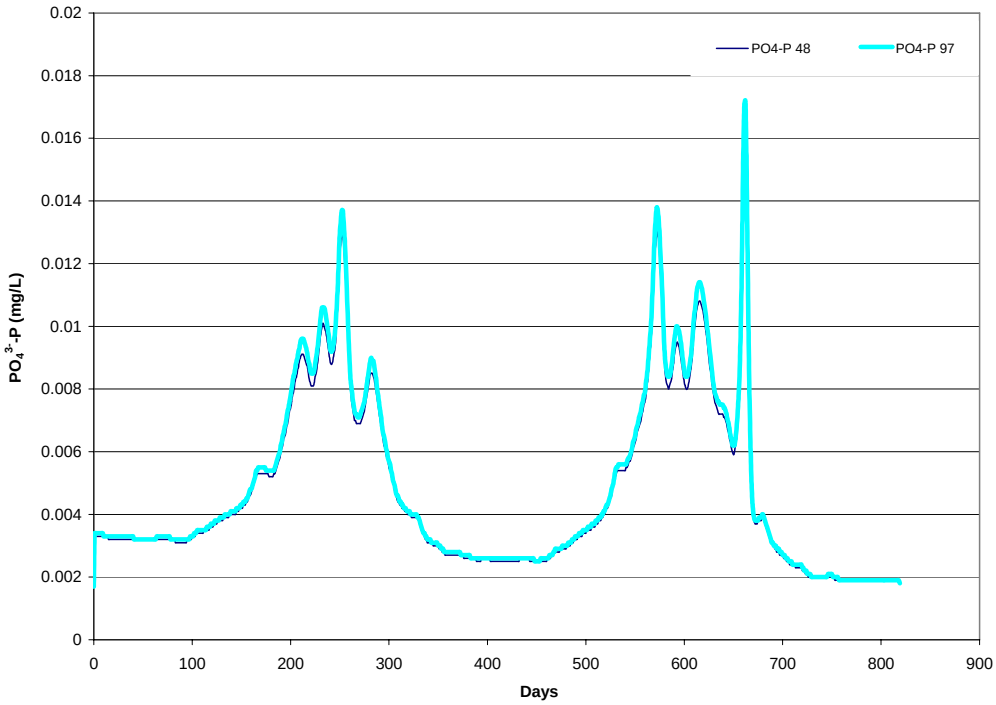

Figure H.7: Scenario 2 Simulation Results of Orthophosphate Phosphorus for the Köyceğiz Lake Boundary Condition

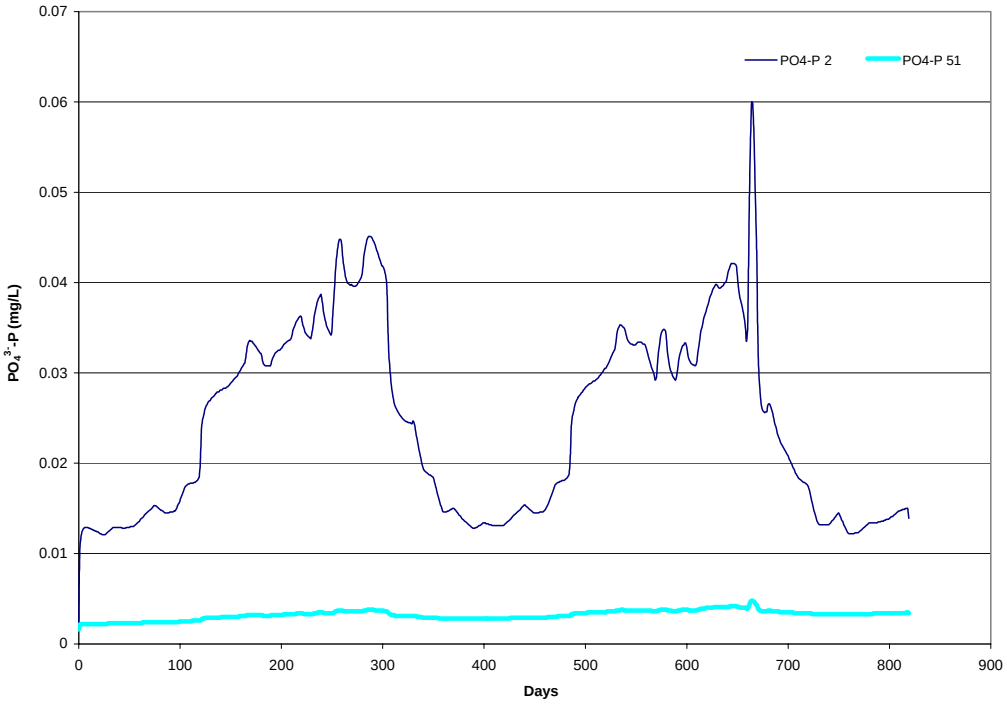

Figure H.8: Scenario 2 Simulation Results of Orthophosphate Phosphorus for the Mediterranean Sea Boundary Condition

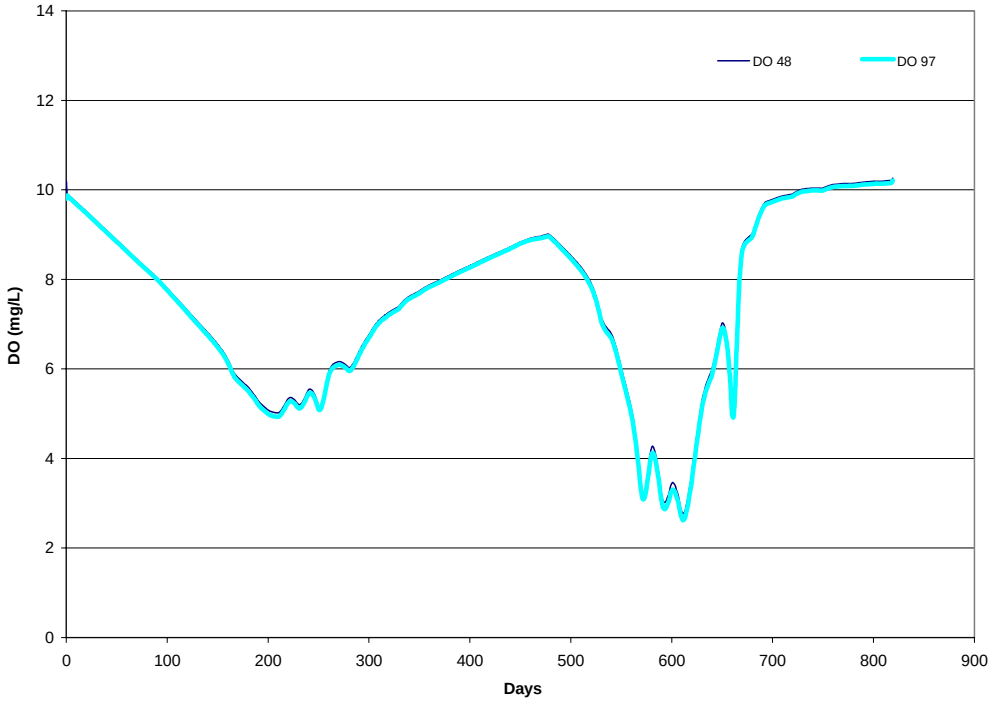

Figure H.9: Scenario 2 Simulation Results of Dissolved Oxygen for the Köyceğiz Lake Boundary Condition

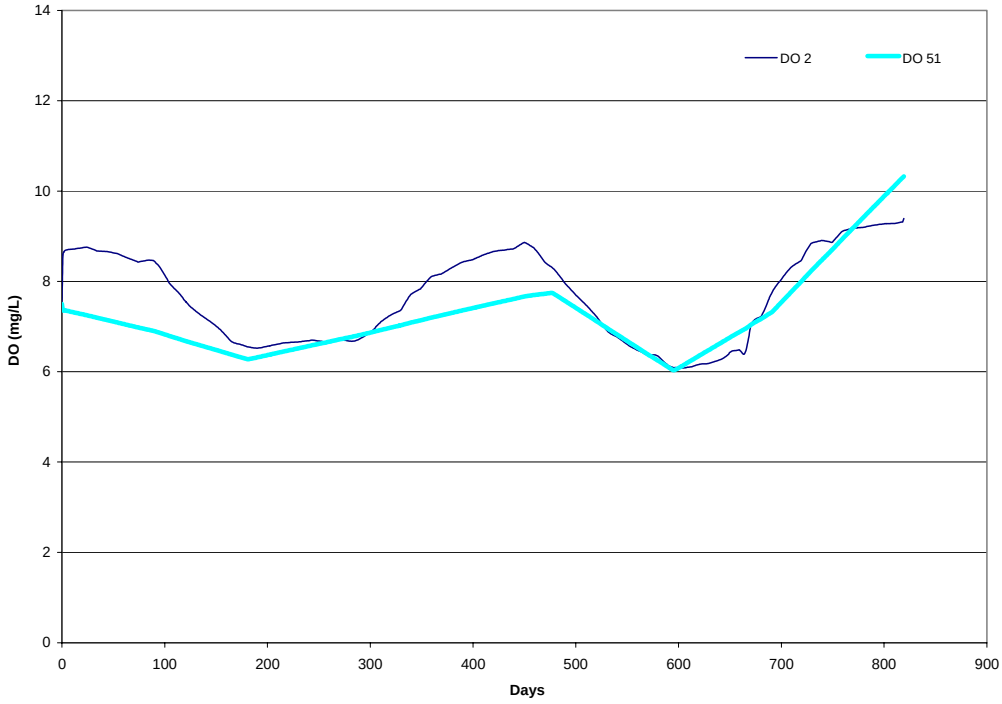

Figure H.10: Scenario 2 Simulation Results of Dissolved Oxygen for the Mediterranean Sea Boundary Condition

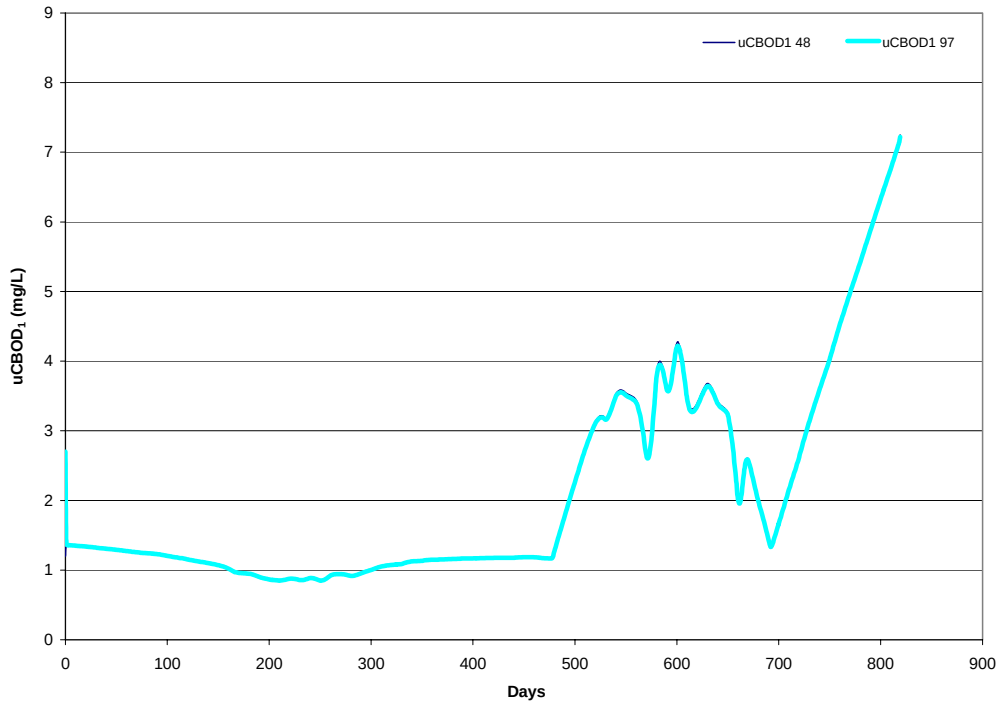

Figure H.11: Scenario 2 Simulation Results of $CBOD_1$ for the Köyceğiz Lake Boundary Condition

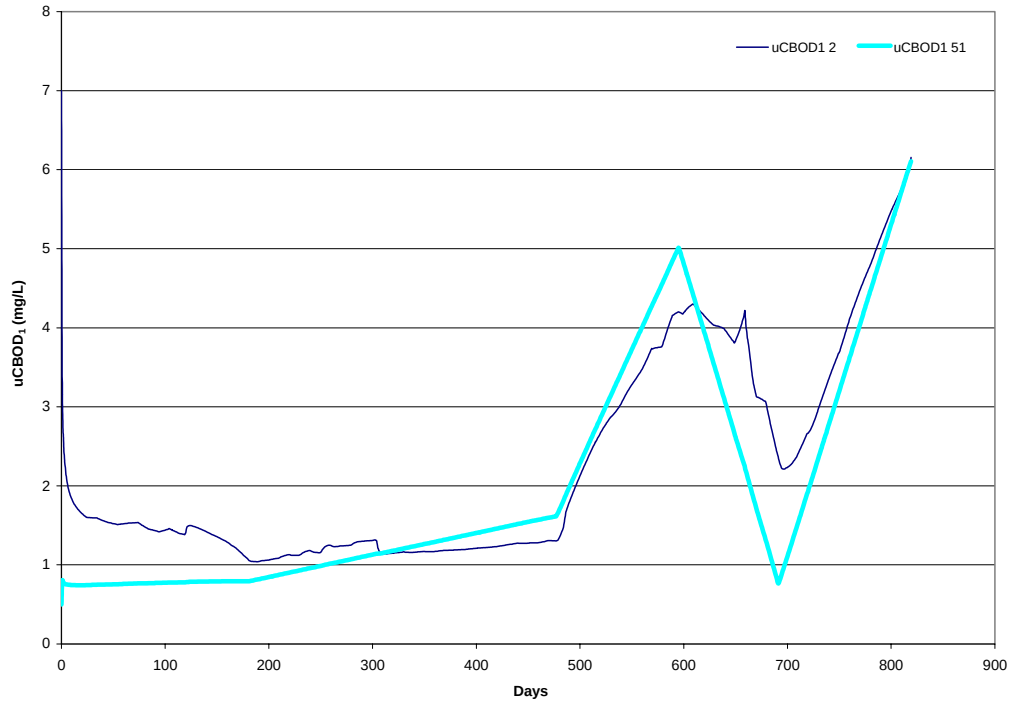

Figure H.12: Scenario 2 Simulation Results of $CBOD_1$ for the Mediterranean Sea Boundary Condition

Annex I
Simulation Results of Load Scenario 3

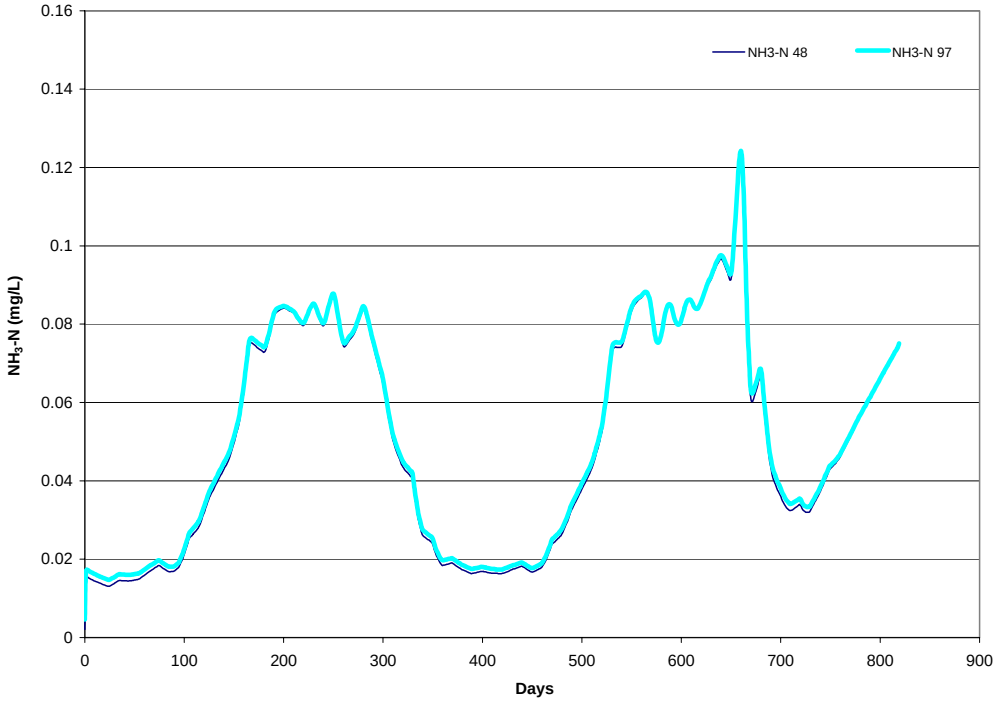

Figure I.1: Scenario 3 Simulation Results of Ammonia Nitrogen for the Köyceğiz Lake Boundary Condition

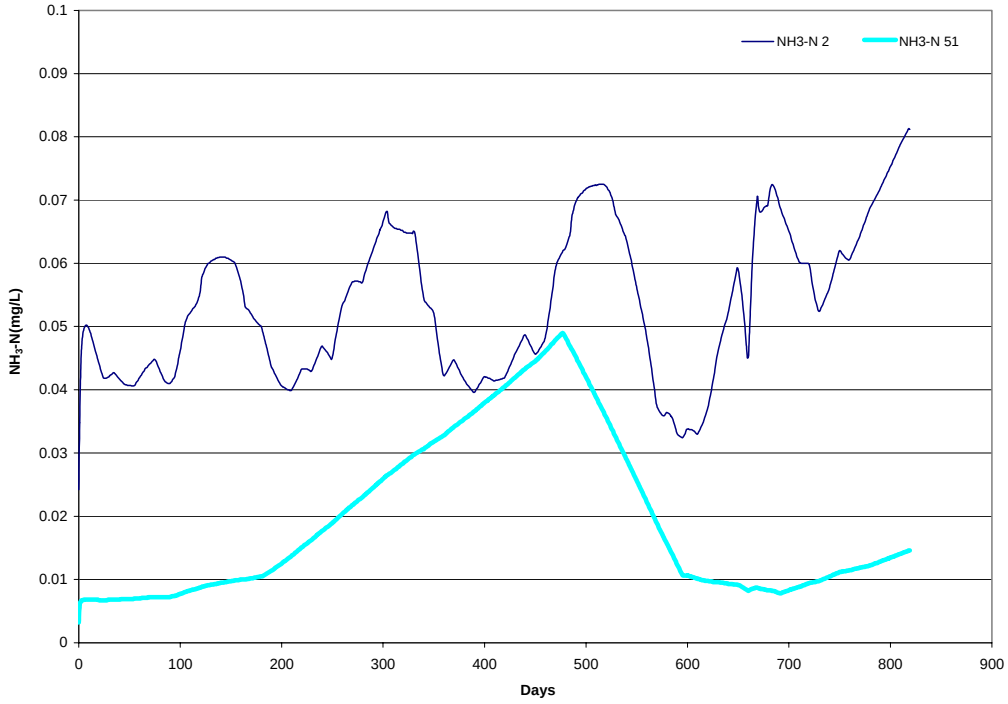

Figure I.2: Scenario 3 Simulation Results of Ammonia Nitrogen for the Mediterranean Sea Boundary Condition

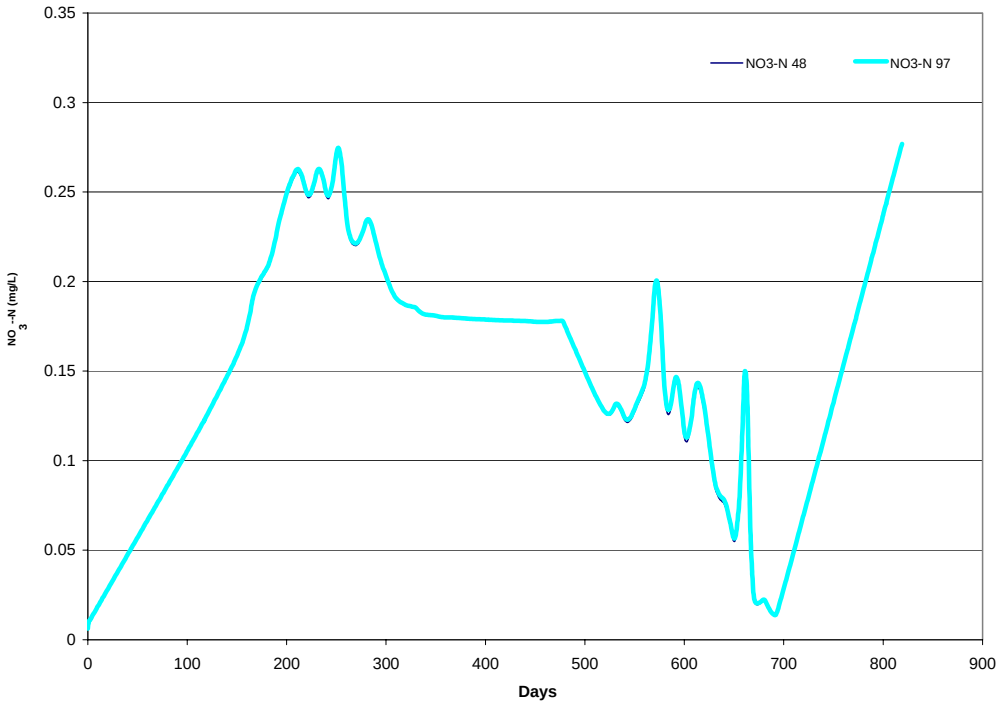

Figure I.3: Scenario 3 Simulation Results of Nitrate Nitrogen for the Köyceğiz Lake Boundary Condition

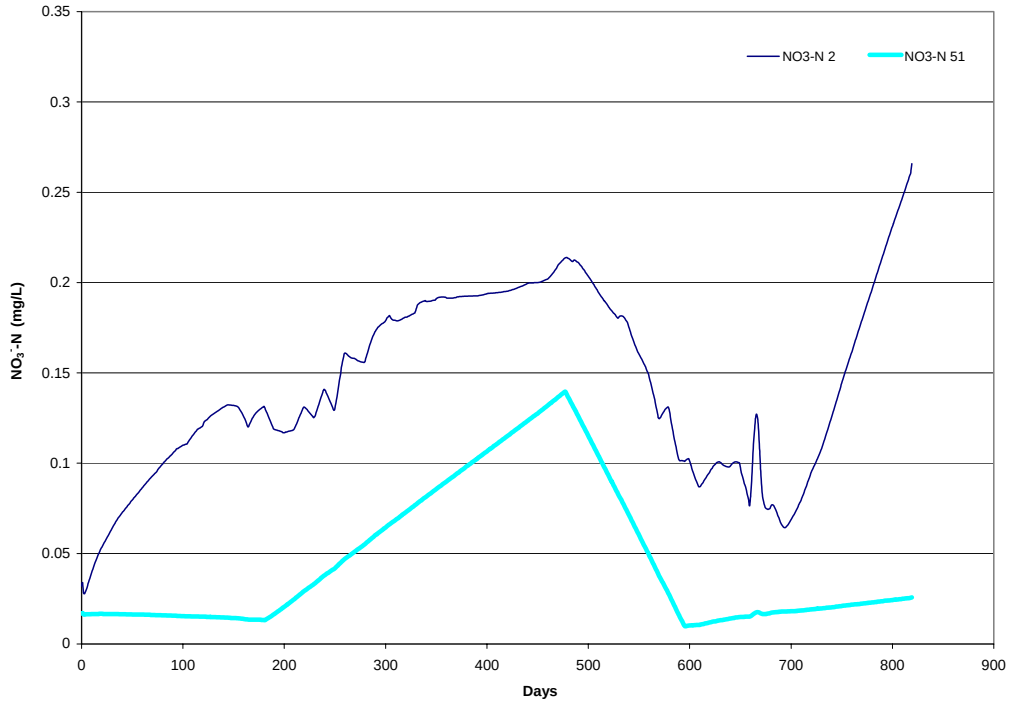

Figure I.4: Scenario 3 Simulation Results of Nitrate Nitrogen for the Mediterranean Sea Boundary Condition

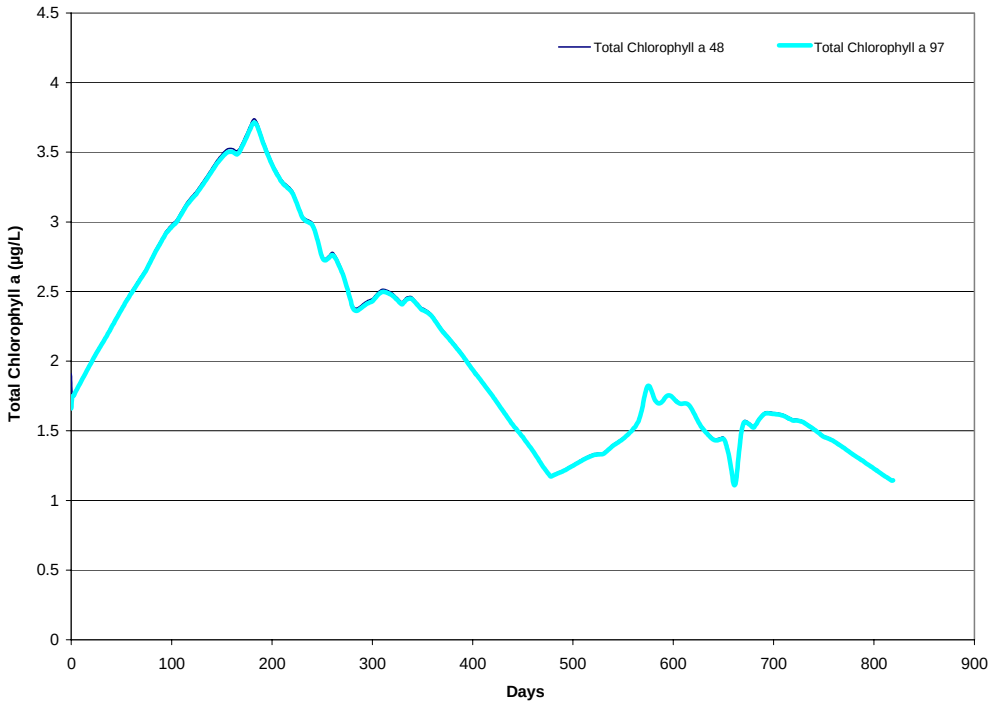

Figure I.5: Scenario 3 Simulation Results of Total Chlorophyll a for the Köyceğiz Lake Boundary Condition

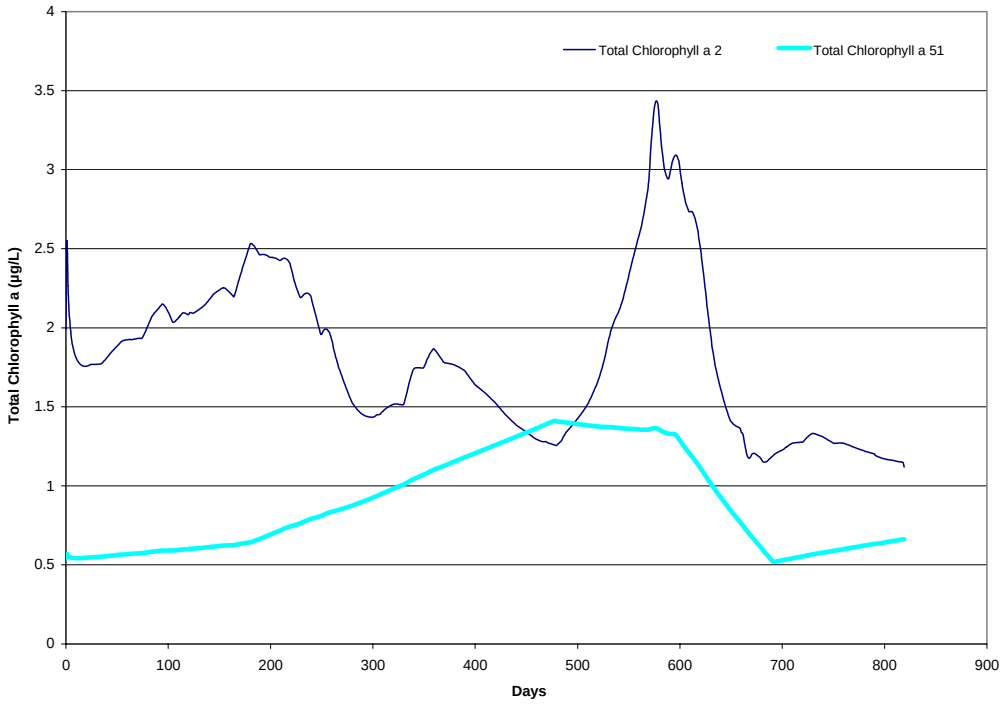

Figure I.6: Scenario 3 Simulation Results of Total Chlorophyll a for the Mediterranean Sea Boundary Condition

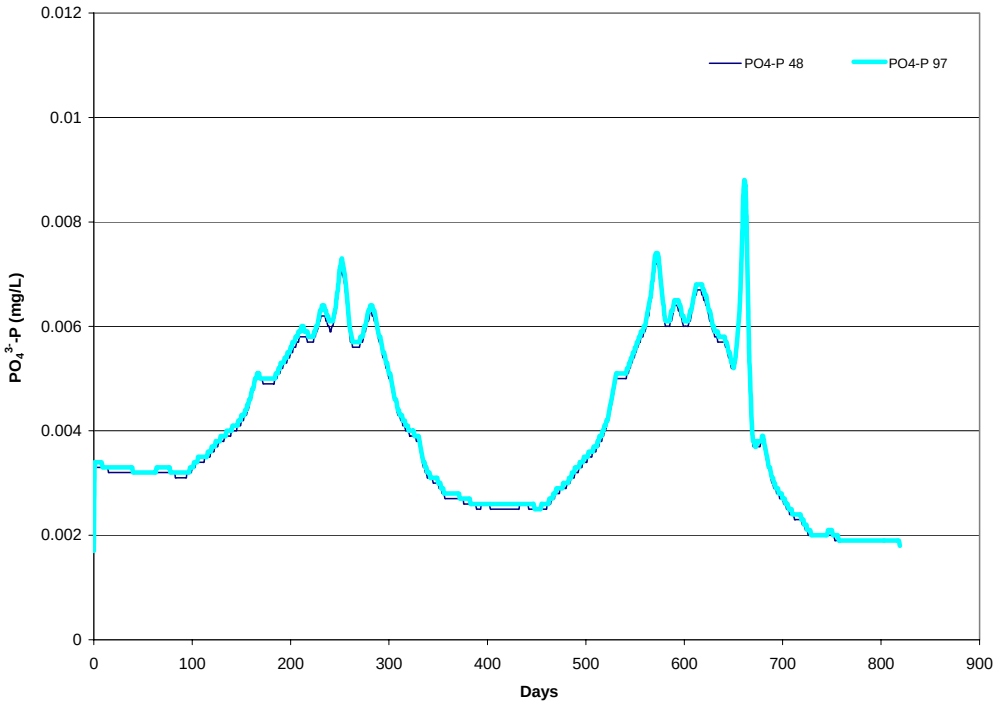

Figure I.7: Scenario 3 Simulation Results of Orthophosphate Phosphorus for the Köyceğiz Lake Boundary Condition

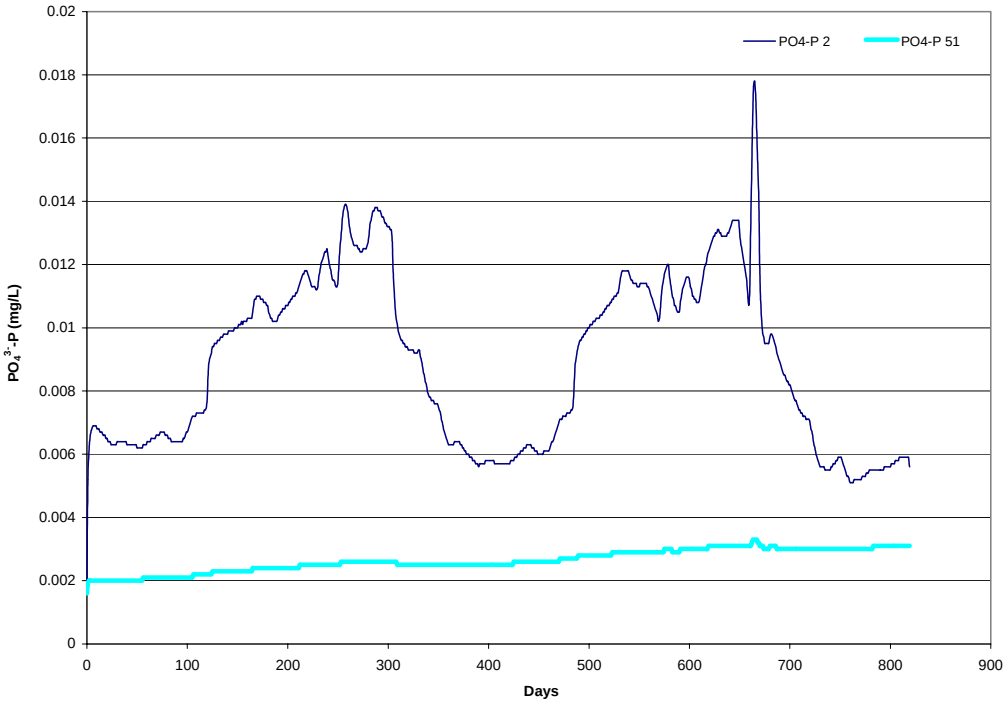

Figure I.8: Scenario 3 Simulation Results of Orthophosphate Phosphorus for the Mediterranean Sea Boundary Condition

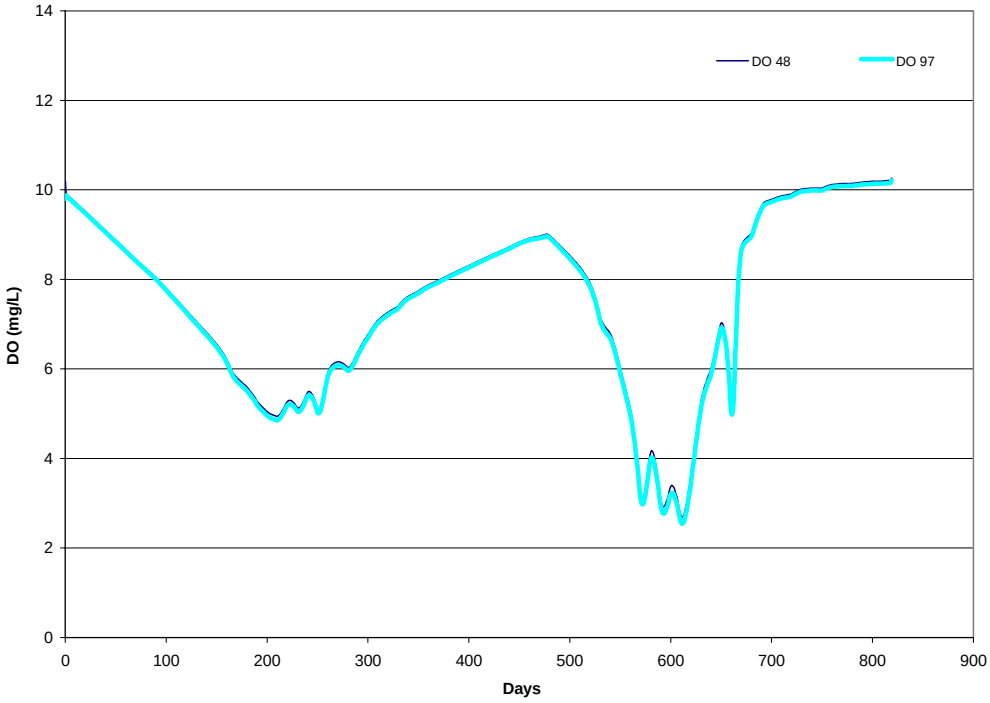

Figure I.9: Scenario 3 Simulation Results of Dissolved Oxygen for the Köyceğiz Lake Boundary Condition

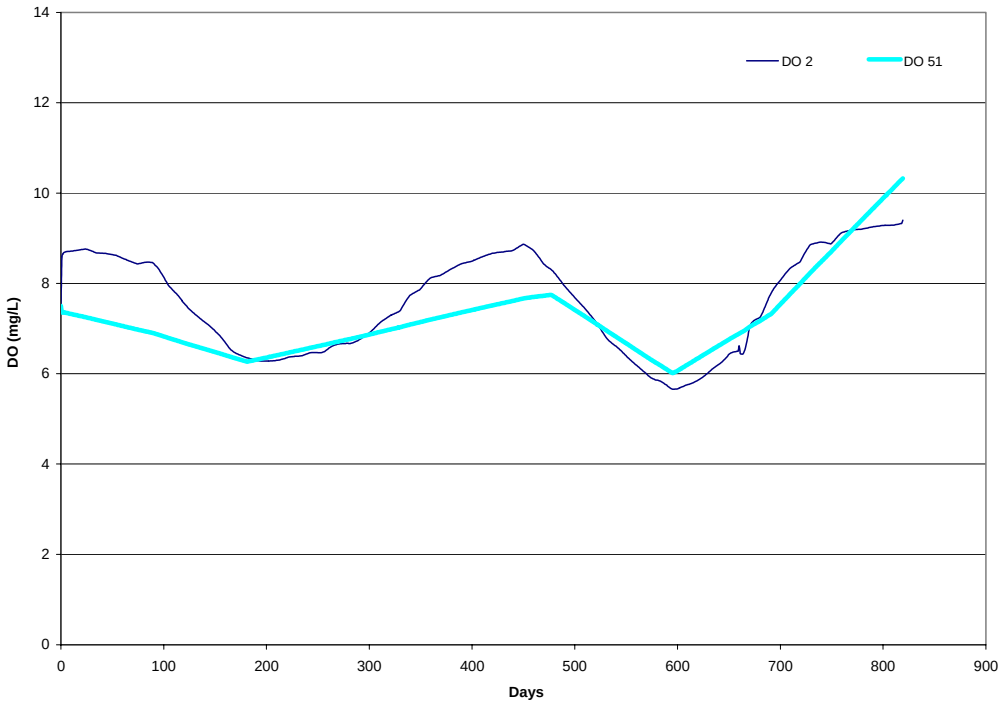

Figure I.10: Scenario 3 Simulation Results of Dissolved Oxygen for the Mediterranean Sea Boundary Condition

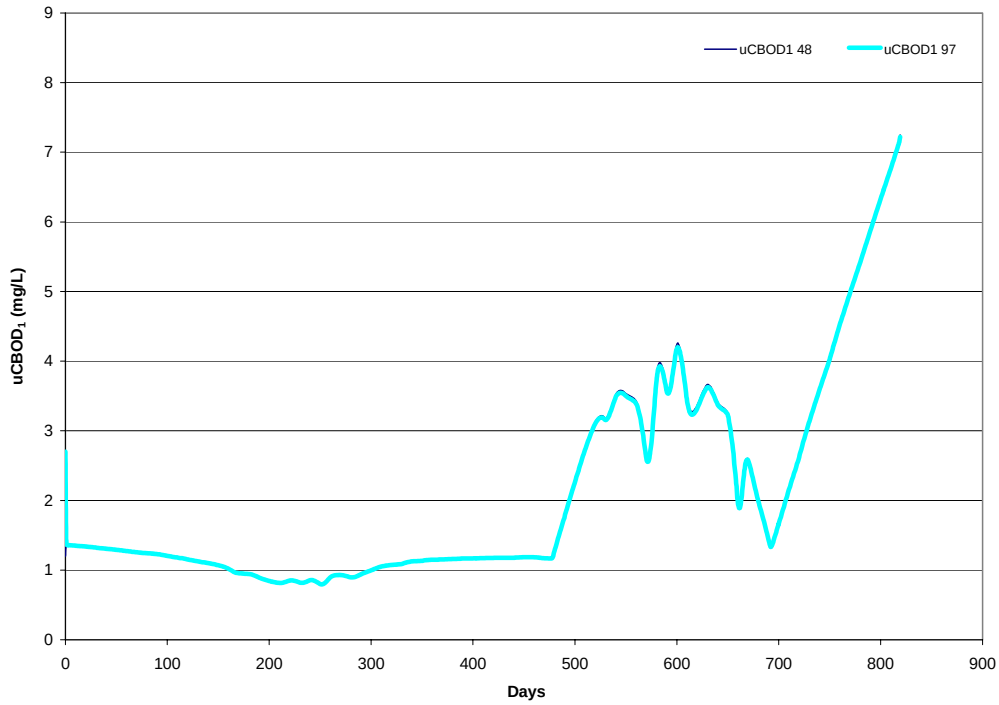

Figure I.11: Scenario 3 Simulation Results of $CBOD_1$ for the Köyceğiz Lake Boundary Condition

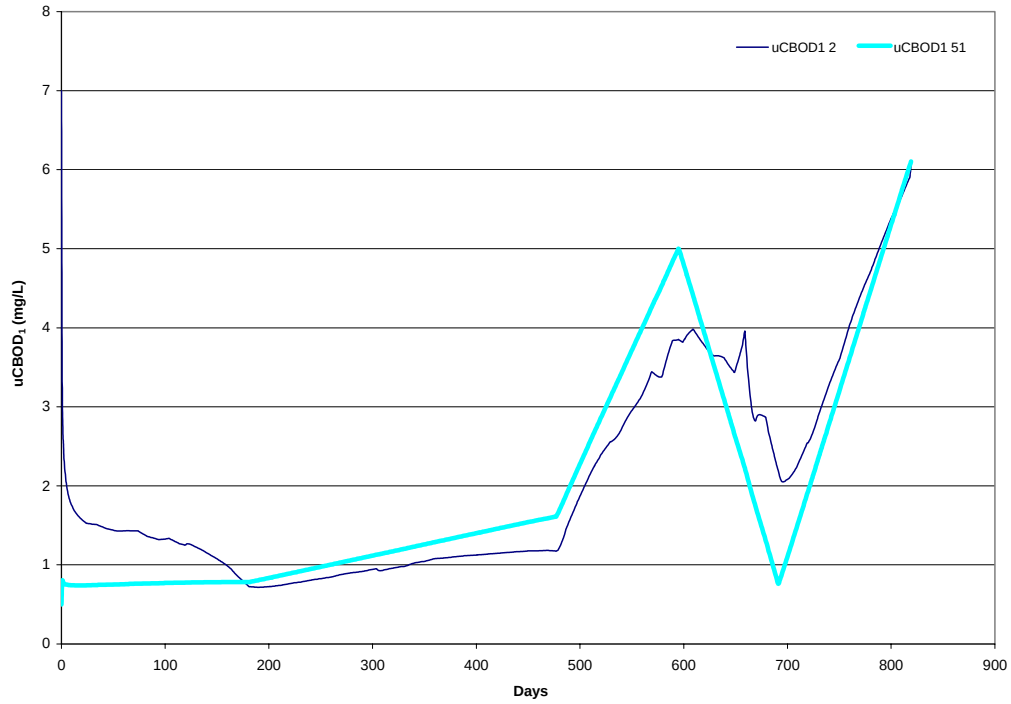

Figure I.12: Scenario 3 Simulation Results of $CBOD_1$ for the Mediterranean Sea Boundary Condition

CURRICULUM VITAE

Alpaslan Ekdal was born in İstanbul, in 1975. He got his B.Sc. degree from Yıldız Technical University, Environmental Engineering Department in 1998. Then, he had completed his M.Sc. studies in 2000 at Istanbul Technical University, Institute of Science and Technology, Environmental Engineering Program. In 2000, he started his Ph. D. studies at the same program. He worked as a visiting scientist at the United States Environmental Protection Agency, National Exposure Research Laboratory, Ecosystems Research Division, Athens, GA to conduct part of his Ph. D. studies between February 25, 2005 and February 25, 2006. He has been working as a research assistant at Istanbul Technical University, Environmental Engineering Department since 2002.